Expression and regulation of zinc-alpha$_2$-glycoprotein in rodent adipose tissue

Thesis submitted in accordance with the requirements of the University of Liverpool for the degree of Doctor in Philosophy by Theodora Tzanavari.

January 2007

Declaration

I declare that the research reported in this thesis has been carried out by myself at the Division of Cellular and Metabolic Medicine, University of Liverpool, and help which was received for any part of the work has been duly acknowledged. I believe that the contents of this thesis are wholly original, except where references are made. The work reported in this thesis has not been presented for any other degree.

Theodora Tzanavari
University of Liverpool
January 2007

Acknowledgements

I would like to thank the following people for their assistance in completing this work:

My supervisors Dr Chen Bing and Professor Paul Trayhurn for providing the required resources and unlimited supervision and patience during the practical and written part of this thesis.

Dr. Stuart Wood for his practical support and advice.

Mr. Leif Hunter for his continued practical advice and patience.

Andy for his help and the staff of the Bioresources Unit for their work in providing and maintaining animals.

Dr. Bohan Wang for her advice and the kind donation of tissues.

Dr. Sarah Dutton for her useful advice and friendship throughout this work.

All the members of my group for making this work a big pleasure and for the useful conversations.

Dr Nikos Migas for his support and his help with the final editing of this thesis.

My family for their love and support.

Abbreviations

α-MSH	α-melanocyte-stimulating hormone
ACE	angiotensin-converting enzyme
AGT	angiotensinogen
ASP	acylation stimulating protein
BAT	brown adipose tissue
BCA	bicinchoninic acid
BMI	body mass index
BSA	bovine serum albumin
cAMP	cyclic adenosine monophosphate
C/EBP	CCAAT/enhancer binding proteins
CNS	central nervous system
CNTF	ciliary neurotrophic factor
COX	cyclooxygenase
CPE	carboxypeptidase E
CRBP	cellular retinol binding protein
CRP	c-reactive protein
DIT	diet induced thermogenesis
DMEM	dulbecco's modified eagle's medium
DNA	deoxyribonucleic acid
DTT	dithiothreitol
ECL	enhanced chemiluminescence
EDTA	ethlyenediaminetetraacetic acid
EGF	epidermal growth factor
FCS	foetal calf serum
FFA	free fatty acid
FGF	fibroblast growth factor
FIAF	fasting-induced adipose factor
GAPDH	glyceraldehyde-3-phosphate dehydrogenase
GH	growth hormone

HEPES	(4-(2-hydroxyethyl)piperazine-1-ethanesulphonic acid)
HIF-1	hypoxia-inducible factor-1
hMADs	human multipotent adipose-derived stem cells
HRP	horse radish peroxidase
HSL	hormone sensitive lipase
IBMX	3-isobutyl-1-methylxanthine
IFN-γ	interferon-γ
IGF-1	insulin-like growth factor-1
IGFBPs	insulin-like growth factor binding proteins
IL-	interleukin-
JAK/STAT	janus kinase/ signal transducer and activator of transcription
LDL	low-density lipoprotein
LIF	leukaemia-inhibitory factor
LMF	lipid mobilizing factor
LPL	lipoprotein lipase
LPS	lipopolysaccharide
MC4R	melanocortin 4 receptor
MCP-1	chemokine monocyte chemoattractant protein 1
MHC	major histocompatibility complex
MIF	macrophage migration inhibitory factor
MSH	melanocyte-stimulating hormone
MT	metallothionein
NCBI	national center for biotechnology information
NEAT	nonexercise activity thermogenesis
NGF	nerve growth factor
NPY	neuropeptide Y
NST	non-shivering thermogenesis
PAI-1	plasminogen activator inhibitor-1
PBS	phosphate buffered saline
PCR	polymerase chain reaction

PG-	prostaglandin-
PIF	proteolysis inducing factor
PKA	protein kinase A
PPAR	peroxisome proliferator activated receptor
POMC	pro-opiomelanocortin
RAR	retinoic acid receptor
RAS	renin-angiotensinogen system
RBP	retinol binding protein
REE	resting energy expenditure
RNA	ribonucleic acid
RT	reverse transcription
SAA	serum amyloid A
SDS	sodium dodecyl sulphate
SEM	standard error of the mean
SNS	sympathetic nervous system
TAGs	triacylglycerols
TBE	tris-borate-EDTA
TBS	tris-buffered saline
TCA	trichloroacetic acid
TGF-β	transforming growth factor-β
Tris-HCl	trizma hydrochloride; tris[hydroxymethyl]-aminomethane hydrochloride
TZD	thiazolidinedione
TNF-	tumour necrosis factor-
UCP	uncoupling protein
UV	ultra violet
VEGF	vascular endothelial factor
WAT	white adipose tissue
ZAG	zinc-alpha$_2$-glycoprotein

Table of contents

Declaration		ii
Acknowledgements		iii
Abbreviations		iv
Table of contents		vii
List of figures		xii
List of tables		xv
Abstract		xvi
CHAPTER 1	INTRODUCTION	1
1.1	Adipose tissue anatomy	2
1.1.1	Adipose tissue morphology	2
1.1.2	Adipocyte differentiation and development	3
1.1.3	Function of WAT	6
1.1.3.1	WAT metabolism: lipolysis and lipogenesis	6
1.1.4	BAT function	8
1.1.5	Adipose tissue and adipocyte studies	9
1.2	Energy balance	11
1.2.1	Obesity	12
1.2.1.1	Epidemiology of obesity	12
1.2.1.2	Obesity as a medical problem	13
1.2.1.3	Obesity as an inflammatory state	14
1.2.1.4	Study of obesity: Genetic models	15
1.2.2	Cancer cachexia	17
1.2.2.1	Pathogenesis of cancer cachexia	17
1.2.2.2	Pathogenesis of cancer cachexia in adipose tissue	19
1.2.2.3	Mediators of cancer cachexia	19
1.3	Endocrine function of adipose tissue	22
1.3.1	Free fatty acids and steroid secretions of WAT	22
1.3.2	Leptin	24
1.3.2.1	Regulation of leptin expression and production	24
1.3.2.2	Functions of leptin	26
1.3.2.3	Leptin receptor	26
1.3.3	Insulin sensitivity and insulin resistance	27
1.3.3.1	Adiponectin	27
1.3.3.1.1	Expression, regulation and function of adiponectin	27
1.3.3.1.2	Adiponectin receptors	28
1.3.3.2	Resistin	29
1.3.3.3	Visfatin	29
1.3.4	Cytokines	30
1.3.4.1	Tumour necrosis factor αα (TNFα)	30
1.3.4.2	Interleukins	31
1.3.5	Chemokines	32
1.3.6	Growth factors	33
1.3.7	Haemostatic factors	34
1.3.8	Acute-phase proteins	36

1.3.9	Prostaglandins	37
1.3.9.1	Prostaglandin synthesis	37
1.3.9.2	Prostaglandin receptors	38
1.3.9.3	Prostaglandins in WAT	40
1.3.10	Proteins of lipid and lipoprotein metabolism	41
1.4	Zinc-α_2-glycoprotein (ZAG)	42
1.4.1	ZAG expression	43
1.4.2	Biological functions of ZAG	43
1.4.3	ZAG is involved in body weight regulation and is expressed in adipose tissue	44
1.5	Aims of this thesis	45
CHAPTER 2	MATERIALS & METHODS	47
2.1	Reagents and Equipment	48
2.1.1	Chemical reagents	48
2.1.2	Commercial kits	50
2.1.3	Equipment	50
2.1.4	Software	51
2.1.5	Suppliers' addresses and URLs	52
2.2	Animals	54
2.2.1	Mice	54
2.2.2	Rats	55
2.3	Mature adipocytes and stromal vascular cell fractionation	56
2.3.1	Reagents	56
2.3.2	Fractionation with collagenase digestion method	57
2.4	3T3-L1 adipocyte cell culture	58
2.4.1	Reagents	58
2.4.2	Cell storage	59
2.4.2.1	Cell generation and maintenance	59
2.4.2.2	Cell passaging and plating	60
2.4.2.3	Cell differentiation	60
2.4.2.4	Cell treatment	60
2.4.2.5	Cell and media collection	61
2.4.3	Light microscopy	61
2.5	Total RNA isolation from cells and tissues using the Trizol - Reagent method	61
2.5.1	Reagents	61
2.5.2	Trizol - Reagent RNA extraction method	62
2.5.3	TURBO DNase treatment of RNA	63
2.5.3.1	Reagents	63
2.5.3.2	Method	63
2.5.4	RNA quantification	64
2.6	Reverse-transcription polymerase chain reaction (RT-PCR)	64
2.6.1	First-strand cDNA synthesis	64
2.6.1.1	Reagents	65
2.6.1.2	Method	65

2.6.2	Polymerase Chain Reaction (PCR)	65
2.6.2.1	PCR primer design	66
2.6.2.2	PCR primer optimization	67
2.6.2.3	Reagents	69
2.6.2.4	Method	69
2.6.3	Agarose gel electrophoresis	69
2.6.3.1	Reagents	70
2.6.3.2	Method	70
2.7	Real-time Polymerase chain reaction (qPCR) – Taqman system	70
2.7.1	Taqman system description	71
2.7.2	Primers and Taqman probes design and optimisation	73
2.7.3	Preparation of 96 well plates for real-time PCR	76
2.7.3.1	Reagents	76
2.7.3.2	Method	76
2.7.4	Taqman system real-time PCR machine setup	77
2.7.5	Analysis of real-time PCR data	78
2.8	Protein detection using western blotting method	78
2.8.1	Protein Isolation	81
2.8.1.1	Protein isolation from frozen tissues	81
2.8.1.1.1	Reagents	81
2.8.1.1.2	Method	81
2.8.1.2	Protein Isolation from TRizol reagent	81
2.8.1.2.1	Reagents	81
2.8.1.2.2	Method	82
2.8.1.3	Protein isolation from 3T3-L1 adipocyte media using TCA precipitation	82
2.8.1.3.1	Reagents	82
2.8.1.3.2	Method	83
2.8.2	Protein quantification by the BCA method	83
2.8.2.1	Reagents and equipment	83
2.8.2.2	Method	83
2.8.3	Sodium dodecyl sulphate Polyacrylamide Gel Electrophoresis (SDS PAGE)	84
2.8.3.1	Reagents	84
2.8.3.2	Equipment	86
2.8.3.3	Method	86
2.8.4	Electroblotting	87
2.8.4.1	Reagents and equipment	87
2.8.5	Immunological detection of proteins	88
2.8.5.1	Reagents and Equipment	88
2.8.5.2	Ponceau S staining	89
2.8.5.3	Detection method	89
2.8.5.4	Determination of optimal primary antibody dilution	90
2.8.6	Protein quantification from western blotting	91
2.9	Statistical analysis	91
CHAPTER 3	ZAG EXPRESSION IN RODENT ADIPOSE TISSUE AND GENETIC MODELS OF OBESITY	92

3.1	Introduction	93
3.2	Methods	95
3.2.1	Animals and tissues	95
3.2.2	RT-PCR and real-time PCR	96
3.2.3	Western blotting	97
3.2.4	Statistical analysis	97
3.3	Results	97
3.3.1	ZAG expression in adult rodent adipose tissue	97
3.3.1.1	ZAG expression in mouse adipose tissue	97
3.3.1.2	ZAG expression in mature adipocytes and the stromal vascular (SV) fraction of WAT depots	99
3.3.1.3	ZAG expression in rat adipose tissue	104
3.3.2	ZAG expression levels in rodent models of obesity	106
3.3.2.1	*ZAG* gene expression in WAT of lean and ob/ob mice	106
3.3.2.2	ZAG expression in WAT of lean and fa/fa Zucker rats	108
3.4	Discussion	108
CHAPTER 4	REGULATION OF ZAG EXPRESSION IN MOUSE ADIPOSE TISSUE: EFFECTS OF FASTING AND HIGH-FAT DIET	115
4.1	Introduction	116
4.2	Methods	118
4.2.1	Animals	118
4.2.2	RT-PCR and real-time PCR	118
4.2.3	Western blotting	119
4.2.4	Statistical analysis	119
4.3	Results	120
4.3.1	Effects of 16h-fasting on ZAG expression in mouse adipose tissue depots	120
4.3.2	Effects of high-fat diet on ZAG expression in mouse adipose tissue depots	128
4.4	Discussion	131
CHAPTER 5	ZAG EXPRESSION IN 3T3-L1 ADIPOCYTES: REGULATION BY HORMONES, INFLAMMATORY CYTOKINES AND PROSTAGLANDINS	135
5.1	Introduction	136
5.2	Methods	138
5.2.1	Cell culture	138
5.2.2	RT-PCR and real-time PCR	139
5.2.3	Statistical analysis	139
5.3	Results	140
5.3.1	*ZAG* gene expression in 3T3-L1 cells	140
5.3.2	Regulation of *ZAG* gene expression in 3T3-L1 adipocytes	140
5.3.2.1	Effects of sympathetic agonists on *ZAG* gene expression	143
5.3.2.2	Effects of peripheral hormones and rosiglitazone on *ZAG* gene expression	143
5.3.2.3	Effects of inflammatory regulators on *ZAG* gene expression	147
5.3.3	Regulation of *ZAG* gene expression by prostaglandins in 3T3-L1	

	adipocytes	147
5.3.3.1	Effects of PGD_2 and J_2-series prostaglandins on *ZAG* gene expression	147
5.3.3.2	Effects of PGE_2, PGF_{2a} and PGI_2 on *ZAG* gene expression	151
5.4	Discussion	157
CHAPTER 6	POSTNATAL DEVELOPMENT OF ZAG IN RODENT ADIPOSE TISSUE	163
6.1	Introduction	164
6.2	Methods	167
6.2.1	Animals	167
6.2.2	RT-PCR and real-time PCR	167
6.2.3	Western blotting	168
6.2.4	Statistical analysis	168
6.3	Results	169
6.3.1	ZAG expression in the early postnatal period	169
6.3.2	Total body weight and adipose tissue depots during early postnatal development	172
6.3.3	ZAG expression patterns in adipose tissue postnatally	172
6.3.4	Postnatal expression of ZAG in the liver of rat neonates	177
6.3.5	Expression patterns of several adipokines in adipose tissue postnatally	177
6.3.5.1	Gene expression pattern of leptin in rat adipose tissue during postnatal development	177
6.3.5.2	Gene expression pattern of adiponectin in rat adipose tissue during postnatal development	180
6.3.5.3	Gene expression pattern of NGF in rat adipose tissue during postnatal development	180
6.3.5.4	Gene expression pattern of MCP-1 in rat adipose tissue during postnatal development	180
6.3.5.5	Gene expression pattern of IL-6 in rat adipose tissue during postnatal development	184
6.3.6	Comparison of ZAG mRNA levels in different adipose depots at days 1, 21 and 32 postnatally	184
6.4	Discussion	190
CHAPTER 7	GENERAL DISCUSSION	196
7.1	Introduction	197
7.2	Previous work	197
7.3	Current study	198
7.4	ZAG expression in adipose tissue	200
7.5	Regulation of ZAG expression in adipose tissue	202
7.6	Future work	205
7.7	Concluding remarks	207
REFERENCES		208

List of figures

Figure 1.1 Stages of adipocyte differentiation 5

Figure 1.2 Pathogenesis of cancer cachexia 21

Figure 1.3 Proteins secreted from white adipose tissue 23

Figure 1.4 Prostaglandin synthetic pathway 39

Figure 2.1 The principle of Taqman assay 71

Figure 2.2 Default baseline plot-log and linear view 79

Figure 2.3 Schematic diagram of protein detection 85

Figure 2.4 Standard curve for protein concentration estimation 80

Figure 3.1 *ZAG* gene expression in adipose tissue depots of mice 98

Figure 3.2 Leptin gene expression adipose tissue depots of mice 100

Figure 3.3 ZAG protein expression in adipose tissue depots of mice 101

Figure 3.4 ZAG mRNA levels in mature adipocytes and stromal vascular fraction of white adipose tissue depots 102

Figure 3.5 ZAG protein expression in mature adipocytes and stromal vascular fraction of subcutaneous white adipose tissue in mice 103

Figure 3.6 Tissue distribution of *ZAG* gene and protein in rat 105

Figure 3.7 *ZAG* gene expression in white adipose tissue depots of lean and *ob/ob* mice 107

Figure 3.8 *ZAG* gene expression in white adipose tissue of lean and obese (*fa/fa)* Zucker rats 109

Figure 3.9 ZAG protein expression in retroperitoneal white adipose tissue of lean and *fa/fa* Zucker rats 110

Figure 4.1 Body weight and adipose tissue weight of mice fasted for 16 h 121

Figure 4.2 ZAG mRNA levels in adipose tissue depots of mice fasted for 16 h 122

Figure 4.3 ZAG protein expression in epididymal WAT of mice fasted for 16 h 123

Figure 4.4 ZAG protein expression in perirenal WAT of mice fasted for 16 h 124

Figure 4.5 ZAG mRNA levels in liver of mice fasted for 16 h 125

Figure 4.6 Leptin mRNA levels in adipose tissue depots of mice fasted for 16 h 126

Figure 4.7 Adiponectin mRNA levels in adipose tissue depots of mice fasted for 16h 127

Figure 4.8 Effects of high-fat diet on ZAG mRNA levels 129

Figure 4.9 Effects of high-fat diet on ZAG protein levels 130

Figure 5.1 Time course of ZAG gene expression in 3T3-L1 adipocytes 141

Figure 5.2 Time course of ZAG mRNA levels in 3T3-L1 adipocytes 142

Figure 5.3 Effect of noradrenaline, isoprenaline and BRL 37344 on ZAG mRNA levels in 3T3-L1 adipocytes 144

Figure 5.4 Effect of Insulin and Adiponectin on ZAG mRNA levels in 3T3-L1 adipocytes 145

Figure 5.5 Effect of rosiglitazone on ZAG mRNA levels in 3T3-L1 adipocytes 146

Figure 5.6 Effect of Leptin on ZAG mRNA levels in 3T3-L1 adipocytes 148

Figure 5.7 Effect of LPS, IL-6 and TNF-α on ZAG mRNA levels in 3T3-L1 adipocytes 149

Figure 5.8 Effect of PGD_2 and J_2- series prostaglandins on ZAG mRNA levels in 3T3-L1 adipocytes 150

Figure 5.9 Dose response of Δ^{12}-PGJ_2 on ZAG mRNA levels in 3T3-L1 adipocytes 152

Figure 5.10 Dose response of PGE_2 on ZAG mRNA levels in 3T3-L1 adipocytes 153

Figure 5.11 Dose response of PGE_2 on adiponectin and IL-6 mRNA levels in 3T3-L1 adipocytes 154

Figure 5.12 Dose response of $PGF_{2\alpha}$ on ZAG mRNA levels in 3T3-L1 adipocytes 155

Figure 5.13 Effect of PGI_2 on ZAG mRNA levels in 3T3-L1 adipocytes 156

Figure 6.1 ZAG is expressed in rat adipose tissue at day 1 postnatally and onwards 170

Figure 6.2 Gene expression of leptin and adiponectin in WAT depots and BAT of rat neonates 171

Figure 6.3 Developmental changes in body weight and weight of adipose tissue depots in rat neonates 173

Figure 6.4 Developmental changes in weight of WAT depots and BAT relative to body weight in rat neonates 174

Figure 6.5 *ZAG* gene expression in adipose tissue depots of neonatal rats 175

Figure 6.6 ZAG protein levels in adipose tissue depots of rat neonates 176

Figure 6.7 *ZAG* gene expression in the liver of rat neonates 178

Figure 6.8 Leptin gene expression in adipose tissue depots of neonatal rats 179

Figure 6.9 Adiponectin gene expression in adipose tissue depots of neonatal rats 181

Figure 6.10 *NGF* gene expression in adipose tissue depots of neonatal rats 182

Figure 6.11 *MCP-1* gene expression in adipose tissue depots of neonatal rats 183

Figure 6.12 *IL-6* gene expression in adipose tissue depots of neonatal rats 185

Figure 6.13 Depot differences in ZAG gene expression in adipose tissue of neonatal rats 186

Figure 6.14 Depot differences in leptin gene expression in adipose tissue of neonatal rats 187

Figure 6.15 Depot differences of adiponectin gene expression in adipose tissue of neonatal rats 189

List of tables

Table 2.1 Sequences of the primers and the PCR conditions 68

Table 2.2 Sequences of primers and Taqman probes of mouse target genes and working conditions for real-time PCR 74

Table 2.3 Sequences of primer and Taqman probe sequences of rat target genes and working conditions for real-time PCR 75

Abstract

Adipose tissue is now recognised as a significant endocrine organ which plays a key role in energy balance and metabolic regulation through the secretion of hormones and other protein factors, known as adipokines. The work in this thesis examined the regulation of zinc-α_2-glycoprotein (ZAG), a novel adipokine, expression in adipose tissue, using a combination of *in vivo* and cell culture (3T3-L1 adipocytes) approaches.

ZAG, both mRNA and protein, was detected in BAT and in all major white adipose tissue (WAT) depots; visceral fat, especially omental, was the main adipose tissue site of ZAG synthesis in adult mice. Following collagenase digestion, ZAG was equally detected both in mature adipocytes and the stromal vascular fraction of mouse subcutaneous, epididymal and perirenal WAT. Obesity was found to be associated with decreased ZAG expression in two rodent models of genetic obesity (the *ob/ob* mouse and the *fa/fa* rat). Fasting (16h) led to a decrease in ZAG mRNA levels in mouse epididymal WAT. ZAG was found to be differentially regulated in WAT depots of mice kept on a high-fat diet for 12 weeks; ZAG mRNA levels were increased in epididymal WAT, while decreased in the subcutaneous depot, and no changes were found in perirenal WAT. The findings suggest that ZAG expression in adipose tissue is subject to dietary regulation with a depot-specific pattern.

In vitro, rosiglitazone, a selective PPARγ agonist with anti-inflammatory properties, induced a dose-dependent increase in *ZAG* gene expression. Isoprenaline, a β-adrenoreceptor agonist and BRL37344, a selective β_3-adrenoreceptor agonist, were also both found to have a small inducing effect on *ZAG* gene expression; however there appears to be only a limited role for the sympathetic system in ZAG regulation. Adiponectin led to a 5-fold increase in *ZAG* gene expression. On the other hand, ZAG was downregulated by leptin, while inflammatory agents, such as LPS, TNFα and IL-6 had no effect on ZAG expression. The possible role of prostaglandins on *ZAG* gene expression was also investigated *in vitro*. While prostaglandin PGD_2 had no effect, the PGD_2 metabolites, PGJ_2, 9-deoxy-Δ^9,$\Delta^{12,13,14}$-dihydro-PGJ_2 (Δ^{12}-PGJ_2) and 15-deoxy-

$\Delta^{12,14}$-PGJ_2 (15d-PGJ_2), a PPARγ ligand and potent anti-inflammatory agent, induced major increases in *ZAG* gene expression; Δ^{12}-PGJ_2 induced a major, dose-dependent increase in ZAG expression. In marked contrast, the pro-inflammatory prostaglandins PGE_2, which is also known for its antilipolytic properties, and $PGF_{2\alpha}$ induced a substantial dose-dependent decrease in ZAG expression in the adipocytes.

Finally, the ontogenic pattern of ZAG expression in WAT and BAT during early postnatal development was examined in female Wistar rats aged 1 to 32 days. Before weaning at day 21, white fat was predominantly subcutaneous, the amount increasing rapidly after birth. The perirenal and gonadal fat depots were evident by around day 5 and were increased significantly at weaning. ZAG mRNA and protein were detected from day 1 in subcutaneous WAT, which appears to be a key source for its synthesis during the suckling period. The relative mRNA and protein levels were unchanged in WAT depots until day 21, when both were significantly reduced. ZAG was also detected in BAT at day 1, while the expression levels were reduced from day 3 onwards. The downregulation of ZAG expression in WAT depots at weaning and thereafter, when fat mass is expanded substantially, suggests that ZAG might be involved in the postnatal development of adipose tissue mass

In conclusion, these studies indicate that WAT and BAT synthesize ZAG, and provide evidence that the adipokine might be involved in the lipolytic process taking place within the tissue. The levels of ZAG are also influenced under various conditions where energy flux changes and by several agents, particularly rosiglitazone and prostaglandins. Finally, there is evidence that ZAG is involved in the inflammatory response of WAT, its role being most probably anti-inflammatory.

Chapter 1

Introduction

1.1 Adipose tissue anatomy

Mammals have two types of adipocytes, namely white and brown adipocytes, which have distinct anatomy and function. These are in turn organized into white and brown adipose tissue (WAT and BAT), both tissue types comprising the adipose organ (Cinti 2001).

Histologically, white and brown adipocytes are quite distinct. Although both types of adipocytes are spherical, brown adipocytes range in diameter from 10 to 25 μm, while white adipocytes can vary from 15 to 150 μm, due to their ability to accumulate different amounts of triglyceride that form a single vacuole in the jaloplasm. In brown adipocytes, which are multilocular in terms of lipid droplets, the nucleus is spherical and situated in the centre of the cell. The cytoplasm is rich in mitochondria, which account for the tissue's brown colour, with well-developed cristae and the lipids are organized in numerous vacuoles. In contrast, in white adipocytes, which are unilocular and also possess fewer and less-developed mitochondria, the nucleus is located peripherally (Cinti, 2001).

Apart from morphological changes, there are numerous quantitative differences between the two tissues. In contrast to WAT, BAT is characterized by high sympathetic innervation and respiratory activity, but has a lower lipid content (30-40%) compared to WAT (up to 90%). Furthermore, although most genes which are expressed in WAT are also expressed in BAT, the abundance and physiological regulation of gene products and their activity can vary considerably between the two tissues (Klaus, 2001). For example, the response of the two tissues to environmental or nutritional stress can be quite opposite, as is the regulation of the activity and gene expression of lipoprotein lipase (LPL) (Klaus, 2001).

1.1.1 Adipose tissue morphology

The two types of adipose tissue are organized in discrete depots throughout the body, which can broadly be categorized as subcutaneous and visceral. In rodents, the main visceral depots are perirenal, mesenteric, omental, retroperitoneal, and epididymal.

Adipocytes exhibiting the white phenotype can also be found in or around many other organs, including the skin, lymph nodes, bone marrow, pancreas, thymus and blood vessels (Cinti, 2001). Although specific depots are predominantly white or brown, some depots contain both types of adipocytes, the relative amount of each type depending on age, strain, as well as the nutritional and environmental conditions to which the animal is exposed (Cinti, 2001). This concominant existence of both cell types may reflect the ability of mature adipocytes to transdifferentiate between the two forms, the effect being possibly mediated by changes in β_3-adrenoreceptor expression level (Cinti, 2005).

However, only 50% of WAT is composed of mature adipocytes (Hausman, 1985), the rest of the tissue being the stromal vascular fraction, which consists of numerous cell types, including pre-adipocytes, fibroblasts, histiocytes, mast cells, and capillary endothelial cells (Cinti, 2001).

In rats, white adipocytes appear in the perinatal period and the biggest white depot in newborns is the subcutaneous depot, visceral fat mass substantially increasing after weaning (around day 20) in rodents (Cinti, 2001), as it will be discussed in more detail in Chapter 6. In contrast to most mammals, including rodents, where WAT is predominantly developed postnatally and is usually below 3% of body weight at birth, human newborns have large amounts of WAT mainly in the subcutaneous regions. There are currently three main explanations for this. The first is that fat compensates for the lack of insulating fur. It has also been suggested that large amounts of fat may represent the increased energy requirements by the brain or that fat is needed by the newborn as it is forced to mobilize fat at birth to compensate for the disruption in flow of maternal nutritional support at parturition before lactation is established (Klaus, 2001).

1.1.2 Adipocyte differentiation and development

When energy intake exceeds energy expenditure, WAT undergoes an increment. White adipocytes enlarge, thus becoming hypertrophic, and subsequently hyperplastic by developing more adipocytes from the precursor pool. It is believed that adipocytes can only enlarge up to a certain maximal size, which is genetically determined and specific for

each depot (Girolamo *et al.*, 1998), and that once adipocytes have reached that size, hyperplasia is triggered (Faust *et al.*, 1978; Bjorntorp, 1991). Contrary to other cell types, the ability to increase the quantity of fat cells is retained into adulthood (Gregoire, 2001). On the other hand, when energy expenditure is greater than energy intake, adipocytes release their triacyglycerols in the form of free fatty acids and glycerol. During extreme fasting conditions, they give up all stored lipid and can no longer be distinguished from preadipocytes, a condition known as hypotrophy (Schling & Löffler, 2002). There has been an ongoing debate on whether totally slimmed-down adipocytes undergo apoptosis or not, with the latest report indicating that this is not the case (Cinti, 2005).

Adipocyte differentiation (adipogenesis), the process during which functioning adipocytes develop from fibroblast-like cells called adipoblasts, is a multi-step, tightly controlled and irreversible process (Ailhaud, 2001). Once adipose tissue is formed, adipocytes represent between one-third and two-thirds of the total number of cells. As illustrated in Figure 1.1, there are many factors involved in each step of the adipogenic process, and every step following adipoblasts reaching confluence is characterized by the presence of specific markers. Adipogenesis is triggered by the production of two key transcription factors, CCAAT/ enhancer-binding protein α (CEBPα) and peroxisome proliferator-activated receptor γ (PPARγ), which are responsible for inducing the expression of adipocyte-specific genes (Warne, 2003). Creation of new adipocytes is always accompanied by development of blood vessels and average blood flow to WAT can vary from 3 to 30 $ml \cdot min^{-1} \cdot 100\ g\ tissue^{-1}$ (Schling & Löffler, 2002).

Numerous factors trigger adipocyte differentiation. Dexamethasone, a synthetic glucocorticoid increases the production of prostacyclin, a potent adipogenic factor, and glucocorticoids also repress at a transcriptional level the expression of preadipocyte factor-1 (pref-1), thus allowing the differentiation process to proceed. Insulin-like growth hormone 1 (IGF-1) has also been shown to stimulate adipogenesis together with insulin-like growth factor binding proteins (IGFBPs). Insulin, which is known for its role in

Figure 1.1 Stages of adipocyte differentiation

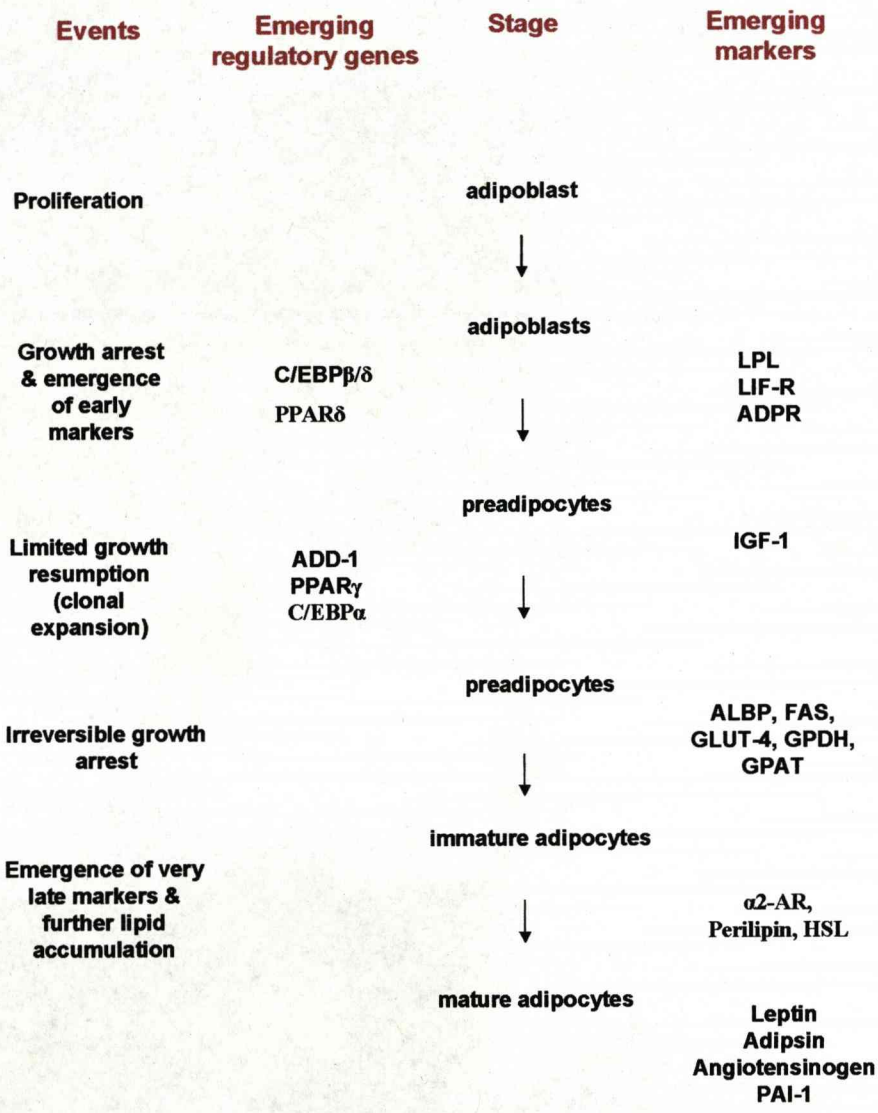

Schematic representation of multiple stages of adipocyte differentiation. This is based on data obtained from 3T3-L1 and 3T3-F442A adipocytes (adapted from Ailhaud, 2001).

lipogenesis, as discussed in the following section, also triggers adipogenesis. Furthermore, prostaglandin I_2 (PGI_2) rapidly upregulates the expression of early transcription factors, such as C/EBPβ and CEBPδ, through activation of its cell surface receptor (Ailhaud, 2001).

In contrast to the above, various factors have been identified which inhibit or abolish differentiation of adipose precursor cells, such as platelet-derived growth factor (PDGF), transforming growth factor-β (TGF-β), most possibly fibroblast growth factor (FGF) and epidermal growth factor (EGF), retinoids, fat-soluble vitamins and prostaglandin $F_{2\alpha}$ (PGF_{2a}) (Ailhaud, 2001).

1.1.3 Function of WAT

WAT plays several important roles in mammalian physiology, and is essential in the maintenance of energy homeostasis. The classical view of WAT is that it serves as an energy storage site that is mobilized during periods of food deprivation to release fatty acids for oxidation in other organs. WAT also provides thermal insulation, this trait being particularly evident in the case of the blubber of marine mammals such as seals and whales (Trayhurn & Beattie, 2001). Fat stores also serve as a source of water (metabolic water), which is important in the case of some desert and marine mammals (Klaus, 2001). However, this traditional view of WAT changed in 1994 with the discovery of leptin (Zhang *et al.*, 1994). Since then more than fifty WAT protein secreted factors have been identified, the number constantly increasing, which are involved in the regulation of energy balance and other physiological processes, thus making WAT a very important endocrine organ. The major products of adipose tissue and their functions will be discussed later in this chapter.

1.1.3.1 WAT metabolism: lipolysis and lipogenesis

The two major metabolic processes of adipose tissue are lipolysis and lipogenesis, fat accumulation being determined by the balance between them. In a restricted sense, lipogenesis, which takes place in the adipose tissue and the liver, is the *de novo* synthesis of fatty acids, but in a broader sense, it is the acylation of glycerol with free fatty acids to

form triacylglycerols (TAGs), which can then be either stored in the adipocyte or incorporated into more complex structures such as lipoproteins. LPL is a key enzyme for the regulation of lipogenesis. In adipose tissue, LPL is the rate-limiting enzyme for the import of triglyceride-derived fatty acids into the adipocytes for storage. LPL levels are higher in adipose tissue of women compared to men, but the fact that its activity is higher in the gluteo-femoral than the abdominal region, explains the difference in fat distribution observed between the sexes. Lipogenesis is directly promoted by insulin in part by increasing LPL activity in adipose tissue. Insulin which acts through binding to its receptor at the surface of the membrane also stimulates glucose transport into the adipocyte by increasing the number of GLUT4 transporters in the plasma membrane. Glucocorticoids, such as cortisol that act though a specific glucocorticoid receptor (GR), also stimulate LPL activity, as well, *in vitro* in the presence of insulin. Elevated cortisol levels can lead to increased accumulation of fat in visceral adipose tissue. However, this combined effect of insulin and cortisol on LPL activity can be totally inhibited by growth hormone (GH). Leptin, which will be discussed later, may also contribute to lipogenesis. Finally, lipogenesis is very responsive to changes in the diet. While high-fat diets decrease lipogenesis, carbohydrates increase lipogenesis in both adipose tissue and liver. LPL activity in obesity is increased. Apart from nutrition, exercise and aging also play a role in lipogenesis (Boschmann, 2001; Kersten, 2001).

Lipolysis is the process by which triglycerides are broken down into glycerol and non-esterified fatty acids (Tisdale, 2002). Lipolysis largely occurs in adipose tissue for the mobilization of fatty acids to serve as a fuel in the body, as well as a precursor for the synthesis of ketone bodies. TAG mobilization is mainly achieved by hormone-sensitive lipase (HSL), a key enzyme in the process, located inside the adipocyte. HSL hydrolyzes TAGs first into diacylglycerol, then monoacylglycerol and finally glycerol and the respective free fatty acids (FFA). FFAs are then transported through blood to the organs of respective destination, mainly liver and muscle. It is believed that the sympathetic nervous system (SNS) is the most important mechanism for controlling lipolysis in adipose tissue and that neuronal signals derived from it are mediated to the adipocyte and the surrounding blood vessels via specific receptors. Catecholamines, including both

epinephrine and norepinephrine act as physiological receptor-binding ligands and there are two types of catecholamine-binding adrenergic receptors, also called adrenoreceptors, the α- and β- adrenergic receptors. All their subtypes (α, α_2, β_1, β_2 and β_3) are expressed in white adipocytes. The β_3-adrenoreceptor shares 40-50% amino acid sequence homology with the β_1 and β_2 subtypes (Howe, 1993). All three mediate lipolysis in white adipose tissue in mice and rats (Arch *et al.*, 1984), and thermogenesis in BAT (Arch *et al.*, 1989). When an agonist binds to a β subtype, adenylyl cyclase is activated and cyclic AMP (cAMP) is synthesized. Its increase activates protein kinase A (PKA), which then phosphorylates, and thus activates HSL. Insulin inhibits lipolysis stimulated by β agonists, whereas GH significantly increases catecholamine-induced lipolysis. In humans, the β_2 adrenoreceptor subtype is considered to be the most important in lipolysis and a possible role of β_3 has been suggested. As in lipogenesis, factors such as nutrition, exercise and aging, also play a role in lipolysis (Boschmann, 2001).

1.1.4 BAT function

In contrast to WAT, which stores energy, BAT is used for the release of energy in the form of heat. BAT, which is probably unique to mammals (Klaus, 2001), is the first form of adipose tissue to appear during development and is characterised by the expression of uncoupling protein 1 (UCP-1), which is uniquely expressed in this tissue (Dulloo & Samec, 2000). This protein is located in the inner mitochondrial membrane and acts by uncoupling mitochondrial respiration (Rousser *et al.*, 2004). BAT has a specialised role in dissipating energy by thermogenesis. Thermogenesis in general can be categorised as either obligatory or regulatory (Pecqueur *et al.*, 2001), the latter being subdivided into heat generated by shivering of skeletal muscles in response to cold, non-shivering thermogenesis (NST), physical activity thermogenesis (exercise), non-exercise activity thermogenesis (NEAT) and diet- and drug- induced thermogenesis (DIT).

BAT is more highly vascularised than WAT, and is also more densely innervated by the SNS, with innervation of individual adipocytes (Cinti, 2005). Increased sympathetic activity in BAT is characterised by both hypertrophic and hyperplastic expansion,

increased blood flow and utilisation of lipid and carbohydrate substrates for oxidative metabolism (Collins *et al.*, 2001).

At birth, BAT is present in most mammals, including rodents. After birth, the surrounding temperature falls and fluids evaporate from the newborn's skin. This cold exposure evokes NST, which is crucial for the survival of the newborn. In rodents, it is necessary at birth, but also needed at a slightly later stage when pups emerge from the nest (Cannon *et al.*, 1988). BAT is also particularly important in animals with a special need to generate heat, such as cold-adapted rodents and hibernating mammals. It is also present in human newborns, where it has a clear role in generating heat. Although tiny amounts of BAT still exist, the tissue has at best a minor thermoregulatory role in adults (Rosen & Spiegelman, 2000). BAT thermogenesis can also be activated after excess dietary energy intake (Klaus, 2001).

The capacity of BAT for NST is determined by the degree of UCP-1 expression, the process being regulated mainly by the SNS basal tone that is modulated in response to cold, diet and photoperiod (Dulloo & Samec, 2000). In rodents, the SNS acts on BAT via β3-adrenoreceptor to induce UCP-1 gene expression (Bays, 2004). It is worth mentioning at this stage that two UCP-1 homologues, UCP-2 and UCP-3 have been identified, the second being primarily expressed in BAT and skeletal muscle. However, their participation in metabolic regulation is not fully understood (Dulloo & Samec, 2000).

1.1.5 Adipose tissue and adipocyte studies

There are two approaches for the study of adipose tissue, *in vitro* and *in vivo* studies. Three main *in vitro* systems are currently available for studying adipocytes. These are isolated mature adipocytes, primary culture and clonal cell lines. Mature adipocytes are harvested from freshly dissected adipose tissue following collagenase digestion. Although mature adipocytes are very fragile and have a very limited life span (usually a maximum of 24 h), they are arguably the most closely related culture system to *in vivo* adipocytes,

since they are a fully differentiated heterogeneous pool of adipocytes directly from the source of interest with the minimum of experimental intervention.

In primary cultures and clonal cell lines, preadipocytes are converted to mature adipocytes once confluent. This is achieved by the addition of three agents used to induce differentiation *in vitro*. These are insulin, dexamethasone and isobutylmethylxanthine (IBMX). While the addition of insulin mimics the effects of *in vivo* insulin and insulin-growth factor 1 (IGF-1), dexamethasone is representative of natural glucocorticoids. Finally, IBMX acts to increase intracellular cAMP levels (Rosen & Spiegelman, 2000).

Primary culture involves the isolation of fibroblastic pre-adipocytes from adipose tissue, usually following collagenase digestion, which are then induced to differentiate into adipocytes. Their life-span is longer than that of mature adipocytes and they can be maintained in culture for 2-4 weeks. An adequate starting amount of adipose tissue is required, as preadipocytes only make up a small proportion of total adipose tissue, and care is required to ensure that preadipocytes are separated from fibroblasts and other stromal vascular cells. However, preadipocytes have a low proliferative capacity. Nevertheless, they are a good tool for adipose tissue study, as they are similar to isolated mature adipocytes, and are sourced directly from adipose tissue.

Probably the most widely used tool for the study of adipose tissue is clonal cell lines, such as the Swiss mouse 3T3-L1 and 3T3-F442A cells, whose use is well established. In particular, the 3T3-L1 fibroblastic cell line provides a unique model for insulin-sensitive primary fat cells, as under defined conditions it can be converted to fully differentiated adipocytes, characterized by increased insulin receptor number and induction of adipogenic specific proteins (Grako *et al.*, 1994). Clonal cell lines have some key advantages compared to primary cells. Firstly, they are homogeneous and at the same stage of differentiation, thus allowing for a consistent response to a treatment. In addition, they are immortal as long as they are passaged and stored correctly. However, their main disadvantage is the fact that they are distant from their original source that has

resulted in gene translocations and that could possibly affect the expression of genes resulting in unexpected results.

Human multipotent adipose-derived stem cells (hMADs cells), which have recently been described (Rodriguez *et al.*, 2004), are the first example of a human preadipocyte clonal cell line. However, due to the lack of a human cell line until recently, the SGBS human preadipocyte cell strain has been increasingly used as a tool for the study of human adipocytes (Wabitsch *et al.*, 2001). SGBS cells are derived from the subcutaneous white adipose tissue of an infant with Simpson-Golabi-Behmel syndrome, a rare disorder characterized by tissue overgrowth. The cells are characterized by a high capacity for adipose differentiation over many generations, thus providing an almost unlimited source of identical human preadipocytes.

In contrast to *in vitro* studies, *in vivo* studies enable the full integrated physiological response to a stimulus, such as fasting or cold exposure, to be ascertained. Studies on the effects of certain compounds may also be studied *in vivo*, using a range of techniques for their administration to the animal. These include oral administration (in food/water or via gavage), internal administration (by cannulation), and injection (subcutaneously, intraperitoneally, intramuscularly, intracutaneously, and intravenously). A key advantage of an *in vivo* study compared to an *in vitro* one is that in the former the adipocytes can interact with neural and endocrine signals and with other cell types that might be present in adipose tissue through paracrine signals. *In vitro* studies on the other hand are better at identifying the specific cause leading to a certain effect, as any effect observed is likely to be the result of a specific and direct response to an applied stimulus.

1.2 Energy balance

Basic metabolic processes, physical activity, food consumption and, as previously discussed, thermogenesis, all use energy. In order to maintain a constant body weight, energy intake must equal energy expenditure. Failure to do so will induce an imbalance, which will either result in excess body fat accumulation, if there is a surplus of energy, or in wasting and cachexia, if there is an energy deficit. Both conditions are accompanied by

changes both in the morphology and regulation of adipose tissue, and very importantly constitute health threatening conditions. In the following sections, obesity and cachexia, with the main focus on cancer-induced cachexia, and the metabolic changes occurring in these two conditions, are discussed in detail.

1.2.1 Obesity

When energy intake exceeds energy expenditure, a state of positive energy is reached resulting in weight gain and subsequently obesity. Obesity is defined as a significant increase above ideal weight, and is a disease in which excess body fat has accumulated such that health may be adversely affected. Clinically, body fat is estimated by using a formula that combines weight and height. This is the body-mass index (BMI), which is the weight in kilograms divided by the square of the height in meters. Because of differences in body composition among individuals, BMI may not always correspond to the same degree of fatness, but it is the commonest way of calculating it. A person with a BMI between 25.0 and 29.9 is classified as overweight, whereas a person with a BMI above 30.0 is classified as obese. In extreme cases where BMI is over 40, a person is classified as morbidly obese (Kopelman, 2000).

1.2.1.1 Epidemiology of obesity

Obesity in modern societies has increased alarmingly, reaching pandemic proportions (WHO, 2000). Different surveys have shown a great increase in the prevalence of obesity over time. At the moment, around 65% of the United States adult population (Daniels, 2006) and a slightly lower percentage of the European population are either overweight or obese, with a higher percentage of women. In the UK the prevalence of obesity has tripled from around 7% to 25% of the adult population since 1980s (Rennie & Jebb, 2005). If the current trend continues, by 2030 half of the British population will be obese, these figures reflecting the fact that the prevalence of obesity in children is increasing rapidly (Deckelbaum & Williams, 2001).

This great recent increase in the percentage of the population being obese has concentrated research on the causes leading to obesity. The leading causes of obesity,

however, are complex as they involve the interaction of many factors. There are an estimated 300 genes which influence body weight and it is estimated that genetics account for about 30% to 40% of the differences in people's weight, and predisposition to excess weight gain (Jequier & Tappy, 1999; Barsh *et al.*, 2000; Damcott *et al.*, 2003), but that the environment determines phenotypic expression (Barsh *et al.*, 2000). Environmental conditions, such as food availability, cultural norms, and the level of physical activity account for about 70% of weight differences (Pi-Sunyer, 2002). It is suggested that evolution favours fat storage, as human bodies have not yet adapted to high-energy food abundance, but instead harbor fat as a safeguard against famine (Daniels, 2006).

1.2.1.2 Obesity as a medical problem

Obesity dramatically increases the risk of developing several other disorders including type 2 diabetes, cardiovascular diseases, dyslipidaemia, arthritis, gallstone formation (Mokdad *et al.*, 2001), and certain cancers, such as breast, colon, uterus, pancreas, and kidney cancer (Calle *et al.*, 2003). In terms of diabetes, during obesity fasting plasma insulin is elevated and there is an increased insulin response to a glucose load. Fat depots and their distribution influence glucose metabolism, increase lipolysis and thus the release of FFAs from abdominal adipocytes, which results in a greater uptake of insulin by the liver and finally in increased gluconeogenesis and dyslipidaemia. These then result in hyperinsulinaemia and decreased skeletal insulin sensitivity. The inability of β-cells to cope long term with this situation and produce more and more insulin, leads to the development of type 2 diabetes. It has been demonstrated that even a modest weight gain of 5 to 7 kg increases the risk of diabetes by 50%, while losing the same amount of weight reduces the risk by the same amount (Kokkoris & Pi-Sunyer, 2003).

Another major health problem is the effects of obesity on cardiovascular function. This is because in obesity there is an increase in both lean and fat mass and in surface area. This results in an increase of total body oxygen consumption and cardiac output. The total blood volume is also increased in proportion to body weight, which leads to an increase in stroke volume and cardiac output. So there is an increase in the blood volume

returning to the heart, which sometimes results in failure of the ventricles and atria to support and thus heart failure (Kopelman, 2000).

1.2.1.3 Obesity as an inflammatory state

Obesity is now considered as a state of chronic low-grade inflammation (Das, 2001; Festa *et al.*, 2001; Trayhurn & Wood, 2004). This notion is basically supported by the observation that obesity is characterized by increased circulating levels of several markers of inflammation, such as pro-inflammatory cytokines and acute-phase proteins (Hotamisligil *et al.*, 1993; Trayhurn & Wood, 2004). As will be discussed in later sections, adipose tissue is a source of some of these factors, contributing either directly to their elevated levels or indirectly via the stimulation of cytokine production elsewhere (Wood & Trayhurn, 2006). Furthermore, since obese subjects have been found to exhibit adipocyte infiltration in tissues such as skeletal muscle, it has recently been suggested that WAT may provide a source of inflammatory markers within other organs (Caspar-Bauguil *et al.*, 2005). It is proposed that this inflammatory state may lead to the development of insulin resistance, hyperlipidaemia and the metabolic syndrome (Festa *et al.*, 2001; Engstrom *et al.*, 2003; Trayhurn & Wood, 2004).

A possible explanation for this is that the inflammatory response is primarily local to adipose tissue as a response to hypoxia in areas of the fat depots as the tissue mass increases during the development of obesity. This is supported by evidence that a transcription factor induced by hypoxia, hypoxia-inducible factor-1 (HIF-1), regulates a number of genes, including angiogenic factors VEGF and PAI-1 (Trayhurn & Wood, 2004). Furthermore, a cross talk between macrophages and adipocytes may also contribute to this inflammatory status (Stout & Suttles, 2004). An infiltration of WAT by macrophages has been evidenced (Weisberg *et al.*, 2003), which is possibly regulated by the increased release of leptin, the chemokine monocyte chemoattractant protein 1 (MCP-1) and macrophage migration inhibitory factor (MIF) from adipocytes during obesity (Trayhurn & Wood, 2004; Skurk *et al.*, 2005). A major role for WAT in the development of inflammation-related complications of obesity, particularly insulin resistance and atherosclerosis is considered plausible (Wood & Trayhurn, 2006).

1.2.1.4 Study of obesity: Genetic models

Much of the current understanding of the mechanisms underlying energy regulation has come from studies on animal models of obesity, including genetically obese (due to specific mutations) and diet-induced obese models. The most extensively studied obese model is the *ob/ob* (obese) mouse (Zhang *et al.*, 1994). This model has an autosomal recessive mutation on chromosome 6 leading to a lack of biologically active leptin and subsequently preventing normal signaling of energy stores by the adipose tissue to the hypothalamus. This results in hyperphagia, decreased energy expenditure and subsequent accumulation of excess fat (Zhang *et al.*, 1994). *ob/ob* mice are also characterized by hyperinsulinaemia, insulin resistance and subsequent hyperglycaemia (Herberg & Coleman, 1977; Coleman, 1978). There are different variants of *ob/ob* mice with specific mutations in the leptin gene, which either prevent gene transcription entirely or most commonly introduce a premature stop codon that results in a truncated and inactive form of leptin (Zhang *et al.*, 1994).

The *db/db* (diabetic) mouse is another widely used model for obesity studies. *db/db* mice are insensitive to leptin due to a mutation in the long isoform of the leptin receptor (OB-Rb) (Chen *et al.*, 1996). As a result, leptin fails to exert its normal satiety and thermogenic effects. Thus *db/db* mice exhibit hyperphagia, obesity and hyperinsulinaemia, leading to insulin resistance followed by increasing hyperglycaemia, as insulin resistance advances, and finally to β-cell hyperplasia (Berglund *et al.*, 1978; Molina *et al.*, 1984). In contrast to the *ob/ob* mouse where fat mass is increased by both hypertrophic and hyperplastic mechanisms, in *db/db* mouse the fat mass is said to be only hypertrophic (Johnson & Hirsh, 1972). Furthermore, in these models brown adipocytes are unilocular and show moderate UCP-1 activity, supporting the fact that obesity due to a lack of leptin or a functional leptin receptor is accompanied by reduced BAT adrenergic stimulation (Cinti *et al.*, 1997; Cinti, 2005).

Other genetic models include the *fa/fa* (Zucker) rat, *fat/fat* (fat) mouse, A^y/A^y (agouti) mouse and the *tub/tub* (tubby) mouse. The *fa* gene lies on rat chromosome 5 and the *fa* phenotype is caused by a single mutation on the extracellular portion of the long form of

the leptin receptor, which leads to a 90% reduction in binding affinity for leptin and impairment of leptin's central effects on energy balance (Phillips *et al.*, 1996). Thus, similarly to *ob/ob* mice, fatty Zucker rats become obese through reduced stimulation of BAT thermogenesis, hyperphagia and hyperinsulinaemia (Phillips *et al.*, 1996). Furthermore, the *agouti* mutation results from gene rearrangements, which change the normally restricted expression of agouti in the skin. In the hypothalamus, agouti acts as an endogenous antagonist of the melanocortin-3 and -4 receptors (MC3-R and MC4-R), through which α-melanocyte-stimulating hormone (α-MSH), released by pro-opiomelanocortin (POMC) neurons in the ARC, acts to inhibit feeding. Loss of melanocortin-mediated inhibition of feeding is responsible for hyperphagia and development of obesity in the A^y mouse (Butler & Cone, 2001). The tubby mouse has an autosomal recessive mutation which leads to mature onset obesity, hearing loss and retinal degradation as a result of a splicing defect in the *tub* gene (Guan *et al.*, 1998). Finally, the *fat* gene is a missense mutation of the *Cpe* gene that encodes carboxypeptidase E, an enzyme involved in the processing of proinsulin to insulin in the β cell, and of POMC and other neuroendocrine prohormones in the hypothalamus and pituitary (Leiter & Herberg, 1997). The loss of *Cpe* activity leads to defects in the processing of pro-hormone forms of neuropeptides associated with the control of satiety, thus leading to hyperphagia and a diabetic and obese phenotype (Utsunomiya *et al.*, 1998).

Further understanding of the development of obesity has been acquired from studies on transgenic knockout mice. For example, the MC4R knockout mouse which is obese, hyperleptinaemic and hyperisulinaemic confirmed that the obese phenotype in the agouti mouse is caused by inhibition of the MC4R signaling by agouti (Butler & Cone, 2003). Similarly, POMC knockout mice exhibit obesity and hyperphagia, while MC3R knockout mice exhibit obesity but not hyperphagia, as well as hyperleptinaemia and hyperinsulinaemia, although they do not develop diabetes (Butler & Cone, 2003). Interestingly, selective knockout of insulin receptors in white fat does not greatly disturb glucose metabolism, but decreases adipose tissue mass, reflecting the normally high sensitivity of adipose tissue to the antilipolytic effects of insulin (Abel *et al.*, 2001). Furthermore, a transgenic mouse with ablated WAT throughout development

emphasized the beneficial effects of adipose tissue on growth, glucose metabolism and survival in fasting (Moitra *et al.*, 1998). Finally, ablation of BAT in mice led to decreased thermogenesis, early onset of obesity without hyperphagia, and obesity with impaired glucose tolerance, confirming that increased metabolic efficiency and less wastage of energy through thermogenesis predispose to impaired glucose homeostasis (Hamann *et al.*, 1996).

1.2.2 Cancer cachexia

Numerous chronic diseases are associated with cachexia, including cancer, AIDS, rheumatoid arthritis, tuberculosis, cystic fibrosis and congestive heart failure (Tisdale, 2002). Cancer cachexia is a complex disorder characterized by progressive weight loss associated with anorexia, asthenia, anaemia, alterations in immune function, and disproportionate muscle wasting. This condition, most commonly seen in patients with gastrointestinal, lung and prostate cancer, occurs in up to 80% of subjects with advanced forms of cancers and accounts for about 20% of deaths, when subjects have lost around 30% of their pre-morbid weight (Warren, 1932; Fearon, 1992; Tisdale, 2002). The survival of cancer patients is directly related to both the total weight loss and the rate of weight loss. Furthermore, it has been estimated that cancer patients who have experienced weight loss respond almost 2.5 times less frequently to chemotherapy than patients who have not (Slaviero *et al.*, 2003).

1.2.2.1 Pathogenesis of cancer cachexia

In contrast to starvation, where weight is primarily lost from adipose tissue, in cachexia, weight loss is observed both in the fat and skeletal muscle compartments. In cachexia, loss of skeletal muscle arises from a fall in protein synthesis and an increase in protein degradation, which then results in weakness, leading to immobility and death, usually because of loss of respiratory muscle function (Tisdale, 2002). Cachexia has often been attributed to anorexia, the loss of appetite and early satiety, as it is present in up to one-half of newly diagnosed cancer patients (Grosvenor *et al.*, 1989). However, anorexia alone is unable to explain all the metabolic processes that occur during cachexia, as it has

been clearly demonstrated by the differences in the metabolic changes taking place between subjects with cachexia and those suffering from starvation. In addition to the depletion of skeletal muscle mass in patients with cachexia, which only occurs at the late stages of starvation conditions, subjects with cachexia show an increase in liver mass due to metabolic recycling activity, while a decrease is observed in starved subjects (Wigmore *et al.*, 1997). Furthermore, although in starvation the weight loss observed is easily reversed by feeding, in patients with cachexia the degree of food intake does not correspond to the extent of malnutrition and attempts to increase body weight fail to reverse the weight loss (Evans *et al.*, 1985). Several appetite stimulants, such as corticosteroids, have been used without success. At present, progestogens are used for the treatment of cachectic patients. These include megestrol acetate and medroxyprogesterone acetate, but although patients seem to gain some weight, there is no change in their body fat-free mass (Tisdale, 2002).

Weight loss can in principle result from decreased energy intake and/or increased energy expenditure. Resting energy expenditure (REE) is the main determinant of energy expenditure. Although REE accounts for 70% of total energy expenditure in normal subjects, it varies considerably among different groups of cancer patients. REE has, for example, been found to be elevated in patients with pancreatic and lung cancer but unaltered in patients with colorectal cancer (Fredrix *et al.*, 1991). This observed increase could be related to the upregulation of UCPs. Although, as previously mentioned, BAT is uncommon in adults where it is present in around 13% of the population tested, it is present in around 80% of patients with cachexia (Shellock *et al.*, 1986). In addition to that, UCP-2 and -3, which are found in skeletal muscle, may also play a significant role in energy balance and lipid metabolism as they are upregulated in rodent models of cachexia, although their exact role and degree of involvement are still unclear, as different studies have presented contradictory results, one even suggesting that anorexia was driving their production (Sanchis *et al.*, 1998; Bing *et al.*, 2000; Busquets *et al.*, 2005).

1.2.2.2 Pathogenesis of cancer cachexia in adipose tissue

In WAT, cachexia results in increased rates of lipolysis, decreased lipogenesis, hyperlipidaemia, raised circulating levels of free fatty acids and glycerol, and finally the loss of up to 85% of adipose tissue mass (Fearon & Preston, 1990). It has been observed in some clinical studies (Costa *et al.*, 1981) that increased fatty acid utilization precedes weight loss, thus suggesting the production of lipid-mobilizing factors either by the tumour or by host tissues. This increased fatty acid mobilization from host adipose tissue may also be an important factor contributing to the tumour growth (Wicha *et al.*, 1979; Hussey & Tisdale, 1994) There are putative factors through which these changes may be mediated, such as pro-inflammatory cytokines and tumour-derived protein factors (Gordon *et al.*, 2005).

1.2.2.3 Mediators of cancer cachexia

The general metabolic abnormalities seen in cancer cachexia are driven by the production of a number of factors, which include cytokines and other cachectic agents, by both the host and tumour. As seen in Figure 1.2, the presence of a tumour results in a persistent host inflammatory response, characterized by the production of T helper 1 (Th1) cytokines, such as tumour necrosis factor α (TNFα), interleukin-1β (IL-1β), interleukin-6 (IL-6) and interferon-γ (IFNγ). On the other hand, tumours also produce specific cachectic factors such as proteolysis inducing factor (PIF) and lipid mobilizing factor (LMF), which promote protein and fat breakdown respectively.

Products of the tumour and/or host cell have been associated with appetite suppression. IL-1 has been shown to be involved in the induction of anorexia, by blocking neuropeptide Y (NPY)-induced feeding, which is a feeding-stimulating peptide (Chance *et al.*, 1994; Plata-Salaman, 2000). TNFα has been associated with cachexia since it promotes lipolysis and inhibits lipogenesis, mainly through suppression of LPL and the induction of proteolysis through the ubiquitin-proteasome proteolytic pathway (Tracey *et al.*, 1990). It has been proposed that an elevation in plasma levels of TNFα is responsible for the metabolic alterations in adipose tissue seen with cancer cachexia (Argilés, 1997). Elevated circulating concentrations of IL-6 have also been shown to be associated with

weight loss in some patients with lymphoma, lung cancer and colorectal cancer (Rubin, 2003). Leukaemia-inhibitory factor (LIF), IL-1 and ciliary neurotrophic factor (CNTF) have also been suggested as mediators of cachexia (Argilés, 2003).

LMF acts specifically on adipose tissue through the cyclic-AMP-mediated pathway and PIF, which is a sulphated glycoprotein that induces protein degradation in skeletal muscle, by upregulating the ubiquitin-proteasome proteolytic pathway. Although there is a strong correlation between these factors and cachexia, there is no effect on appetite (Tisdale, 2002). LMF, which appears to act through the β_3-adrenoreceptor, is able to induce lipolysis in adipose tissue. It was first purified from the cachexia-inducing mouse colon adenocarcinoma, MAC16. It has also been found in the urine of cancer patients, suggesting that it can induce lipid mobilization in these subjects. LMF is homologous to the plasma protein Zinc-α_2-glycoprotein (ZAG) (Todorov *et al.*, 1998), which is the main focus of this study and is going to be discussed in the following sections.

PIF has been shown to be present in patients with weight losses greater than 10%, which were not attributed to cytokines. PIF has been found to be present at its maximum in the serum of mice bearing the MAC16 tumour, with a weight loss between 11% and 20%. PIF has also been found in the urine of patients with different types of carcinoma. These patients, in whose urine PIF was present, experienced great weight losses, especially of lean body mass, and the action of PIF is mainly mediated on skeletal muscle. Additionally, PIF may also be involved in cancer cachexia by contributing to a continuous cycle of cytokine and acute phase protein production. Finally, the high degree of structural conservation between murine and human PIF suggests that cachexia in mice and humans is produced by the same tumour product (Tisdale, 2002).

Figure 1.2 Pathogenesis of cancer cachexia

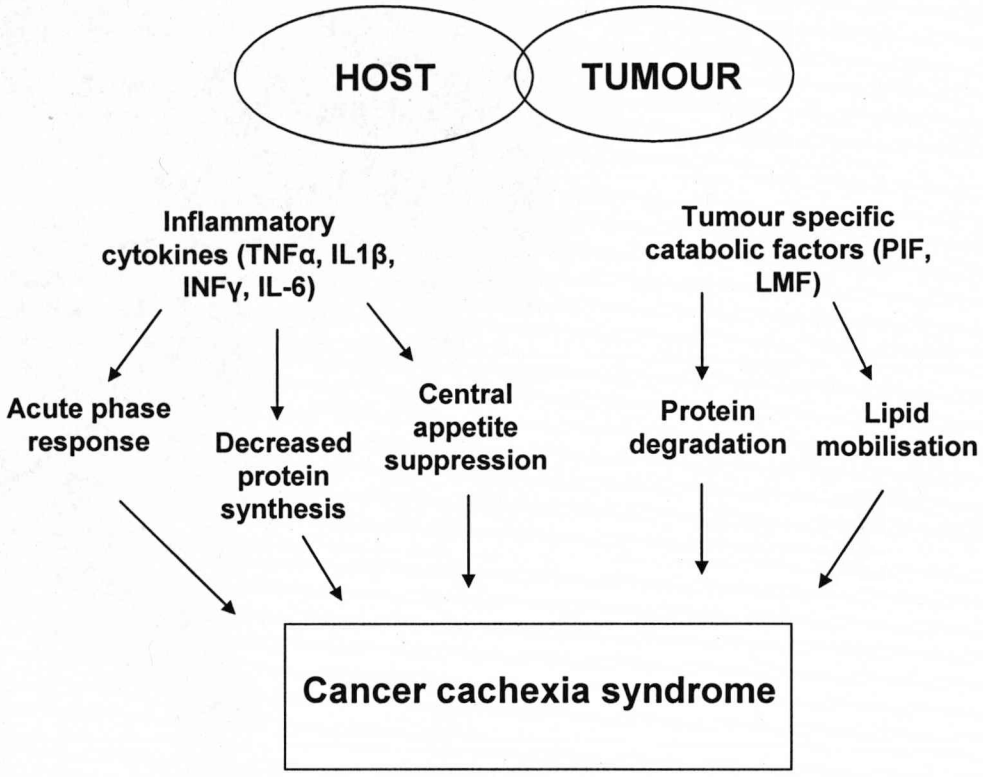

(Source: Gordon *et al.*, 2005)

Schematic representation of the mediators involved in the development of the cancer cachexia syndrome.

1.3 Endocrine function of adipose tissue

The traditional view of adipose tissue as an energy storage organ has dramatically changed during the last few years, with the identification of various factors, termed adipokines, which are secreted from the tissue and have been shown to be involved in a wide range of physiological and metabolic processes. For a factor to be classified as an adipokine, its secretion from adipocytes has to be demonstrated. This is usually demonstrated *in vitro*, using either freshly isolated adipocytes, or adipocytes derived by differentiation from fibroblastic pre-adipocytes. When a factor is found to be expressed in adipose tissue, it is essential to determine whether it is expressed within mature adipocytes, or whether it is only found in the other cell types that constitute the tissue, such as fibroblasts, macrophages and endothelial cells. At present, more than fifty adipokines have been identified, which according to their known physiological functions can be categorized as presented in Figure 1.3 (Trayhurn & Beattie, 2001; Trayhurn & Wood, 2004). Lipoprotein lipase was in effect the first adipokine to be identified, however a major finding, which subsequently led to the focus on adipose tissue, was the discovery of leptin (Zhang *et al.*, 1994). The wide range and diversity of the factors secreted from WAT have made it evident that WAT is a major secretory and endocrine organ, which plays a key role in many metabolic and physiological processes in mammals. In the following sections, the major adipokines and their functions are discussed in more detail.

1.3.1 Free fatty acids and steroid secretions of WAT

Before discussing the adipose tissue secreted protein factors, it is appropriate to mention that quantitatively fatty acids are the major secretory product of WAT, reflecting the fuel storage role of the tissue. Fatty acids are the product of TAG lipolysis mediated by HSL. FFAs released from adipose tissue are a major source of plasma FFAs, and both adipose tissue and plasma FFAs are elevated in obesity (Lewis *et al.*, 2002). Furthermore, the largest percentage of circulating FFAs is derived from subcutaneous adipose tissue; thus FFA lipolysis is unlikely to be the link between visceral adiposity and metabolic syndrome disorders (Nielsen *et al.*, 2004). In addition, WAT stores cholesterol and is involved in the metabolism of steroid hormones. Although the tissue does not synthesize steroid

Figure 1.3 Proteins secreted from white adipose tissue

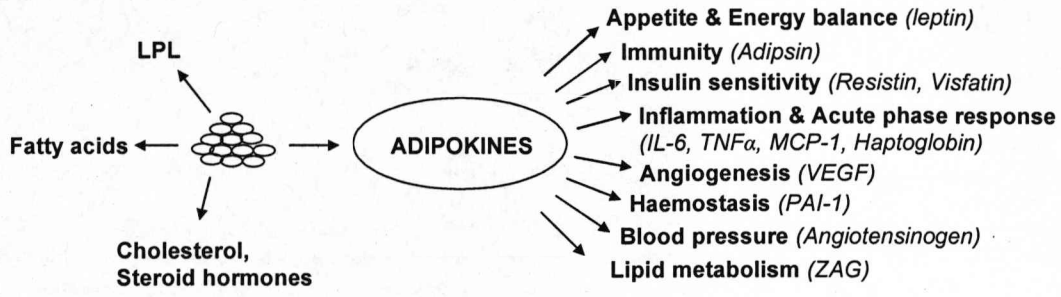

A schematic presentation of white adipose tissue and its products. Not all secreted proteins are listed. IL-6, interleukin-6; TNFα, tumour-necrosis factor α; MCP-1, monocyte chemattractant protein 1; PAI-1, plasminogen activator inhibitor-1; VEGF, vascular endothelial factor.

hormones *de novo*, it expresses the enzymes involved in the conversion of glucocorticoids and sex hormones, such as 17βHSD which is responsible for the conversion of oestrone to oestradiol and androstenedione to testosterone, these being additional secretory WAT products (Mohamed-Ali *et al.*, 1998; Trayhurn & Beattie, 2001).

1.3.2 Leptin

Leptin was originally identified in 1994 as a satiety factor secreted by adipose tissue and the *obese* (*ob*) gene which encodes the protein was first identified in genetically obese (*ob/ob*) mice using positional cloning (Zhang *et al.*, 1994). The leptin gene (Lep (*ob*)) encodes an 18-kDa protein containing a signal sequence which is cleaved to produce the mature 16-kDa hormone (Zhang *et al.*, 1994). Sequence analysis has shown that the rat *ob* gene has 96% homology with the mouse one, while the nucleotide and protein are 84% and 82% homologous to the human *ob* gene, respectively (Clement *et al.*, 1996).

Although it was initially suggested that leptin was only synthesized in WAT, it has since been detected in several additional sites, including BAT, the stomach, placenta, mammary gland, ovarian follicles, the heart and bone and possibly the brain (Trayhurn *et al.*, 1999; Trayhurn *et al.*, 2001). Nevertheless, WAT remains the major site of leptin synthesis and the major contributor to leptin circulating levels (Considine *et al.*, 1996).

1.3.2.1 Regulation of leptin expression and production

The levels of leptin mRNA in WAT and the circulating levels of leptin are closely associated with the amount of fat mass, both in rodents (Frederich *et al.*, 1995) and in humans (Considine *et al.*, 1996), its levels increasing with fatness. Furthermore, serum leptin levels are significantly higher in females compared to males (Havel *et al.*, 1996) and exhibit a significant 24h pattern with a nocturnal maximum (Heptulla *et al.*, 2001).

Leptin is expressed in all WAT depots; however there are substantial differences in the levels of leptin mRNA between sites. Differences are also observed depending on the developmental stage and on species. It has been reported that although in mature rodents leptin mRNA levels are higher in the epididymal and perirenal depots compared to

subcutaneous, where leptin mRNA levels are lowest (Trayhurn *et al.*, 1995), in humans, the subcutaneous depots exhibits higher levels of leptin mRNA compared to the omental site (Hube *et al.*, 1996; Montague *et al.*, 1997). Furthermore, and as will be discussed in greater detail in Chapter 6, studies in rodents indicate that there are major developmental changes in the expression of leptin in WAT (Rayner *et al.*, 1997).

Both *in vitro* and *in vivo* studies have demonstrated that a number of factors substantially influence leptin synthesis in WAT. Leptin expression is regulated by nutritional status. Fasting induces a rapid reduction both in *ob* gene expression in WAT and in the levels of circulating leptin, which are however reversed upon refeeding (Trayhurn *et al.*, 1995; Hardie *et al.*, 1996). Similar to fasting, acute cold exposure leads to a rapid reduction in *ob* mRNA levels, which is subsequently reversed by rewarming (Trayhurn *et al.*, 1995; Hardie *et al.*, 1996).

Furthermore, leptin expression in WAT is regulated by a number of hormones. Catecholamines, both noradrenaline and adrenaline, have a major suppressive effect on leptin production (Trayhurn *et al.*, 1995), which is primarily mediated through the β_3-adrenoreceptor (Giacobino *et al.*, 1996; Trayhurn *et al.*, 1996), since selective β_3-agonists strongly suppress *ob* gene expression and reduce leptin circulating levels (Mantzoros *et al.*, 1996; Trayhurn *et al.*, 1996). It has also been demonstrated that thiazolidinediones (TZDs) repress both *ob* gene expression and circulating leptin levels through the activation of peroxisome proliferator activator γ (PPARγ) (Mantzoros *et al.*, 1996; Trayhurn *et al.*, 1996). On the other hand insulin (Havel, 2001), glucocorticoids and oestrogens (Castracane *et al.*, 1998) stimulate leptin production, with the opposite effect occurring with the administration of testosterone (Blum *et al.*, 1997). Finally, leptin levels increase in response to inflammatory cytokines, such as TNFα, sepsis, and acute infection (Sarraf *et al.*, 1997; Faggioni *et al.*, 1998; Gualillo *et al.*, 2000). It has been proposed that the sympathetic nervous system is the main physiological regulator of leptin production and that it provides a negative feedback loop to adipose tissue in the production of the hormone (Trayhurn *et al.*, 1998).

1.3.2.2 Functions of leptin

Apart from its neuroendocrine effects on food intake and energy expenditure, a number of other functions have been attributed to leptin, including its action in the reproductive system, in angiogenesis and in the immune system. As will be discussed in the next section, leptin interacts with several central neuroendocrine systems leading to the inhibition of food intake (Campfield *et al.*, 1995; Halaas *et al.*, 1995). Overall, leptin is involved in a wide and diverse spectrum of physiological and metabolic processes (Trayhurn & Beattie, 2001).

1.3.2.3 Leptin receptor

The leptin receptor (OB-R) is a member of the class I cytokine family (Tartaglia *et al.*, 1995). As a result of alternative splicing, in mice OB-R can exist as six isoforms: an OB-R long form (OB-Rb), four short forms (OB-Ra, -Rc, -Rd, and –Rf), and a soluble isoform (OB-Re) (Lee *et al.*, 1996). Furthermore, there are four known isoforms of the human leptin receptor (OB-R5, -15, -67, and -274) (Barr *et al.*, 1999). All isoforms have identical extracellular ligand binding domains; they differ, however, at the intracellular carboxy terminus (Koerner *et al.*, 2005).

Ob-Rb is the longer form and is essential for leptin's weight reducing effects. Ob-Rb is highly expressed in hypothalamic neurons, as well as in T cells and vascular endothelial cells. In the central nervous system, Ob-Rb is mainly expressed in the hypothalamic arcuate nucleus (ARC), dorsomedial nucleus (DMH), paraventricular nucleus (PVN), ventromedial nucleus (VMH) and the lateral hypothalamic area (LHA) (Ahima *et al.*, 2000; Elmquist, 2001). These nuclei express neuropeptides and neurotransmitters that regulate food intake and body weight. Key examples are the orexigenic neuropeptide Y (NPY), which responds through its receptors to absent or low levels of leptin and the melanocyte-stimulating hormone (MSH), which acts through its melanocortin-4 receptor in response to an increased plasma leptin concentration. NPY mRNA levels are increased in *ob/ob* mice and decreased after leptin treatment (Friedman & Halaas, 1998). The leptin receptor activates the janus-kinase/ signal transducer and activator of transcription-3 (STAT-3) pathway. Leptin administration induces STAT-3 translocation,

phosphorylation of phosphoinositide 3-kinase (PI (3) K) and the expression of several leptin-responsive genes (Niswender *et al.*, 2001; Zigman & Elmquist, 2003).

1.3.3 Insulin sensitivity and insulin resistance

1.3.3.1 Adiponectin

Adiponectin, which is also known as ACRP30, apM1, adipoQ and GPB28, is a 247 amino acid hormone produced exclusively by adipocytes (Ouchi *et al.*, 1999). It was initially identified from a cDNA, adipose most-abundant gene transcript 1, reflecting a gene that is specifically expressed in adipose tissue (Maeda *et al.*, 1997). Adiponectin is a 30-kDa polypeptide that belongs to the collagen superfamily sharing strong sequence homologies with type VIII and X collagens, complement factor C1q and TNFα (Scherer *et al.*, 1995; Maeda *et al.*, 1996; Chandran *et al.*, 2003).

1.3.3.1.1 Expression, regulation and function of adiponectin

As aforementioned, adiponectin is exclusively expressed in adipocytes, with increasing expression and secretion in adipocytes after the induction of differentiation (Ouchi *et al.*, 1999). In humans, adiponectin expression is higher in subcutaneous compared to visceral adipose tissue (Fain *et al.*, 2004). In human blood, adiponectin occurs in high concentrations of about 10 μg/ml, accounting for 0.01% of total serum protein (Böttner *et al.*, 2004). Females have significantly higher levels of plasma adiponectin than males, this sexual dimorphism developing during pubertal development in relation to serum androgens (Böttner *et al.*, 2004). In contrast to most adipokines, its expression in WAT and circulating levels are decreased in obesity (Arita *et al.*, 1999), in conditions of insulin resistance and diabetes (Hotta *et al.*, 2000) and in cardiovascular disease with increasing severity (Matsuzawa *et al.*, 2004). In these conditions, the reduction of adiponectin levels precedes the development of the disorders (Yamamoto *et al.*, 2004), and low adiponectin levels have been demonstrated to predict the development of type 2 diabetes (Spranger *et al.*, 2003). On the other hand, adiponectin levels increase when insulin sensitivity improves, such as after weight reduction, or treatment with insulin-sensitising drugs (Yang *et al.*, 2001; Matsazawa *et al.*, 2004). It has thus been suggested that adiponectin

has a role in the development of the metabolic syndrome (Diez *et al.*, 2003; Matsazawa *et al.*, 2004)

Furthermore, adiponectin exhibits anti-inflammatory and anti-atherogenic properties, including the inhibition of NFκB activation and the modulation of endothelial adhesion molecules in response to inflammatory stimuli (Ouchi *et al.*, 2000; Diez & Iglesias, 2003; Matsazawa, 2005). It has also been proposed that the protein is involved in the link between atherosclerosis and obesity (Ouchi *et al.*, 1999). Adiponectin may play a role in modulating insulin action and it is thought to mediate the insulin sensitizing effects of TZDs (Stefan & Stumvoll, 2002).

Finally, overexpression of adiponectin in 3T3-L1 adipocytes was reported to result in more rapid cell proliferation and differentiation to adipocytes alongside increased expression of adipogenic genes, increased lipid content, and improved insulin responsiveness for glucose transport (Fu *et al.*, 2005).

1.3.3.1.2 Adiponectin receptors

The effects of adiponectin are mediated through two recently identified receptors, AdipoR1 and AdipoR2, which are predominantly expressed on muscle and liver cells respectively, although they are widely expressed in the body (Yamauchi *et al.*, 2003). Adiponectin binds to both receptors and mediates the activation of AMP kinase, PPARα activation, and consequently glucose uptake and fatty acid oxidation, which is most probably the main molecular mechanism accounting for the increase in insulin sensitivity mediated by adiponectin (Gil-Campos *et al.*, 2004).

The expression levels of adiponectin receptors are decreased in obesity (Kadowaki & Yamauchi, 2005), but are increased during fasting and decreased in re-fed mice (Tsuchida *et al.*, 2004). In particular, AdipoR1 expression seems to be associated with insulin sensitivity and insulin secretion in mice (Staiger *et al.*, 2004) and humans (Civitarese *et al.*, 2004), as diabetes and insulin treatment decrease AdipoR1 expression, while AdipoR2 remains constant (Inukai *et al.*, 2005).

1.3.3.2 Resistin

Resistin (also referred to as FIZZ3 and ADSF) is a ~12kDa protein that is secreted exclusively by mature adipocytes in the mouse, and is a marker for adipocyte differentiation (Kim *et al.*, 2001). However it is expressed primarily in macrophages and monocytes in humans (Steppan & Lazar, 2004). Resistin was initially reported to be elevated in obese rodents and to promote insulin resistance. In murine studies resistin administration was shown to induce insulin resistance, while it was demonstrated that anti-resistin strategies improved insulin sensitivity (Steppan *et al.*, 2001). It was thus suggested that resistin functions as a link between obesity and insulin resistance. However, subsequent studies in rodents revealed contradictory results and thus a physiological role for the protein has failed to be established (Way *et al.*, 2001). The role of resistin in humans is also not clear (Smith, 2002), as human serum resistin levels are associated with adiposity and insulin resistance in many, but not all, studies (Janke *et al.*, 2002; Steppan & Lazar, 2004), and it was even shown in a recent report that resistin levels are actually decreased in *db/db* mice compared to lean controls, the levels being increased by the administration of metformin, an anti-diabetic agent with insulin sensitizing effects (Fujita *et al.*, 2002). Due to the differences observed between resistin in human and rodents, it has been suggested that the adipokine may exert diverse effects and that further studies are required in order to understand its role (Steppan & Lazar, 2004).

1.3.3.3 Visfatin

Visfatin (pre-B cell colony-enhancing factor) is a 52 kDa secreted protein and is one of the most recently identified adipokines (Hug & Lodish, 2005). In adipose tissue, visfatin is specifically expressed in the visceral depot of both humans and mice, and visfatin serum levels are positively correlated with visceral adiposity. It was also demonstrated that visfatin has a high affinity for the insulin receptor, and thus a linkage between the functions of the two proteins has been suggested (Fukuhara *et al.*, 2005; Bae *et al.*, 2006; Krzyzanowska *et al.*, 2006). Unlike insulin however, visfatin levels appear to be unaffected by fasting or feeding (Fukuhara *et al.*, 2005). *In vitro*, dexamethasone was

shown to increase visfatin expression, while growth hormone, TNFα and isoproterenol decreased its levels in 3T3-L1 adipocytes (Kralisch *et al.*, 2005).

1.3.4 Cytokines

Adipose tissue is the source of several inflammatory cytokines, which are key regulators of the inflammatory response (Trayhurn & Beattie 2001).

1.3.4.1 Tumour necrosis factor α (TNFα)

TNFα was firstly identified in adipose tissue of rodents in 1993, where it was shown to be markedly induced in obese animal models (Hotamisligil *et al.*, 1993). TNFα is a 26-kDa protein that is subsequently cleaved into a 17-kDa biologically active protein that exerts its effects via type I and II TNFα receptors (Fain *et al.*, 2004). TNFα is expressed both in mature adipocytes and the stromovascular cells of WAT, its levels being higher in human subcutaneous than visceral adipose tissue (Fain *et al.*, 2004). Similarly, TNFα is expressed in preadipocytes; however, its levels increase with the degree of differentiation (Hube & Hauner, 1999). Both types of TNFα receptor are also expressed within adipocytes (Ruan & Lodish, 2003).

Although TNFα was originally thought to be involved in cachexia, it has now been implicated in the pathogenesis of obesity and insulin resistance, its expression both in human and rodent adipose tissue being positively correlated with adiposity and insulin resistance (Hotamishigil *et al.*, 1993; Ruan & Lodish, 2003). In adipose tissue, TNFα suppresses genes involved in the uptake and storage of nonesterified fatty acids (NEFAs) and glucose, as well as genes for transcription factors involved in adipogenesis and lipogenesis. Furthermore, it affects the expression of several adipocyte-secreted factors, including IL-6, MCP-1 and nerve growth factor (NGF), whose levels are substantially increased with the administration of TNFα *in vitro* (Ruan *et al.*, 2002; Wang & Trayhurn, 2006). Multiple effects have also been described in terms in relation to insulin action, such as the inhibition of the insulin receptor signaling pathway (Coppack, 2001). TNFα is an important mediator of inflammation and can induce several other inflammatory cytokines (Ruan & Lodish, 2003; Wang & Trayhurn, 2006).

1.3.4.2 Interleukins

Both IL-6 and its receptor, IL-6R, are expressed by adipocytes and by the adipose tissue, IL-6 expression and secretion being 2 to 3 times greater in visceral, mainly omental, relative to subcutaneous adipose tissue (Fain *et al.*, 2004). IL-6 circulates at high levels in the bloodstream (Mohamed-Ali *et al.*, 1997), and it has been estimated that about one third of circulating IL-6 originates from adipose tissue (Fernandez-Réal & Ricart, 2003). IL-6 circulates in multiple glycosylated forms ranging from 22 to 27-kDa in size, while its receptor, which is homologous to the leptin receptor, exists in two forms, an 80-kDa membrane-bound form and a 50-kDa soluble form (Fain *et al.*, 2004). Both plasma levels of IL-6 and IL-6 expression in WAT are positively correlated with obesity, impaired glucose tolerance, and insulin resistance (Mohamed-Ali *et al.*, 1997; Vozarova *et al.*, 2001), while circulating levels fall in response to weight loss (Bastard *et al.*, 2000). Peripheral administration of IL-6 induces hyperlipidaemia, hyperglycaemia and insulin resistance both in humans and rodents. Furthermore, IL-6 inhibits adipogenesis and has been implicated in stimulating lipolysis (Path *et al.*, 2001) and in decreasing adiponectin secretion (Fernandez-Real & Ricart, 2003). Furthermore, IL-6 is produced in the murine hypothalamus, suggesting a central role for this interleukin in the central regulation of appetite and energy expenditure, similarly to leptin (Jones, 1994). IL-6 levels in the CNS are negatively correlated with fat mass in overweight humans, suggesting central IL-6 deficiency in obesity and central administration of IL-6 increases energy expenditure and decreases body fat in rodents (de Benedetti *et al.*, 1997; Wallenius *et al.*, 2002). *In vitro*, IL-6 expression in adipocytes is increased by insulin (Krogh-Madsen *et al.*, 2004), and TNFα (Wang *et al.*, 2005), as well as by prostaglandin D_2 and its metabolites PGJ_2 and $\Delta^{12}PGJ_2$ (Peeraully *et al.*, 2006).

Other interleukins expressed in white adipose tissue include IL-1β, IL-8, IL-10, IL-17D and IL-18. IL-1β has been shown to stimulate leptin release from human adipocytes (Flower *et al.*, 2003), and to mediate leptin induction in mice administered with inflammatory stimuli (Faggioni *et al.*, 1998). The *IL-8* gene is expressed in human adipocytes, the protein being secreted by the cells (Bruun *et al.*, 2000). IL-8 release is stimulated by IL-1β and TNFα, while being inhibited by dexamethasone (Bruun *et al.*,

2001). Furthermore, IL-8 plasma levels are increased in obesity (Straczkowski *et al.*, 2002).

The anti-inflammatory cytokine IL-10 is also secreted from human adipocytes, as well as from the stromal vascular fraction of human fat depots (Fain *et al.*, 2004*b*), its levels being elevated in obesity both in humans and rodents (Esposito *et al.*, 2003; Juge-Aubry *et al.*,2005). Finally, IL-8 expression is induced by LPS and TNFα (Juge-Aubry *et al.*, 2005). Similarly, IL-18 circulating levels are increased in obesity and fall with weight reduction (Esposito *et al.*, 2002). IL-18 is a pro-inflammatory cytokine and it has recently been demonstrated that IL-18 is expressed in human adipose tissues and cultured human adipocytes, where its levels are increased by the administration of TNFα (Skurk *et al.*, 2005; Wood *et al.*, 2005). However, its release from adipocytes has not been documented, so it is only considered as a putative adipokine (Wood *et al.*, 2005). Similarly to IL-18, IL-17D expression in adipocytes has been reported and it has demonstrated to stimulate the production of IL-6 and IL-8 (Starnes *et al.*, 2002); however, there has been no report of its release from these adipocytes.

1.3.5 Chemokines

It has been demonstrated during the last few years that obesity is associated with increased adipose tissue infiltration by macrophages (Weisberg *et al.*, 2003; Wellen & Hotamisligil, 2003). Monocyte chemoattactant protein-1 (MCP-1), a chemokine that recruits monocytes to sites of inflammation, is expressed and secreted by adipose tissue, both by adipocytes and the stromal vascular fraction (Wellen & Hotamisligil, 2003), its levels being higher in visceral compared to subcutaneous human adipose tissue (Bruun *et al.*, 2005). The observation that MCP-1 expression levels in adipose tissue and circulating levels are elevated in obesity, has suggested that MCP-1-mediated macrophage infiltration of adipose tissue may contribute to the metabolic abnormalities related with obesity and insulin resistance (Sartipy & Loskutoff, 2003; Dahlman *et al.*, 2005). Furthermore, increased circulating MCP-1 levels in obesity are associated with increased circulating monocytes (Takahashi *et al.*, 2003). On the other hand, weight loss leads to a

reduction in MCP-1 levels (Christiansen *et al.*, 2005). When MCP-1 is applied to cultured adipocytes, both insulin-stimulated glucose uptake and insulin-induced insulin receptor tyrosine phosphorylation are decreased, suggesting that MCP-1 directly contributes to adipose tissue insulin resistance (Gerhardt *et al.*, 2001; Sartipy & Loskutoff, 2003). In addition, MCP-1 inhibits adipocyte growth and differentiation by decreasing the expression of a number of adipogenic genes (Sartipy & Loskutoff, 2003). *In vitro*, MCP-1 expression and secretion by adipocytes is stimulated by TNFα (Wang *et al.*, 2005) and prostaglandin D_2 and J_2-series prostaglandins (Peeraully *et al.*, 2006). However, adipose tissue is not a major contributor to circulating MCP-1 levels (Dahlman *et al.*, 2005).

Macrophage migratory inhibitory factor (MIF) is another factor possibly involved in the macrophage infiltration process in WAT. MIF is secreted by human adipocytes, its levels positively relating to BMI. It has thus been suggested that it may be an obesity-dependent regulator of macrophage infiltration into adipose tissue (Skurk *et al.*, 2005; Trayhurn, 2005).

1.3.6 Growth factors

Several growth factors are synthesized in WAT. Transforming growth factor-β (TGFβ) is a multifunctional cytokine produced by a variety of cells that regulates the growth and differentiation of various cell types. It is involved in cell adhesion and migration, extracellular matrix production, tissue remodeling and wound repair (Sporn *et al.*, 1987). TGFβ is expressed in adipose tissue, its levels being elevated in murine models of obesity (Samad *et al.*, 1997). Since TGFβ has been shown to increase preadipocyte cell proliferation, it has been suggested that its increased levels in obese adipose tissue may contribute to the elevated cellularity of fat depots related to the obese phenotype (Frühbeck *et al.*, 2001). *In vitro*, TNFα stimulates TGFβ production, which in turn leads to an increase in the production of PAI-1 (Samad *et al.*, 1997).

Insulin-like growth factor-1 (IGF-1) is another growth factor secreted from WAT acting to stimulate preadipocyte proliferation and differentiation (Hausman *et al.*, 2001).

Vascular endothelial factor (VEGF) is a potent angiogenic factor and a WAT product. Its levels are increased in the plasma of *db/db* mice compared to their lean counterparts and it is mainly synthesized by visceral WAT (Miyazawa-Hoshimoto *et al.*, 2005). *In vitro*, VEGF is upregulated by insulin, while dexamethasone has the opposite effect (Fain & Madan, 2005).

As discussed in a previous section, WAT is innervated by the SNS, the sympathetic system being a major physiological regulator of lipolysis in WAT (Hales *et al.*, 1978; Bartness & Bamshad, 1998), cell number (Bartness & Bamshad, 1998) and adipokine synthesis, particularly leptin (Trayhurn *et al.*, 1995; Rayner & Trayhurn, 2001). In various tissues, the development and survival of sympathetic neurons depend on the presence of neurotrophins, NGF being the best characterized one (Vega *et al.*, 2003). NGF is a newly identified adipokine, the *NGF* gene being expressed in human and mouse WAT, and the protein being secreted from murine adipocytes in culture (Peeraully *et al.*, 2004). Various factors have been identified which affect NGF expression and release by these adipocytes. TNFα strongly upregulates NGF expression, while both dexamethasone and rosiglitazone suppress its expression, suggesting a role for the neurotrophin in the inflammatory response of WAT (Peeraully *et al.*, 2004). Furthermore, it has been demonstrated that NGF synthesis is regulated by prostaglandins, the levels being upregulated by PGD_2, PGJ_2 and $\Delta^{12}PGJ_2$, while downregulated by 15d-PGJ_2, PGE_2, $PGF_{2\alpha}$, and PGI_2 (Bulló *et al.*, 2005). NGF is also synthesized and released by BAT, with expression in brown adipocytes being inhibited by prolonged cold exposure and norepinephrine (Néchad *et al.*, 1994; Nisoli *et al.*, 1996).

1.3.7 Haemostatic factors

Plasminogen-activator inhibitor 1 (PAI-1) is a serine protease inhibitor, whose elevated plasma levels are a risk factor for thrombosis (Fay, 2004). PAI-1 is produced both by adipocytes and the stromal vascular fraction of WAT, its secretion and expression being greater in visceral relative to subcutaneous white tissue (Fain *et al.*, 2004). Adipose tissue is thought to be a major source of PAI-1 in obesity, its circulating levels positively

correlating with visceral adiposity, as well as insulin resistance (Kershaw & Flier, 2004). On the other hand, weight loss and treatment with TZDs significantly reduce PAI-1 circulating levels (Mertens & Van Gaal, 2002). TNFα is a major regulator of elevated PAI-1 levels in obesity (Mertens & Van Gaal, 2002; Juhan-Vague *et al.*, 2003). Furthermore, a possible role for PAI-1 in the development of adipose tissue has been proposed, as PAI-1 deficient mice show less weight gain, smaller adipocyte size and lower tissue triglyceride levels compared with wild-type mice in response to a high-fat diet (Schafer *et al.*, 2001; Ma *et al.*, 2004).

The renin-angiotensin system (RAS) is an important regulator of systemic blood pressure and renal electrolyte homeostasis (Engeli *et al.*, 2000). Numerous RAS proteins are synthesized and secreted by WAT, including renin, angiotensinogen (AGT), angiotensin I and II, angiotensin receptors type I (AT1) and II (AT2), and angiotensin-converting enzyme (ACE), with the expression of AGT, ACE and AT1 receptors being higher in visceral compared to subcutaneous tissue (Engeli *et al.*, 2003). RAS expression is positively correlated with adiposity in humans, while AGT expression is decreased by fasting and increased by refeeding, the changes being accompanied by changes in blood pressure. It has been demonstrated in rodents that inhibition of RAS decreases weight and increases insulin sensitivity (Engeli *et al.*, 2003; Goossens *et al.*, 2003). Furthermore, RAS proteins influence adipose tissue development in multiple ways. For example, both RAS and angiotensin II are induced during adipogenesis; the latter promotes adipocyte growth and differentiation as it inhibits lipolysis, promotes lipogenesis and decreases insulin-dependent glucose uptake. Furthermore, RAS proteins affect the expression of other adipose tissue-secreted factors, such as prostacyclin, PAI-1 and leptin (Engeli *et al.*, 2003). Further evidence for the role of RAS in obesity and hypertension has been provided by different murine models, as it has been demonstrated that AGT-knockout mice have decreased blood pressure and adipose tissue mass (Massiera *et al.*, 2001a), while transgenic mice overexpressing AGT in adipose tissue exhibit the opposite traits (Massiera *et al.*, 2001b).

1.3.8 Acute-phase proteins

Several acute-phase proteins are now recognized as adipokines, with adipose tissue being a potential contributor to the raised circulating levels of these factors in obesity (Trayhurn & Wood, 2004).

Haptoglobin is a tetrameric glycoprotein which binds haemoglobin, preventing both iron loss and kidney damage during haemolysis. It has an antioxidant function and has been reported to be angiogenic, stimulating endothelial cell differentiation, and vascularisation (Cid *et al.*, 1993). Haptoglobin is expressed and secreted by mouse and human adipose tissue solely by mature adipocytes and, similarly to resistin (Haugen *et al.*, 2001), it is a late marker of adipocyte differentiation (do Nascimento *et al.*, 2004). Its circulating levels are increased in obesity and type 2 diabetes (Engstrom *et al.*, 2003), the same having been observed in *ob/ob* mice (do Nascimento *et al.*, 2004). *In vitro*, haptoglobin levels are enhanced by glucocorticoids, catecholamines, and TNFα while being suppressed by TZDs (do Nascimento *et al.*, 2004). Thus, haptoglobin in adipose tissue might be involved in the inflammatory response, or play a role as an antioxidant and in angiogenesis (do Nascimento *et al.*, 2004), functions which have also been proposed for metallothionein (MT), another acute phase response protein (Trayhurn & Beattie, 2001).

MT is mainly synthesized in the liver and kidney and it has been suggested to have an antioxidant role in BAT (Beattie *et al.*, 2000). Both MT-1 and MT-2 are expressed in all major WAT depots, with no substantial site differences and their expression is adipocyte specific, with no expression in the stromal vascular fraction (Trayhurn *et al.*, 2000). *In vitro*, MT levels are stimulated by dexamethasone and forskolin and it has been suggested that it might function in WAT as an antioxidant protecting fatty acids from oxidative stress (Trayhurn *et al.*, 2000).

Serum amyloid A (SAA) is the precursor of amyloid A protein found in secondary amyloid plaques, recognized as a risk factor for coronary artery disease. WAT has only recently been identified as a source of SAA. Serum SAA positively correlate with weight

gain, adiposity and SAA mRNA levels in adipose tissue (Sjoholm *et al.*, 2005). Both SAA adipose tissue expression levels and circulating levels decrease in response to weight loss, thus indicating that SAA could be a possible link between obesity and cardiovascular disease (Poitou *et al.*, 2005; Sjoholm *et al.*, 2005).

1.3.9 Prostaglandins

1.3.9.1 Prostaglandin synthesis

White adipose tissue is known to synthesise various prostaglandins, adipocytes themselves producing prostaglandins and expressing several of the receptors through which PGs exert their effects (Bell-Parikh *et al*, 2003). Prostaglandins are lipid-derived autacoids generated by sequential metabolism of arachidonic acid by the cyclooxygenase (COX) and prostaglandin synthase enzymes. There are two COX isoforms, COX-1 and COX-2, with prostaglandins produced via the former being ascribed a role in physiological homeostasis, while those produced via the latter usually being responsible for inflammatory effects. COX-2 is thus a major target for non-steroidal anti-inflammatory drugs such as aspirin and indomethacin. In general, phospholipase A_2 catalyzes the release of arachidonic acid from membrane phospholipids. Upon its release, arachidonic acid undergoes oxidation by COX to PGG_2 followed by reduction to the unstable endoperoxide PGH_2, the central prostanoid precursor. PGH_2 serves as a substrate for the prostaglandin synthase enzymes, namely PGD_2, PGE_2, $PGF_{2\alpha}$, prostacyclin and thromboxane synthase, which are responsible for the production of the five principal bioactive prostaglandins generated *in vivo*, PGD_2, PGE_2, $PGF_{2\alpha}$, TXA_2 (thromboxane) and PGI_2 (prostacyclin) (Fig 1.4) (Straus & Glass, 2001; Hata & Breyer, 2004).

Prostaglandins are ubiquitously produced and act locally in an autocrine or paracrine manner to elicit a diverse set of pharmacological effects modulating many physiological systems, including the endocrine, respiratory and immune systems. However, they are only locally active, due to their rapid breakdown. PGD_2 is sequentially degraded to PGJ_2, which then isomerizes to yield 9-deoxy-Δ^9,$\Delta^{12,13,14}$-dihydro-PGJ_2 (Δ^{12}-PGJ_2). Furthermore, PGJ_2 may be converted directly to 15-deoxy-$\Delta^{12,14}$-PGJ_2 (15d-PGJ_2) in the presence of

albumin. In contrast to conventional prostaglandins, PGJ_2 and its derivatives possess a highly reactive cyclopentenone ring that permits them to ligate nuclear receptors and to modify intracellular signaling molecules (Bell-Parikh *et al.*, 2003). Similarly, PGE_2 may be converted to PGA_2, PGC_2 and PGB_2, while 6-keto-$PGF_{1\alpha}$ is the natural metabolite of PGI_2 (Fig. 1.4) (Straus & Glass, 2001).

Prostaglandins exhibit both pro-inflammatory and anti-inflammatory effects in many pathophysiological conditions, this usually depending on cell population, and the context of activation, but mainly on the receptor subtype that they bind to (Hata & Breyer, 2004).

1.3.9.2 Prostaglandin receptors

The physiological effects of prostaglandins are partly mediated by a family of rhodopsin-like seven transmembrane spanning G-protein-coupled prostanoid receptors (GPCRs). The prostaglandin receptor subfamily comprises eight members (DP, EP1-4, FP, IP and TP), which are classified according to the prostaglandin ligand that each binds with the highest affinity. More specifically, DP binds PGD_2, PGJ_2 and Δ^{12}-PGJ_2, while PGE_2 exerts its effects by binding and activating four receptors, EP1 to EP4. Furthermore, PGI_2 binds IP, $PGF_{2\alpha}$ to FP and TXA_2 to TP (Hata & Breyer, 2004). A ninth prostaglandin receptor has recently been identified, the chemoattractant receptor homologous molecule expressed on Th2 cells (CRTH2), which binds PGD_2 and its metabolite 15d-PGJ_2 (Hirai *et al.*, 2001; Sawyer *et al.*, 2002). However, the CRTH2 receptor is more closely related to chemoattractant receptors rather than the other prostaglandin receptors. The exact roles of prostaglandin receptors in physiologic and pathologic conditions are determined by ligand-receptor interactions which depend on multiple factors such as ligand affinity, receptor expression profile, differential coupling to signal transduction pathways and the cellular context in which the receptor is expressed, and prostaglandins may activate more than one subtype of prostaglandin receptors (Hata & Breyer, 2004).

Figure 1.4 Prostaglandin synthetic pathway

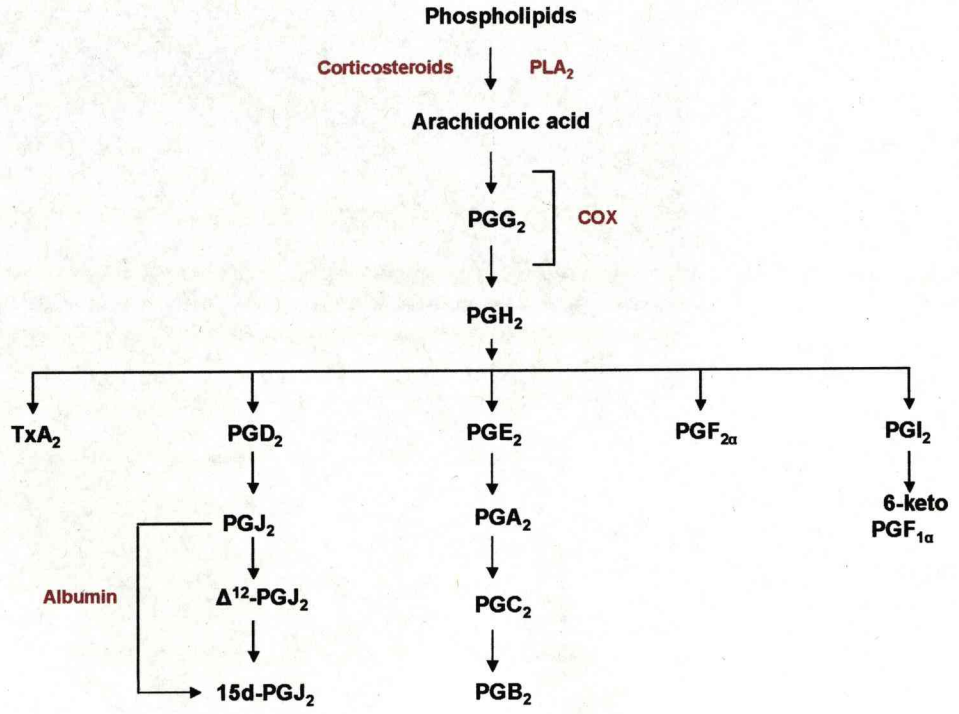

Schematic representation of the general pathway for prostaglandin synthesis. Phospholipids are converted into arachidonic acid, which is metabolized by COX-1 and -2 to PGH2, the common precursor for the five principal prostaglandins, generated by individual prostaglandin synthase enzymes. (adapted from Hata & Breyer, 2004)

In addition to the G-protein coupled receptors, prostaglandins act through intracellular targets, the PPAR family of nuclear receptors. Both 15d-PGJ_2 and Δ^{12}-PGJ_2 bind to PPARγ, the former representing the highest affinity ligand for PPARγ identified (Forman *et al.*, 1995; Kliewer *et al.*, 1995), its anti-inflammatory effects most probably being mediated through stimulation of this receptor (Ricote *et al.*, 1998; Bell-Parikh *et al.*, 2003). 15d-PGJ_2 also activates PPARα and PPARδ, although less potently than PPARγ (Forman *et al.*, 1997). Similarly, PGI_2 has been proposed as a ligand for PPARα and PPARδ, through which it possibly mediates angiogenic effects (Kubis & Levy, 2004; Pola *et al.*, 2004).

1.3.9.3 Prostaglandins in WAT

As aforementioned, it has been known for some time that adipocytes can synthesize prostanoids (Shillabeer *et al.*, 1998), with PGE_2, 6-keto-$PGF_{1\alpha}$, $PGF_{2\alpha}$ and 15d-PGJ_2 being secreted by 3T3-L1 adipocytes (Borglum *et al.*, 1999). Similarly, the capacity of 3T3-L1 adipocytes and human adipose tissue to synthesize PGD_2 and its derivatives has been demonstrated (Jowsey *et al.*, 2003) and both PGI_2 and PGE_2 are secreted by isolated human adipocytes, although their expression is higher in the stromal vascular fraction (Fain *et al.*, 2002) and in rat adipocytes (Shillabeer *et al.*, 1998). Various roles have been attributed to prostaglandins in WAT.

Prostaglandins play various roles in adipogenesis. $PGF_{2\alpha}$ has been shown to inhibit adipocyte development (Curtis-Prior, 1975). Diverse actions have been attributed to PGE_2 most possibly explained by it binding to four EP subtypes, which differ in their signal transduction pathways (Negishi *et al.*, 1995). Although PGE_2 and PGI_2 are the two prostaglandins predominantly synthesized by adipocytes, they appear to have opposing effect on early adipogenesis, the former inhibiting adipocyte differentiation (Vassaux *et al.*, 1992) through the EP4 receptor (Tsuboi *et al.*, 2004), while the latter promotes it (Vassaux *et al.*, 1992). Furthermore, PGE_2 has been reported to stimulate leptin release by adipose tissue (Fain *et al.*, 2000), to have an antilipolytic effect on mammalian adipocytes (Castan *et al.*, 1994) and to stimulate metabolism of BAT via the EP1 receptor (Tsuboi *et al.*, 2004). Additionally, studies with 3T3-F442A adipocytes have

demonstrated that the stimulation of lipolysis induced by some cytokines such as IL-1β is mediated through a cytokine-induced stimulation of prostaglandin synthesis, as the lipolytic effect of these agents on the adipocytes is blocked by indomethacin, a non-selective COX inhibitor (Feingold *et al.*, 1992).

1.3.10 Proteins of lipid and lipoprotein metabolism

Several proteins involved in lipid and lipoprotein metabolism are released from white adipocytes. The enzyme lipoprotein lipase (LPL), the first identified secreted protein factor of adipocytes, is responsible for the breakdown of circulating TAGs to release fatty acids for uptake by adipocytes and its expression is stimulated by insulin and glucocorticoids (Enerback & Gimble, 1993; Trayhurn *et al.*, 2001). WAT also secretes cholesteryl ester transfer protein, which plays an important role in the accumulation of cholesteryl ester by adipose tissue, and apolipoprotein E (Trayhurn & Beattie, 2001). Furthermore, WAT is a major site of retinol-binding protein (RBP) synthesis (Makover *et al.*, 1989), although liver and kidney are the main contributors to the circulating levels of this protein. RBP which is required for the transport of retinol (vitamin A) from the liver and adipose tissue to target tissues (Trayhurn & Beattie, 2001), has recently been reported to be involved in the development of insulin resistance in obesity and type 2 diabetes (Yang *et al.*, 2005)

Adipsin, also known as complement factor D, is an adipose tissue derived factor required for the enzymatic production of acylation-stimulating protein (ASP), also known as C3ades-Arg, a complement factor protein that affects both lipid and glucose metabolism (Cianflone *et al.*, 2003). Although adipsin was initially shown to be reduced in rodent obesity (Flier *et al.*, 1987), later studies in humans have positively correlated both adipsin and ASP levels with adiposity, insulin resistance and dyslipidemia (Cianflone *et al.*, 2003). Furthermore, ASP enhances fatty acid uptake by increasing LPL activity and triglyceride synthesis, as well as glucose transport in adipocytes, while on the other hand it decreases lipolysis and release of FFAs from adipocytes (Cianflone *et al.*, 2003). Finally, adipocytes express C5L2, a G protein-coupled receptor for ASP (Kalant *et al.*, 2003).

Fasting-induced adipose factor (FIAF) is an angiopoietin-like protein and a target for PPARα (Kersten *et al.*, 2000). FIAF, whose circulating levels generally increase with fasting (Kersten *et al.*, 2000), has been shown to inhibit LPL activity affecting the accumulation of TAGs by adipocytes (Bäckhed *et al.*, 2004). Finally, zinc-alpha2-glycoprotein is a recently identified adipokine (Bao *et al.*, 2005) with a possible role in adipose tissue lipid metabolism.

1.4 Zinc-α_2-glycoprotein (ZAG)

ZAG is a soluble protein first identified in human plasma in 1961. Its name is attributed to the fact that it can be precipitated by adding zinc ions and it displays electrophoretic mobility in the α_2 region of the plasma globulins (Bürgi & Schmid, 1961). The human *ZAG* gene is composed of four exons and has been mapped to human chromosome band 7q22.1 (Ueyama *et al.*, 1994). Human ZAG consists of a single polypeptide chain of 276 amino acid residues and has a molecular weight of 38,487 daltons as calculated from its polypeptide and carbohydrate structure (Araki *et al.*, 1988), very close to the original estimate of Mr 41,000 based on physiological studies (Bürgi & Schmid, 1961). The rat and mouse proteins are slightly longer, consisting of 279 and 290 residues in the mature form, respectively. Comparison among them has shown that there is a 59.4% overall amino acid sequence identity between human and rat and a 58.6% identity between human and mouse ZAG (Ueyama *et al.*, 1994). However, murine and human ZAG can share up to 100% identity in regions that are thought to be involved in lipid metabolism (Hale *et al.*, 2001). On the other hand, identity between rat and mouse ZAG reaches 88.5% (Ueyama *et al.*, 1994).

ZAG has been associated with antigens of the major histocompatibility complex, due to similarities in their amino acid sequence and in domain structure (Sanchez *et al.*, 1997; Sanchez *et al.*, 1999). Furthermore, it has been shown to be a member of the immunoglobulin gene superfamiy (Araki *et al.*, 1988). These findings have been further confirmed by the crystal structure of human ZAG, which reveals an MHC-like fold without a β_2M light chain, and a groove that closely resembles the peptide-binding sites

of classical class I MHC molecules. But instead of a peptide, the ZAG groove contains a nonpeptidic compound that might be implicated in lipid metabolism under pathological conditions (Sanchez *et al.*, 1999).

1.4.1 ZAG expression

ZAG protein has been found within the cytoplasm of many normal secretory epithelial cells, such as those in breast, prostate and liver. Consistent with that, ZAG is expressed in most body fluids, including serum, sweat, saliva, seminal plasma, cerebrospinal fluid, breast milk, colostrum, amniotic fluid, urine and synovial fluid (Bürgi & Schmid, 1961; Tada *et al.*, 1991). The expression of ZAG in various differentiated cell types is of great interest, and the observation that its expression increases with the degree of differentiation (Lei *et al.*, 1997; Brysk *et al.*, 1999; Hale *et al.*, 2001) explains its use as a clinical marker. ZAG is present in breast cysts and is produced by 40% of breast carcinomas. It has also been shown that it is inducible in breast cancer cell lines by glucocorticoids and androgens and that its expression correlates with tumour differentiation and does not independently affect prognosis (Tada *et al.*, 1991; Díez-Itsa *et al.*, 1993).

1.4.2 Biological functions of ZAG

ZAG is a putative mediator of cancer cachexia, although the mechanisms of its action are yet to be determined. As discussed earlier, the function of ZAG was recently indicated when it was found to be identical, in terms of molecular weight, amino-acid sequence, electrophoretic mobility, and immunoreactivity, to the lipid-mobilising factor (LMF) isolated from a cachexia-inducing murine adenocarcinoma (MAC16) and from the urine of patients with unresectable pancreatic carcinoma and established weight loss. It was thus suggested that tumour-produced ZAG may contribute to the development of cancer cachexia (Todorov *et al.*, 1998). Both ZAG and LMF were shown to stimulate adenylate cyclase in murine adipocyte plasma membranes and release glycerol from isolated adipocytes (Hirai *et al.*, 1998). ZAG is produced by normal prostate epithelium. In addition to that, the protein is produced by around 73% of prostate cancers and as with

breast cancer, the greater the degree of differentiation, the greater the production of ZAG (Hale *et al.*, 2001).

1.4.3 ZAG is involved in body weight regulation and is expressed in adipose tissue

The involvement of ZAG in the induction of lipolysis has been demonstrated both *in vivo* and *in vitro*. The *in vivo* administration of ZAG to mice induces a rapid and selective reduction on body fat and increases serum-free fatty acid levels, by activating hormone-sensitive lipase through increased intracellular cAMP levels. Furthermore, *in vitro*, ZAG stimulates lipolysis in a dose-dependent manner when applied to adipocytes isolated from murine adipose tissue (Hirai *et al.*, 1998). It has recently been demonstrated that the lipolytic effect of ZAG is attenuated by the specific β_3-adrenoreceptor antagonist SR59230. This finding indicates that ZAG activity in rodents is mediated via the β_3 adrenoreceptor with up-regulation of the cAMP pathway (Russell *et al.*, 2002). Furthermore, it has been shown in a recent study using KK/Ta mice, a spontaneous model of type 2 diabetes (Ikeda, 1994), that ZAG might be a possible candidate gene for the regulation of body weight and age-dependent changes in the genetic control of obesity, its overexpression in 3T3-L1 adipocytes leading to an increase in adiponectin mRNA levels (Gohda *et al.*, 2003).

The secretory function of adipocytes, together with the lipolytic effect of ZAG led to a recent study examining whether ZAG is produced locally in WAT. Indeed, it was shown that ZAG is expressed both in human and mouse WAT, and 3T3-L1 murine adipocytes, while its levels are elevated in WAT of mice bearing the MAC16 tumor (Bing *et al.*, 2004). ZAG stimulates adipose tissue breakdown through the cAMP-dependent pathway, as mentioned above, and upregulates uncoupling proteins found in adipose tissue, potentially contributing to changes in REE (Sanders & Tisdale, 2004). It was further demonstrated that the protein is a new adipokine secreted by human SGBS adipocytes, its expression being regulated particularly through the PPARγ receptor and by TNFα (Bao *et al.*, 2005).

1.5 Aims of this thesis

As indicated in the preceding sections, WAT is now recognized as a major endocrine and secretory organ in addition to its traditional role in the storage of energy and thermal insulation. WAT is a heterogeneous organ, consisting of multiple specific depots with distinct anatomical locations and different molecular characteristics, as shown by the differential expression of most adipokines in these sites.

ZAG is a potent mediator of cancer cachexia, which induces lipolysis and lipid utilization. ZAG is expressed in murine WAT and in BAT and human WAT (Bing *et al.*, 2004) and it was subsequently shown that ZAG protein is secreted from human adipocytes, thus being a novel adipokine with a possible role in lipid metabolism and inflammation in WAT (Bao *et al.*, 2005).

In this context, it is important to study in more detail the expression and regulation of ZAG in adipose tissue and thus further explore the function of this adipokine. In this work, two approaches were employed. The first was *in vivo* studies using rodents, and the second was *in vitro* studies using the 3T3-L1 murine fibroblastic clonal cell line. These studies would allow the investigation of the following:

1. A comparison of *ZAG* gene and protein expression among different WAT depots and BAT to determine whether there are key depot differences.
2. *ZAG* gene and protein expression in mature adipocytes and the stromal vascular fraction of WAT depots in order to determine the fraction relative importance of the different cell in WAT.
3. A comparison of *ZAG* gene and protein expression in WAT depots of lean and obese mice.
4. Examination of whether alterations in the nutritional status affect ZAG expression *in vivo*.
5. Examination of the early postnatal development of ZAG in rat adipose tissue to assess how early is ZAG expressed in development.

6. Expression of the *ZAG* gene *in vitro* at different stages of adipocyte differentiation.
7. The role of sympathetic agonists, hormones and inflammatory mediators in the regulation of ZAG expression in 3T3-L1 adipocytes.

Chapter 2

Materials & Methods

2.1 Reagents and Equipment

2.1.1 Chemical reagents

Reagents	*Supplier*
40% Acrylamide/ Bis	Sigma
Adiponectin	Sigma
Agarose	BDH
Ammonium persulfate	Sigma
Antibodies	Santa-Cruz
β – Mercaptoethanol	Sigma
Bicinchoninic acid solution (BCA)	Sigma
Bovine Serum Albumin	Sigma
BRL37344	Tocris
Bromophenol Blue	Sigma
Calcium chloride	BDH
Chloroform	Fisher Scientific
Collagenase	Sigma
Copper sulphate	Sigma
Dexamethasone	Sigma
di-sodium hydrogen phosphate	Sigma
Dulbecco's modified Eagle's medium (DMEM)	Invitrogen
ECL hyperfilm	Amersham
100% ethanol	Sigma
Ethidium bromide	Sigma
Fetal calf serum	Invitrogen
GeneRuler™ 100 bp DNA ladder	Helena
Glucose	Sigma
Glycerol	Sigma
Glycine	Sigma
Guanidine hydrochloride (thiocynate salt)	Calbiochem

HEPES (4-(2-hydoxyethyl)piperaxine-1-ethanesulphonic acid)	Sigma
IBMX (3-Isobutyl-1-methylxanthine)	Sigma
Insulin	Sigma
Interleukin-6	Sigma
Isoprenaline	Sigma
Isopropanol	Sigma
Leptin	Sigma
Lipopolysaccharide (LPS)	Sigma
Magnesium chloride	BDH
Magnesium sulphate	BDH
Methanol	BDH
Noradrenaline	Sigma
Phosphate buffered saline (PBS)	Invitrogen
Photographic developer	Sigma
Photographic fixer	Sigma
Ponceau	Sigma
Potassium chloride	BDH
Prostaglandins	Alexis
Rainbow molecular weight marker	Amersham
RNase AWAY	Molecular BioProd
Rosiglitazone	GlaxoSmithKline
Sigmaclean® water bath treatment	Sigma
Skimmed milk powder	Tesco
Sodium acetate	BDH
Sodium chloride	BDH
Sodium citrate	BDH
Sodium dodecyl sulphate	BDH
Sodium dihydrogen orthophosphate	BDH
Sodium EDTA	BDH
Sodium hydroxide	BDH

Sucrose	BDH
Taqman primers	Eurogentec
Taqman probes	Eurogentec
Tris – Borate - EDTA 10x buffer pH8.3 (TBE)	Fisher Scientific
TEMED	Sigma
TNFα	Sigma
Trichloroacetic acid (TCA)	Sigma
TRIzol reagent	Sigma
Tris – Base	Sigma
Tris hydrochloride	Qbiogene
Trypsin	Calbiochem
Tween 20 (polyoxyethylene sorbitan monolaurate)	Sigma
Ultra pure water	DakoCytomation
ZAG monoclonal antibody	Santa-Cruz

2.1.2 Commercial kits

Kits	*Supplier*
ECL Western Blotting detection reagents and analysis system	Amersham
qPCR™ Core Kit	Eurogentec
ReddyMix Master PCR Master Mix Kit	ABgene
Reverse-iT™ 1st strand synthesis	ABgene
TURBO DNA-*free*™	Ambion

2.1.3 Equipment

Equipment	*Supplier*
ABI Prism 7700 real-time PCR machine	Applied Biosystems
Beckman Preparative Ultracentrifuge	Beckman
Benchmark™ Plus microplate spectrophotometer	Bio-Rad

Biophotometer	Eppendorf
Centrifuge 5415D	Eppendorf
Centrifuge 5417R	Eppendorf
Corning filter system (0.22 µm membrane)	Fisher Scientific
Compact Electro-blotting unit	Scie-Plas
GallenKamp shaking water bath	Sanyo
Glass homogenisers (borosilicate)	Fisher Scientific
HB-1000 hybridisation oven	Ultra-Violet products
Hetovac VR-1 vacuum centrifuge	Thermo
Hybond ECL Nitrocellulose Membrane	Amersham
Hyperfilm ECL	Amersham
Kodak Digital Science DC 120 digital camera	Kodak
Mx3005P QPCR system	Stratagene
Nescofilm® membrane	Fisher Scientific
PCR express thermal cycler	Hybaid
PolytronUltra-Turrax T25 electric homogenizer	Janke & Kunkel
Real-time PCR plates	ABgene
Real-time PCR cover slips	ABgene
SARAN wrap	Norlab
UVette plastic disposable cuvettes	Eppendorf
Vertical electrophoresis unit	Scie-Plas

2.1.4 Software

Software	*Supplier*
Beacon Designer, PREMIER	Biosoft
Excel, 2003	Microsoft
HP Precision Scan Pro 2.5	Hewlett-Packard Co
Kodak Digital Science ID 1 image analysis software	Kodak
MCID Basic 7.0 Software	Imaging Research Inc
Microplate Manager 5.2 Software	Bio-rad

MxPro QPCR Software	Stratagene
Primer Express® Software	Applied Biosystems
Primer Premier 5.0 Software	Premier Biosoft

2.1.5 Suppliers' addresses and URLs

ABgene, ABgene House, Blenheim Road, Epsom KT19 9AP, UK. *http://www.abgene.com*

Alexis Biochemical, 6181 Cornerstone Court East Suites 102-104, 92121-4727 San Diego, USA. *http://www.alexis-corp.com*

Antec Europe BV, Sydneystraat 33, 3047 BP Rotterdam, the Netherlands. *http://www.antec.com*

Ambion Ltd, Spitfire Close, Ermine Business Park, Huntingdon, Cambridgeshire, PE29 6XY, UK. *http://www.ambion.com*

Amersham Biosciences UK Ltd, Amersham Place, Little Chalfont, Buckinghamshire, HP7 9NA, UK. *http://www.amersham.co.uk*

Applied Biosystems, Kelvin Close, Birchwood Science Park North, Warrington, Cheshire, WA3 7PB, UK. *http://www.appliedbiosystems.com*

Beckman Instruments Inc, Palo Alto, Fullerton, CA 92634, USA. *http://www.beckman.com*

BDH laboratory supplies, Poole Dorset, BH15 1TD, UK. *http://www.bdh.com*

Bio-Rad Laboratories Ltd, Bio-Rad House, Maxted Road, Hemel Hempstead, Hertfordshire, HP2 7DX, UK. *http://www.bio-rad.com*

Dako, Denmark House Angel Drove Ely, Cambridgeshire, CB7 4ET, UK. *http://www.dako.co.uk*

Eppendorf UK Ltd, Endurance House, Chivers Way Histon, Cambridge, CB4 9ZR, UK. *http://www.eppendorf.com/uk/*

EMD Biosciences Inc, Calbiochem Brand, 10394 Pacific Center Court, San Diego, California, 92121, USA. *http://www.merckbiosciences.co.uk/html/CBC/*

Eurogentec Ltd, P.C House, 2 South Street, Hythe, Southampton, Hampshire SO45 6EB, UK. *http://www.eurogentec.com*

Fisher Scientific, Bishop Meadow Road, Loughborough, Leicestershire, LE11 5RG, UK. *http://www.fisher.co.uk*

GlaxoSmithKline Ltd, Stockley Park West, Stockley Park, Uxbridge, UB11 1BT, Middlesex, UK. *http://www.glaxowellcome.co.uk*

Helena Laboratories (UK) Ltd, Colima Avenue, Sunderland Enterprise Park, Sunderland SR5 3XB, UK. *http://www.helena.co.uk*

Hybaid (UK) Ltd, Action Court, Ashford Road, Ashford, Middlesex, TW15 1XB, UK. *http://www.hybaid.com*

Imaging Research Inc, Brock University, 500 Glenridge Avenue, St. Catherines, Ontario, Canada L2S 3A1. *http://www.imagingresearch.com*

Invitrogen Ltd, 3 FountainDrive, Inchinnan Business Park, Paisley, PA4 9RF, UK. *http://www.invitrogen.com*

Janke & Kunkel, Janke-&-Kunkel- Str 10, 79219 Staufen, Germany. *http://www.ika.net*

Kodak Ltd, P.O. Box 66, Station Road, Hemel Hempstead, Hertfordshire, HP1 1JU, UK. *http://www.kodak.co.uk*

Roche Diagnostics Ltd, Bell Lane, Lewes, East Sussex, BN7 1LG, UK. *http://www.biochem.roche.com*

Microsoft Ltd, Microsoft Campus, Reading, RG6 1WG, UK. *http://www.microsoft.com/uk/*

Norlab Lab Care, Unit 6, Aberdeen, AB21 7HG, UK.

PREMIER Biosoft International, 3786 Corina Way, Palo Alto, CA 94303-4504, Cilicon Valley, USA. *http://www.premierbiosoft.com*

QBiogene, Wellington House, East Road, Cambridge, CB1 1BH, UK. *http://www.qbiogene.com*

SANYO UK, SANYO House, 18 Colonial Way, Watford, Hertfordshire, WD24 4PT, UK. *http://www.sanyo.co.uk*

Santa-Cruz Biotechnology Inc, 2145 Delaware Avenue, Santa Cruz, California 95060, USA. *http://www.scbt.com*

Scie-Plas, Unit 3 Gainsborough, Trading Estate, Old Road, Southam, Warwickshire, CV47 1HP, UK. *http://www.scie-plas.com*

Sigma-Aldrich Company Ltd, Fancy Road, Poole, Dorset, BH12 4QH, UK. *http://www.sigma-aldrich.com*

Stratagene, Hogehilweg 15, 1101 CB Amsterdam Zuidoost, Netherlands. *http://www.stratagene.com*

Tocris Cookson Ltd, Northpoint, Fourth Way, Avon Mouth, Bristol, BS11 8TA, UK. *http://www.tocris.com*

Ultra-Violet Products Ltd, Unit 1, Trinity Hall Farm Estate, Nuffield Road, Cambridge, CB4 1TG, UK. *http://www.uvp.com*

Whatman PLC, Whatman House, St Leonards Rd, 20/20 Maidstone, Kent, ME16 0LS, UK. *http://www.whatman.co.uk*

2.2 Animals

All animal studies were conducted according to the U.K. Home Office Guidelines for the care and use of laboratory animals.

2.2.1 Mice

Ten-week old male mice (CD1) from an inbred colony at the University of Liverpool were housed at an ambient temperature of 22 ± 1^{0}C under a 12:12 h light – dark cycle (lights were on at 07:00 h) and fed a standard pelleted diet (CRM diet, LAbsure, Witham, U.K.) containing 19.2% protein and 4.3% lipid (wt/ wt). Both food and water were available *ad libitum*. The mice were killed by cervical dislocation and the following tissues were rapidly dissected and frozen in liquid nitrogen: WAT (subcutaneous, epididymal, perirenal, mesenteric, and omental depots), interscapular brown adipose tissue (BAT), liver, spleen, heart, kidneys, lungs, skeletal muscle (gastrocnemius), whole brain and the hypothalamus. All tissues were stored at -80^{0}C until RNA extraction.

For a fasting experiment, sixteen ten-week mice (CD1) were used. The mice were kept under the aforementioned conditions and two days prior to the experiment were divided into the fed and the fasted groups and were housed in grid bottomed cages. On commencing the experiment, mice of the control group were still kept on the same diet.

In contrast, all food was removed from the fasted group's cage, while they still had *ad libitum* access to water. Sixteen hours later, animals were sacrificed by cervical dislocation and the following tissues were rapidly dissected and frozen in liquid nitrogen: WAT (subcutaneous, epididymal, perirenal, mesenteric, and omental), BAT and liver.

For the study of the effects of diet composition on ZAG expression, WAT (subcutaneous, epididymal, and perirenal) from lean and diet–induced obese female C57BL/6J mice from Lund University (Lund, Sweden) was provided by Dr Wang (University of Liverpool, U.K.). The mice were purchased from Taconic (Skensved, Denmark) and maintained at 22^{0}C on a 12:12 h light - dark cycle. One week after arrival, the mice were divided into two groups. The first group was on a low-fat diet (11% fat by energy) while the second one was on a high-fat diet (58% fat by energy, Research Diets, New Brunswick, USA). Both groups were kept on these diets for 12 weeks before being sacrificed.

For the study of the effects of obesity on ZAG expression, WAT (subcutaneous, epididymal, perirenal, and omental) from eight–week old lean (+/+ or +/*ob*) and genetically obese (*ob/ob*) C57BL/6J male mice (Charles River Laboratories, Wilmington, MA, USA) was also utilised. After being received, the mice were housed for one week under controlled environmental conditions (22 ± 1^{0}C; 12:12 h light-dark cycle and lights on at 07:00) to allow recovery from stress induced by the transportation. They were then killed by cervical dislocation and dissected tissues were snap frozen in liquid nitrogen.

2.2.2 Rats

Ten-week old male Wistar rats from an inbred colony at the University of Liverpool were housed at an ambient temperature of 22 ± 1^{0}C under a 12:12 h light – dark cycle (lights on at 07:00) and fed a standard pelleted diet (CRM diet, Labsure, Witham, U.K.) containing 19.2% protein and 4.3% lipid (wt/wt). Both food and water were available *ad libitum*. The rats were killed by CO_2 inhalation and the following tissues were rapidly dissected and frozen in liquid nitrogen: WAT (subcutaneous, epididymal, perirenal, mesenteric, and omental depots), interscapular brown adipose tissue (BAT), liver, spleen,

heart, kidneys, lungs, esophagus, stomach, skeletal muscle (gastrocnemius), whole brain and the hypothalamus. All tissues were stored at -80^{0}C until RNA extraction.

For the study of ZAG expression during early postnatal development, WAT (as soon as it was large enough to sample), BAT and liver were dissected from 1, 3, 5, 7, 10, 15, 21, and 32-days-old female Wistar rats (University of Liverpool, U.K). The animals were housed at an ambient temperature of 22 ± 1^{0}C under a 12:12 h light – dark cycle (lights were on at 07:00 h). The animals were weaned at day 21 and had *ad libitum* access to lab chow from day 18. Animals were killed by CO_2 inhalation.

For the study of the effects of obesity on ZAG expression, WAT (epididymal and retroperitoneal) from three - month old lean (+/+ or +/*fa*) and genetically obese (*fa/fa*) male Zucker rats, bred at Rowett Research Institute (Aberdeen, Scotland) were a gift from Dr Rayner.

2.3 Mature adipocytes and stromal vascular cell fractionation

2.3.1 Reagents

(i) 10 x Mixed salts:

1.35 M sodium chloride

47 mM Potassium chloride

25 mM Calcium chloride

12.5 mM Magnesium sulphate

Sterile water

The mix was filtered through a 0.2 µm filter disc and stored at -20^{0}C.

(ii) 10 x HEPES:

100 mM HEPES

12.5 mM Sodium dihydrogen orthophosphate

12.5 mM *di*-sodium hydrogen phosphate

Sterile water

The pH of the mix was adjusted to 7.6 at room temperature; it was then filtered through a 0.2 µm filter disc and stored at -20°C.

(iii) 10 % BSA

After the 10% solution was made up in water, it was left at 4°C overnight to dissolve. Its pH was then adjusted to 7.4 and the mix was then filtered through a 0.2 µm filter disc and stored at -20°C.

(iv) Collagenase buffer:

1 mg/ ml Collagenase

0.1 mg/ ml Glucose

3.5 % BSA

1 x Mixed salts

1 x HEPES

Sterile water

The collagenase and glucose were mixed in a sterile universal, while the rest of the components were mixed into another container and were then added to the first mix. The buffer was then put through a 0.2 µm filter, and into a fresh universal.

2.3.2 Fractionation with collagenase digestion method

The six mice were sacrificed and the subcutaneous, epididymal and perirenal fat depots were dissected, using different scissors among depots. Each sample was placed in a 7 ml 1% albumin buffer aliquot. The albumin aliquots containing the fat were then transferred to a sterile cell culture hood. An aliquot of 5 ml of albumin buffer was added into each half of a sterile Petri dish, and the fat from one aliquot was transferred onto one side of the Petri dish and cleaned of any visible blood vessels and any other non-adipose tissue fragments. The cleaned fat was then transferred to the other side of the Petri dish, where it was finely chopped using two disposable scalpels, before transfer it into a 7 ml aliquot of collagenase buffer. The universals were then sealed using parafilm wrap and placed in a shaking water bath at 37°C for 1 h (or until the fat had been digested). During this time the universals were removed every 15 min and shaken vigorously. After

the collagenase digestion was complete, the samples were passed through a 250 µm mesh into fresh universals. The samples were then centrifuged for 10 min at 1,000 rpm at room temperature. At this stage, the mature adipocytes had floated to the top and were removed to a clean tube and left to settle for a short time, after which, any unwanted buffer was carefully removed with a needle. The remaining buffer was then removed from the original universals and the stromal vascular pellet was left at the bottom and transferred into a fresh tube. Both fractions were then stored at -80^{0}C until further analysis.

2.4 3T3-L1 adipocyte cell culture

For 3T3-L1 adipocyte culture, all precautions needed were taken to prevent any infection passing onto the cells. All glassware was autoclaved and plastic ware was sterile. All bottles and universals were opened within a sterile cell culture hood, firstly wiped with 1% vircon solution followed by 70% ethanol. All media components were mixed together and then filter sterilised through a 0.22 µm filter membrane. Prepared media were kept at 4^{0}C for one week maximum and were always pre-warmed at 37% in a water bath, which was kept sterile with the addition of Sigmaclean, before adding to the cells to avoid cell shock. However, induction medium was always freshly prepared prior to actual use and any excess was discarded afterwards.

2.4.1 Reagents

(i) Culture medium:

1 x DMEM

10% Fetal Calf serum

(ii) Induction medium:

1 x DMEM

10% Fetal Calf serum

5 µg/ ml Insulin

0.25 mM Dexamethasone

0.5 mM IBMX

Both dexamethasone and IBMX stock solutions were made fresh each time in 95% ethanol.

(iii) Feeding medium post-differentiation:

1 x DMEM

10% Fetal Calf Serum

5 µg/ ml Insulin

(iv) Trypsin/ EDTA:

For 10 ml stock: 8 ml sterile water

Stock trypsin/ EDTA (0.05% / 0.02%)

10 x PBS

2.4.2 Cell storage

3T3-L1 cells were obtained from the American Type Culture Collection (Manassas, Virginia, USA) and aliquots were stored in liquid nitrogen. Cells were cultured at 37°C in an incubator with a humidified atmosphere of 5% CO_2/ 95% air.

2.4.2.1 Cell generation and maintenance

To start a cell culture experiment, a frozen aliquot of cells was removed from liquid nitrogen storage and defrosted in a water bath at 37°C. One ml of pre-warmed culture medium was then added to the aliquot to help defrosting and the sample was gently pipetted up and down a few times to aid thawing. The thawed aliquot was then added to a 25 cm^2 flask containing 3 ml of culture medium and placed in an incubator. The culture medium was replaced with fresh medium every 48h to ensure the survival of the cells.

2.4.2.2 Cell passaging and plating

Once the cells were around 80% confluent, the medium was aspirated off, 1 ml of Trypsin/EDTA was added and the flask was placed in the incubator for 1-2 min until the cells detached. The detachment of the cells was verified by light microscopy. After the cells had been detached, 9 ml of pre-warmed culture medium was added to neutralise the trypsin and prevent cell lysis and the suspension was then gently pipetted up and down to break up any clumps. The cells were then either plated out to six well plates or into 25 cm^2 flasks to increase the numbers. In the first case, 300 µl of the cell suspension was added to each well, where 1.5 ml of culture medium had already been placed, whereas in the latter, 1 ml of the cell suspension was added to 3 ml of media already placed in the flasks, to be plated out to six well plates as soon as they were confluent using the same procedure.

2.4.2.3 Cell differentiation

Once plated out, the cells were allowed to grow confluent, and then left for another 24 h. The cells were induced to differentiate by replacing the culture medium with 1.5 ml of differentiation medium. The feeding medium also remained in the wells for 48 h, and as with culture medium it was replaced with fresh medium every subsequent 48 hours. This continued up until 24 h before the cells were ready for treatment. Differentiation of cells into adipocytes was confirmed by the accumulation of lipid droplets, which usually started around day 3 after the induction of differentiation.

2.4.2.4 Cell treatment

In the first instance, the time-course of ZAG gene expression in 3T3-L1 cells was studied. For this experiment, 6 wells of cells were collected from 2 days before differentiation up to 15 days post-differentiation. As soon as that was established, the effect of different agents on ZAG mRNA levels of expression was investigated.

At day 7 after induction of differentiation, the feeding medium was aspirated off the cells and was replaced with fresh feeding medium, insulin-free feeding medium, or FCS-free medium as appropriate. After 24 h, the different treatment agents were mixed in feeding

media, or insulin-free media or FCS-free media and 1 ml was added to the cells as appropriate. Cells used as controls also had their feeding media replaced. Cells were incubated with the treatment agents for 24 h before being collected. When a dose-response experiment was performed, cells were treated with increasing concentrations of the agent for 24 h.

2.4.2.5 Cell and media collection

The medium was first collected in 2 ml sterile RNase free tubes, and then 700 µl of Trizol reagent was added in each well to remove cells from the bottom of the well. The Trizol/cell mixture was gently pipetted up and down to ensure collection of the maximum number of cells and was then placed into sterile RNase free tubes and stored at -80^{0}C to prevent RNA degradation until further analysis. Collected medium was first centrifuged at 1,000 g for 10 min, the supernatant was transferred to a fresh tube and was then stored at -80^{0}C as well.

2.4.3 Light microscopy

Cells were visualised using phase contrast light microscopy. The image was captured and photographed using a CCD video camera (WILD MPS 515, SPOT, Switzerland).

2.5 Total RNA isolation from cells and tissues using the Trizol - Reagent method

2.5.1 Reagents

(i) RNAse AWAY

(ii) Trizol - Reagent

(iii) Chloroform

(iv) Isopropanol

(v) 75% Ethanol

(vi) UV-irradiated distilled water

(vii) Ultra-pure water

2.5.2 Trizol - Reagent RNA extraction method

Before starting, scissors, tweezers and the homogeniser blade attachments to be used were sprayed with RNase AWAY, left for 30 min and then rinsed with UV-irradiated distilled water to remove any RNases present. The homogeniser blade was rinsed four times between samples in four different universal flasks containing UV-irradiated water, with the flasks being changed between samples from different groups.

A sample of 100 mg of WAT and BAT, or 50 mg in the case of other tissues, either fresh or frozen was placed in a sterile 5 ml tube containing 1 ml of Trizol reagent, the volumes being adjusted accordingly. The samples were disrupted using an electronic homogeniser. In the case of RNA extraction from cells, cells were already kept frozen in 700 µl of Trizol reagent per well of cells and were then passed through a 23 gauge needle ten times, ensuring that the needle was changed between different groups of cells.

If WAT was used, then an intermediate step was required in order to remove the lipid. After homogenisation the sample was centrifuged at 14,000 rpm for 10 min at 4°C. This usually resulted in a fatty layer on top of the supernatant which was avoided while the supernatant was transferred to a fresh tube, taking care not to disrupt the cell debris pellet formed at this stage.

The sample was then incubated for 5 min at room temperature, before adding 200 µl of chloroform. It was then shaken vigorously for 15 sec, let stand at room temperature for 10 minutes and centrifuged at 14,000 rpm for 15 min at 4°C creating three layers, a colourless upper aqueous phase containing RNA, a white interphase containing DNA and a bottom red phenol phase containing protein. The top layer was transferred to a fresh tube, the interphase was discarded, while the lower layer was transferred to a new tube and kept at -80°C for protein extraction. Fifty µl of isopropanol were then added to the sample, which was vortexed and kept for 10 min at room temperature. The sample was centrifuged at 14,000 rpm for 10 min at 4°C and the supernatant was transferred to a new tube. Another 450 µl of isopropanol was then added to the sample, which was vortexed, let stand for 10 min at room temperature and then centrifuged at 14,000 rpm

for 10 min at 4°C. Following that, the supernatant was discarded taking care of the pellet, which was vortexed in 500 µl of 75% ethanol. The sample was then centrifuged at 14,000 rpm for 10 min at 4°C. The supernatant was removed and the pellet was allowed to air dry for 5-10 min. The pellet was dissolved in 10-30 µl of ultra-pure water and stored at -80°C until further use.

2.5.3 TURBO DNase treatment of RNA

Although all possible care was taken not to contaminate RNA samples, a certain degree of contamination could not be avoided. DNA contamination of RNA samples however would later result in inaccurate quantification. To minimise this problem, whenever RNA samples were used for real-time RT-PCR analysis, a TURBO DNA-free Kit was used to remove any remaining traces of DNA from RNA preparations and thus improve the efficiency of the quantification analysis.

2.5.3.1 Reagents

(i) 10x TURBO DNase buffer

(ii) TURBO DNase (2 units/ µl)

(iii) DNase Inactivation Reagent

2.5.3.2 Method

According to manufacturer's instructions, 0.1 volume of 10x TURBO DNase Buffer and 1 µl TURBO DNase, which is suitable for removing up to 1 µg of DNA from RNA in an up to 100 µl reaction volume, were added to the RNA sample and mixed gently. The sample was then incubated at 37°C in a hybridisation oven for 30 min with gentle shaking. Two µl or 0.1 volume DNase Inactivation Reagent, whichever was greater, was then added and the sample was incubated for 2 min at room temperature, mixing occasionally to redisperse the Inactivation Reagent, which removes the DNase and any divalent cations from the sample. The sample was then centrifuged at 10,000 g for 1.5 min, and the supernatant, which contains the RNA, was carefully transferred into a fresh tube.

2.5.4 RNA quantification

RNA samples were quantified using a spectrophotometer (Biophotometer). One µl of the RNA was diluted, the diluted sample was placed in a disposable plastic cuvette and the absorbance was measured at 260 nm and 280 nm with distilled water used as a blank. The concentration of RNA (µg/ µl) was automatically calculated.

Since the maximum absorbance of nucleic acids is at 260 nm and RNA has an extinction coefficient of approximately 44 at that wavelength, the concentration of RNA can be calculated by the spectrophotometer using the Beer-Lambert law:

$$[\text{RNA}]\ \mu g/\ \mu l = A_{260} \times 44 \times \text{Dilution Factor}/\ 1000$$

The ratio between A_{260} and A_{280} was used as a measure of the purity of the RNA. A value of 2 indicated a pure sample, whereas a value of 1.6 or less indicated contamination (essentially from protein).

2.6 Reverse-transcription polymerase chain reaction (RT-PCR)

2.6.1 First-strand cDNA synthesis

This procedure is used to generate single-stranded DNA (ssDNA) strands (cDNA) complementary to the mRNA sequences in the total RNA samples. For this, anchored oligo-dT primers were used instead of standard dT primers or random decamers. Standard dT primers anneal at random points within the poly-(A) tail and cDNAs generated this way contain long 3' poly (dA/dT) sequences that are largely responsible for the low efficiency of identification of the genes expressed at lower levels. Oligo-dT primers also generate truncated cDNA through internal poly (A) priming which in turn interrupts the generation of full-length cDNA (Wang *et al.*, 2000). Furthermore, random decamers anneal at a random point along the mRNA sequence. It has been demonstrated (Nam *et al.*, 2002) that this problem of internal poly-(A) can be minimized with replacement of these primers with anchored oligo-dT primers, since they are designed to

anneal at the mRNA/ poly-(A) junction instead, thus starting transcription at the start of the 3' end of the coding mRNA sequence. This minimizes the generation of truncated cDNA, thus providing high-quality cDNAs, and further improving the efficacy of PCR and real-time PCR for the study of genes that are not highly expressed.

2.6.1.1 Reagents

First strand DNA was reverse transcribed from total RNA by using a Reverse-iT™ first strand synthesis kit (ABgene, UK), which contained:

(i) Anchored oligo-dT (500 ng/ µl)

(ii) dNTP mix (5 mM each)

(iii) 5x 1st strand synthesis buffer

(iv) DTT (1 M)

(v) Reverese iT™ RTase Blend (50 units/ µl)

(vi) Ultra-pure water

2.6.1.2 Method

The procedure was carried out using sterile RNase/ DNase – free tubes and filter tips. For a 20 µl reaction, 1 µg of RNA, 1 µl oligo dT primer and up to 12 µl sterile water were added to a 0.5 ml tube, vortexed, and then heated to 70°C for 5 min in order to remove any secondary structure. The sample was then immediately placed on ice, before adding the following: 4 µl of 5x buffer, 2 µl of dNTP mix, I µl of 1M DTT, and 1 µl of reverse transcriptase. The sample was then vortexed and incubated at 47°C for 30 min. To inactivate the Reverse-iT RTase, the sample was finally incubated at 75°C for 19 min. The sample was then either stored at -20°C or immediately used for polymerase chain reaction (PCR).

2.6.2 Polymerase Chain Reaction (PCR)

For PCR, first the cDNA sequence is used to design a pair of primers, one complementary to each strand of the DNA double helix and lying on opposite sites of the region to be amplified. How this pair of primers is designed is discussed in the following

section. Previously made cDNA is used as a template for PCR reaction and DNA polymerase is used to amplify the quantity of the cDNA of interest. The process starts with a denaturation phase at 94°C, which is followed by 20 to 40 amplification cycles. Each cycle doubles the amount of DNA synthesized in the previous cycle and consists of three steps; denaturation, annealing and extension. Denaturation results in the dissociation of double-stranded DNA (dsDNA) into single-stranded DNA (ssDNA) and the unwinding of its helical structure. Annealing enables the primers to hybridise to their complementary bases on the ssDNA. Annealing temperature, as further discussed in the following section, is primer specific and depends on the primer length and GC content. Finally, during extension, the DNA polymerase synthesises a complementary DNA strand starting from the primer. The duration of the extension phase depends on the size of the product being amplified and as general rule it is 60 sec/ kb of the target gene.

There are a number of potential housekeeping genes. These should be expressed at a constant level in different tissues, and at a constant level within the same tissue in all conditions, and they include β-actin, glyceraldehyde-3-phosphate dehydrogenase (GAPDH), hypoxanthine guanine phosphoribosyl transferase (HPRT), 18S ribosomal RNA and RNA PolyA II. Housekeeping genes are used to assess the relative degrees of expression of the genes of interest and also indicate the quality of the template material. In this study, β-actin was used for both PCR and real-time PCR assays (see section 2.7.5). In PCR assays, a β-actin PCR was performed as soon as the cDNA samples had been synthesised to check the samples' quality, thus verifying the integrity of the original RNA. If bands had been faint or undetectable, suggesting degradation of the original isolated RNA, then the RNA integrity could have been checked directly by denaturing gel electrophoresis, which would allow RNA visualisation. However, no problems of this nature were encountered throughout this study.

2.6.2.1 PCR primer design

Primers were designed using Primer Premier 5 software (Biosoft International, Palo Alto, CA, USA) and synthesised commercially (MWG Biotech. Ebersberg, Germany or Eurogentec, Romsey, UK).

There a few rules that apply to PCR primer design, which were followed in the studies described in this thesis for optimal results. Primers were designed to span at least one intron, in order to avoid the generation of PCR products from any genomic DNA contaminants present in the cDNA template solution. Intron locations were identified using the NCBI 's Map Viewer utility. Primers need only be 18-30 nucleotides long. The longer the primer the more specific it is during amplification but longer primers are more likely to form secondary structures. Both primers had similar G+C content, between 40% and 60% (so that they had similar annealing temperatures), with a minimal degree of self-complementarity (to avoid formation of secondary structures) and no complementarity to each other (so that primer duplexes were not formed).

Annealing temperatures (T_a) are based around melting temperature (T_m), the temperature at which 50% of the primers are annealed to their target sequence. For primers of <20 bases, Tm can be calculated in ^{0}C from the equation: Tm = 4(G+C) + 2(A+T), where G, C, A and T are the number of bases in the primer. Using this as a starting point, the optimum annealing temperature can be determined by trial and error. The individual primer T_ms were between 60^0 and 65^{0}C, and within 2^{0}C of each other, so that the T_a of the pair would not be below 55^{0}C, as low T_a promotes non-specific binding. The primers were ideally designed to amplify a 180-600 bp product, as larger products would require longer annealing times to be amplified. The sequence of both primers and that of the expected product were finally BLAST searched to ensure specificity.

Table 2.1 includes all primers used for PCR analysis in the studies to follow.

2.6.2.2 PCR primer optimization

Primers were tested on receipt by performing PCR on some cDNA samples in which a signal for that particular gene was expected. During that first step of the optimization, a high number of cycles (35-38) was used and a gradient analysis was performed to determine the optimal annealing temperature. To do that, samples containing the same cDNA underwent PCR amplification over a range of annealing temperatures. The highest temperature at which a strong signal was obtained with no non-specific products

Table 2.1 Sequences of the primers and the PCR conditions

Gene	Primer Sequence (5'-3')	T_a ^0C	Cycles no.	Size bp	Accession No.
mZAG s	GCCTTCTTCCACTACAACAG	54	30	396	NM_013478
mZAG as	TTCAGGACACTCCTCCTCTA				
mβ-actin s	TGCTGTCCCTGTATGCCTCT	60	23	463	NM_007393
mβ-actin as	AGGTCTTTACGGATGTCAACG				
mresistin s	GAAGAACCTTTCATTTCCCCTCC	60	25	266	NM_022984
mresistin as	CTTCACGAATGTCCCACGAGCC				
rZAG s	AAATAACAGAAGCAGTGGAGCAG	54	30	322	NM_012826
rZAG as	TTTGTGGGTAGAAGTCATAGGC				
rLeptin a	GTCCAGGATGACACCAAAACCC	60	30	239	NM_013076
rLeptin as	TCTCGCAGGTTCTCCAGGTCAT				
rAdip. a	GTCCCTCCACCCAAGGAAACT	56	28	271	NM_144744
rAdip. as	GCCCTACGCTGAATGCTGAGT				
rβ-actin s	GCCCATCTATGAGGGTTACGC	62	23	543	NM_031144
rβ-actin as	GAGCCACCAATCCACACAGAG				

T_a ^0C, annealing temperatures; Cycle no, cycle numbers; bp, base pair indicating size of the expected products. m, mouse; r, rat; s, sense primer; a, antisense primer. Adip, adiponectin.

was selected. In general, primer optimization was performed using cDNA from a source with a relatively weak signal of the specific gene of interest, so as to ensure that it could then be detected in samples expressing it at a low level.

2.6.2.3 Reagents

(i) Ultra-pure water

(ii) 100 µM stock solution of each sense and antisense primers

(iii) 1.1x ReddyMix (ReddyMix PCR MasterMix kit)

2.6.2.4 Method

The procedure was carried out using sterile RNase/ DNase – free tubes and filter tips. One µl of each RT reaction, 2 µl in the case of ZAG, was amplified in a 25 µl PCR reaction containing 0.02 mM of each primer and 1.1x Reddy Mix™ PCR Master Mix that consists of 1.5 mM $MgCl_2$, 1.25 units Taq polymerase, 75 mM Tris HCl (pH 8.8 at 25°C), 20 mM $(NH_4)_2SO_4$, 0.01% Tween 20 (v/v) and 0.2 mM each of the dNTPs. Sterile water was used to make up to 25 µl reaction when needed.

PCR was performed on a thermal cycler (Hybaid, U.K). The sample was incubated with an initial denaturation at 94°C for 2 min, followed by 23-35 cycles, depending on the gene amplified (see Table 2.1), consisting of denaturation at 94°C for 20 sec, annealing, whose temperature varied among different genes (see Table 2.1), and extension at 72°C for 40 sec, or 60 sec in the case of ZAG. After the last cycle, the sample underwent elongation at 72°C for 5 min in all cases. Negative control RT-minus reactions were carried out to establish that the target RNA was not contaminated with DNA.

2.6.3 Agarose gel electrophoresis

PCR products were visualised on 1% agarose gels stained with ethidium bromide. Ethidium bromide is fluorescent and contains a planar group that intercalates between the stacked bases of DNA and is the most convenient method for visualising DNA under UV irradiation in agarose gels.

2.6.3.1 Reagents

(i) Agarose

(ii) 5 mg/ml Ethidium bromide

(iii) 1x TBE buffer

(iv) 100 bp DNA ladder

2.6.3.2 Method

Gel casting trays were used for running gels, assembled with tape at each end. The amplification of targeted genes was checked on a 1% agarose gel. The volumes of gel made up varied, according to the size of the tank and tray used. Agarose was weighed out into a 250 ml conical flask and then 1 x TBE was added to the required volume. The mixture was then heated in a microwave oven, mixing occasionally, until the agarose melted. Once melted the mixture was allowed to cool slightly, before adding 5 ng/µl ethidium bromide. The gel was then poured into the gel - casting tray, and allowed to set for at least 30 min. Once the gel had set, the tape was removed and it was placed into the electrophoresis tank. 1 x TBE was added until the gel had completely submerged, and the comb was then removed. Ten – 20 µl of PCR product was loaded into each well, taking care that wells did not overflow, and run alongside 2 µl of 100 bp ladder, at a constant 100 – 120 V and maximum current for 30 – 60 min.

When the samples had been electrophoresed, the gel was placed on a UV transiluminator (2011 Macrovue) to allow visualisation of the products. The images were recorded using a digital camera (KDS DC120) and analyzed using KDS ID 1 image analysis software.

2.7 Real-time Polymerase chain reaction (qPCR) – Taqman system

Real-time PCR has become the most popular method and the 'gold standard' for quantitating steady-state mRNA levels. It measures formation during the exponential phase, by taking advantage of the fact that DNA amplifications do occur efficiently early

in the reaction process. This measurement correlates to the amount of specific starting DNA, thereby allowing quantification.

2.7.1 Taqman system description

The real-time work performed in this study used the Taqman system. This system continuously measures PCR product accumulation using a set of primers and a dual-labeled fluorogenic oligonucleotide probe called the Taqman probe. This probe is composed of a short oligodeoxynucleotide (20-30 bases) that is labelled with two different fluorescent dyes. As schematically presented in Figure 2.1, on the 5' terminus is a reporter dye and on the 3' terminus is a quenching dye (usually TAMRA). This probe sequence is homologous to an internal target sequence present in the PCR amplicon. When the probe is intact, energy transfer occurs between the two fluorophores and emission from the reporter is quenched by the quencher (FRET – fluorescence resonance energy transfer). During the extension phase of PCR, the probe is cleaved by 5' nuclease activity of Taq polymerase thereby releasing the reporter from the oligonucleotide quencher, thus ending FRET and producing an increase in reporter emission intensity (at 518 nm for FAM), which increases in each cycle proportional to the rate of probe cleavage. In the real-time machine, the laser light source excites each well and a CCD camera measures the fluorescence spectrum and intensity from each well to generate real-time data during PCR amplification. The software examines the fluorescence intensity of reporter and quencher dyes and calculates the increase in normalized reporter emission intensity over the course of amplification (ΔR). The results are then plotted [usually as ΔR_N, after normalisation of the reporter dye signal to a reference dye (usually ROX) to correct for differences in reaction mix volumes between wells] versus time, represented by cycle number, to produce a continuous measure of PCR amplification. To provide precise quantification of initial target in each PCR reaction, the amplification plot is examined at a point during the early log phase of product accumulation. This is accomplished by assigning a fluorescence threshold above background and determining the time point at which each sample's amplification plot reaches the threshold (C_T) (Bustin, 2002; Giulietti *et al.*, 2001; Valasek & Repa, 2005).

Figure 2.1 The principle of Taqman assay

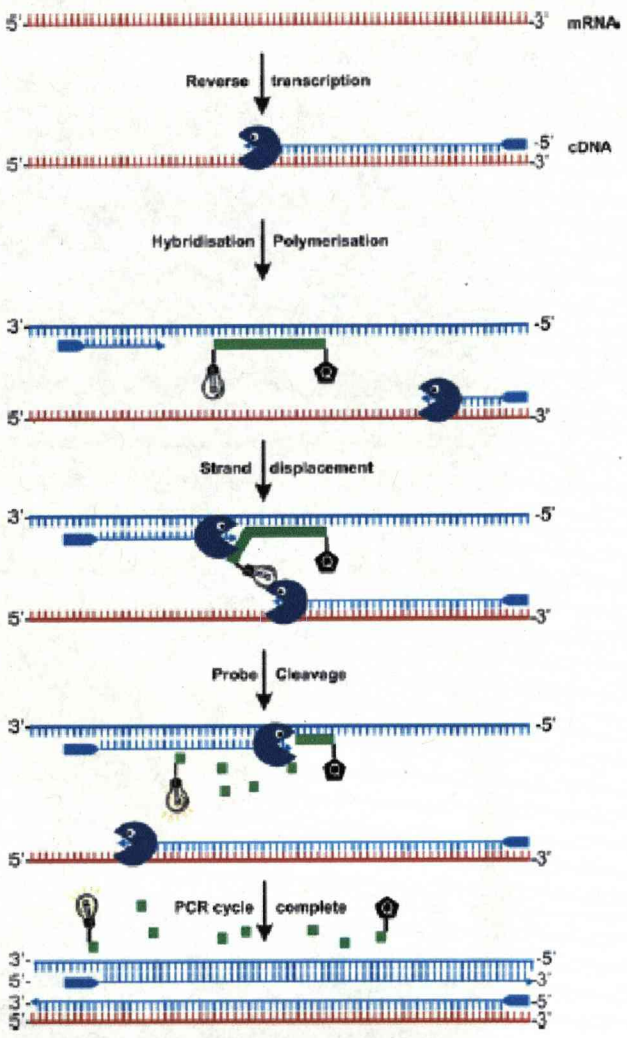

(Source: Bustin & Mueller, 2005)

This diagram shows the steps at each Taqman cycle. After denaturation, primers and probes anneal to their targets. The probe contains a reporter dye at the 5' end and a quencher (Q) at the 3' end. During the polymerisation step, the 5' nuclease activity of the Taq polymerase displaces and cleaves the probe. This physically separates the reporter dye and quencher dyes, resulting in reporter fluorescence. The increase in signal is directly proportional to the number of molecules released during that cycle. Accumulation of PCR products is detected directly by monitoring the increase in fluorescence of the reporter dye.

2.7.2 Primers and Taqman probes design and optimisation

Murine and rat primers (apart from ZAG rat primers) and Taqman probe sequences were designed (with the kind assistance of Dr J Jenkins) with Primer Express software (Applied Biosystems). ZAG rat primers and probe were designed using Beacon Designer software (PREMIER, Biosoft International). All sets of primers and probes were synthesised commercially (Sigma-Genosys, Haverhill, UK and Eurogentec, Romsey, UK). They were all designed to be 20-30 bases in length, while the PCR product size was designed to be no more than 150 bases, as PCR is more efficient with smaller amplicons. Primers' T_ms were 58-60^{0}C, while their individual T_ms did not differ more than 1-2^{0}C. In addition the forward primer contained no more that 2 G + Cs in the last 5 bases of the 3' and T_m of the probes was significantly greater (approximately 10^{0}C) than that of the primers, to ensure that they hybridise before the primers. The probes did not overlap with, or have sequence complementarity with either of the primers and they did not contain a G at their 5' ends, as a G adjacent to the reporter dye quenches reporter fluorescence even after the probe has been cleaved. Finally, they were designed so that there were no more than 4 Gs in a row and the number of Gs was smaller than that of Cs. Finally, as for RT-PCR, primers were designed to span an intron.

All the sequences for primers and probes used in Taqman assays in this study are presented in Tables 2.2 and 2.3, together with the optimised final reaction concentrations. For each new set of primers and probe an optimisation of the concentrations was first conducted. An assay was performed with final primer concentrations ranging from 50 nM to 900 nM (in all possible combinations of 50 nM, 300 nM and 900 nM), while the probe concentration was fixed at 200 nM. The combination that gave the lowest C_T and the highest R_N was then selected and was used to determine the probe optimal final concentration, which ranged from 25 nM to 225 nM. As with the primers, amplification plots were used to select the optimal concentration.

Table 2.2 Sequences of primers and Taqman probes of mouse target genes and working conditions for real-time PCR

Gene	Sequence (5'-3')	Conc. nM	Size, bp
mZAG			
S	GAGCCTGTGGGACCTTGGA	900	
A	CCTCCCTGGCCCTCTGAA	900	
P	AATGGAGGACTGGGAGAAGGAAAGCCA	225	
mLeptin			76
S	CATCTGCTGGCCTTCTCCAA	900	
A	ATCCAGGCTCTCTGGCTTCTG	900	
P	AGCTGCTCCCTGCCTCAGACCAGTG	225	
mAdipo			97
S	GGCTCTGTGCTCCTCCATCT	900	
A	AGAGTCGTTGACGTTATCTGCATAG	900	
P	CCCATACACCTGGAGCCAGACTTGGT	225	
mβ-actin			
S	ACGGCCAGGTCATCACTATTG	900	97
A	CAAGAAGGAAGGCTGGAAAAG	900	
P	ACGAGCGGTTCCGATGCCCTG	225	

Conc, the working concentrations for each primer and probe; bp, base pair indicating the product sizes (S, sense primer; A, antisense primer; P, probe; m, mouse. Adipo, adiponectin.

Table 2.3 Sequences of primer and Taqman probe sequences of rat target genes and working conditions for real-time PCR

Gene	Sequence (5'-3')	Conc. (nM)	Size (bp)
rZAG			
S	CCTTCAGGAGACTGGGTCTTATTC	900	99
A	GTTGAGAAATGCGGTGGCTTG	900	
P	CCTCTACACCGGGTTGTCCAGGCC	225	
rLeptin			
S	AACCCTCATCAAGACCATTGTCA	900	100
A	CCCGGGAATGAAGTCCAAA	900	
P	TGACATTTCACACACGCAGTCGGTATCC	225	
rAdipo.			
S	CCCCTGGCAGGAAAGGA	900	64
A	CCTACGCTGAATGCTGAGTGAT	900	
P	AGCCCGGAGAAGCCGCTTACATG	225	
rMCP-1			
S	CTGTCTCAGCCAGATGCAGTTAA	300	69
A	TGGGATCATCTTGCCAGTGA	300	
P	CCCCACTCACCTGCTGCTACTCA	225	
rNGF			
S	TGAAAGGCTGGGTGCATAGC	900	76
A	GCCTGTACGCCGATCAAAA	900	
P	TCCATGTTGTTCTACACTCTGATCACAGCG	225	
rIL-6			
S	CGAAAGTCAACTCCATCTGCC	300	80
A	GGCAACTGGCTGGAAGTCTCT	300	
P	TCAGGAACAGCTATGAAGTTTCTCTCCG	225	
rβ-actin			
S	GACAGGATGCAGAAGGAGATTACTG	300	101
A	GAGCCACCAATCCACACAGA	300	
P	CACCATGAAGATCAAGATCATTGCTCCTCCT	225	

Conc, the working concentrations for each primer and probe; bp, base pair indicating the product sizes (S, sense primer; A, antisense primer; P, probe; r, rat; adipo, adiponectin).

2.7.3 Preparation of 96 well plates for real-time PCR

2.7.3.1 Reagents

(i) qPCR Core Kit:

10x Reaction Buffer

50 mM Magnesium chloride

5 mM dNTP mix

5 U/µl Hot Goldstar enzyme

(ii) Sense primer (300 nM), antisense primer (300 nM) and taqman probe (100 nM stock solutions.

(iii) Ultra-pure water

2.7.3.2 Method

Working solutions of the primers and probes were prepared at 10x concentrations by diluting the stock solution with ultra-pure water. Each 25 µl reaction contained the following:

10x Reaction buffer	2.5 µl (1x final concentration)
50 mM $MgCl_2$	2.5 µl (5mM)
5 mM dNTP	1 µl (200mM)
Sense primer	2.5 µl (see Table 2.2 and 2.3)
Antisense primer	2.5 µl (see Table 2.2 and 2.3)
Taqman probe	2.5 µl (see Table 2.2 and 2.3)
5 U/µl Hot Goldstar enzyme	0.125 µl (0.025 U/ µl)
Ultra-pure water	11.375 µl

A master mix was made up, with 5-10% excess to allow for pipetting errors, which contained all the above components for the PCR, minus the cDNA template. Twenty-four µl, or 23 µl in the case of ZAG, of the master mix were then aliquoted to each well. One or 2 µl cDNA was then added to each well for a total reaction volume of 25 µl. All

samples were added on the plate in duplicate or triplicate if that was possible. 'No primer', 'no probe' and 'no template' control samples were also added on the plate for each set of primers and probe and the plate was sealed with an optical cover. The plate was then spun at 1000 rpm for 1 min to ensure the reaction mix was not sticking to the sides of the well. Since the Stratagene machine (see section 2.7.4) was more sensitive, in most cases 12.5 µl reactions were prepared instead of 25 µl. In that case 11.5-12 µl of master mix were placed in each well before adding the cDNA. If two or more plates needed to be compared, a number of standards were used in all the plates.

2.7.4 Taqman system real-time PCR machine setup

Some studies described in this thesis were performed using an ABI Prism 7700 instrument (Applied Biosystems), while the rest were performed using the Mx3005P QPCR system (Stratagene). The same sets of primers and probes were used in both systems. The ABI Prism 7700 system requires an Apple Macintosh which runs the Sequence Detector v1.7a software (Applied Biosystems). The Mx3005 system was connected to a PC (Dell Optiplex GX280) and data was collected and analysed with Mx3005P v2.02 software (Stratagene). In both programs, wells were labelled according to content on the plate setup screen. In the latter, FAM was specified as the reporter dye and ROX as the reference dye. The plate was inserted into the heat block and an optical pad placed on top so that the holes aligned with the well positions. The cover was locked into position and the run started.

Amplifications were performed starting with a 2 min activation stage at 50°C, then a 10 min denaturation step at 95°C followed by 40 cycles consisting of a denaturation step of 15 sec at 95°C and a combined primer annealing and extension step of 60 sec at 60°C. Data was collected automatically by the software, and analysed once the run was complete.

2.7.5 Analysis of real-time PCR data

The amplification plots were displayed in log scale using the Sequence Detector software and the threshold was then manually adjusted. The representations were then switched back to linear and the software automatically recalculated the C_T value for each well (Figure 2.2). As mentioned above, the C_T is defined as the cycle number at which the fluorescence emitted from the well crossed the threshold. The results were then exported as a Microsoft Excel file and mRNA levels of expression were analysed by relative quantitation with the $2^{-\Delta\Delta CT}$ method (Livak & Schmittgen, 2001). All samples were normalised to values of β-actin, which was used as the internal standard in all experiments. Results were expressed as fold changes of C_T values relative to controls.

2.8 Protein detection using western blotting method

Western blotting (Towbin *et al.*, 1979) is a method used to detect protein in a given sample of tissue homogenate or extract. It uses gel electrophoresis to separate denatured proteins by mass. The proteins are then transferred out of the gel and onto a nitrocellulose membrane where they are probed using antibodies specific to the protein of interest. The technique relies on the primary antibody to detect the protein of interest from the total of proteins found on the membrane. The secondary antibody then recognizes the primary antibody and binds to it. Horse radish peroxidase (HRP) conjugated to the secondary antibody converts a luminol substrate to a light releasing substance and this light is detected as a spot on a film (Figure 2.3). Western blotting is broadly used to examine the amount of protein in a sample, or compare protein expression in different groups.

Figure 2.2 Default baseline plot-log and linear view

(A)

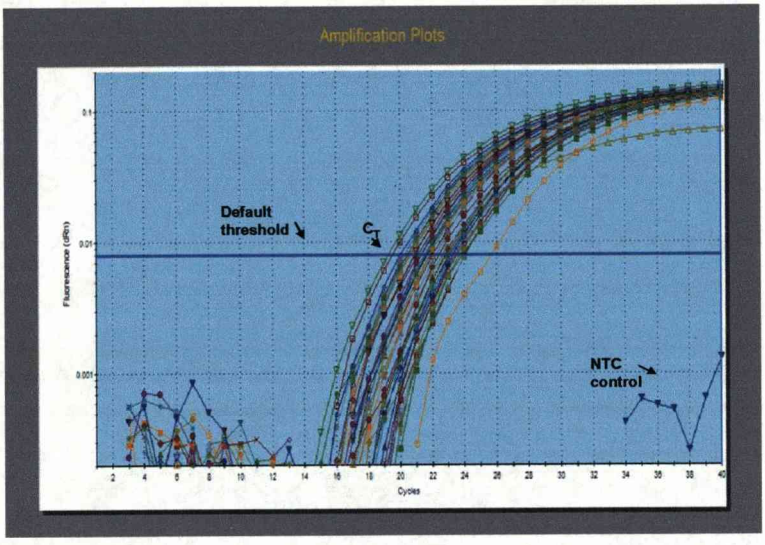

(B)

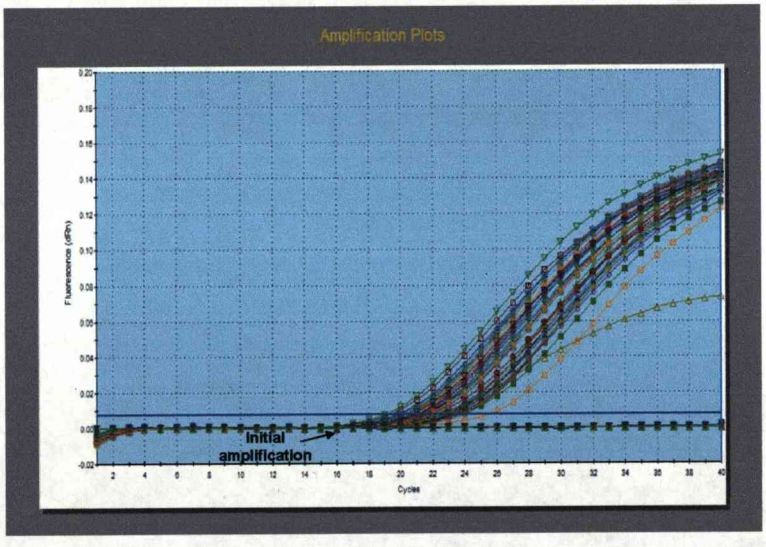

The figure shows an image of an amplification plot with default settings, as seen on the Mx3005P v2.02 software (Stratagene). (A) Log view: while here the plot could be adjusted, ideally set above the background fluorescence, within the exponential phase of the PCR. (B) shows the linear view of the same assay.

Figure 2.3 Schematic diagram of protein detection

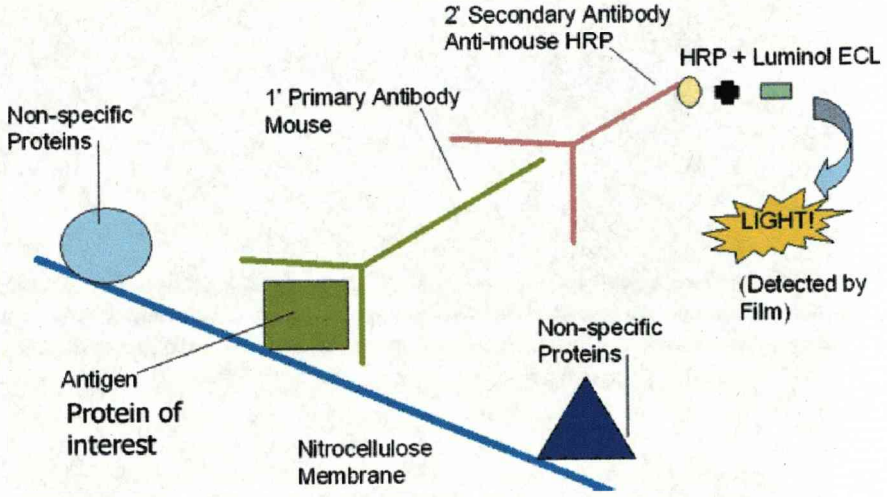

(Source: http://www.molecularstation.com/images/western-blot.gif)

This schematic diagram represents the detection procedure during immunoblotting. The membrane is shown in dark green. Milk proteins block non-specific antibody binding. The protein of interest is shown in light green. Primary and secondary antibodies are shown as upside-down Ys. HRP is shown in yellow. When the membrane is soaked into the ECL detection reagents, a peroxidase catalyzed oxidation of luminol is elicited and subsequently enhanced chemiluminescence, where the HRP labeled protein is bound to the antigen on the membrane. The resulting light is detected on the Hyperfilm.

2.8.1 Protein Isolation

Different methods were used for protein isolation from frozen and frozen tissues, through Trizol reagent after RNA had been extracted first, and from 3T3-L1 cells.

2.8.1.1 Protein isolation from frozen tissues

2.8.1.1.1 Reagents

(i) SHE buffer:

250 mM Sucrose

1 mM HEPES

0.2 mM EDTA

Distilled water

Protease Inhibitors (1 tablet per 10 ml buffer)

The pH of the solution was adjusted to 7.2 and stored at 4^{0}C for up to three months.

2.8.1.1.2 Method

One hundred mg of tissue sample were homogenised in a glass homogeniser in 500 µl SHE buffer. The sample was then centrifuged at 12,000 g for 15 min at 4^{0}C. The supernatant containing the protein was retrieved, while the pellet, which contained cell debris, nuclei and mitochondria, was discarded. The protein concentration was then determined using the BCA assay (Section 2.8.2) and the sample was either used or stored at -80^{0}C.

2.8.1.2 Protein Isolation from TRizol reagent

2.8.1.2.1 Reagents

(i) Wash Solution [0.3 M Guanidine Hydrochloride in 95% ethanol (0.3M GHCl)

(ii) 100% ethanol

(iii) 1% Sodium dodecyl sulphate (SDS) containing protease inhibitors (I tablet per 10 ml)

2.8.1.2.2 Method

As previously described in the RNA extraction method (Section 2.5.2), the phenol (bottom) layer after the chloroform precipitation was stored to perform protein extraction. Three-hundred µl of 100% ethanol was then added to the sample per 1 ml of TRizol reagent used for the initial homogenization. Volumes were adjusted accordingly when 700 µl had originally been used, as in 3T3-L1 cells. The sample was then mixed by inversion and allowed to stand at room temperature for 2-3 min before being centrifuged at 2,000 x g for 5 min at 4°C to pellet any remaining traces of DNA. The supernatant containing the protein was then carefully transferred into a fresh tube and 1.5 ml of isopropanol was added per 1 ml of TRizol initially used, to precipitate the protein. The sample was then incubated for 10 min at room temperature and centrifuged at 12,000 x g for 10 min at 4°C. The supernatant was discarded and the pellet containing the protein was washed in 2 ml of wash solution per 1 ml of TRizol used initially. The sample was allowed to stand for 20 min at room temperature and was centrifuged at 7,500 x g for 5 min at 4°C. The wash solution was then discarded, replaced by fresh one and the whole washing procedure was repeated twice more. After discarding the wash solution the third time, the protein pellet was vortexed in 2 ml of 100% ethanol and incubated for 20 min at room temperature. The sample was then centrifuged at 7,500 x g for 5 min at 4°C. The ethanol was discarded and the protein pellet was vacuum dried for 5 min. The sample was then sonicated, in 20-30 µl of 1% SDS containing protease inhibitors, three times each lasting 10 sec with a ten sec interval between them in order for the pellets to dissolve. The sample was finally centrifuged at 10,000 x g for 10 min at 4°C to sediment any insoluble material and the protein supernatant was transferred into a fresh tube. The sample was stored at -80°C or immediately used to proceed with the rest of the western blotting procedure.

2.8.1.3 Protein isolation from 3T3-L1 adipocyte media using TCA precipitation

2.8.1.3.1 Reagents

(i) 50% TCA solution in water (used cold)

(ii) 1% SDS with protease inhibitors (1 tablet per 10 ml)

(iii) 1x PBS

2.8.1.3.2 Method

Five hundred µl of TCA solution was added in 1.5 ml of medium, collected as previously described in Section 2.3.2.5, giving a final TCA concentration of 12.5%. The sample was then incubated for 3 h on ice before being centrifuged at 14,000 rpm for 30 min at 4°C. The supernatant was then discarded and the pellet containing the protein was first washed in 200 µl of 1x PBS and then dissolved in 1% SDS. If the medium did not contain serum, it was dissolved in 10 µl, whereas otherwise in 300 µl of 1% SDS. The sample was then stored at -80°C.

2.8.2 Protein quantification by the BCA method

2.8.2.1 Reagents and equipment

(i) Bicinchoninic acid (BCA) solution

(ii) Copper (II) sulphate solution

(iii) Protein standard (2 mg/ ml BSA)

(iv) 1% SDS

(v) 96-well microplate

2.8.2.2 Method

A standard curve was created using Bovine serum albumin (BSA) as a protein standard with final concentrations of 0, 4, 8, 12, 16, 24 and 40 µg/ well. To do that, 0, 2, 4, 6, 8, 12 and 20 µl of BSA were added to the wells in duplicate and made up to 20 µl with 1% SDS. In terms of the samples, 1 µl of each sample of unknown concentration was added to the wells and then made up to 20 µl with 1% SDS. A 1:50 dilution of copper sulphate in BCA solution, which contains BCA, sodium carbonate, sodium tartrate and sodium bicarbonate in 0.1 M NaOH (pH 11.25), was prepared and 200 µl of this solution was added into each well. The plate was then incubated for 30 min at 37°C in a hybridization oven and after that time the samples containing the protein could be seen changing from green to purple. The extinction was then measured at 570 nm in a Benchmark Type plate reader. Data was collected with Microplate Manager 5.2 software and a standard

curve was made relative to which the protein concentration of the samples was determined (see Figure 2.4). The correlation coefficient (r) of the standard curve should ideally be 1. In cases where r was lower than 0.996 the process was repeated. Furthermore, in cases when protein samples were either too concentrated or too diluted for the reader to determine a concentration, the reactions were repeated by adjusting the volume of the samples accordingly.

2.8.3 Sodium dodecyl sulphate Polyacrylamide Gel Electrophoresis (SDS PAGE)

2.8.3.1 Reagents

(i) Loading buffer:

125 mM Tris-HCL pH 6.8

2.5% SDS

2.5% β – Mercaptoethanol

6.25% Glycerol

2.5 mg/ml Bromophenol blue

Once the ingredients had been added together, loading buffer was aliquoted and stored at -20^{0}C up to a few months.

(ii) Separating gel (10 ml) (10%):

4.825 ml distilled water

2.475 ml 40% Acrylamide/ bis

2.5 ml 1.5 M Tris pH 8.8

100 µl 10% SDS

100 µl 10% Ammonium Persulfate (AP)

10 µl TEMED

AP was made fresh each time

(iii) Stacking gel (5ml) (4%):

3.732 ml Distilled water

498 µl 40% Acrylamide/ bis

Figure 2.4 Standard curve for protein concentration estimation

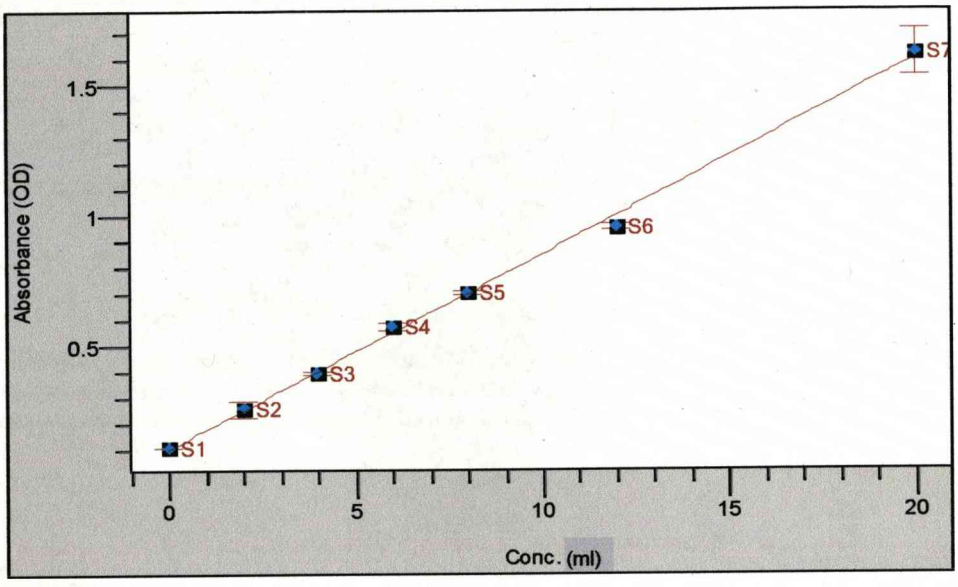

Standard Curve: Abs = 0.0749 * Conc + 0.108
Correlation Coefficient 0.999

This figure represents a standard curve for protein concentration estimation using the BCA assay as obtained by MicroplateManager 5.2 software. BSA was used as a protein standard at final concentrations of 0, 2, 4, 6, 8, 12, and 20 µg. The optimum correlation coefficient (r) is as close to 1 as possible. Concentration is in ml.

630 µl 1.0 M Tris-HCl pH 6.8

50 µl 10% SDS

50 µl 10% AP

5 µl TEMED

(iv) Running buffer:

25 mM Tris-base

192 mM Glycine

0.1% SDS

Distilled water

The running buffer was stored at room temperature and was used only once.

2.8.3.2 Equipment

(i) Main vertical electrophoresis unit with safety lid

(ii) 2.0 mm notched glass plates

(iii) 2.0 mm plain glass plates

(iv) 1.0 mm spacers

(v) 1.0 mm comb, 12 or 16 wells

(vi) Casting base with silicone seals

2.8.3.3 Method

At first all the gel components were cleaned with ethanol, dried and then assembled following the manufacturer's instructions (*Scie-Plas,* Instruction manual for vertical electrophoresis units). Once assembled and locked onto the casting base, distilled water was poured between the glass plates to check for leaks. The water was then removed using filter paper. The separating gel was prepared and injected between the glass plates, without delay, using a 5 ml syringe and 21-gauge needle, leaving about 1/3 of the space for the stacking gel. Minimum pressure was applied to the syringe while injecting to avoid the formation of bubbles and using a fresh syringe and needle, 0.01% SDS was added to the top of the gel to a depth of 5 mm to stop it drying out and to keep the gel

level. Once the separating gel had set (10-20 min), the SDS was removed using filter paper, the stacking gel was prepared, injected between the glass plates the same way and the comb was inserted. It was then allowed to set for 20-30 min.

The protein concentration had already been estimated using the BCA method (see section 2.8.2). From the protein stock, 5 to 20 µg were run on the gel. The samples were made up to equal volume by adding 0.1% SDS and were then diluted 1:1 with loading buffer. They were then heated at a 95°C waterbath for 5 min, to denature the proteins allowing them to unfold completely. The SDS in the sample then surrounded the protein with a negative charge and the β-mercaptoethanol prevented the reformation of disulfide bonds.

The gel was then removed from the casting base and placed into the gel tank, which was filled with running buffer until both ends of the gel apparatus were completely submerged. The comb was then removed, the wells were repaired with a gauge needle if needed and the samples were loaded slowly so as not to overflow and run alongside 5 µl of rainbow protein marker at 40 mAmps constant and maximum voltage until the bromophenol blue dye was seen running off the gel (usually 1.5-2 h). During the run the tank was connected to cold water so that the system was kept cool. The electrophoresis unit was then disassembled and the gel transferred for electroblotting.

2.8.4 Electroblotting

2.8.4.1 Reagents and equipment

(i) Transfer buffer:

25 mM Tris-base

192 mM Glycine

20% Methanol

Distilled water

The buffer was made fresh and only used once

(ii) Fibre pads

(iv) Extra thick blotting paper

(v) Hybond ECL Nitrocellulose Membrane

(vi) Compression Cassettes (black (-) and white (+))

(vii) Running tank and lid

(viii) Internal Electroblotting module for two gels

All the components for the transfer were soaked into transfer buffer for about 15 min before assembling the blotting unit in the following order while still in buffer to prevent the formation of bubbles which interfere with the transfer procedure:

1.+ cassette, 2. foam pad, 3. blotting paper, 4. transfer membrane, 5. gel, 6. blotting paper, 7. foam pad, 8. – cassette

Before finalising and while still in buffer, it was made sure that there were no bubbles in between the components. The tank was filled with running buffer until the whole system was fully submerged and transfer was performed at 100 V constant for an hour, while cold water was constantly circulating at the bottom of the tank to keep it cool.

2.8.5 Immunological detection of proteins

2.8.5.1 Reagents and Equipment

(i) 0.1 % Ponceau S

(ii) Tris Buffered Saline (TBS) pH 7.5:

20 mM Tris - Base

500 mM Sodium Chloride

Distilled water

(iii) TTBS:

TBS

0.05% Tween-20

(iv) Blocking solution:

10% skimmed milk powder in TTBS

(v) Antibody diluent:

3% skimmed milk powder in TTBS

(vi) Primary and secondary antibodies

(vii) ECL Western blotting detection reagents

(viii) Photographic Developer (stored in the dark)

(ix) Photographic Fixer (stored in the dark)

(x) Intensifying screen cassette

(xi) Hyperfilm ECL

2.8.5.2 Ponceau S staining

Before proceeding with the detection, Ponceau S staining was performed on the membrane to ensure the success of the transfer and the equal loading of protein in all the lanes. As soon as the transfer was finished, the blotting unit was disassembled and the membrane was carefully placed in a small container face up and was submerged into Ponceau S. It was then placed onto a shaking platform for 15 min. The Ponceau was then tipped off and the membrane was washed in TBS buffer. After a period the protein bands could be visualised. TBS was then replaced until all red colour disappeared. The detection steps then followed.

2.8.5.3 Detection method

The membrane was placed in a box containing 100 ml of blocking solution and was incubated at room temperature for 1 h on a shaking platform or overnight at 4^0C. The primary antibody solution was prepared by making up 2 ml of antibody diluent containing 1:1000 antibody. The ZAG primary antibody was a mouse monoclonal (Santa-Cruz, USA). Monoclonal antibodies are better than polyclonal ones for western blotting since they create lower background on the blot and are more specific, thus producing cleaner results as less non-specific bands are detected. The membrane was placed into a pouch together with the primary antibody solution and incubated at 4^0C overnight on a shaking platform. The following day the membrane was placed into a clean box and washed with 50 ml of TTBS at room temperature for 10 min on a shaking platform. The TTBS was then replaced and the procedure was repeated twice more. The

membrane was then once again placed into a pouch and incubated with 2 ml of secondary antibody (HRP conjugated goat anti-mouse) solution (1:1000) at room temperature for 1 h on a shaking platform. After 1 h the membrane was once again placed in a box and washed three times in TTBS buffer, for 10 min each time. These were followed by 3 washes in TBS for ten min each. All 6 washes took place at room temperature on a shaking platform. The TBS was then replaced and the membrane was left standing for about 15 min while preparing for the development procedure.

For detection, 1.5 ml of each of the two ECL (Enhanced Chemiluminescence) reagents were mixed together, gently poured over the membrane, and incubated for 1 min at room temperature. After that any excess ECL detection reagent was discarded and the membrane was heat-sealed in Saran wrap membrane, gently smoothing out any air bubbles with tissue, and immediately preceded with the development procedure as the chemiluminescent signal only lasts for 1 h.

The development procedure took place in a dark room. The sealed membrane was placed face up into the intensifying screen with a piece of High performance chemiluminescence on top. The cassette was then shut and the membrane was exposed (usually for 30 sec – 1 min for tissue samples and 30 min for cell extracts). The film was then placed into the developer solution, shaking it gently, and as soon as the bands appeared, it was transferred to the fixer solution, again shaking gently, for 1-2 min. The film was finally rinsed in water for 15 min, to clean it from the fixer solution, before it was allowed to air dry.

The membrane was handled very carefully and with forceps at all stages. It was then stored at 4^0C and if desired could be re-probed with another antibody.

2.8.5.4 Determination of optimal primary antibody dilution

To obtain clean results with low background, it was important to determine the optimal primary antibody dilution for detection, as the secondary antibody dilution was known. For this purpose, a series of dot blots were carried out. A dilution range of protein sample was applied directly onto the nitrocellulose membrane, one blot being prepared for each

antibody dilution to be tested, and the membrane was allowed to air dry. The membranes were then blocked and washed exactly as described above. Several dilutions of primary antibody were then prepared (usually 1:100, 1:500, 1:1000 and 1:2000) and incubated with the membranes overnight at 4^0C. All subsequent steps were then the same as the ones mentioned above.

2.8.6 Protein quantification from western blotting

Once dried, the film was scanned using HP Precision Scan Pro 2.5 software and the optical density of the bands was then measured with MCID Basic 7.0 software. Density was measured as D x A-ROD and values were exported to Excel for further statistical analysis.

2.9 Statistical analysis

Statistical analysis was performed using Microsoft Excel 2003 or SPSS for Window v12 software. Comparisons between samples from two groups were assessed by Student's *t*-test (either paired or unpaired), while for 3 or more groups of samples one-way ANOVA with post-hoc multiple comparisons using a Bonferroni correction was employed. Differences were considered to be significant when $P<0.05$. All results are presented as means ± standard error of the mean (SEM), the group size varying between experiments (usually 5-8).

Chapter 3

ZAG expression in rodent adipose tissue and genetic models of obesity

3.1 Introduction

As previously discussed in Chapter 1, it has been demonstrated that ZAG is involved in lipid metabolism. Briefly, both *in vivo* and *in vitro* studies have shown that ZAG induces a rapid reduction in body fat and that it stimulates lipolysis (Hirai *et al.*, 1998), its lipolytic effect probably being mediated through the β_3-adrenoreceptor with upregulation of the cAMP pathway (Russell *et al.*, 2002). The possibility that ZAG is a candidate gene in the regulation of body weight has been raised (Gohda *et al.*, 2003). It was thus intriguing when ZAG (mRNA and protein) was recently shown to be expressed both in white and brown adipose tissue of mice, as well as in white fat of human (Bing *et al.*, 2004) and might thus contribute to the local modulation of lipid metabolism within the tissue.

Rodents are a good animal model for studying ZAG, due to the degree of homology in the protein between them and humans. Although both rat and murine ZAG display 59% amino acid sequence homology with the human counterpart (Ueyama *et al.*, 1994), they share up to 100% identity in specific regions thought to be important in lipid metabolism (Sanchez *et al.*, 1999). Furthermore, there is an 88.5% identity between rat and mouse ZAG amino acid sequence (Ueyama *et al.*, 1994).

The adipose organ is a multidepot organ consisting of several subcutaneous and visceral depots, with distinct anatomical locations, which are different both in terms of fat cell size and function (Pond & Mattacks, 1991). Rodents have two main subcutaneous fat depots, anterior and posterior, and several visceral depots including retroperitoneal, perirenal, omental, and mesenteric depots. In terms of functional differences, it is important to mention that the omental adipose tissue contains more blood vessels and sympathetic nerve fibres than the subcutaneous depot, implying a greater degree of metabolic activity in the former (Kelley, 2004). Furthermore, there are more monocytes/macrophages present in omental compared to subcutaneous adipose tissue (Bornstein *et al.*, 2000). In addition to that, a higher degree of lipolytic activity has been demonstrated in the omental site (Harmelen *et al.*, 2002). It has been suggested that

omental and subcutaneous adipocytes might originate from different precursor cells that are genetically different or that are programmed differentially by the surrounding tissue before their differentiation (van Harmelen *et al.*, 2002). These differences further justify the fact that different adipose tissue depots show differential capacity with respect to adipokine secretion (Trayhurn & Beattie, 2001). It is thus of great interest, after having established the expression of a factor in adipose tissue to explore, using quantitative methods, its differential presence in different depots.

Another important issue is that adipocytes do not account for the whole of the organ. Mature adipocytes constitute around 50% of the total cell content of WAT (Hausman, 1985). The remaining stromal vascular fraction consists of a number of different cell types including fibroblasts, macrophages and endothelial cells. Thus, when a factor is expressed in adipose tissue, it is important to establish whether it is indeed expressed in mature adipocytes.

In the present chapter, in terms of the ZAG expression in murine adipose tissue, the first consideration was to investigate whether there are differences in *ZAG* gene and protein expression among depots, and thus gain a greater insight into ZAG's potential physiological functions in adipose tissue. Furthermore, since it has been previously shown by RT-PCR that ZAG is expressed in both mature adipocytes and the stromal vascular fraction of mouse epididymal WAT (Bing *et al.*, 2004), the second aim of this study was to explore, again quantitavely, in which fraction ZAG (mRNA and protein) is mostly expressed.

Further studies were also designed to focus on examining ZAG expression in pathophysiological conditions in which energy balance and substrate flux are changed to determine whether ZAG is a component of local fat mobilisation in adipocytes. Obesity is a low-grade inflammatory state (Festa *et al.*, 2001) resulting from chronically positive energy balance by excess energy intake and/or energy expenditure. As a result, the levels of many adipokines change in the obese state (Trayhurn & Wood, 2004). Obese rodent models are commonly used to study possible factors in the pathogenesis of obesity and to

investigate the biochemical, physiological and morphological changes that are present in obesity. Therefore, the third aim of this study was to compare ZAG mRNA levels in WAT between lean and obese animals in two rodent models of obesity: the genetically obese (*ob/ob)* mouse, which was first identified in 1950 (Ingalls *et al.*, 1950), and the genetically obese (*fa/fa)* Zucker rat (Zucker & Zucker, 1961). A specific mutation of the leptin gene is responsible for the obese phenotype of the *ob/ob mouse* (Zhang *et al.*, 1994), which is characterised by the lack of biologically active leptin and this effectively prevents normal signalling of energy stores by the adipose tissue to the hypothalamus. Thus, one of its first symptoms is hyperphagia, while othes include hyperinsulinaemia, insulin resistance and hyperglycaemia (Friedman & Halaas, 1998; Fruhbeck & Salvador, 2000). The *fa/fa* rat on the other hand has a point mutation in the gene encoding the leptin receptor (OB-R) that has been identified as the underlying cause of its phenotype, and it is characterised by hyperinsulinaemia (Chua *et al.*, 1996).

All experiments described in this chapter were conducted in reference to leptin. Leptin is the most studied adipokine in terms of differential expression both in humans and rodents. In addition to that, its upregulation in obesity is well documented.

3.2 Methods

3.2.1 Animals and tissues

Ten-week-old male CD-1 mice and Wistar rats were from an inbred colony maintained at the University of Liverpool. Animals were housed at an ambient temperature of 22 ± 1^{0}C under a 12:12 h light-dark cycle (lights on at 07:00 h) and fed a standard pelleted diet (CRM diet, Labsure, Witham, U.K.). Both food and water were available *ad libitum.* Animals were killed by cervical dislocation and the following tissues were rapidly dissected and frozen in liquid nitrogen: WAT (subcutaneous, epididymal, perirenal, mesenteric, and omental depots), interscapular brown adipose tissue (BAT), liver, spleen, heart, kidneys, stomach, skeletal muscle (gastrocnemius), hypothalamus, lung and esophagus. All tissues were stored at -80^{0}C until further analysis. For part of this study,

collagenase digestion was employed to separate mature adipocytes from the stromal vascular fraction, and the two fractions of subcutaneous, epididymal and perirenal WAT depots were kept separately at -80^{0}C until further analysis.

WAT from 8-week-old male lean (+/+ and +/*ob*) and genetically obese (*ob/ob*) C57BL/6J mice (Harlam Olac) was also used. Upon arrival, the mice were housed for one week under controlled environmental conditions (22 ± 1^{0}C under a 12:12 h light-dark cycle, lights on at 07:00 h) to allow recovery from any transportation-induced stress. They were killed by cervical dislocation and WAT depots (subcutaneous, epididymal, perirenal and omental) were quickly dissected, snap-frozen in liquid nitrogen and stored at -80^{0}C until further analysis.

Retroperitoneal and epididymal WAT samples from 3-month-old male Zucker rats (both lean (+/+ or +/*fa*) and genetically obese (*fa/fa*), bred at the Rowett Research Institute (Aberdeen, Scotland), were a gift from Dr DV Rayner.

All animal studies were conducted according to the U.K. Home Office Guidelines for the care and use of laboratory animals.

3.2.2 RT-PCR and real-time PCR

Total RNA was extracted from tissues using Tri-Reagent as previously described in section 2.5. RNA was then treated using a DNA-free kit (section 2.5.3) and quantified using a BioPhotometer (section 2.5.4). First-strand DNA was reverse-transcribed from 1 μg of total RNA using the Reverse-iT First Strand Synthesis kit (section 2.6) and the patterns of gene expression were analysed by RT-PCR (section 2.6.2). For the studies of *ZAG* gene expression on adipose tissue 2 μl of cDNA (equivalent to 100 ng of RNA) were used, while 1 μl of cDNA was used as a template for expression analysis of *ZAG* and other target genes in all other tissues. Relative mRNA levels were quantitated by real-time PCR using a qPCR Core Kit on a ABI Prism 7700 instrument (section 2.7).

3.2.3 Western blotting

Protein was extracted from tissues using Tri-Reagent after the RNA had been removed for total RNA extraction (section 2.8.1.2) or from frozen tissues (section 2.8.1.1). The concentration of samples was determined using the BCA method (section 2.8.2) and 10 μg of protein were mixed with equal volumes of loading buffer and separated by electrophoresis on 10% SDS-polyacrylamide gels (section 2.8.3). Immunoblotting was then performed as described in section 2.8.4 by using an anti-mouse ZAG monoclonal primary antibody (Santa Cruz Biotechnology, USA) at a 1:1000 dilution, followed by incubation with a goat anti-mouse secondary antibody conjugated to horseradish peroxidase at a 1:1000 dilution. Densitometric analysis was carried out (section 2.8.6) and gels were stained with Ponceau S to confirm equal loading (section 2.8.5.2).

3.2.4 Statistical analysis

Data are expressed as mean values ± SE. Comparisons between two groups were assessed by Student's *t*-test, while for differences among more than two groups one-way ANOVA coupled with Bonferroni's *t*-tests was employed, as previously described in section 2.9. Differences were considered as statistically significant when $P < 0.05$.

3.3 Results

3.3.1 ZAG expression in adult rodent adipose tissue

3.3.1.1 ZAG expression in mouse adipose tissue

As part of the present study, the expression of the *ZAG* gene in WAT depots was verified by RT-PCR. Although RT-PCR indicated that the *ZAG* gene is expressed in all WAT sites tested, the signal intensity appeared to vary among depots, which suggests that there are inter-depot differences in ZAG expression levels. Real-time PCR was therefore used to quantify ZAG mRNA levels in different depots (Figure 3.1). The results clearly demonstrate that ZAG mRNA levels varied considerably between depots. The mRNA levels were significantly higher in perirenal and omental WAT when compared to

Figure 3.1 *ZAG* gene expression in adipose tissue depots of mice

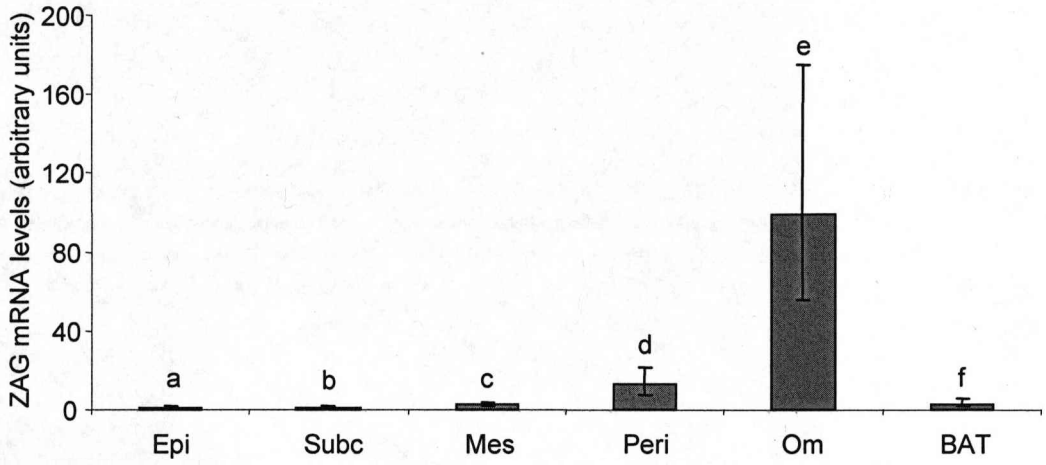

Six adipose tissue depots were dissected from mice and total RNA was extracted. Real-time PCR was used for the relative quantification of ZAG mRNA levels. Results are presented relative to the ZAG mRNA levels in epididymal WAT and are presented as means ± SE (bars) for 5-6 mice. Epi, epididymal; subc, subcutaneous; mes, mesenteric; peri, perirenal; om, omental; BAT, interscapular brown adipose tissue. [a]$P < 0.01$ vs peri, $P < 0.01$ vs om; [b]$P < 0.01$ vs peri, $P < 0.01$ vs om; [c]$P < 0.05$ vs peri, $P < 0.05$ vs om; [d]$P < 0.05$ vs om; [e]$P < 0.01$ vs BAT (One-way ANOVA, post-hoc multiple comparisons with Bonferroni correction).

epididymal, subcutaneous, and mesenteric depots, while the lowest levels were detected in epididymal WAT. ZAG was expressed in BAT, its levels in the tissue being significantly lower than the levels in omental WAT. As a comparison, leptin mRNA levels were also determined in the same WAT depots and leptin levels were at their highest in epididymal and at the lowest in omental adipose tissue (Figure 3.2).

Following mRNA analysis, ZAG protein levels in the same depots were measured. Similar to mRNA, ZAG protein levels were significantly higher in perirenal and omental WAT when compared to mesenteric, subcutaneous and epididymal WAT and BAT. However, in contrast to mRNA, the lowest ZAG protein levels were detected in BAT (Figure 3.3).

3.3.1.2 ZAG expression in mature adipocytes and the stromal vascular (SV) fraction of WAT depots

In order to explore whether ZAG is mainly produced in the mature adipocytes or the stromal vascular fraction of mouse white adipose tissue, subcutaneous, epididymal and perirenal WAT depots were dissected from six mice, and following collagenase digestion the two fractions were separated. Real-time PCR was employed to analyse the mRNA levels of expression. The results showed that there were no significant differences in ZAG mRNA levels between the two fractions in all the depots examined (Figure 3.4A). ZAG protein was also detected in both fractions, and as with the mRNA results there was no significant difference between them (Figure 3.5).

Leptin gene expression was also determined in subcutaneous adipose tissue as a reference, by real-time PCR (Figure3.4B), and leptin was found to be expressed exclusively in mature adipocytes no signal being detected in the SV fraction.

Figure 3.2 Leptin gene expression adipose tissue depots of mice

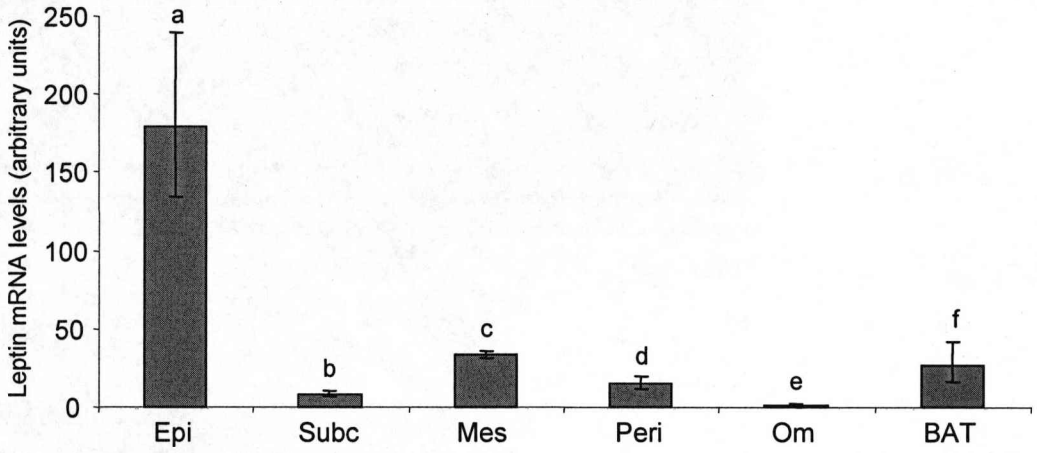

Six adipose tissue depots were dissected from mice and total RNA was extracted. Real-time PCR was used for the relative quantification of leptin mRNA levels. Results are presented relative to the leptin mRNA levels in omental WAT and are presented as means ± SE (bars) for 5-6 mice. Om, omental; subc, subcutaneous; peri, perirenal; mes, mesenteric; epi, epididymal; BAT, interscapular brown adipose tissue. [a]$P < 0.05$ vs BAT; [b]$P < 0.01$ vs peri, $P < 0.01$ vs epi; [c]$P < 0.01$ vs epi; [d]$P < 0.01$ vs mes; [e]$P < 0.05$ vs subc, $P < 0.01$ vs peri, $P < 0.01$ vs mes, $P < 0.001$ vs epi, $P < 0.01$ vs BAT (One-way ANOVA, post-hoc multiple comparisons with Bonferroni correction)

Figure 3.3 ZAG protein expression in adipose tissue depots of mice

(A)

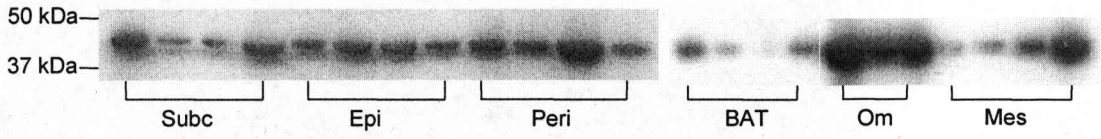

(B)

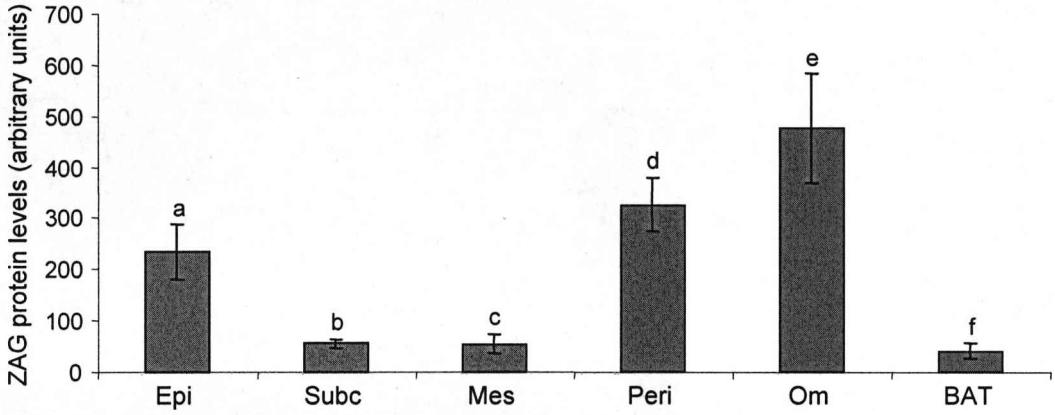

Six adipose tissue depots were dissected from mice and protein was extracted. Western blotting (A) was used for detection of ZAG and quantification of ZAG protein expression levels (B). Results are presented relative to ZAG protein levels in BAT and are presented as means ± SE (bars) for 4 mice. BAT, interscapular brown adipose tissue; mes, mesenteric; subc, subcutaneous; epi, epididymal; peri, perirenal; om, omental. $^{b}P < 0.05$ vs peri; $P < 0.05$ vs om; $^{c}P < 0.05$ vs epi; $P < 0.01$ vs peri; $P < 0.05$ vs om; $^{f}P < 0.05$ vs epi, $P < 0.01$ vs peri, $P < 0.01$ vs om (One-way ANOVA, post-hoc multiple comparisons).

Figure 3.4 ZAG mRNA levels in mature adipocytes and stromal vascular fraction of white adipose tissue depots

(A)

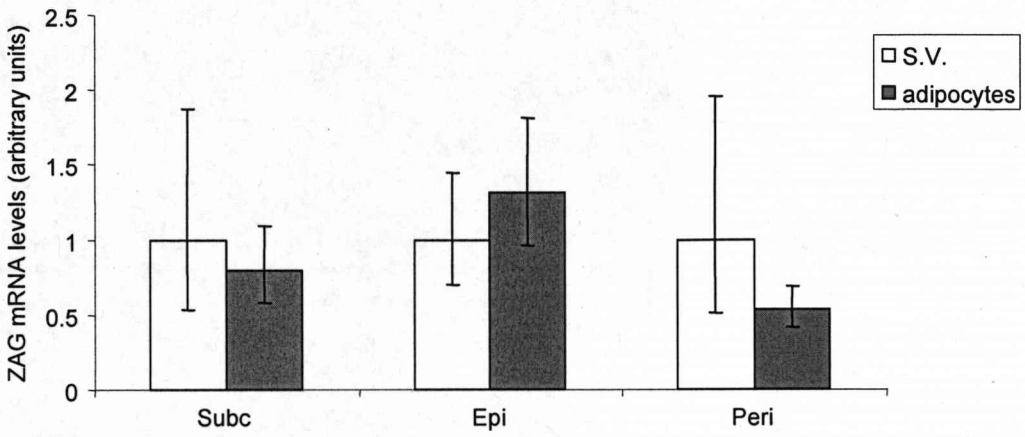

(B) **Subcutaneous WAT**

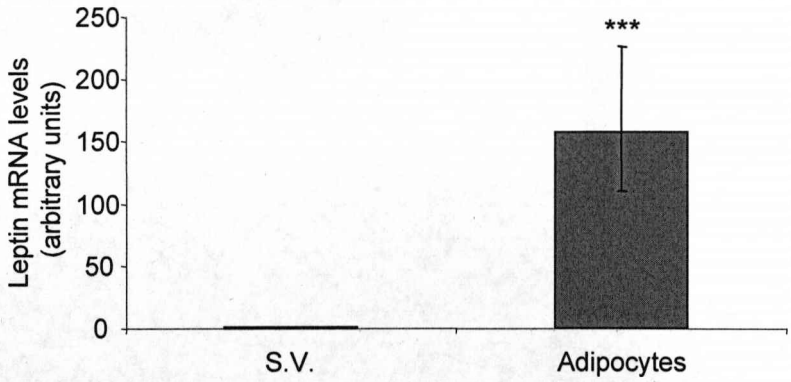

Three WAT depots were dissected from normal mice and following collagenase digestion mature adipocytes were separated from the SV fraction. Real-time PCR was used for relative quantification of ZAG (A) and leptin (B) mRNA levels. Results are expressed relative to SV for each depot and are presented as means ± SE (bars) for 5-6 mice. Subc, subcutaneous; epi, epididymal; peri, perirenal; SV, stromal vascular. ***$P < 0.001$ (paired Student's t test) compared to SV group and normalized to β-actin.

Figure 3.5 ZAG protein expression in mature adipocytes and stromal vascular fraction of subcutaneous white adipose tissue in mice

(A)

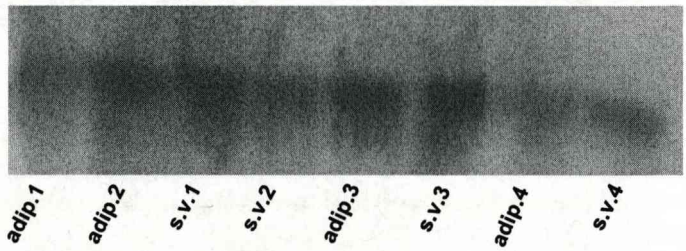

(B)

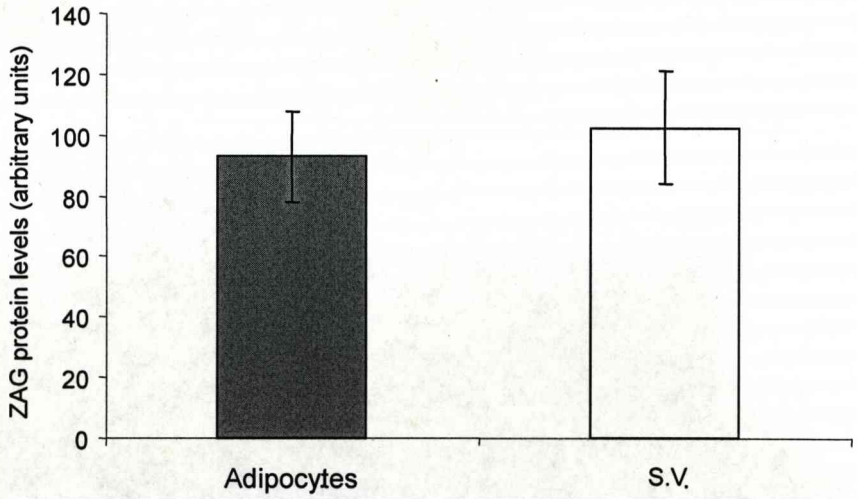

Protein samples were extracted from the mature adipocytes and SV fraction of subcutaneous WAT. Western blotting (A) was used for detection of ZAG protein and quantification of protein levels (B). Results are expressed as means ± SEM (bars) for 4 mice. Adip, mature adipocytes; sv, stromal vascular fraction. $P > 0.05$ (paired Student's *t*-test).

3.3.1.3 ZAG expression in rat adipose tissue

To this point, studies have demonstrated the detailed expression pattern of ZAG in mouse adipose tissue, which has led to subsequent studies on ZAG expression in rat adipose tissue. Since it has not been reported previously, it was important to first establish the expression pattern of ZAG in the tissues, including rat WAT and BAT. Since the *ZAG* gene contains 4 exons, primers were designed to span two exon-exon boundaries to ensure that no product could be derived from genomic DNA contamination. The presence of ZAG mRNA would be expected to result in a 322-bp product being generated. For this purpose, tissues were collected from a 10-week old Wistar rat and ZAG mRNA distribution was studied by RT-PCR, while the protein expression was analysed by western blotting.

As shown in Figure 3.6A, in addition to the liver, which is known as the main source of ZAG production, a strong signal for ZAG mRNA was also detected in the stomach, kidney, spleen, oesophagus, muscle and lung. However, ZAG mRNA was barely detectable in the heart and hypothalamus. Most importantly *ZAG* gene expression was detected in all the WAT depots tested, subcutaneous, gonadal. perirenal, mesenteric and omental, as well as in BAT. ZAG mRNA was also detected in pericardial fat.

Following mRNA analysis, ZAG protein expression pattern in all the tissues was analysed using western blotting (Figure 3.6B). The results revealed a very similar pattern to that of the mRNA expression. In particular, ZAG protein was detected in all the WAT depots examined, subcutaneous, omental, epididymal, perirenal, mesenteric and pericardial and in BAT.

Figure 3.6 Tissue distribution of *ZAG* gene and protein in the rat

(A)

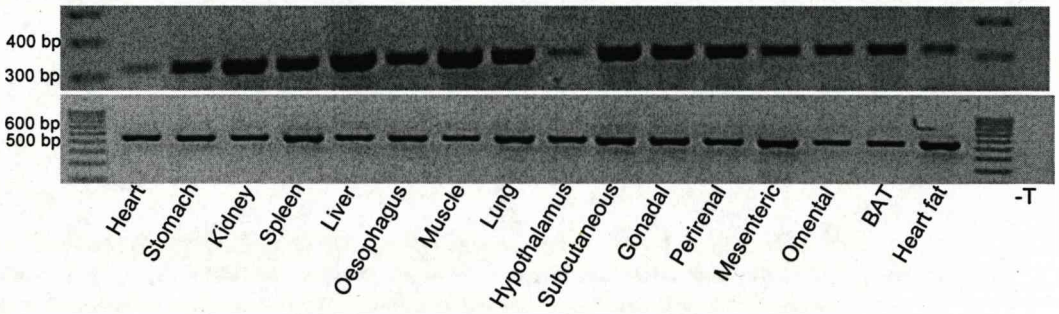

(B)

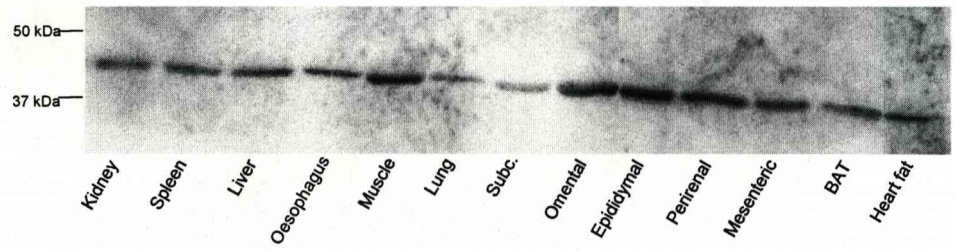

ZAG gene and protein expression in tissues dissected from a 3-month old female wistar rat. (A) ZAG mRNA by RT-PCR, (B) Western blot of ZAG.

3.3.2 ZAG expression levels in rodent models of obesity

Having studied the levels of ZAG expression in adipose tissue depots under normal conditions, it was investigated whether expression of *ZAG* gene was changed in obesity. For this purpose two models were used: the genetically obese mouse (*ob/ob*) and the genetically obese (*fa/fa*) Zucker rat.

3.3.2.1 ZAG gene expression in WAT of lean and ob/ob mice

ZAG mRNA levels were examined in subcutaneous, epididymal, perirenal and omental WAT depots of lean and *ob/ob* mice using real-time PCR. As a comparison, leptin gene expression was also studied in the same samples.

In subcutaneous and epididymal WAT, *ZAG* gene expression was significantly lower ($P < 0.05$) in the obese compared to the lean mice, the difference being 3- fold and 10-fold for the two tissues respectively (Figure 3.7A). It can be seen from the results that a similar trend was observed in the perirenal and omental depots, although the differences were not statistically significant ($P > 0.05$).

Leptin gene expression, on the other hand, was significantly higher in the obese than in the lean mice in all depots tested, with differences varying from 9-fold in subcutaneous ($P < 0.001$) to 4-fold ($P < 0.05$) in epididymal WAT (Figure 3.7B).

Figure 3.7 *ZAG* gene expression in white adipose tissue depots of lean and *ob/ob* mice

(A)

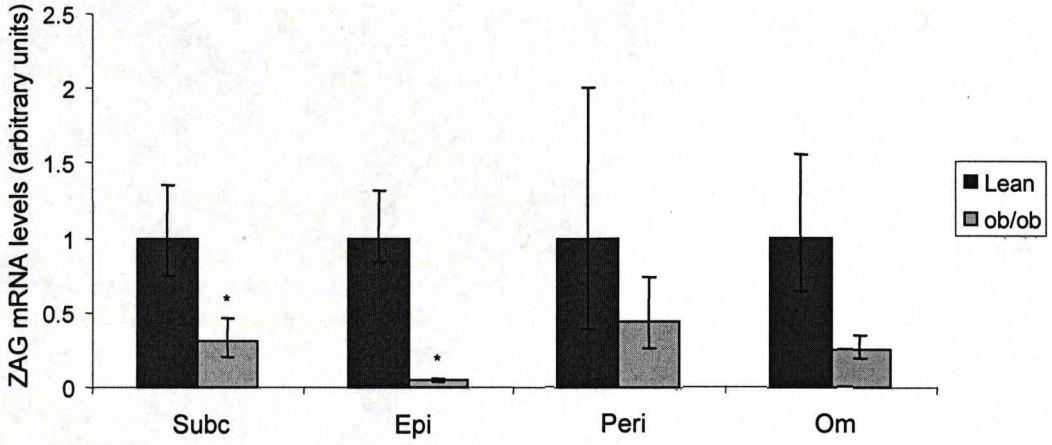

(B)

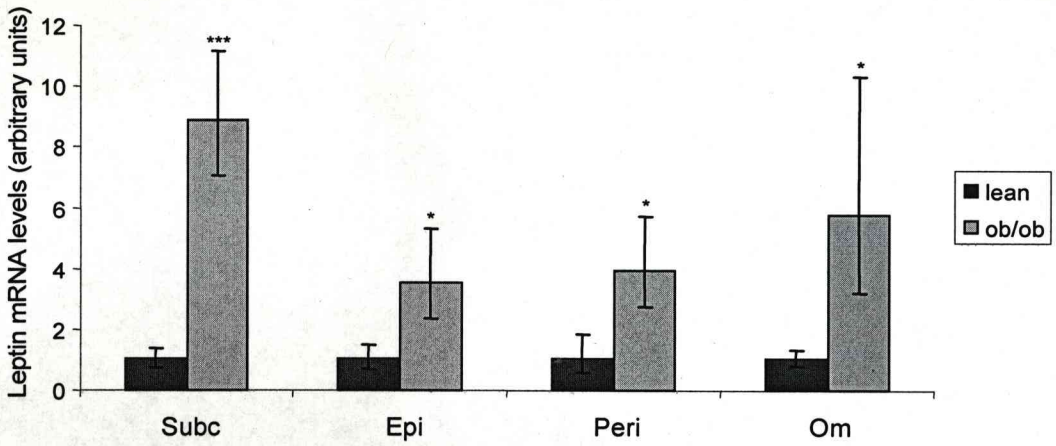

Four WAT depots were dissected from lean and *ob/ob* mice and total RNA was extracted. Real-time PCR was used for relative quantification of ZAG (A) and leptin (B) mRNA levels. Results are expressed relative to the expression levels in the lean group for each depot and are presented as means ± SE (bars) for 4-6 mice. Subc, subcutaneous; epi, epididymal; peri, perirenal; om, omental. $^{*}P < 0.05$, $^{***}P < 0.001$ compared to leans and normalized to β-actin (unpaired Student's *t*- test).

3.3.2.2 ZAG expression in WAT of lean and fa/fa Zucker rats

ZAG mRNA levels were examined in epididymal and retroperitoneal WAT of 3-month old *fa/fa* Zucker rats and their lean counterparts.

ZAG mRNA levels were significantly downregulated in the *fa/fa* group both in epididymal and retroperitoneal WAT by ~5-fold ($P < 0.05$) (Figure 3.8A). ZAG protein expression was also analysed in retroperitoneal WAT samples. Although, there was an indication that ZAG is downregulated in the obese group, statistical analysis revealed no significant difference between the two groups (Figure 3.9).

Leptin mRNA levels were also analysed in retroperitoneal WAT. As shown in Figure 3.8B, leptin was upregulated in the *fa/fa* group compared to their lean counterparts by ~2.5-fold ($P < 0.05$).

3.4 Discussion

Consistent with previous studies (Bing *et al.*, 2004), it has been shown in this study that ZAG (mRNA and protein) is expressed in adipose tissue. A signal for ZAG was detected in all major adipose tissue sites, both in mice and rats. As part of this study, the tissue distribution of ZAG in the rat was explored using RT-PCR and western blotting. Consistent with previous screening using northern blotting analysis (Ueyama *et al.*, 1994), a strong signal for ZAG mRNA was detected in the liver, which is a major production site of ZAG in the body, and in lung, kidney and stomach. Furthermore, the current study is the first indication of ZAG expression in rat spleen, oesophagus and skeletal muscle. Importantly, it is the first study reporting the expression of ZAG in all the major rat WAT depots and in rat BAT. ZAG protein was also detected in all the aforementioned tissues. It is interesting to note that although liver gave a strong signal in mRNA analysis, a weak signal was seen in the protein analysis. A possible explanation for this observation, which has previously been reported in humans (Tada *et al.*, 1991), is

Figure 3.8 *ZAG* gene expression in white adipose tissue of lean and obese (*fa/fa*) Zucker rats

(A)

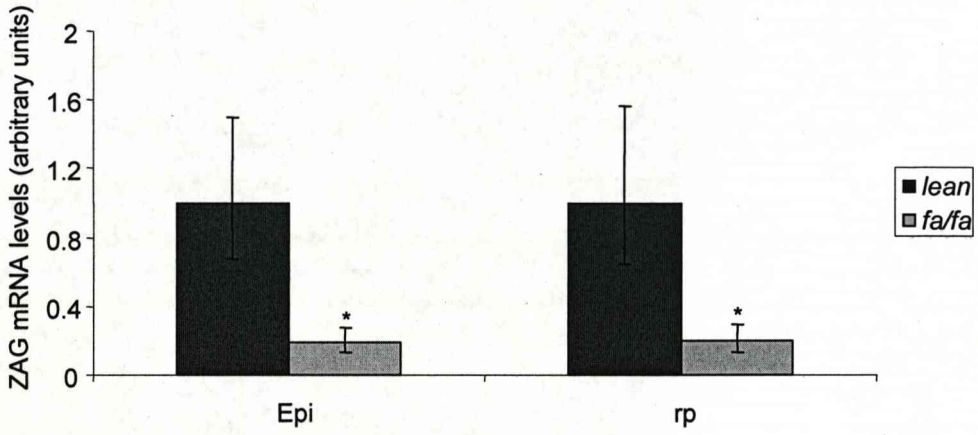

(B) **Retroperitoneal WAT**

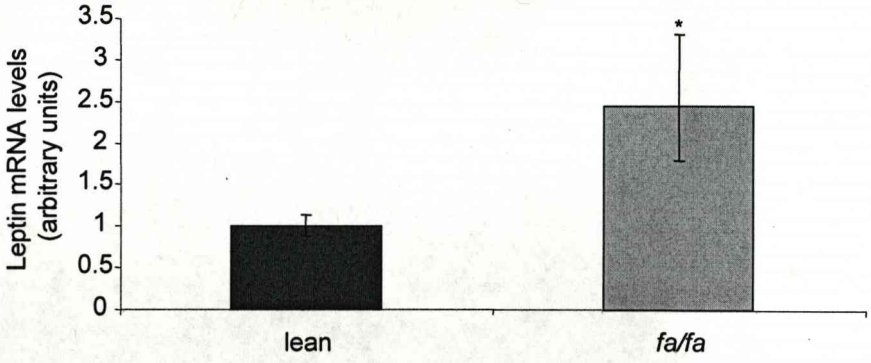

Epididymal and retroperitoneal depots were dissected from 3-month old lean and *fa/fa* Zucker rats and total RNA was extracted. Real-time PCR was used for relative quantification of ZAG (A) and leptin (B) mRNA levels in retroperitoneal. Results are expressed relative to the expression levels in the lean group for each depot and are presented as means ± SE (bars) for 6-8 rats. Epi, epididymal; rp. Retroperitoneal. *P < 0.05 compared to leans and normalized to β-actin (unpaired Student t-test).

Figure 3.9 ZAG protein expression in retroperitoneal white adipose tissue of lean and *fa/fa* Zucker rats

(A)

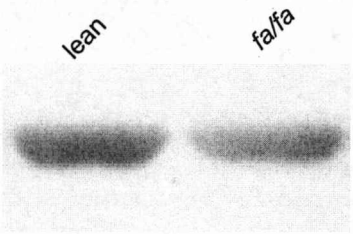

(B)

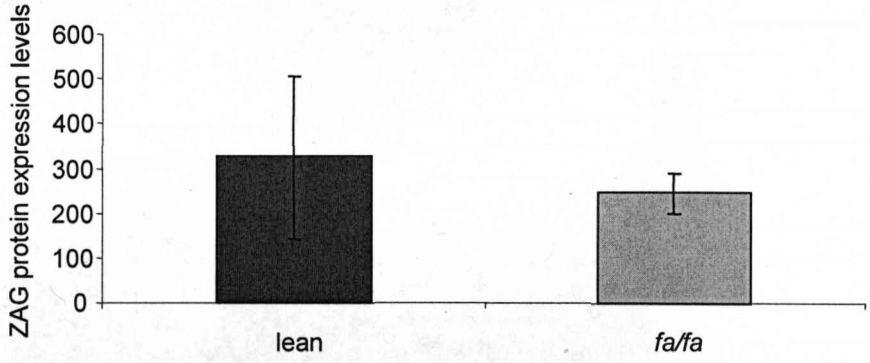

Protein was extracted from the retroperitoneal samples from lean and *fa/fa* Zucker rats aged 3 and 9 months. Western blotting (A) and densitometric analysis (B) were used for relative uantitation of ZAG protein levels. Results are expressed relative to the expression level in retroperitoneal WAT of 3-month old lean animals and are presented as means ± SE (bars) for 4-5 rats.

that the liver may secrete ZAG into the blood immediately after its synthesis, or ZAG protein in the liver may be in a masked state that does not allow the antibodies to bind (Ueyama *et al.*, 1994). Although, WAT is not the major site of ZAG production, the fact that ZAG is an adipokine produced locally by adipose tissue and the possible functions that have been attributed to it has led to further study, particularly the characterisation of its expression patterns, in adipose tissue.

Differences were clearly evident between the levels of ZAG mRNA and protein in the different adipose tissue depots of mice, as measured by real-time PCR and western blotting, ZAG levels being significantly elevated in perirenal and omental depots. Differences in the degree of lipolysis/ lipogenesis may account for this variability in ZAG expression levels among depots. As mentioned above, visceral adipose tissue has higher lipolytic activity compared to subcutaneous adipose tissue. This can be attributed to regional variation in the action of the major lipolysis-regulating hormones, catecholamines and insulin, the lipolytic effect of the former being more pronounced and the antilipolytic effect of the latter being weaker in visceral than in subcutaneous adipose tissue (Bolinder *et al.*, 1983; Arner, 1998). IL-6, which decreases adipose tissue LPL activity (Fried *et al.*, 1998) and similar to ZAG (Bing *et al.*, 2004) has been implicated in stimulating lipolysis (Path *et al.*, 2001; Vantall *et al.*, 2003) is also mostly expressed in the omental compared to the subcutaneous depot (Fried *et al.*, 1998).

Furthermore, this site variation has been attributed to the amount of adrenoreceptors present in visceral fat (Wajchenberg, 2000). In rodents, the β_3-adrenoreceptor is viewed as the principle receptor-subtype through which the stimulation of lipolysis occurs (Giacobino, 1996). Visceral tissue is characterised by the increased expression and function of β_3-adrenoreceptors and a decreased insulin receptor affinity and signal transduction in visceral adipocytes (Arner *et al.*, 1990). Furthermore, studies on isolated adipocytes from different adipose sites in humans showed that the β_3-adrenoreceptor is functionally expressed mainly in omental adipose tissue (Lönnqvist *et al.*, 1993). It has been reported that *in vitro* the potent lipolytic effect of ZAG is attenuated by the specific

β_3-adrenoreceptor antagonist SR59230, suggesting that ZAG activity in rodents is mediated via the β_3-adrenoreceptor (Russell *et al.*, 2002).

Consistent with previous reports (Masuzaki *et al.*, 1995; Hardie *et al.*, 1996; Hube *et al.*, 1996; Montague *et al.*, 1997; van Harmelen *et al.*, 1997; Zhang *et al.*, 1999), leptin production was higher in the subcutaneous than in the omental depot in this study, the highest levels being observed in epididymal WAT.

A number of cell types have been shown to secrete ZAG, including epithelial cells of breast, prostate and liver (Tada *et al.*, 1991). The SV fraction of adipose tissue contains a variety of other cell types, such as fibroblasts and macrophages, as well as preadipocytes. It has previously been shown, both in mice (Bing *et al.*, 2004) and in human (Bao *et al.*, 2005) that ZAG is expressed in both fractions. In the present study, it has been demonstrated that there are no statistically significant differences in the levels of ZAG expression in the two fractions, both at the mRNA and protein levels, in all three mouse depots tested. However, studies in human subcutaneous and omental WAT indicated that the *ZAG* gene was expressed primarily in mature adipocytes (Bao *et al.*, 2005), although a non-quantitative approach was used. It could be that this is a difference in ZAG expression between human and rodents. The fact that leptin is solely expressed in mature adipocytes was also verified as part of this study, consistent with previous observations (Einstein *et al.*, 2005).

When ZAG mRNA levels were analysed in WAT depots from lean and genetically obese (*ob/ob*) mice, a significant difference between the two genotypes was shown as ZAG expression was reduced in subcutaneous and epididymal WAT. Although the results were not statistically significant, the same trend of reduced expression was observed in perirenal and omental WAT of *ob/ob* mice. As a reference point it was also shown that leptin mRNA level was higher in the depots of *ob/ob* mice as previously reported (Frederich *et al.*, 1995). In genetically obese rats (*fa/fa*), ZAG mRNA was significantly downregulated in the epididymal and retroperitoneal WAT of 3-month-old obese animals. Consistent with previous studies which have shown that leptin mRNA levels are

markedly elevated in rats with the *fa/fa* mutation (Masuzaki *et al.*, 1996), mRNA levels of leptin were increased in the retroperitoneal WAT of obese compared to lean animals. It thus seems that there is a link between obesity and decreased ZAG expression and the fact that some of the results were not statistically significant may be a consequence of small sample groups and variation among animals.

Obesity is now considered to represent a state of chronic low-grade inflammation (Das, 2001), an assumption based on the increased circulating levels of several markers of inflammation in obesity, including IL-6, TNFα, haptoglobin and MCP-1 (Das 2001; Bulló *et al.*, 2003; Sartipy & Loskutoff, 2003). Contrary to other adipokines, adiponectin levels decrease in the obese state (Arita *et al.*, 1999), and it is considered to have anti-inflammatory (Ouchi *et al.*, 1999), as well as insulin sensitising properties (Spranger *et al.*, 2003). Similarly to adiponectin, ZAG has been shown in the present study to be reduced in genetically obese rodent models. Similar results were demonstrated in a recent study on obese women (Dahlman *et al.*, 2005). Assuming that relative mRNA levels of ZAG in adipose tissue reflect relative rates of ZAG production within the tissue, and based on the similar patterns observed for the two adipokines, an anti-inflammatory role for ZAG in the obese state might be suggested. The potential involvement of ZAG in anti-inflammatory processes in WAT has also been suggested in a recent *in vitro* study which demonstrated that rosiglitazone increases, while TNFα reduces ZAG mRNA levels in human adipocytes (Bao *et al.*, 2005) and is also suggested by *in vitro* studies on the regulation of ZAG expression in murine adipocytes as part of the present thesis (see Chapter 5).

Furthermore, the suppression of ZAG in obesity could also be related to a role of ZAG in the regulation of energy metabolism. It has previously been shown that ZAG induces lipolysis *in vitro* and that *in vivo* administration of ZAG reduces body fat (Hirai *et al.*, 1998). However, as a result of increased insulin resistance, obesity is characterised by increased basal lipolysis, reduced antilipolytic action of insulin and reduced LPL expression and activity (Hauner & Skurk, 2001). In addition, the degree of obesity is correlated with the extent of loss of β_3- and β_1-adrenoreceptors in WAT in both genetic

and dietary obesity in mice (Boschman, 2001). It might be suggested that ZAG is not only affected by lipolysis but is also inversely regulated by the degree of adipogenesis, which increases in the obese state.

It should be noted that most observations of ZAG expression in obesity presented in this chapter are only based on ZAG mRNA levels, which do not always represent protein expression levels in the tissue or circulatory levels of the protein. Further studies would thus provide stronger indications of the role of ZAG in adipose tissue in obesity.

In conclusion, ZAG (both gene and protein) is expressed in all the major white adipose tissue depots and BAT in mouse and rats, its levels being higher in perirenal and omental fat. Crucially, ZAG has been shown to be present in both mature adipocytes and stromal vascular fraction of all major depots. Finally, there is evidence that obesity has an association with decreased levels of ZAG in white adipose tissue, and this suggests that ZAG could conceivably have an anti-inflammatory role and act locally in the modulation of lipolysis in rodent adipose tissue.

Chapter 4

Regulation of ZAG expression in mouse adipose tissue: effects of fasting and high-fat diet

4.1 Introduction

In Chapter 3, the differential expression of ZAG in adipose tissue was explored revealing that ZAG is mostly produced in visceral depots, and equally by mature adipocytes and the stromal vascular fraction of the tissues. It was also demonstrated using two rodent genetic models of obesity that in contrast to most adipokines, ZAG is down-regulated in obesity. It is known that nutritional status can alter the gene expression and /or plasma levels of adipose-secreted factors as demonstrated by various studies (Trayhurn *et al.*, 1995; Zhang *et al.*, 2001; Bertile & Raclot, 2004; Rajala *et al.*, 2004; Einstein *et al.*, 2005; Korhonen & Saarela, 2005), such as the downregulation of leptin in response to fasting (Trayhurn *et al.*, 1995; Zhang *et al.*, 2001), presumably to contribute to adapting overall metabolism to the new nutritional environment (Giordano *et al.*, 2005). In the current chapter the effects of changes in the diet on ZAG expression are explored.

To examine nutritional effects on ZAG expression two studies were carried out. In the first one, mice were fasted for 16 h, after which time, ZAG mRNA and protein expression were analysed and compared to those in the normally fed group. In the second study, mice were kept on a high-fat diet (58% lipid by energy) for twelve weeks and ZAG levels were then compared to those in mice fed a low-fat diet (11% lipid by energy).

Fasting is a state when food intake has been arrested for a significant amount of time. Long-term food deprivation is characterized by changes in fuel availability and in adipose tissue lipid content (Goodman *et al.*, 1980). The absence of energy entering the body evokes a complex physiological response aimed at maintaining whole body homeostasis. An important event in the fasting response is the exhaustion of carbohydrate reserves. As a result, the lipids stored in white adipocytes as triacylglycerols are catabolised by lipolysis and secreted as fatty acids. The metabolic adaptations accompanying fasting are governed by numerous endocrine and cellular factors (Kersten *et al.*, 2000). Fasting results in marked changes in the plasma concentrations of important metabolic hormones such as reduced insulin, leptin, glucocorticoids, (Trayhurn *et al.*, 1995), resistin (Rajala *et al.*, 2004) and glucagon (Kersten *et al.*, 2000). In addition, fasting causes altered expression

levels of important transcription factors such as sterol response element-binding protein, c-Myc and PPARα, directing specific changes in the expression of metabolic enzymes (Kersten *et al.*, 2000). Some differences have also been evidenced in terms of the differential response to fasting depending on the anatomical location of adipose tissue, the mobilization of visceral fat pads being greater than that of subcutaneous WAT (Sugden *et al.*, 1994). Furtheromore, when refeeding, a preferential restoration of internal adipose tissue is observed (Bertile *et al.*, 2003).

There has been evidence that this fasting-dependent lipid mobilization in WAT is primarily due to sympathetic noradrenergic innervation (Bartness & Bamshad, 1998; Giordano *et al.*, 2005). BAT, which functions as a heat-producing organ, both for thermoregulation through the action of UCP-1 in rodents and in relation to the regulation of whole-body energy balance (Rothwell & Stock, 1979; Himms-Hagen, 1990), exhibits a suppressed capacity for nonshivering thermogenesis both in mice and rats as a result of food deprivation (Jourdan *et al.*, 1983). It has recently been demonstrated that during fasting BAT is ~7 times more innervated than epididymal WAT (Giordano *et al.*, 2005).

In Chapter 3, the regulation of *ZAG* gene expression in two rodent genetic models of obesity was studied. However, obesity arises as a consequence of a prolonged imbalance between energy intake and expenditure (Bray, 2004). Recent studies in rats have demonstrated that high-fat diets, in which the animal consumes a substantial energy surplus for a certain period leading to obesity, influence gene expression in WAT (Lopez *et al.*, 2003).

Most of the experiments described in this chapter were conducted in reference to leptin and in some cases adiponectin, as the effects of diet alterations on both adipokines have been previously documented (Trayhurn *et al.*, 1995; Zhang *et al.*, 2001; Bertile & Raclot, 2004; Rajala *et al.*, 2004; Einstein *et al.*, 2005; Korhonen & Saarela, 2005).

4.2 Methods

4.2.1 Animals

Sixteen ten-week old male mice (CD1) from an inbred colony at the University of Liverpool were housed at an ambient temperature of 22 ± 1°C under a 12:12 h light – dark cycle (lights were on at 07:00 h) and fed a standard pelleted diet (CRM diet, LAbsure, Witham, U.K.) containing 19.2% protein and 4.3% lipid (wt/ wt). Two days prior to the initiation of the fasting experiment mice were divided into two groups (the fed and fasted groups) and housed in grid bottomed cages. On commencing the experiment all food was removed from the fasted group's cage, while they still had *ad libitum* access to water. This lasted for 16 h, at which point the animals were sacrificed by cervical dislocation and the following tissues were rapidly dissected: WAT (subcutaneous, epididymal, perirenal, mesenteric, and omental), BAT, and liver. Animals were sacrificed according to the regulations for animal treatment of the University of Liverpool. As soon as the tissues were dissected, samples were weighed, snap frozen in liquid nitrogen and stored at -80°C until further analysis.

Subcutaneous, gonadal and perirenal WAT depots from lean and diet-induced obese female C57BL/6J mice from Lund University (Lund, Sweden) were provided by Dr B Wang (University of Liverpool). The mice, weighing 18g, were purchased from Taconic (Skensved, Denmark) and kept in a temperature-controlled room (22°C) on a 12h:12h light:dark cycle. The study was approved by the Local Animal Ethics Committee. One week after arrival the mice were divided into two groups and subsequently fed either a low-fat (11% fat by energy) or a high-fat diet (58% fat by energy; Research Diets, New Brunswick, NJ, USA) for 12 weeks (Winzell *et al.*, 2004).

4.2.2 RT-PCR and real-time PCR

Total RNA was extracted from tissues using Tri-Reagent as previously described in section 2.5. RNA was then treated using a DNA-free kit (section 2.5.3) and quantified using a BioPhotometer (section 2.5.4). First-strand DNA was reverse-transcribed from 1

μg of total RNA using the Reverse-iT First Strand Synthesis kit (section 2.6) and relative mRNA levels of expression were assessed by real-time PCR using the qPCR Core Kit on the Stratagene Mx3005P instrument (section 2.7).

4.2.3 Western blotting

In the study of the effects of the high-fat diet, protein was extracted from tissues using Tri-Reagent after the RNA had been removed for total RNA extraction (section 2.8.1.2), while for the fasting study, protein was extracted from frozen tissues (section 2.8.1.1). The concentration of samples was determined using the BCA method (section 2.8.2) and 10 μg of protein were mixed with equal volumes of loading buffer and separated by electrophoresis on 10% SDS-polyacrylamide gels (section 2.8.3). Immunoblotting was then performed as described in section 2.8.4 by using an anti-mouse ZAG monoclonal primary antibody at a 1:1000 dilution, followed by incubation with a goat anti-mouse secondary antibody conjugated to horseradish peroxidase at a 1:1000 dilution. Densitometric analysis was carried out (section 2.8.6) and gels were stained with Ponceau S to confirm equal loading (section 2.8.5.2).

4.2.4 Statistical analysis

Data are expressed as mean values ± SE. Comparisons between two groups were assessed by unpaired Student's *t*-test, as previously described in section 2.9. Differences were considered as statistically significant when $P < 0.05$.

4.3 Results

4.3.1 Effects of 16h-fasting on ZAG expression in mouse adipose tissue depots

As shown in Figure 4.1A, the body weight of fasted animals was considerably reduced compared to that of normally fed mice. The same was observed for net weight of individual depots (Figure 4.1B), and when the data was presented as a proportion of individual depot weights to whole body weights (Figure 4.1C).

As shown in Figure 4.2, in epididymal WAT, ZAG mRNA levels were significantly lower in the fasted compared to the fed group ($P < 0.01$). Although not statistically significant, the same trend was observed in subcutaneous, epididymal, and perirenal depots. In contrast to what was observed in WAT, in BAT, fasting induced an 8-fold increase in ZAG mRNA levels ($P < 0.01$). After examining the ZAG response to fasting at the mRNA levels, it was important to explore its possible effect at the protein level. In the epididymal WAT, fasting had no effect in ZAG protein expression levels (Figure 4.3). In perirenal WAT (Figure 4.4), there was an indication that the protein expression levels of ZAG were reduced in the fasted group, but the results were not statistically significant ($P > 0.05$).

ZAG mRNA levels were also examined in liver samples of the two groups. As shown in Figure 4.5, a 2.8-fold increase was induced in ZAG mRNA levels ($P < 0.001$) in the liver as a result of 16 h fasting.

Fasting induced an acute and marked reduction of leptin mRNA levels in all WAT depots tested and in BAT, the highest effect being observed in the epididymal and perirenal depots (both ~15-fold, $P < 0.001$) (Figure 4.6). A depot-specific response to fasting was on the other hand observed for adiponectin gene expression (Figure 4.7). Fasting induced a decrease in adiponectin mRNA levels in subcutaneous WAT ($P < 0.01$), while no response was observed in the epididymal depot. However, a 2-fold ($P < 0.01$) and a 4-fold ($P < 0.001$) increase was induced in perirenal WAT and BAT respectively, in response to fasting.

Figure 4.1 Body weight and adipose tissue weight of mice fasted for 16 h

(A)

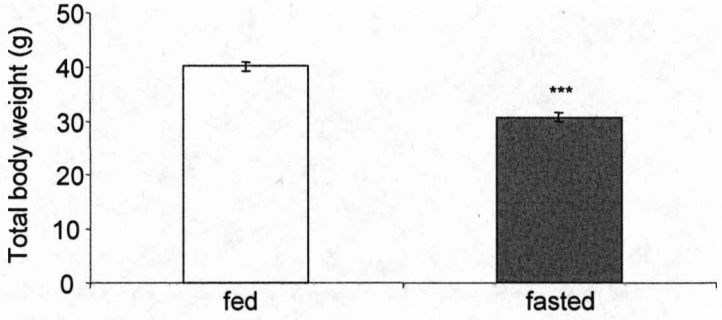

(B)

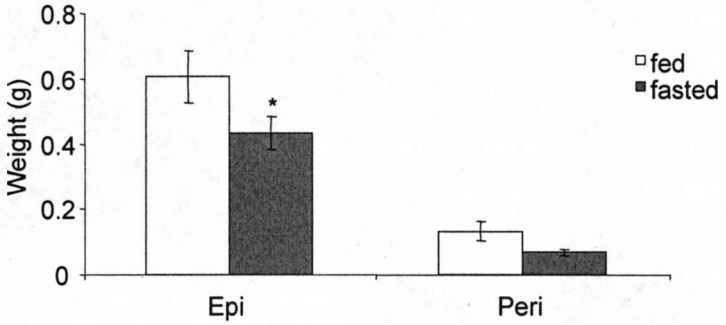

(C)

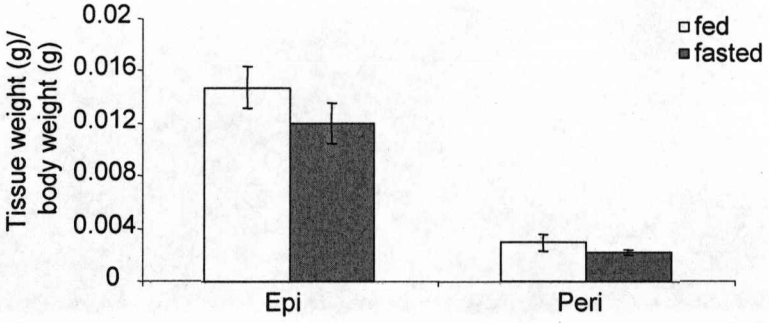

For total body weight (g), mice were weighed as soon as sacrificed, while individual WAT depots were weighed immediately after dissection. Results are presented as mean ± SEM (bars) for 8 mice for each group. $^{*}P < 0.05$, $^{***}P < 0.001$ compared to fed group.

Figure 4.2 ZAG mRNA levels in adipose tissue depots of mice fasted for 16 h

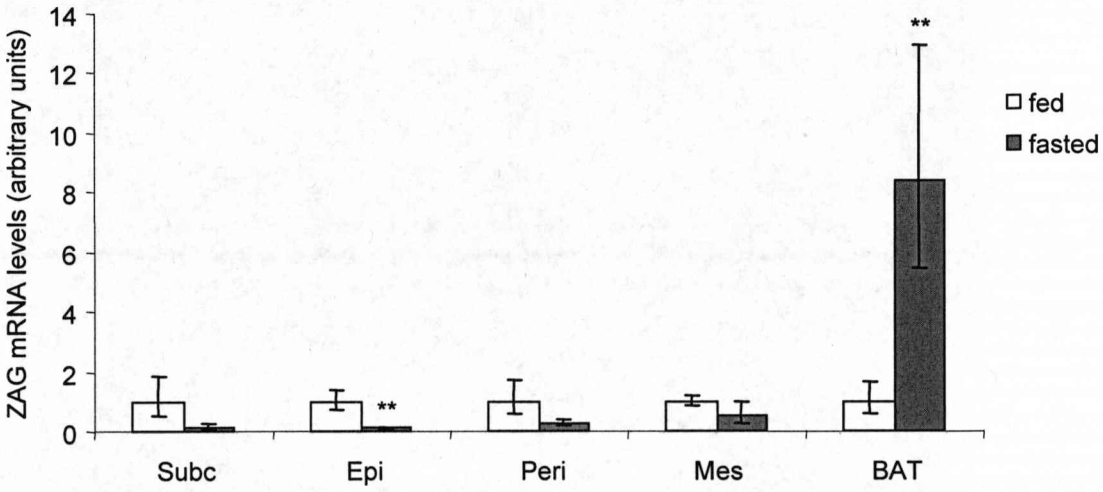

Four WAT depots and interscapular BAT were dissected from fed and 16h-fasted mice and total RNA was extracted. Real-time PCR was used for relative quantification of ZAG mRNA levels. Results are expressed relative to the expression levels in the fed group for each depot and are presented as means ± SE (bars) for 6-8 mice. Subc, subcutaneous; epi, epididymal; peri, perirenal; mes, mesenteric; BAT, interscapular brown adipose tissue. $^{**}P < 0.01$ compared to the fed group for each depot and normalized to β-actin (unpaired Student's *t*- test).

Figure 4.3 ZAG protein expression in epididymal WAT of mice fasted for 16 h

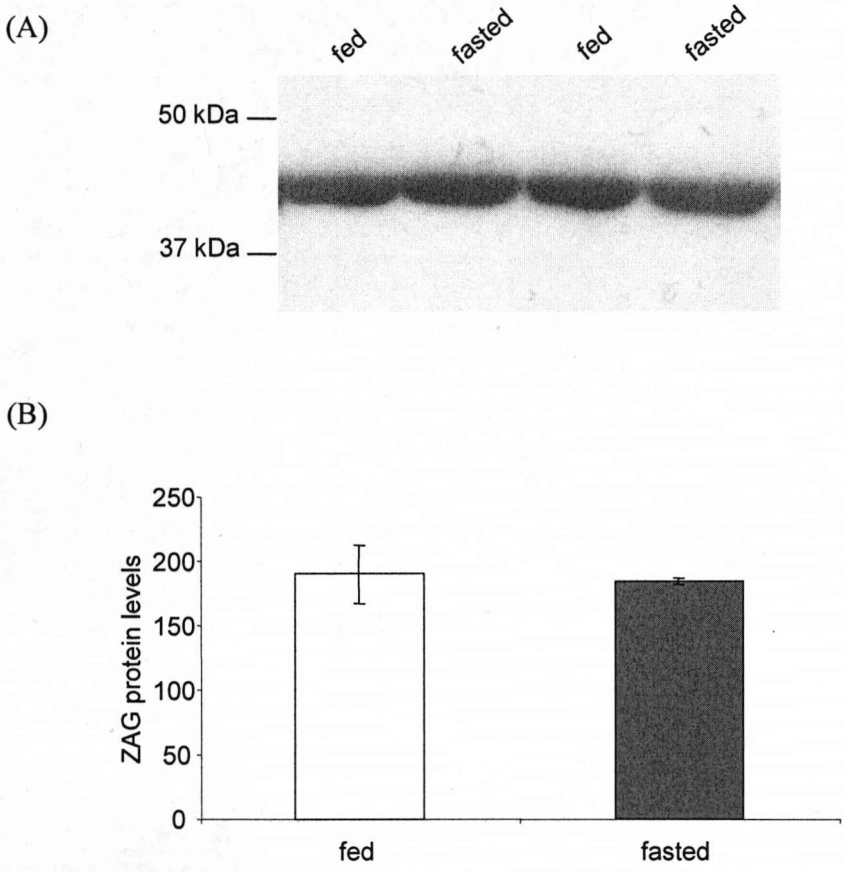

Protein samples were extracted from epididymal WAT of fed and 16h-fasted mice. Western blotting (A) followed by densitometric analysis (B) was used for quantification of ZAG protein levels. Results are expressed as means ± SEM (bars) for 5 mice. $P > 0.05$ compared to fed group (unpaired Student's *t*-test).

Figure 4.4 ZAG protein expression in perirenal WAT of mice fasted for 16 h

(A)

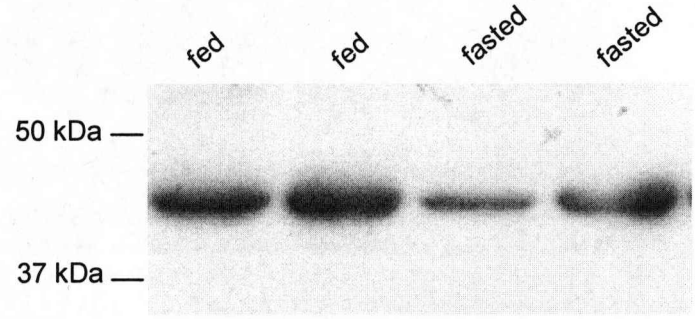

(B)

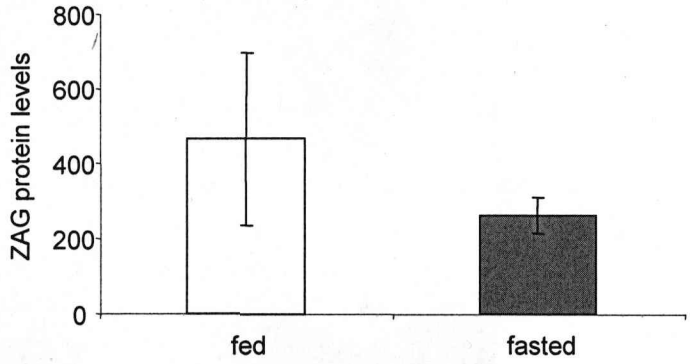

Protein samples were extracted from perirenal WAT of fed and 16h fasted mice. Western blotting (A) followed by densitometric analysis (B) was used for quantification of ZAG protein levels. Results are expressed as means ± SEM (bars) for 5 mice. $P > 0.05$ compared to fed group (unpaired Student's *t*-test).

Figure 4.5 ZAG mRNA levels in liver of mice fasted for 16 h

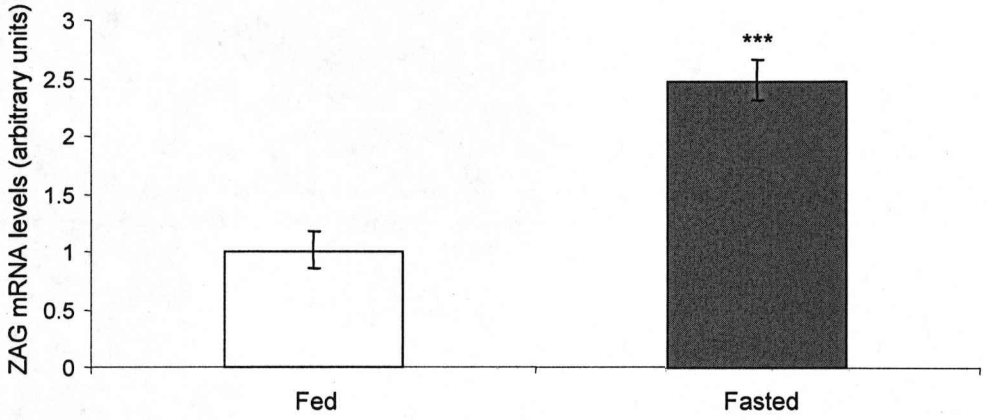

Liver samples were dissected from control (fed) and 16h-fasted mice. Real-time PCR was used for relative quantification of ZAG mRNA levels. Results are expressed relative to the expression levels in the fed group and are presented as means ± SE (bars) for 8 mice. $^{***}P < 0.001$ compared to the fed group and normalized to β-actin (unpaired Student's *t*-test).

Figure 4.6 Leptin mRNA levels in adipose tissue depots of mice fasted for 16h

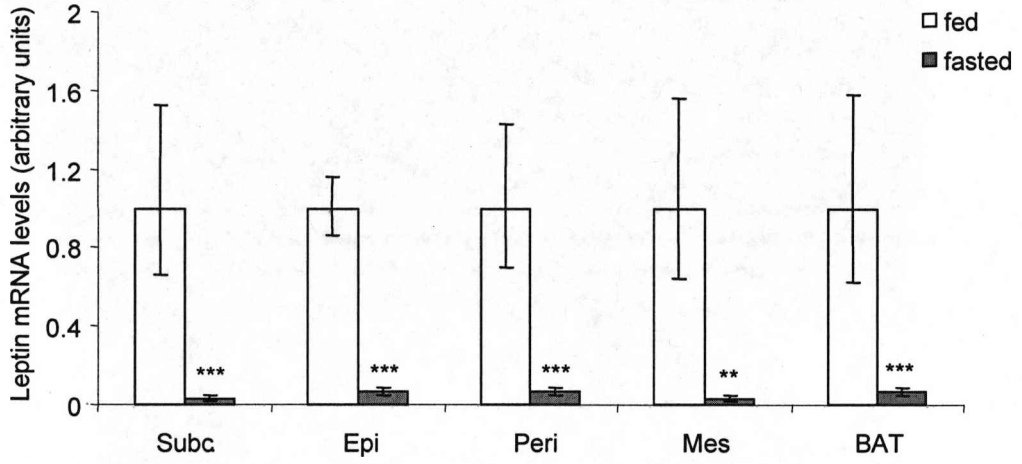

Four WAT depots and interscapular BAT were dissected from fed and 16h-fasted mice and total RNA was extracted. Real-time PCR was used for relative quantification of leptin mRNA levels. Results are expressed relative to the expression levels in the fed group for each depot and are presented as means ± SE (bars) for 6-8 mice. Subc, subcutaneous; epi, epididymal; peri, perirenal; mes, mesenteric; BAT, interscapular brown adipose tissue. $^{**}P < 0.01$, $^{***}P < 0.001$ compared to the fed group for each depot and normalized to β-actin (unpaired Student's *t*- test).

Figure 4.7 Adiponectin mRNA levels in adipose tissue depots of mice fasted for 16 h

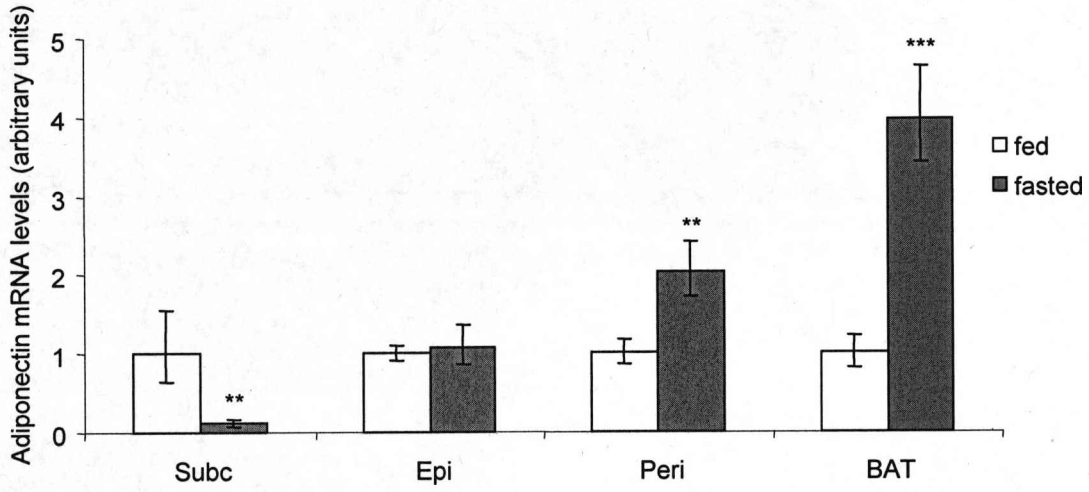

Three WAT depots and interscapular BAT were dissected from fed and 16h-fasted mice and total RNA was extracted. Real-time PCR was used for relative quantification of adiponectin mRNA levels. Results are expressed relative to the expression levels in the fed group for each depot and are presented as means ± SE (bars) for 6-8 mice. Subc, subcutaneous; epi, epididymal; peri, perirenal; BAT, interscapular brown adipose tissue. $^{**}P < 0.01$, $^{***}P < 0.001$ compared to the fed group for each depot and normalized to β-actin (unpaired Student's *t*- test).

4.3.2 Effects of high-fat diet on ZAG expression in mouse adipose tissue depots

Feeding the mice with a high-fat diet (58% fat by energy) for 12 weeks led to a substantial increase in body weight to the extent that they were considered obese. Net weight of adipose tissue depots was also substantially increased (weight data not shown).

As shown in Figure 4.8, *ZAG* gene expression displayed a site-specific pattern in response to the high-fat diet. The high-fat diet for 12 weeks induced a 2.8-fold decrease ($P < 0.01$) in ZAG mRNA levels in subcutaneous WAT. However, it led to a 4.7-fold increase ($P < 0.001$) in gonadal WAT. There was a small, but not statistically significant effect on ZAG mRNA levels in perirenal WAT similar to gonadal WAT. Similar patterns were observed for ZAG protein levels in subcutaneous and perirenal WAT, as a slight decrease was observed in the former and a slight increase in the latter. However, the results were not statistically significant ($P > 0.05$) (Figure 4.9).

Figure 4.8 Effects of high-fat diet on ZAG mRNA levels

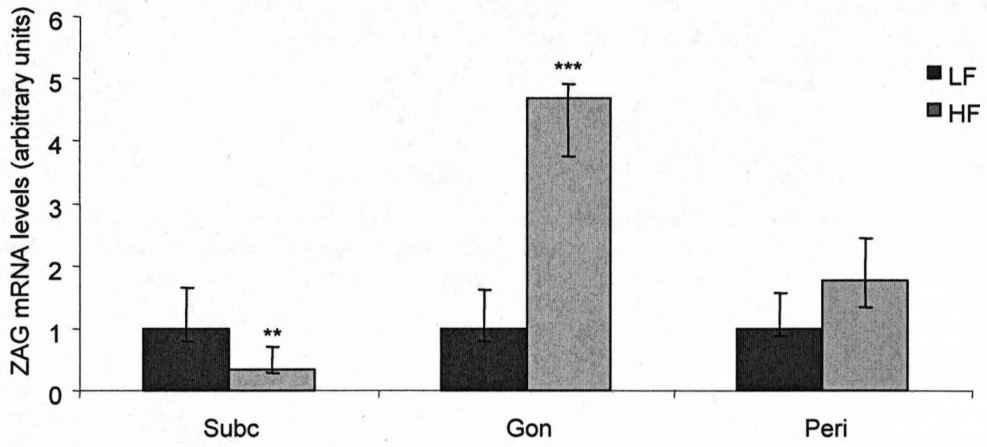

Three WAT depots were dissected from mice fed with low- and high-fat diet and total RNA was extracted. Real-time PCR was used for relative quantification of ZAG mRNA levels. Results are expressed relative to the expression levels in the low-fat diet fed group for each depot and are presented as means ± SE (bars) for 7-8 mice. Subc, subcutaneous; gon, gonadal; peri, perirenal. $^{**}P < 0.01$, $^{***}P < 0.001$ compared to normally fed group for each depot and normalized to β-actin (unpaired Student's *t*- test).

Figure 4.9 Effects of high-fat diet on ZAG protein levels

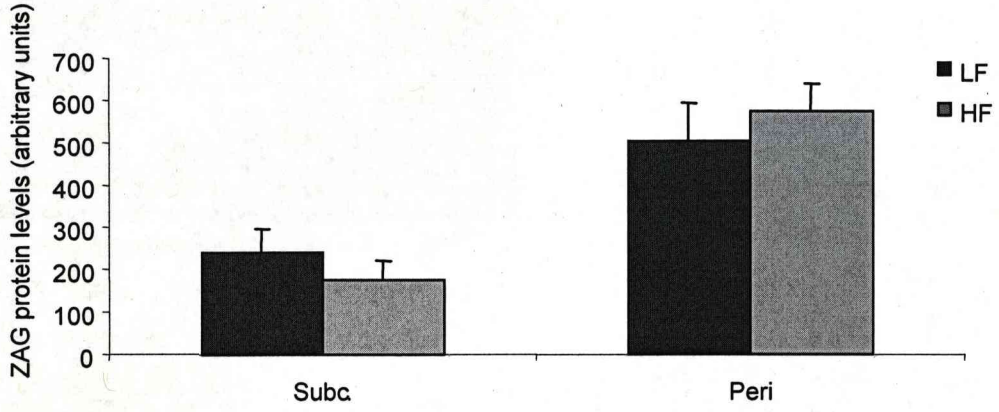

Protein samples were extracted from subcutaneous and perirenal WAT of mice fed with low- and high-fat diet. Western blotting followed by densitometric analysis was used for quantification of ZAG protein levels. Results are expressed as means ± SEM (bars) for 5 mice. $P > 0.05$ compared to normally fed group for each depot (unpaired Student's *t*-test).

4.4 Discussion

The effects of fasting and feeding a high-fat diet on the expression of various adipokines in rodent adipose tissue, including leptin and adiponectin, has been reported previously (Zhang *et al.*, 2002; Lopez *et al.*, 2003; Bertile & Raclot, 2004). It has been demonstrated that the degree to which adipose tissue secreted factors are affected by such changes in the diet may vary depending on several factors, the most important being the duration of the dietary change (Bertile & Raclot, 2004; Lopez *et al.*, 2005). Regional variations within WAT in response to changes in the nutrient supply have also been demonstrated (Sugden *et al.*, 1994; Einstein *et al.*, 2005). The current study is the first to examine the site-specific effect of fasting and high-fat diet on ZAG expression in mouse adipose tissue.

Fasting is characterised by changes in fuel availability and in adipose tissue lipid content. During food deprivation carbohydrate reserves are exhausted, resulting in protein sparing with increased lipid mobilization providing the main energy fuel for the needs of the organism (Goodman *et al.*, 1980). ZAG is a lipid-mobilising factor, strongly induced in WAT of MAC16 tumour-bearing mice, a cancer cachexia model, characterised by fat depletion (Bing *et al.*, 2004). *In vivo* administration of ZAG to mice induces a rapid reduction in body fat and increases serum free fatty acid levels (Hirai *et al.*, 1998). Based on that, it could be assumed that ZAG would be increased in adipose tissue during food deprivation.

However, the present study has demonstrated that 16h fasting induced a significant reduction in ZAG mRNA levels in epididymal WAT of mice, a similar trend being observed for subcutaneous, perirenal and mesenteric WAT. The more pronounced decrease in *ZAG* gene expression in epididymal WAT would be in line with the indication that the mobilization of intra-abdominal fat pads is greater during fasting (Sugden *et al.*, 1994). This response is not however consistent with a local role for ZAG in lipid mobilization in adipose tissue. However, ZAG expression was substantially increased both in BAT and liver samples of the same animals. This observed response of

ZAG to fasting may suggest that the overall production of ZAG is increased during food deprivation.

In the present study, 16h fast led to a decreased ZAG expression in WAT. Since ZAG is lipolytic in a full-grown animal, its decreased expression at times of food deprivation may be assumed to be part of an energy saving mechanism present in WAT as an initial response to fasting. A similar response to 16h fasting in adipose tissue has previously been reported for growth hormone (GH) (Korhonen & Saarela, 2005), another lipolytic factor (Harper, 1973).

The present study shows that 16h fasting decreased the body weight of the mice by as much as 8g. There was also a significant reduction in the net weight of the epididymal and perirenal depots, although not as a proportion to total body weight. Although the effect of fasting on body composition was not determined, it could be assumed that the weight reduction is largely due to decreased gut contents (food and faeces) and only secondarily due to WAT utilization. So it might be possible that the reduction of fat mass is not a direct factor for the decreased ZAG expression in WAT in response to fasting, which might be due to other changes occurring in the body in response to fasting, such as insulin resistance (Schwartz *et al.*, 1997). Further studies would be necessary to demonstrate whether the response is reversed by longer food deprivation, when WAT utilization would be more substantial.

In contrast to its decreased expression in WAT, ZAG was upregulated in BAT of fasted animals, possibly due to the high degree of sympathetic activity in the tissue during fasting (Giordano *et al.*, 2005). However, as discussed later in Chapter 4, studies on the regulation of ZAG in 3T3-L1 adipocytes, indicate that the sympathetic system may play at best a small role in the regulation of ZAG expression.

As part of the present study, the effect of fasting on leptin and adiponectin mRNA levels was also explored. As previously demonstrated (Trayhurn *et al.*, 1995; Zhang *et al.*, 2002), leptin mRNA levels were acutely and substantially decreased in all WAT depots tested in fasted mice. Leptin expression was also downregulated in the BAT of fasted

animals. The response of leptin to fasting is due to the whole body energy conservation evoked by food deprivation. Although the same would be expected in the case of adiponectin, both previous data and the results presented in the current study show the complex response to fasting. Reports available on the effects of fasting on adiponectin expression in WAT are not consistent. At first it was shown that adiponectin is decreased in perirernal WAT as a result of short-term fasting (Zhang *et al.*, 2002), although it was later shown that short-term fasting has no significant effect on adiponectin levels in WAT and that a decrease in its levels is only observed in subcutaneous and epididymal WAT after long-term food deprivation (5-7 days), when body lipid content nears exhaustion and the main energy is provided from protein utilization, suggesting that adiponectin may be involved in the adaptive response to long-term fasting (Bertile & Raclot, 2004). However, in the present study, similarly to the initial studies, adiponectin was significantly reduced in subcutaneous WAT after 16h fasting; however, its levels were increased in perirenal WAT and BAT. The possibility that the expression of adiponectin in BAT is differentially regulated compared to WAT has been previously raised (Zhang *et al.*, 2002). Although no conclusion can be made from the current observations, the data may suggest that there is a significant depot difference for adiponectin in response to 16h-fasting and some further analyses are needed.

The high fat diet induced a site specific response of ZAG expression in WAT. While ZAG mRNA levels were significantly downregulated in subcutaneous WAT, at the same time a substantial increase in its levels was observed in epididymal WAT and a similar trend was noticed in perirenal WAT. As previously discussed in more detail in Chapter 3, there are major differences among WAT depots, in particular between subcutaneous and visceral fat. In terms of the effects of changes in the diets, it has previously been reported that visceral fat is not biologically static and is probably regulated by nutrients (Einstein *et al.*, 2004). Furthermore, it is important to mention that the observed effects could be due to the lipid composition of the specific diet and different dietary lipids intake may possibly have a different effect.

In Chapter 3, it was shown that ZAG expression is reduced in WAT of genetically obese rodents, suggesting that it might be regulated by the increased adipogenesis occurring in the obese state. The mice used in the present study were kept for 12 weeks on a high fat diet and by the end of that period, a substantial increase in their body weight was observed. However, ZAG exhibits a different pattern of expression in genetic models of obesity as opposed to obese models as a result of changes in the diet. This finding might suggest that ZAG is sensitive to the component of the diet, such as fat content. Furthermore, it suggests that this effect depends on the anatomical location, possibly due to the different characteristics of WAT depots.

In conclusion, the current study provides information on the regulation of ZAG in mouse WAT and BAT by alterations in the diet. Inconsistent with its potential role in lipid mobilization in WAT, ZAG was downregulated in epididymal WAT of fasted mice, although its expression increased in BAT and liver. ZAG exhibited a depot specific response to high-fat diet. Taken together, these results suggest that ZAG expression in WAT is sensitive to diet alterations.

Chapter 5

ZAG expression in 3T3-L1 adipocytes: Regulation by hormones, inflammatory cytokines and prostaglandins

5.1 Introduction

In Chapters 3 and 4, a number of *in vivo* studies were conducted to explore the function of ZAG in adipose tissue. It was shown that ZAG is expressed in white adipose tissue, its mRNA and protein levels being equal in mature adipocytes and stromal vascular fraction of murine WAT depots. It was further demonstrated that ZAG expression is reduced in obesity, while ZAG exhibits differential patterns of expression in response to diet alterations in rodents. Another approach to studying the regulation of a certain gene is *in vitro* cell culture systems.

In contrast to *in vitro* studies, in *in vivo* studies the full physiological response to a stimulus can be seen and certain investigations, such as fasting or cold exposure can only be conducted *in vivo*. However, a key disadvantage of *in vivo* studies is that the exact cause leading to an effect cannot be easily isolated and identified as a certain stimulus may be acting directly or indirectly via downstream mediators. This can be resolved by *in vitro* studies, where a stimulus is directly applied to the cells of interest and thus any effect seen most likely results from their interaction.

In the present study, 3T3-L1 adipocytes, a widely employed murine clonal cell line, were used. These provide a unique model for insulin-sensitive primary fat cells, as under defined conditions they can be converted to fully differentiated adipocytes, characterized by increased insulin receptor number and induction of adipogenic specific proteins (Grako *et al.*, 1994). In contrast to primary culture systems, these cells are easier to maintain, and at an unlimited supply, as long as they are passaged and stored correctly.

ZAG has recently been shown to be expressed in 3T3-L1 adipocytes. As part of that study, it has been reported that *ZAG* gene expression in 3T3-L1 adipocytes is increased by dexamethasone, thus suggesting a role for glucocorticoids in its regulation, and by BRL37344, a selective β_3-adrenoreceptor agonist (Bing *et al.*, 2004).

The aim of the current study was to identify further key agents that play a role in the regulation of *ZAG* gene expression in 3T3-L1 adipocytes. In the first part of this study,

the expression of *ZAG* gene in these adipocytes was further investigated and the day of maximum ZAG expression post-differentiation was identified. Subsequently, adipocytes were treated with several important groups of agents, known to modulate the expression of several adipokines. The agents included catecholamines, inflammatory agents, interleukins and peripheral hormones, and their effects on ZAG expression in the system were assessed.

In the second part, the effect of prostaglandins on ZAG expression in 3T3-L1 adipocytes was investigated. As discussed in detail in Chapter 1, prostaglandins (PGs) are lipid-derived autacoids generated by sequential metabolism of arachidonic acid by the cyclooxygenase (COX) and prostaglandin synthase enzymes. Prostaglandins have been implicated in a broad array of diseases, such as cancer, inflammation and hypertension and exert their effects by activating rhodopsin-like seven transmembrane spanning G protein-coupled receptors (GPCRs), which include eight members (DP, EP1-4, FP, IP and TP) and a recently identified ninth receptor, the chemoattractant receptor homologous molecule expressed on Th2 cells (CRTH2). Very importantly, prostaglandins are known to be synthesized and released within WAT (Shillabeer *et al.*, 1998; Fain *et al.*, 2002; Bell-Parikh *et al.*, 2003; Jowsey *et al.*, 2003). There are no reports on the effects of prostaglandins on ZAG expression; however it has been observed that arachidonic acid has a stimulatory effect on ZAG mRNA levels in SGBS human adipocytes (Bao, personal communication); and prostaglandins on the other hand have been shown to affect a number of other adipokines including adiponectin, leptin, MCP-1, IL-6 (Peeraully *et al.*, 2006) and NGF (Bulló *et al.*, 2005) in 3T3-L1 adipocytes.

5.2 Methods

5.2.1 Cell culture

3T3-L1 cells were maintained and cultured as previously described in section 2.4. Briefly, cells were obtained from the American Type Culture Collection (Manassas, USA) and cultured at 37^{0}C in a humidified atmosphere of 5% CO_2/95% air. The cells were maintained in culture medium containing the following: DMEM with 25 mM glucose, 1 mM pyruvate, 4.02 mM L-alanyl-L-glutamine and 10% v/v FCS. Differentiation of the cells was initiated 2 days after confluence by incubation for two days in induction medium that consisted of culture medium with additional 10% FCS, 1 µM dexamethasone, 0.5 mM IBMX, and 2 µM insulin. The adipocytes were then kept in feeding medium, which was subsequently changed every 2 days. Differentiation of cells into adipocytes was confirmed by the visualized accumulation of lipid droplets.

The cells were maintained for up to 15 days post-differentiation and sampled every day, or for seven days after which time specific agents were added. The cells were pre-incubated at 7 days after differentiation for 24 h either with feeding medium (containing insulin and FCS), insulin-free medium (for the study on the effect of insulin), or FCS-free medium (for the studies on the effects of TNF-α, IL-6, LPS and Prostaglandins). Control cells were also pre-incubated with the same media.

Cells were then treated with media containing each of the specific agents at two different dose levels ('low' and 'high'). The control cells had no agents added. Agents used were; rosiglitazone (100 nM & 1 µM), noradrenaline (100 nM & 1 µM), isoprenaline (100 nM & 1 µM), BRL 37344 (100 nM & 1 µM), insulin (1 µM & 10 µM), leptin (100 nM & 2 µM), adiponectin (0.5 µg/ml & 2 µg/ml), LPS (10 ng/ml & 100 ng/ml), IL-6 (1 ng/ml & 25 ng/ml), TNF-α (5 ng/ml & 100 ng/ml), PGD_2 (50 µM & 100 µM), PGI_2 (50 µM & 100 µM), PGJ_2 (7.5 µM & 25 µM), Δ^{12}-PGJ_2 (7.5 µM & 25 µM) and 15d-PGJ_2 (25 µM & 75 µM). The concentrations used were derived from other studies in the Obesity Biology Unit. Between four and six individual wells in cell culture plates were treated with each agent or used as controls; different batches of cells were used for each

set of experiments. After 24 h cells were harvested, lysed in Trizol reagent, and stored at -80^{0}C until further analysis.

To investigate the dose dependent effect of Δ^{12}-PGJ_2, PGE_2 and PGF_{2a} on ZAG expression, cells were incubated for 24h with different concentrations (0-100 μM) of these agents.

5.2.2 RT-PCR and real-time PCR

Total RNA was extracted from tissues using Tri-Reagent as previously described in section 2.5. RNA was then treated using a DNA-free kit (section 2.5.3) and quantified using a BioPhotometer (section 2.5.4). RNA was reverse-transcribed using the Reverse-iT First Strand Synthesis kit (section 2.6.1) and the patterns of gene expression were analysed by RT-PCR (section 2.6.2). mRNA levels were assessed by real-time PCR (section 2.7) using a qPCR Core Kit and a ABI Prism 7700 machine, while for the prostaglandins treated samples a Mx3005P Stratagene machine was used.

5.2.3 Statistical analysis

Data are expressed as mean values ± SE. Comparisons between two groups were assessed by Student's *t*-test, while for differences among more than two groups they were analysed by one-way ANOVA coupled with Bonferroni's *t*-tests, as previously described in section 2.9. $P < 0.05$ was considered as statistically significant.

5.3 Results

5.3.1 *ZAG* gene expression in 3T3-L1 cells

Although the expression of ZAG in 3T3-L1 cells has previously been demonstrated (Bing *et al.*, 2004), it was important to establish its detailed expression pattern in the cells both pre- and post-differentiation before assessing the regulation of *ZAG* gene expression. *ZAG* gene expression was examined in 3T3-L1 cells by RT-PCR (Figure 5.1) and although the signal was relatively low, ZAG mRNA was detected at all time points tested before and after the induction of differentiation. The expression of resistin, known to be expressed in adipocytes post-differentiation (Haugen *et al.*, 2001), was tested in the same samples as a reference point and a strong signal was detected from day 2 after induction of differentiation and thereafter.

In order to identify a suitable time point for treating the cells with the agents, a time course of the relative mRNA levels of ZAG in 3T3-L1 adipocytes pre- and post-differentiation was established. As shown in Figure 5.2, there are no significant differences in ZAG mRNA levels at the different time-points, as well as pre- and post-differentiation. Therefore, the subsequent studies on the regulation of ZAG in 3T3-L1 adipocytes were conducted at day 8 post- differentiation, by which time lipid droplets are well established and molecular markers characteristic of fat cells are expected.

5.3.2 Regulation of *ZAG* gene expression in 3T3-L1 adipocytes

At day 8 post- differentiation, cells were treated with various specific agents and the regulation of *ZAG* gene expression in 3T3-L1 adipocytes was investigated using real-time PCR to quantify the relative ZAG mRNA levels. These agents can be grouped into the following categories, according to their properties; sympathetic agents, peripheral hormones, rosiglitazone, inflammatory regulators and prostaglandins.

Figure 5.1 Time course of *ZAG* gene expression in 3T3-L1 adipocytes

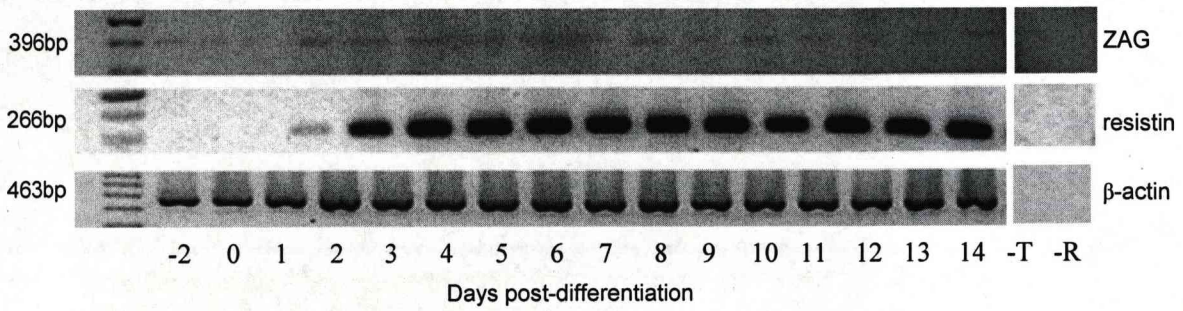

3T3-L1 cells in culture were collected at various time points pre- and post- induction of differentiation into adipocytes. RNA was examined by RT-PCR to detect gene expression of ZAG (35 cycles) and resistin (25 cycles) over the time course. Differentiation was induced at day 0. –T, no template control; -R, no RT control.

Figure 5.2 Time course of ZAG mRNA levels in 3T3-L1 adipocytes

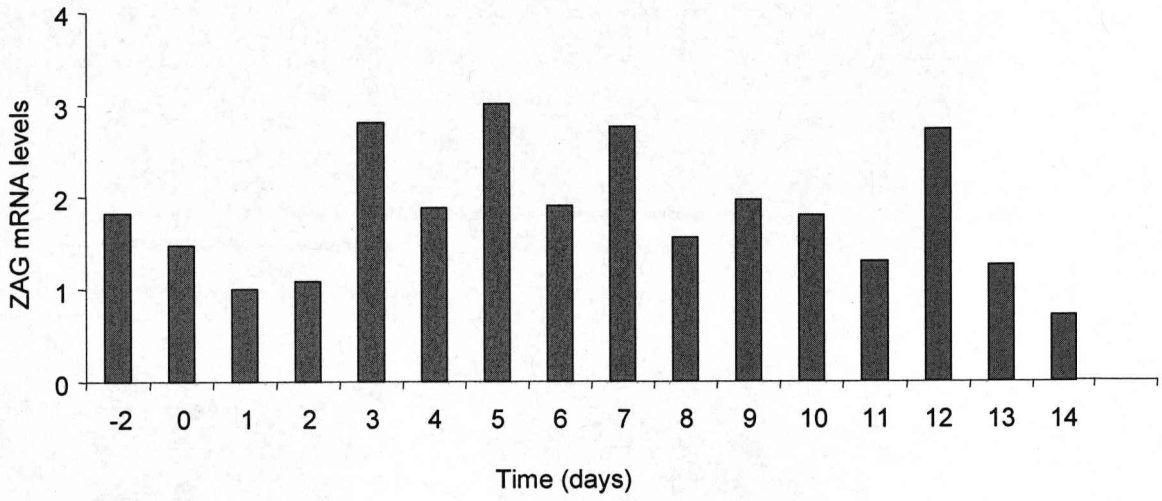

3T3-L1 cells in culture were collected at various time points pre- and post- induction of differentiation into adipocytes. RNA was extracted and examined by real-time PCR to determine ZAG relative mRNA levels over the time course. Differentiation was induced at day 0. Results are given as single value/means.

5.3.2.1 Effects of sympathetic agonists on ZAG gene expression

The first set of experiments was aimed to investigate the effects of sympathetic mediators on the regulation of *ZAG* gene expression. Adipocytes were treated at two dose levels of each of noradrenaline, isoprenaline and BRL 37344. Treatment with noradrenaline at either low or high doses had no effect on ZAG mRNA level (Figure 5.3A). The addition of isoprenaline led, however, to a statistically significant increase in ZAG mRNA level (~2.5-fold) at both low and high doses ($P < 0.01$) (Figure 5.3B). Finally, the addition of a β_3-adrenoreceptor agonist, BRL 37344, induced a statistically significant response (~3-fold) only at the low dose ($P < 0.05$) (Figure 5.3C).

5.3.2.2 Effects of peripheral hormones and rosiglitazone on ZAG gene expression

The aims of the following experiments were to examine the effects of insulin, adiponectin, rosiglitazone and leptin on ZAG mRNA levels in 3T3-L1 adipocytes.

As shown in Figure 5.4A, insulin had no effect on ZAG mRNA levels. Adiponectin on the other hand induced a statistically significant dose-dependent increase in ZAG mRNA levels, with the effect of the high dose being a 5-fold elevation ($P < 0.01$) (Figure 5.4B).

The largest increase in ZAG mRNA levels was observed with rosiglitazone, which resulted in a 3.5-fold and 5-fold increase at the low and high doses respectively ($P < 0.001$) (Figure 5.5A). To assess the specificity of the effect of rosiglitazone on ZAG expression in 3T3-L1 adipocytes, mRNA levels of two other adipokines, adiponectin and IL-6, were measured. Adiponectin mRNA levels were increased significantly at the low and high doses (both ~2.5-fold) ($P < 0.01$ and $P < 0.05$) (Figure 5.5B), while IL-6 showed a trend of a dose-dependent reduction, although the changes were not statistically significant ($P > 0.05$) (Figure 5.5C).

Figure 5.3 Effect of noradrenaline, isoprenaline and BRL 37344 on ZAG mRNA levels in 3T3-L1 adipocytes

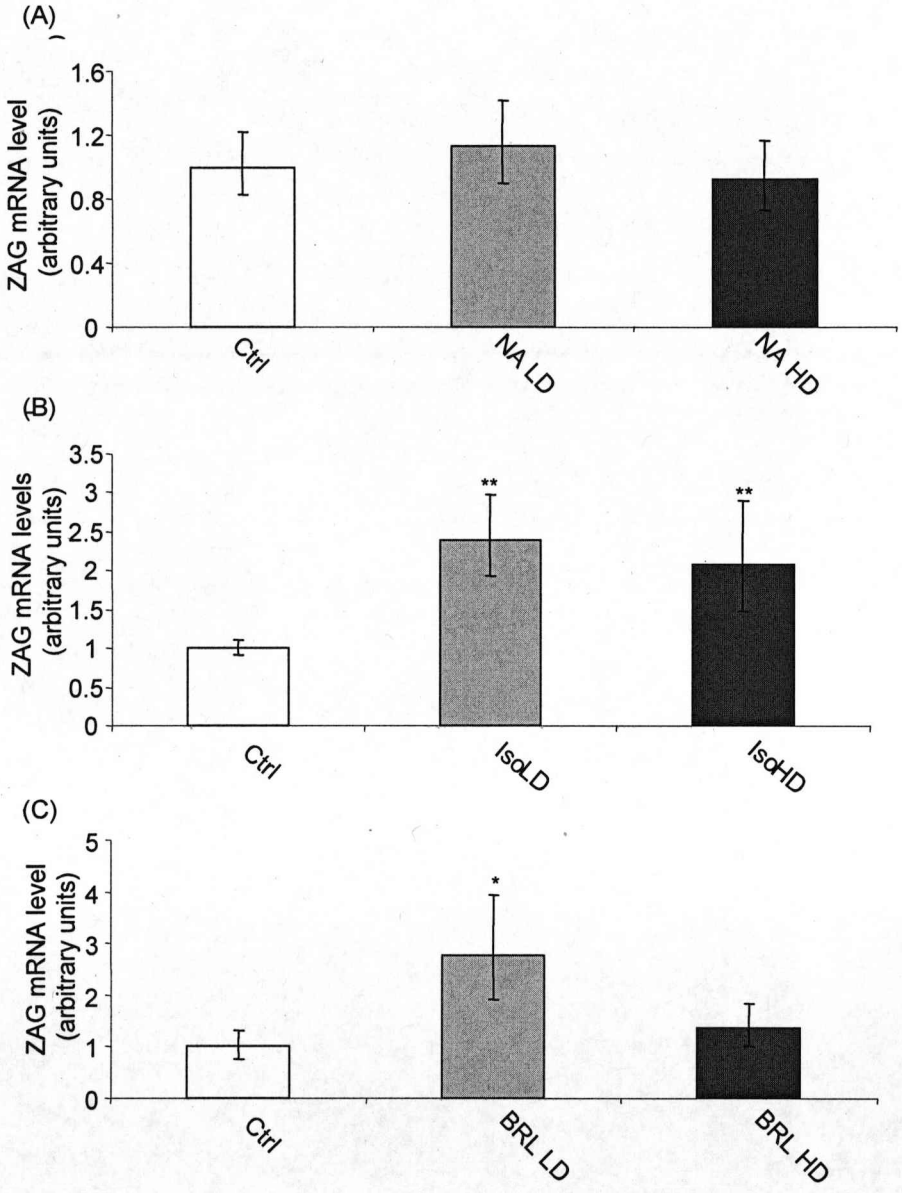

Cells were harvested at day 8 after the induction of differentiation and were incubated for 24 h in a medium containing noradrenaline (NA; A), isoprenaline (Iso; B) and BRL 37344 (BRL; C) (LD, low dose; HD, high dose). No reagent was added to the medium of control cells. NA LD, 100 nM; NA HD, 1 μM; Iso LD, 100 nM; Iso HD, 1 μM; BRL LD, 100 nM, BRL HD, 1 μM. ZAG mRNA levels, measured by real-time PCR, are expressed relative to controls. Results are given as means ± SE (bars) for groups of 5-6. $^{*}P < 0.05$, $^{**}P < 0.01$ compared with controls and normalised to β-actin.

Figure 5.4 Effect of Insulin and Adiponectin on ZAG mRNA levels in 3T3-L1 adipocytes

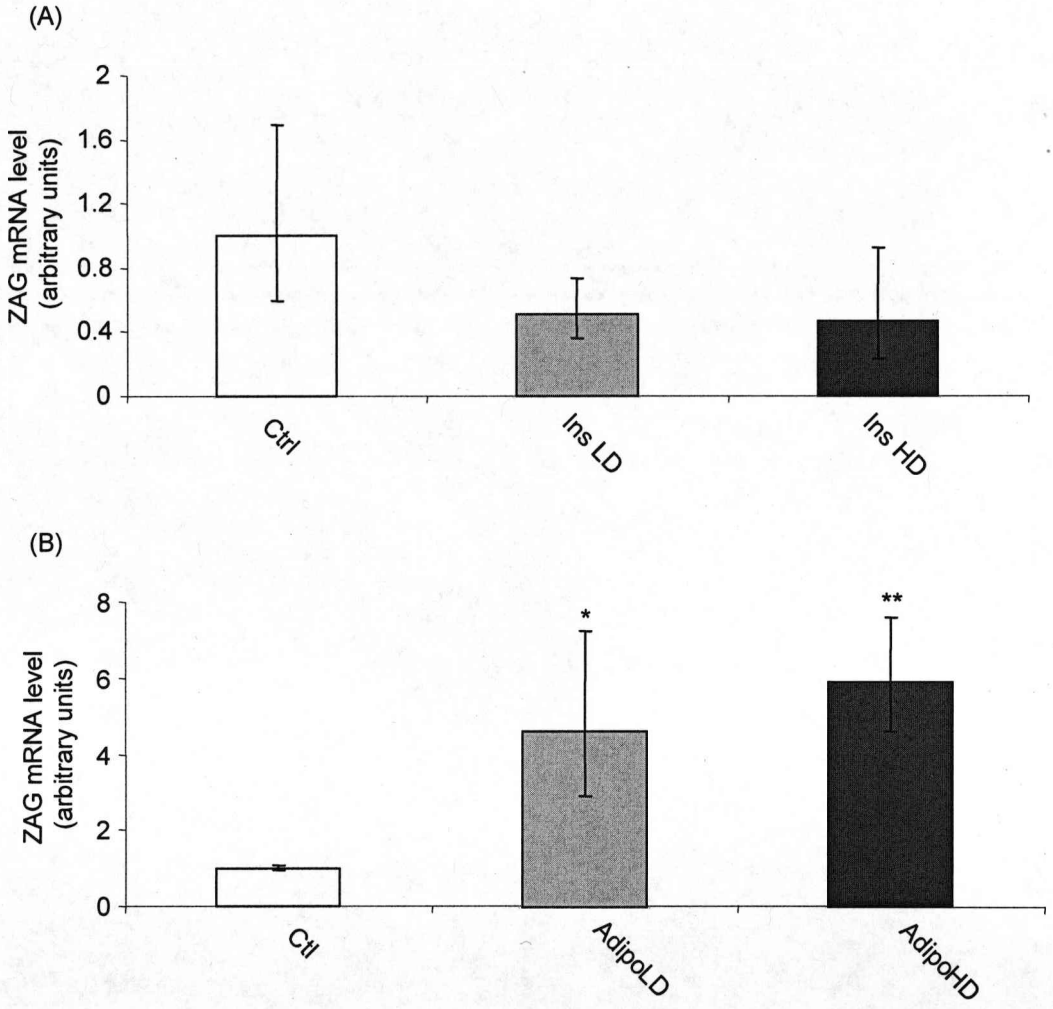

Cells were harvested at day 8 after the induction of differentiation and were incubated for 24 h in a medium containing insulin (Ins; A) and adiponectin (adipo; B) (LD, low dose; HD, high dose). No reagent was added to the medium of control cells. Ins LD, 1 μM ; Ins HD, 10 μM; Adipo, 0.5 μg/ml, adipo HD, 2 μg/ml. ZAG mRNA levels, measured by real-time PCR, are expressed relative to controls. Results are given as means ± SE (bars) for groups of 5-6. $^{*}P < 0.05$, $^{**}P < 0.01$ compared with controls and normalised to β-actin.

Figure 5.5 Effect of rosiglitazone on ZAG mRNA levels in 3T3-L1 adipocytes

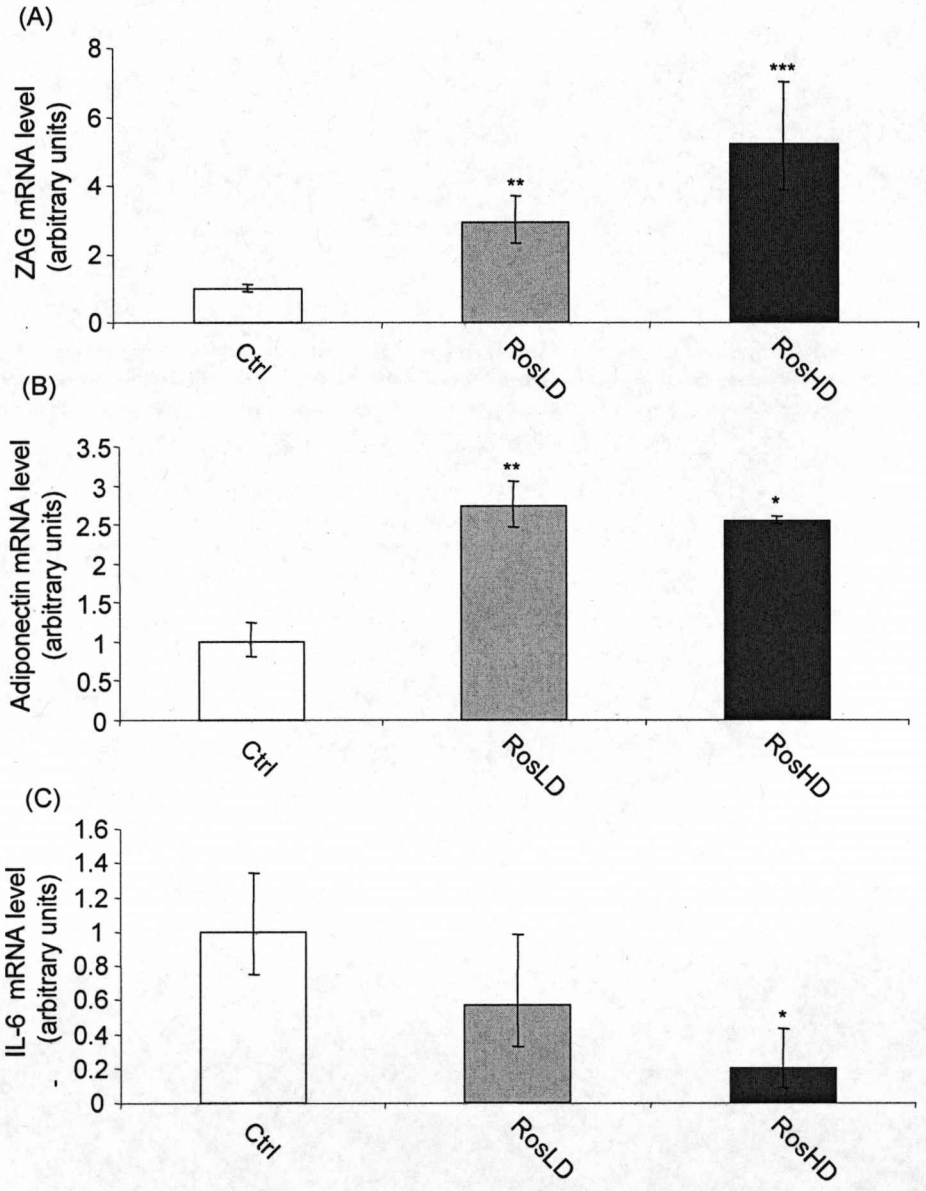

Cells were harvested at day 8 after the induction of differentiation and were incubated for 24h in a medium containing rosiglitazone (LD, low dose, 100 nM; HD, high dose, 1 μM). No reagent was added to the medium of control cells. ZAG (A), adiponectin (B) and IL-6 (C) mRNA levels, measured by real-time PCR, are expressed relative to controls. Results are presented as means ± SE (bars) for groups of 5-6. $*P < 0.05$, $**P < 0.01$ compared to controls and normalised to β-actin.

Leptin induced a statistically significant reduction in ZAG mRNA with low and high dose, (both ~5-fold, $P < 0.01$) (Figure 5.6A). The effect of leptin on ZAG expression was compared with that on adiponectin and IL-6. Leptin induced a 1.7-fold reduction in adiponectin levels at the lower dose ($P < 0.01$), a similar effect being observed at the high dose ($P < 0.05$) (Figure 5.6B), and similarly a 2.5-fold reduction in IL-6 mRNA levels at the higher dose ($P < 0.01$) (Figure 5.6C).

5.3.2.3 Effects of inflammatory regulators on ZAG gene expression

In this set of experiments, the effects of LPS, IL-6 and TNFα on ZAG mRNA levels were investigated. All three agents are known for their pro-inflammatory nature in adipocytes. As shown in Figure 5.7, ZAG mRNA levels in 3T3-L1 adipocytes were unaffected by any of these agents at either of the two dose levels used.

5.3.3 Regulation of *ZAG* gene expression by prostaglandins in 3T3-L1 adipocytes

5.3.3.1 Effects of PGD_2 and J_2-series prostaglandins on ZAG gene expression

Addition of PGD_2 did not affect *ZAG* gene expression at either the low and high doses (Figure 5.8). As previously noted, in culture medium, PGD_2 can spontaneously be converted to PGJ_2 and the latter to its metabolites Δ^{12}-PGJ_2 and 15d-PGJ_2. Thus, the possible effect of each of the prostaglandin derivatives of PGD_2 on *ZAG* gene expression was explored. The high doses used for both PGJ_2 and Δ^{12}-PGJ_2 induced a significant increase in ZAG mRNA levels by ~3- ($P < 0.05$) and 23-fold respectively ($P < 0.001$). 15d-PGJ_2 induced a ~19-fold ($P < 0.001$) increase in ZAG mRNA levels at the low dose, its levels declining to those of the control group with the high dose (Figure 5.8).

Considering the substantial effect of $\Delta^{12}PGJ_2$ on ZAG mRNA levels at the high concentration, an extended dose-response study was undertaken with this prostaglandin with doses ranging from 1 to 100 μM of $\Delta^{12}PGJ_2$ being used. ZAG mRNA levels in 3T3-

Figure 5.6 Effect of Leptin on ZAG mRNA levels in 3T3-L1 adipocytes

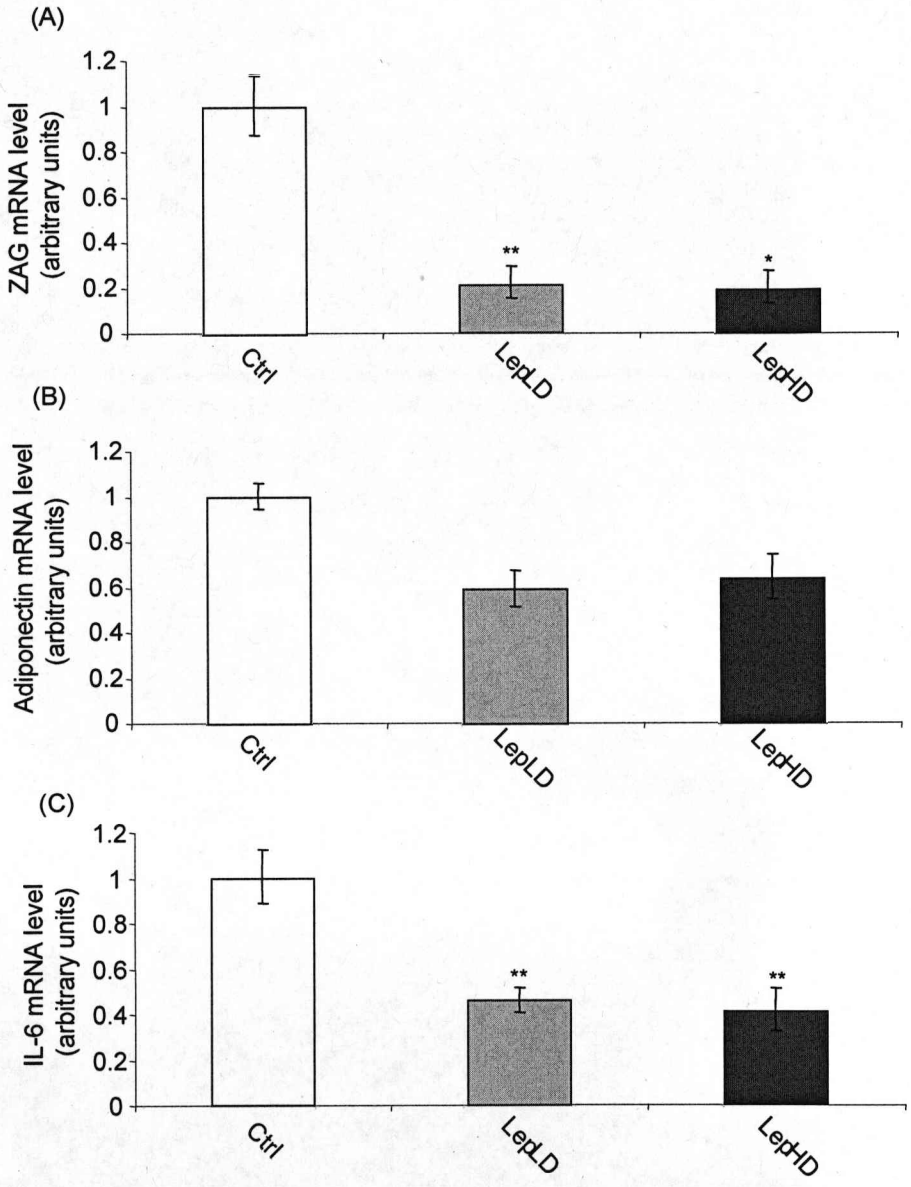

Cells were harvested at day 8 after the induction of differentiation and were incubated for 24h in a medium containing leptin (LD, low dose, 100 nM; HD, high dose, 2 μM). No reagent was added to the medium of control cells. ZAG (A), adiponectin (B) and IL-6 (C) mRNA levels, measured by real-time PCR, are expressed relative to controls. Results are presented as means ± SE (bars) for groups of 5-6. $*P < 0.05$, $**P < 0.01$ compared to controls and normalised to β-actin.

Figure 5.7 Effect of LPS, IL-6 and TNF-α on ZAG mRNA levels in 3T3-L1 adipocytes

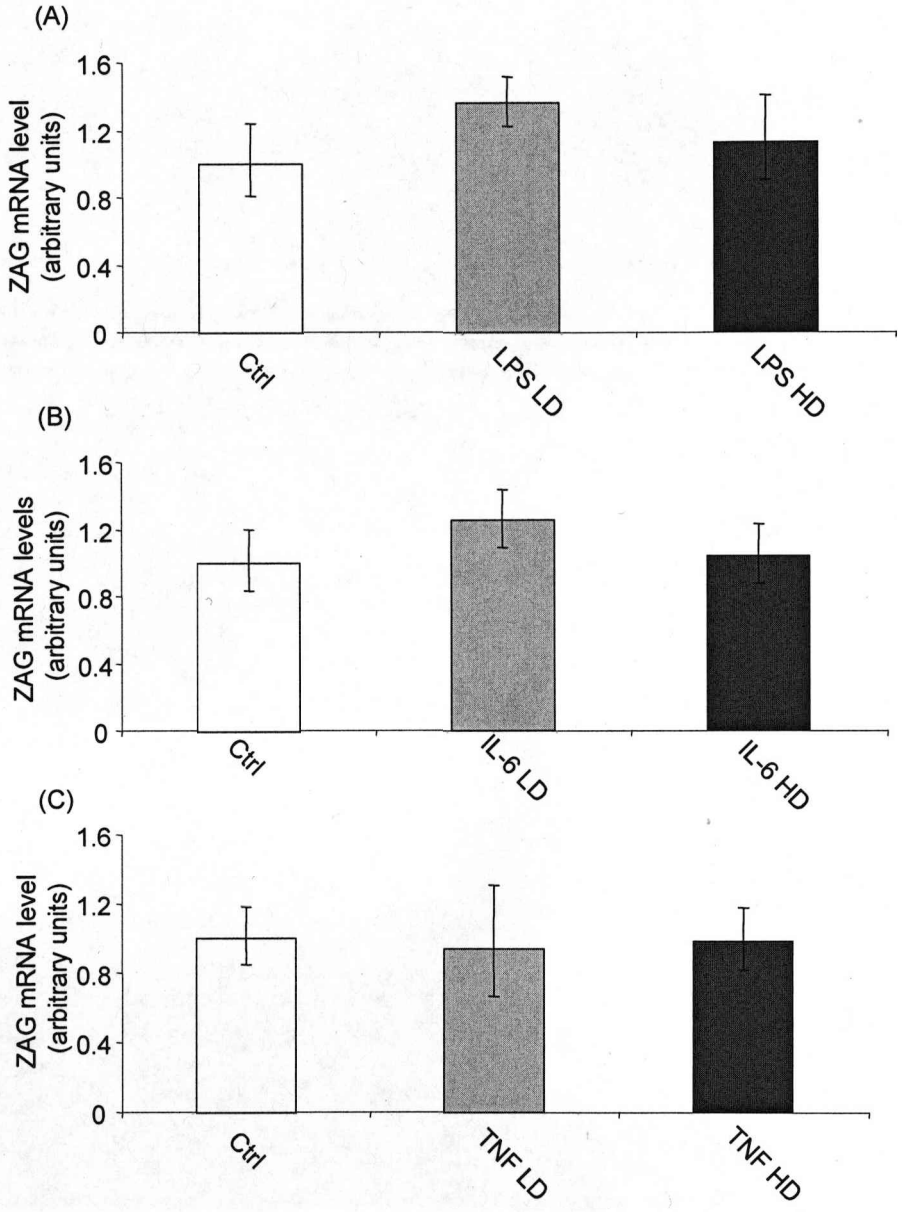

Cells were harvested at day 8 after the induction of differentiation and were incubated for 24h in a medium containing lipopolysacharide (LPS; A), Interleukin-6 (IL-6; B) and tumour-necrosis factor-alpha (TNF-α; C) (LD, low dose; HD, high dose). No reagent was added to the medium of control cells. LPS LD, 10 ng/ml; LPS HD, 100 ng/ml; IL-6 LD, 1 ng/ml ; IL-6 HD, 25 ng/ml; TNF-α, 5 ng/ml, TNF-α HD, 100 ng/ml. ZAG mRNA levels, measured by real-time PCR, are expressed relative to controls. Results are given as means ± SE (bars) for groups of 5-6. There were no significant differences ($P > 0.05$).

Figure 5.8 Effect of PGD_2 and J_2 - series prostaglandins on ZAG mRNA levels in 3T3-L1 adipocytes

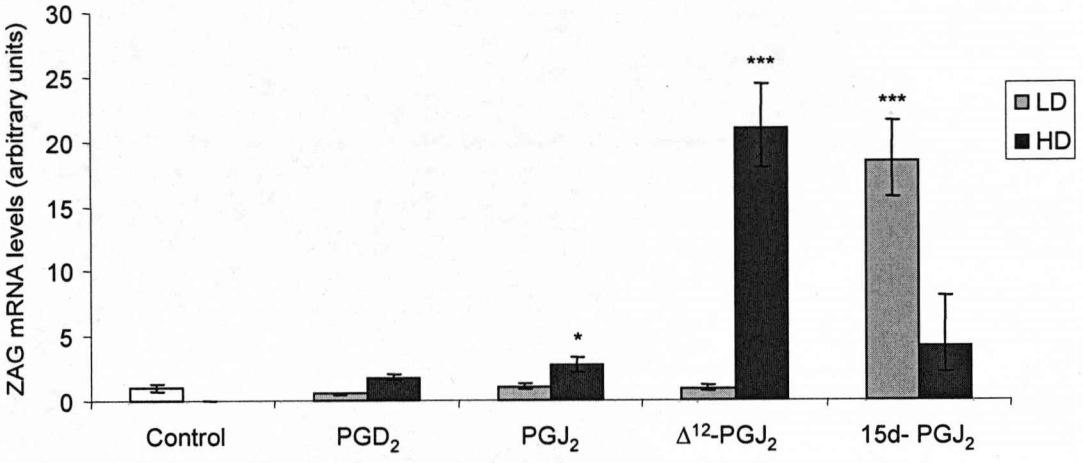

Cells were harvested at day 8 after the induction of differentiation and were incubated for 24h in a medium containing PGD_2, PGJ_2, Δ^{12}-PGJ_2 and 15d- PGJ_2 (LD, low dose; HD, high dose). No reagent was added to the medium of control cells. PGD_2 LD, 50 μM; PGD_2 HD, 100 μM ; PGJ_2 LD, 7.5 μM ; PGJ_2 HD, 25 μM; Δ^{12}-PGJ_2 LD 7.5 μM , Δ^{12}-PGJ_2 HD, 25 μM; 15d- PGJ_2 LD, 25 μM; 15d- PGJ_2 HD, 75 μM. ZAG mRNA levels, measured by real-time PCR, are expressed relative to controls. Results are given as means ± SE (bars) for groups of 5-6. $^*P < 0.05$, $^{**}P < 0.01$, $^{***}P < 0.001$ compared to controls and normalised to β-actin.

L1 adipocytes were significantly increased with treatment of Δ^{12}-PGJ_2 and the increase was dose-dependent. There was a 5-fold increase in ZAG mRNA levels at 1 μM, the highest response being observed with 75 μM when the increase was ~90-fold (figure 5.9).

5.3.3.2 Effects of PGE_2, $PGF_{2\alpha}$ and PGI_2 on ZAG gene expression

Since a pilot study had indicated that both PGE_2 and $PGF_{2\alpha}$ have an inhibitory effect on ZAG expression in 3T3-L1 adipocytes (data not shown), an extended dose-response study was undertaken to explore the effect of these prostaglandins in detail. In both experiments, cells were treated with PGE_2 and $PGF_{2\alpha}$ at doses varying from 10 nM to 100 μM. PGE_2 significantly reduced ZAG mRNA levels with a concentration of 100 nM and above, and the biggest effect was seen at a dose of 100 nM, which induced a 20-fold reduction in ZAG mRNA levels ($P < 0.001$) (Figure 5.10).

To further assess the specificity of PGE_2 on ZAG expression, its effect on adiponectin and IL-6 mRNA levels were also examined. As demonstrated in Figure 5.11, PGE_2 led to a significant gradual decrease in adiponectin mRNA levels with a concentration of 300 nM and above, while it induced a significant increase in IL-6 mRNA levels with a concentration of 3 μM and above.

$PGF_{2\alpha}$ induced a significant reduction in ZAG mRNA levels with a concentration of 100 nM and above, the biggest effect being observed at a dose of 3 μM which induced a 30-fold decrease ($P < 0.001$) (Figure 5.12). Finally, the effect of PGI_2 on ZAG mRNA levels was investigated. PGI_2 had no significant effect on ZAG mRNA level neither at the low or high doses used (Figure 5.13).

Figure 5.9 Dose response of Δ^{12}-PGJ_2 on ZAG mRNA levels in 3T3-L1 adipocytes

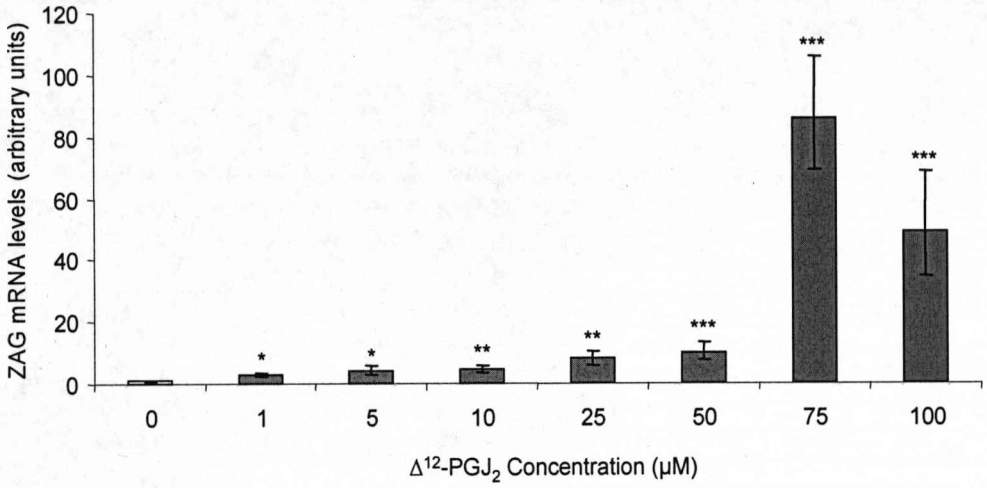

Cells were harvested at day 8 after the induction of differentiation and were incubated for 24h in a medium containing different doses of Δ^{12}-PGJ_2. No reagent was added to the medium of control cells. ZAG mRNA levels, measured by real-time PCR, are expressed relative to controls. Results are given as means ± SE (bars) for groups of 4. $^{*}P < 0.05$, $^{**}P < 0.01$, $^{***}P < 0.001$ compared to controls and normalised to β-actin.

Figure 5.10 Dose response of PGE_2 on ZAG mRNA levels in 3T3-L1 adipocytes

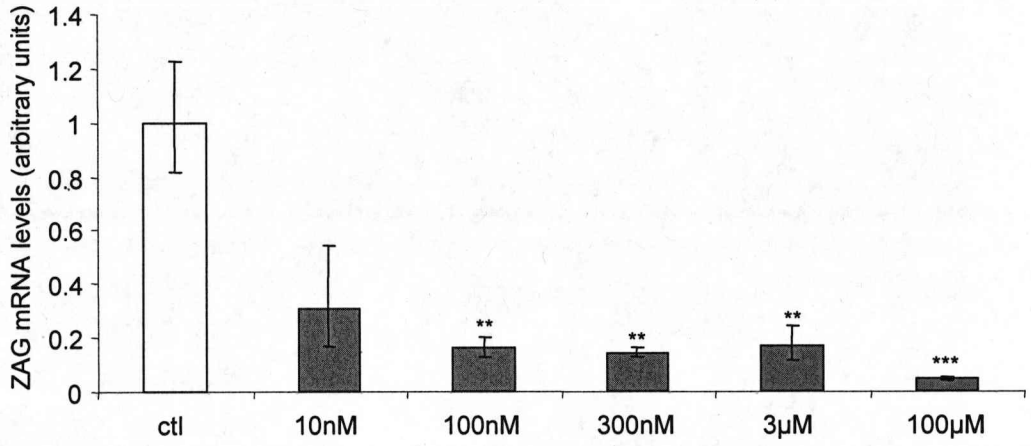

Cells were harvested at day 8 after the induction of differentiation and were incubated for 24h in a medium containing different doses of PGE_2. No reagent was added to the medium of control cells. ZAG mRNA levels, measured by real-time PCR, are expressed relative to controls. Results are given as means ± SE (bars) for groups of 5-6. $^{**}P < 0.01$, $^{***}P < 0.001$ compared to controls and normalised to β-actin.

Figure 5.11 Dose response of PGE_2 on adiponectin and IL-6 mRNA levels in 3T3-L1 adipocytes

(A)

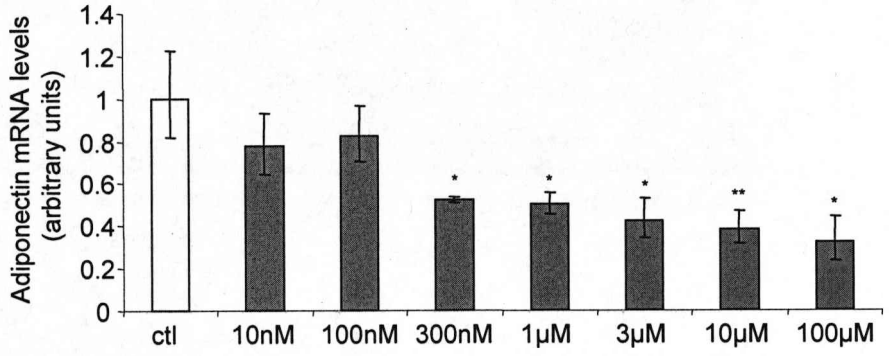

(B)

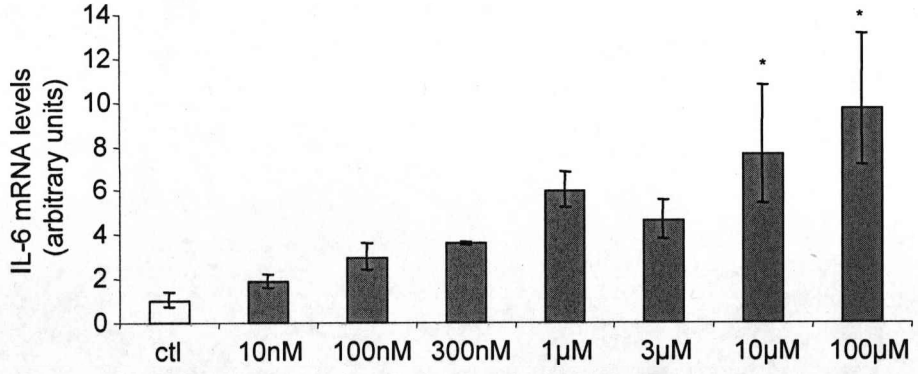

Cells were harvested at day 8 after the induction of differentiation and were incubated for 24h in a medium containing different doses of PGE_2. No reagent was added to the medium of control cells. Adiponectin (A) and IL-6 (B) mRNA levels, measured by real-time PCR, are expressed relative to controls. Results are given as means ± SE (bars) for groups of 5-6. $^*P < 0.05$, $^{**}P < 0.01$ compared to controls and normalised to β-actin.

Figure 5.12 Dose response of $PGF_{2\alpha}$ on ZAG mRNA levels in 3T3-L1 adipocytes

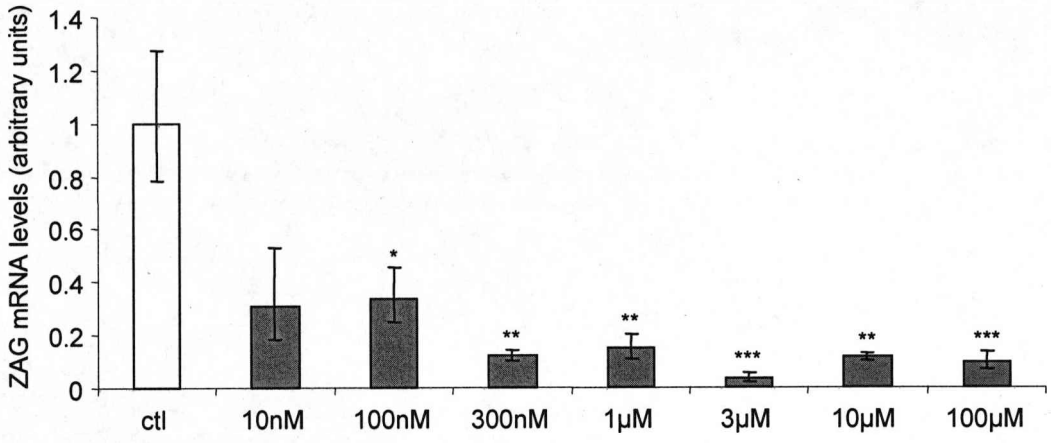

Cells were harvested at day 8 after the induction of differentiation and were incubated for 24h in a medium containing different doses of $PGF_{2\alpha}$. No reagent was added to the medium of control cells. ZAG mRNA levels, measured by real-time PCR, are expressed relative to controls. Results are given as means ± SE (bars) for groups of 5-6. $^{*}P < 0.05$, $^{**}P < 0.01$, $^{***}P < 0.001$ compared to controls and normalised to β-actin.

Figure 5.13 Effect of PGI_2 on ZAG mRNA levels in 3T3-L1 adipocytes

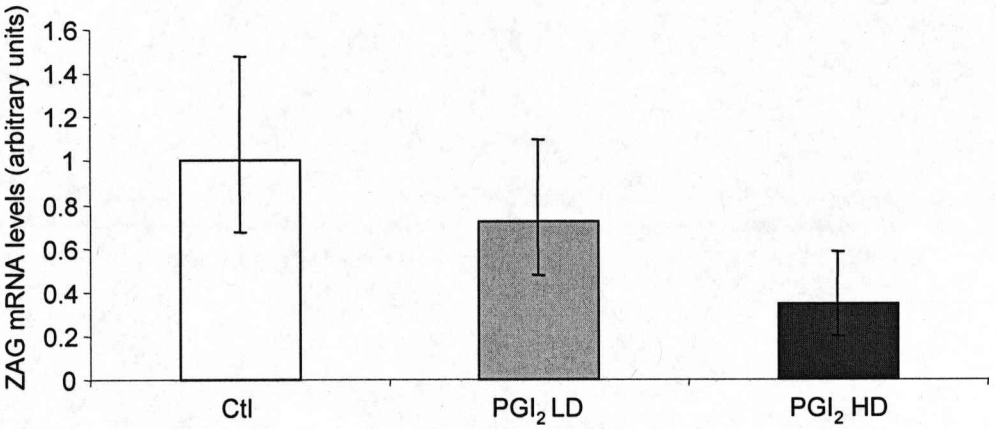

Cells were harvested at day 8 after the induction of differentiation and were incubated for 24h in a medium containing PGI_2 (LD, low dose; HD, high dose). No reagent was added to the medium of control cells. PGI_2 LD 50 μM , PGI_2 HD, 100 μM. ZAG mRNA levels, measured by real-time PCR, are expressed relative to controls. Results are given as means ± SE (bars) for groups of 5-6. There were no significant differences ($P >$ 0.05).

5.4 Discussion

In Chapter 3, it was demonstrated that both ZAG mRNA and protein are expressed in mouse white adipose tissue. Furthermore, it was shown that mature adipocytes express the *ZAG* gene and protein, consistent with a previous report of *ZAG* gene expression in human adipocytes (Bao *et al.*, 2005). This is further evidence that ZAG is an adipokine and could have a local autocrine/ paracrine effect on white adipose tissue and ZAG produced locally could also contribute to the circulating level of the protein. However, from the data presented in this chapter, it is evident that in contrast to what has been demonstrated in human adipocytes, and unlike other adipokines such as resistin, ZAG in murine adipocytes is not a marker of adipocyte differentiation, as it is expressed at similar levels in the fibroblastic 3T3-L1 preadipocytes. This is in line with results presented in Chapter 3, where it was demonstrated that ZAG is equally expressed in mature adipocytes and stromal vascular fraction of murine white adipose tissue depots, as a large portion of the stromal vascular fraction consists of preadipocytes.

There is little information on the regulation of ZAG expression in mouse adipose tissue, although a previous study has suggested that in 3T3-L1 adipocytes, both dexamethasone and a β_3-adrenoreceptor agonist (BRL 37344) have a stimulatory effect on ZAG mRNA levels (Bing *et al.*, 2004). Studies conducted in this chapter focused on identifying key factors, known to modulate the expression of several adipokines, which may also regulate ZAG expression in murine adipocytes. The data presented in this study indicates that a number of hormones and factors can modulate ZAG mRNA levels in 3T3-L1 adipocytes. At the same time the current study was being conducted, a study on the regulation of *ZAG* gene expression on SGBS cell strain, a model of human adipocytes, was published (Bao *et al.*, 2005). A number of factors were also identified in that study; comparisons between the two models are mentioned here, when appropriate.

Noradrenaline, an α- and β- adrenoreceptor agonist, had no effect on *ZAG* gene expression. On the other hand, isoprenaline, a β- adrenoreceptor selective agonist and BRL 37344, a selective β_3-adrenoreceptor agonist, both induced an increase in ZAG

mRNA levels in adipocytes. These results suggest that the sympathetic system may play some role in the regulation of ZAG expression, especially via β_3-adrenoreceptors, which are the dominant receptor type in the stimulation of lipolysis in rodent adipose tissue (Arch, 2001). However, given the small size of these effects, the SNS is unlikely to be a major player in the regulation of ZAG expression.

One of the more substantial effects on *ZAG* gene expression was obtained with rosiglitazone, a selective PPARγ agonist, which induced a 5.5-fold increase in ZAG mRNA levels at the high dose. Its effect on ZAG paralleled its stimulatory effect on adiponectin mRNA, while having the opposite effect on IL-6, as previously reported (Lagathu *et al.*, 2003), indicating that the PPARγ nuclear receptor is involved in the regulation of ZAG synthesis. A number of studies have previously demonstrated that PPARγ ligands regulate the expression of several adipokines by suppressing those linked to insulin resistance and inflammatory response, such as resistin (Haugen *et al.*, 2001), TNFα (Sigrist *et al.*, 2000) and IL-6 (Lagathu *et al.*, 2003), while stimulating adiponectin (Maeda *et al.*, 2001), an insulin-sensitizing and anti-inflammatory adipokine. Since rosiglitazone has anti-inflammatory properties, upregulation of *ZAG* gene expression in murine adipocytes by rosiglitazone observed in the current study and a previous report using human SGBS adipocytes (Bao *et al.*, 2005) may suggest that ZAG might have an anti-inflammatory role in adipose tissue. Rosiglitazone's stimulatory effect on *ZAG* gene expression might also suggest a role for ZAG in insulin sensitivity, however further investigations would be necessary to substantiate this. The observation that pro-inflammatory agents, such as LPS, IL-6 and TNFα had no effect on ZAG mRNA levels in murine adipocytes might suggest that rosiglitazone acts directly to increase ZAG expression and not via the regulation of pro-inflammatory cytokines.

In the present study, it was shown that in 3T3-L1 adipocytes treated with adiponectin, ZAG was increased by 6-fold. Adiponectin, along with its other effects, has an anti-inflammatory action which includes the inhibition of NFκB activation (Ouchi *et al.*, 2000). In contrast to many adipokines, adiponectin gene expression in adipose tissue and the circulating levels of the protein fall in obesity (Matsuzawa, 2005). The observation

that adiponectin has a stimulatory effect on *ZAG* gene expression in adipocytes might be suggestive of ZAG's anti-inflammatory role in adipose tissue and it is further evidence that there might be a functional link between the two adipokines, as it has been previously reported that overexpression of ZAG in 3T3-L1 adipocytes leads to an increase in adiponectin mRNA levels, thus suggesting a possible role for ZAG in body weight regulation (Gohda *et al.*, 2003). Furthermore, since adiponectin falls in obesity, this might explain, at least in part, the reduction in ZAG mRNA level in WAT depots of obese rodents.

Finally, leptin led to the most marked decrease in ZAG mRNA levels in 3T3-L1 adipocytes. Similarly leptin induced a decrease in both adiponectin and IL-6 mRNA levels. Leptin is induced in obesity, its levels increasing with the degree of adiposity. Both *in vivo* and *in vitro* studies have shown that *ob* gene expression is reduced by catecholamines (Hardie *et al.*, 1996; Trayhurn *et al.*, 1998), the effect occurring primarily through the β_3-adrenoreceptors (Giacobino, 1996; Trayhurn *et al.*, 1996). Its regulation in adipocytes is thus opposite to what seems to be the case for ZAG and thus administration of leptin induces a decrease in *ZAG* gene expression. This might be a further explanation for the reduction in ZAG in obese rodents.

The results of the second part of this study have demonstrated that *ZAG* gene expression is largely modulated by key prostaglandins. PGD_2 had no significant effect on ZAG mRNA levels in 3T3-L1 adipocytes. In solution, PGD_2 spontaneously breaks down to PGJ_2 (Straus & Glass, 2001). Although the former did not induce a significant increase in *ZAG* gene expression, the latter induced a 4-fold increase in ZAG mRNA levels. Depending on the conditions, PGJ_2 is converted further to yield Δ^{12}-PGJ_2 and 15d-PGJ_2 (Straus & Glass, 2001). Both these metabolites have strong stimulatory effects on *ZAG* gene expression (figure 5.8). Thus, while PGD_2 does not have a direct effect on *ZAG* gene expression, derivatives, particularly Δ^{12}-PGJ_2, potently stimulate expression.

PGD_2 has been shown to stimulate lipolysis in adipocytes via a mechanism involving the elevation of cAMP levels through activation of adenylate cyclase (Kather & Simon,

1979), this effect being mediated through its DP receptor. 15d-PGJ_2 is a high affinity endogenous ligand for PPARγ nuclear receptor and it actually represents the highest affinity natural ligand for PPARγ identified so far (Straus & Glass, 2001). Δ^{12}-PGJ_2 also binds to PPARγ, although with considerably lower affinity than 15d-PGJ_2 (Forman *et al.*, 1995). This further supports the data presented in the first part of this chapter, where it was demonstrated that the PPARγ agonist rosiglitazone induced a dose-dependent increase in ZAG mRNA levels. Furthermore, 15d-PGJ_2 is a potent anti-inflammatory agent that represses the expression of a number of inflammatory response genes, including iNOS, TNFα and COX-2 genes. It also inhibits the transcription factors NFκB and AP-1; and inhibits NFκB-mediated transcriptional activation by PPARγ-dependent and independent mechanisms. There is also evidence that it functions as a physiological negative feedback regulator of prostaglandin synthesis, as of the inflammatory mediator PGE_2, via inhibition of COX-2 synthesis (Straus & Glass, 2001). It is therefore likely that the observed stimulatory effect of 15d-PGJ_2 on ZAG expression occurs via PPARγ activation, but its anti-inflammatory role may also be involved.

The strong stimulatory effect of PGJ_2, Δ^{12}-PGJ_2 and 15d-PGJ_2, however, is in contrast with the response to PGE_2 and $PGF_{2\alpha}$, which had a strong inhibitory effect on ZAG expression even at very low doses. However, little is known about the functions of these prostaglandins in adipose tissue. Very interestingly, PGE_2 has been found to act as an antilipolytic-hypertrophic agent promoting terminal differentiation of preadipocytes, while PGI_2 may act as an adipogenic-hyperplastic effector. Thus it has been proposed that both contribute to the development of adipose tissue mass (Vassaux *et al.*, 1992 a & b). Furthermore, PGE_2 has been shown to stimulate leptin secretion in rodent adipose tissue and in mature adipocytes (Fain *et al.*, 2000). Similar observations have been made in the heart, where it has been demonstrated that PGE_2 and PGI_2 act as inhibitory modulators of β-adrenergic receptor-stimulated cardiac lipolysis (Ruan *et al.*, 1996). Thus, the anti-lipolytic properties of these prostaglandins could possibly be responsible for the inhibition of *ZAG* gene expression in adipocytes treated with these prostaglandins. The downregulation of ZAG by PGE_2 might also be attributed to the possible role of this prostaglandin as an inflammatory mediator (Straus & Glass, 2001). The upregulation of

IL-6, an inflammatory regulator in adipose tissue, by PGE_2 further supports this suggestion.

As aforementioned, it has been known for some time that adipocytes can synthesize prostaglandins (Shillabeer *et al.*, 1998), with PGE_2, 6-keto-$PGF_{1\alpha}$ (the natural metabolite of PGI_2), $PGF_{2\alpha}$ and 15d-PGJ_2 being secreted by 3T3-L1 adipocytes (Borglum *et al.*, 1999). Similarly, PGD_2 is expressed in both 3T3-L1 adipocytes and human adipose tissue (Jowsey *et al.*, 2003) and both PGI_2 and PGE_2 are secreted by isolated human adipocytes, although their expression is higher in the stromal vascular fraction (Fain *et al.*, 2002). Thus WAT, either mature adipocytes, or other cells in the tissue, such as macrophages and preadipocytes, produce the prostaglandins that affect *ZAG* gene expression in 3T3-L1 adipocytes.

Finally, it should be noted that the concentrations of PGD_2 and the J_2 series PGs used in the present study were based on recent studies demonstrating the effects of prostaglandins on a number of adipokines on 3T3-L1 cells (Bulló *et al.*, 2005; Peeraully *et al.*, 2006). Physiological concentrations of PGs in the body fluids are found to be in the pico-nanomolar range, their levels rise considerably under pathological conditions reaching the micromolar range at the site of damage (Herschman *et al.*, 1997). In the case of PGD_2 and PGJ_2, however, the fact that there is a fall in their initial concentrations during culture because of their conversion to their metabolites has to be taken into consideration. However, their synthesis was found to be increased in the late phases of inflammation (Gilroy *et al.*, 1999).

In conclusion, in the present study, a number of key factors regulating ZAG expression in 3T3-L1 adipocytes were identified. Briefly, it has been demonstrated that rosiglitazone, isoprenaline, and adiponectin have a stimulatory effect on *ZAG* gene expression, while leptin inhibits its expression in 3T3-L1 adipocytes. According to their properties, prostaglandins exert different, but potent, effects on *ZAG* gene expression. While *ZAG* gene expression is strongly induced by PGJ_2-series prostaglandins, pro-inflammatory prostaglandins PGE_2 and $PGF_{2\alpha}$ inhibit its expression in the murine adipocytes. Of

course, the effects of these factors have only been studied at the mRNA levels in this study and further analysis of the secretion of the protein by adipocytes would provide stronger evidence of the regulation of ZAG in WAT.

Chapter 6

Postnatal development of ZAG in rodent adipose tissue

6.1 Introduction

In Chapter 3, it was shown that ZAG is expressed in both adult mouse and rat adipose tissue, as both the mRNA and protein were detected in all WAT depots as well as in BAT. Quantitative analysis also showed that ZAG is mainly expressed in the internal WAT depots. When, however, the physiological functions of a gene are studied, it is important to establish the time at which its system first becomes functional in the young animal and how this changes during early postnatal life. This is particularly so as adipose tissue itself undergoes a number of major morphological and metabolic changes (Herrera & Amusquivar, 2000). There are also suggestions from the study of other adipose tissue factors, such as leptin and resistin, that the distribution of a particular factor in different depots might also undergo changes during early development (Rayner *et al.*, 1997; Oliver *et al.*, 2001a, b; Oliver *et al.*, 2003).

Rats are a good model for studies on the postnatal development of factors relating to adipose tissue and this is mainly due to two reasons. The first is that in the rat the development of white adipose tissue occurs mainly after birth. At day 1 after birth, white fat is barely detectable, usually solely in the subcutaneous area and not internally. However, rats rapidly lay down fat stores during the suckling period, while internal fat depots appear in tiny amounts, only to expand after weaning, around day 21 (Greenwood & Hirsch, 1974; Cryer & Jones, 1978). The second reason for using the rat as a model is that BAT is well developed in newborn rats, where it is present throughout neonatal and adult life (Dessolin *et al.*, 1997). Rats are preferable to mice as the WAT depots are inevitably much smaller in mice and especially at these early stages they are not substantial enough to sample.

The metabolism of rat adipose tissue during the time course of postnatal development undergoes some major changes. Briefly, these can be grouped into the suckling period that usually lasts until day 21 after birth (weaning), the period of highest hyperplasia between birth and 40 days after birth, which is followed by a period of highest cell hypertrophy occurring between 40 and 80 days after birth due to the intense increase in

both LPL activity and lipogenesis (Herrera & Amusquivar, 2000). In the early suckling period, the high-fat and low-carbohydrate diet present in milk (14.8g fat/100g milk) contributes to the marked hyperketonaemia normally present in both humans and rats during this time, since nonesterified fatty acids are the major precursors for ketone body synthesis (Williamson, 1998). Immediately after birth, and less intensively during suckling, the rate of lipolysis has been shown to be enhanced (Gruen *et al.*, 1980). During the first hours after birth, this appears to be regulated by catecholamine release, resulting in cAMP production and increased protein kinase C activity (Kimura *et al.*, 1983). Later, during suckling, enhanced lipolysis is most possibly caused by an enhanced sensitivity to lipolytic hormones, and a decreased plasma insulin/ glucagon ratio (Issad *et al.*, 1987; Marcus *et al.*, 1988). Moreover, LPL activity, which is representative of the tissue's capability to take up circulating triglycerides, peaks at mid-suckling (Ramírez *et al.*, 1998), thus contributing to the enhanced rate of cell proliferation observed at this period. Finally, the suckling period is characterised by a very low lipogenic activity (Smith & Kaplan, 1980).

Weaning at day 21, which is the switch from a high-fat to a high-carbohydrate (the animals gradually consume lab chow from day 18) diet is characterised by many metabolic changes in rat adipose tissue. LPL activity declines around weaning, only to increase again at 30-40 days of age (Cryer & Jones, 1978; Ramírez *et al.*, 1998). Furthermore, lipogenic activity rapidly increases during this period. Because of these changes, from weaning up to around 40 days after birth, although the number of adipocytes is still increasing, they start to be filled up with fat. Finally, lipolysis, which declines as the suckling period advances, slightly peaks after weaning to decline afterwards (Gruen *et al.*, 1980).

Finally, rat foetal liver contains a high level of LPL activity, which increases after birth. This activity declines with age, but still remains higher in the liver of the suckling rat than after weaning, when it declines to undetectable levels (Llobera *et al.*, 1979; Ramirez *et al.*, 1998). Since changes in liver LPL activity in the newborn rat are accompanied by changes in the hepatic content of triglycerides, circulating triglycerides and ketone bodies

(Grinberg *et al.*, 1985), it has been proposed that in the suckling neonate, long chain fatty acids derived from milk lipids are channelled to liver due to its LPL, and such a change possibly contributes to the high ketogenic capacity of that organ during the suckling period (Herrera & Amusquivar, 2000).

Little is known about the occurrence and roles of different adipokines at the early stages of adipose tissue development, leptin being the only adipokine whose fetal and early postnatal development both in WAT and BAT have been documented (Dessolin *et al.*, 1997; Rayner *et al.*, 1997). In this study, the ontogenic pattern of *ZAG* gene and protein expression during postnatal development up to day 32, is reported in different WAT depots (subcutaneous, perirenal, gonadal), BAT and liver in rats. The expression pattern of leptin in rat adipose tissue during this period is also studied as a reference. Furthermore, the ontogenic patterns of adiponectin, the neurotrophin NGF, and the inflammatory factors IL-6 and MCP-1 during early postnatal development in the rat are explored, in order to provide reference points and to gain further information on the physiological role of these adipokines. Each of these adipokines has been linked to body weight control, obesity, insulin sensitivity, as well as inflammation in adipose tissue (Prins, 2002; Wood & Trayhurn, 2006). Thus the present study provides information on the expression patterns of ZAG and the aforementioned adipokines in different WAT depots during early postnatal development in the rat, thus providing a greater insight into the possible function of these adipokines in early adipose tissue development.

6.2 Methods

6.2.1 Animals

For the purposes of this study, two sets of experiments were carried out. In the first experiment, the aim was to explore whether ZAG is expressed in rat WAT and BAT in the first 24 hours after birth, or if not when it first appears in the early postnatal period. For this experiment four female wistar rats were sacrificed at days 1, 3, 5 and 10 after birth and liver, BAT and WAT depots were dissected as soon as they were sufficient to sample. After having established that ZAG was expressed in rat WAT and BAT from day 1 postnatally, the aim was to explore the detailed ontogenic pattern of ZAG expression in the early postnatal period. In the second extended experiment, five female rats were sacrificed at each of the following time points, days 1, 3, 5, 7, 10, 15, 21, and 32 postnatally and again liver, BAT and WAT depots were dissected. Rats were kept under controlled environmental conditions (20-24^{0}C; 12h:12h light:dark cycle) and were sacrificed between 10:00 and 11:00 h at the allocated days. Since their stomachs were invariably full, they were considered to be in the fed state. All animals used for each experimental cycle shared the same genetic background and were kept in mixed sex litters.

Animals were sacrificed by cervical dislocation and according to the regulations for animal treatment of the University of Liverpool. As soon as the tissues were dissected, samples were weighed, snap frozen in liquid nitrogen and stored at -80^{0}C until further analysis.

6.2.2 RT-PCR and real-time PCR

Total RNA was extracted from tissues using Tri-Reagent as previously described in section 2.5. RNA was then treated using a DNA-free kit (section 2.5.3) and quantified using a BioPhotometer (section 2.5.4). RNA was reverse-transcribed using the Reverse-iT First Strand Synthesis kit (section 2.6.1) and the patterns of gene expression were

analysed by RT-PCR (section 2.6.2). mRNA levels of expression were assessed by real-time PCR (section 2.7) using the qPCR Core Kit and a Stratagene Mx3005 instrument.

6.2.3 Western blotting

Protein was extracted from tissues using Tri-Reagent after the RNA had been removed for total RNA extraction, as previously described in section 2.8.1. The protein concentration of samples was determined using the BCA method (section 2.8.2) and 10 μg of protein were mixed with equal volumes of loading buffer and separated by electrophoresis on 10% SDS-polyacrylamide gels (section 2.8.3). Immunoblotting was then performed as described in section 2.8.4 by using an anti-mouse ZAG monoclonal primary antibody at a 1:1000 dilution, followed by incubation with a goat anti-mouse secondary antibody conjugated to horseradish peroxidise at a 1:1000 dilution. Densitometric analysis was carried out as previously described in section 2.8.6 and gels were stained with Ponceau S to confirm equal loading (section 2.8.5.2).

6.2.4 Statistical analysis

Data are expressed as mean values ± SEM. Comparisons between two groups were assessed by unpaired Student's *t*-test, while differences among more than two groups were analysed by one-way ANOVA coupled with Bonferroni's *t*-tests, as previously described in section 2.9. Differences were considered as statistically significant when $P < 0.05$.

6.3 Results

6.3.1 ZAG expression in the early postnatal period

An initial study was conducted in order to explore whether ZAG is expressed in rat neonates in the first 24 hours after birth or if not when it first appears. Experiments were also carried out in the liver as a further reference point on ZAG's availability in the body. For this, ZAG mRNA and protein expression were studied using RT-PCR and western blotting respectively, in the liver, BAT and WAT depots of 1, 3, 5, and 10 day old female rats. Liver and BAT were available from day 1, whereas subcutaneous and gonadal were sufficient to sample at days 3 and 5 respectively.

Both ZAG mRNA and protein were expressed in liver and BAT postnatally at day 1 onwards, and in subcutaneous and gonadal at all days tested (Figures 6.1A&B). Further to ZAG, the expression of leptin and adiponectin mRNA was studied as a reference. Consistent with what has previously been reported for leptin (Rayner *et al.*, 1997), it was expressed in adipose tissue from day 1 and although not quantified, its expression was clearly increasing with time (Figure 6.2A). The adiponectin gene was also found to be expressed at all time points tested (Figure 6.2B).

Although RT-PCR indicated that the *ZAG* gene is expressed in all sites tested postnatally, as soon as they are sufficient to be sampled, the signal intensity varied between time points, suggesting that the expression of ZAG changes postnatally. Thus real-time PCR was used and some initial results showed an interesting pattern of ZAG mRNA and protein expression postnatally (data not shown). It thus led to the studies on the postnatal ontogenic pattern of *ZAG* gene and protein expression in a more extensive manner.

Figure 6.1 ZAG is expressed in rat adipose tissue at day 1 postnatally and onwards

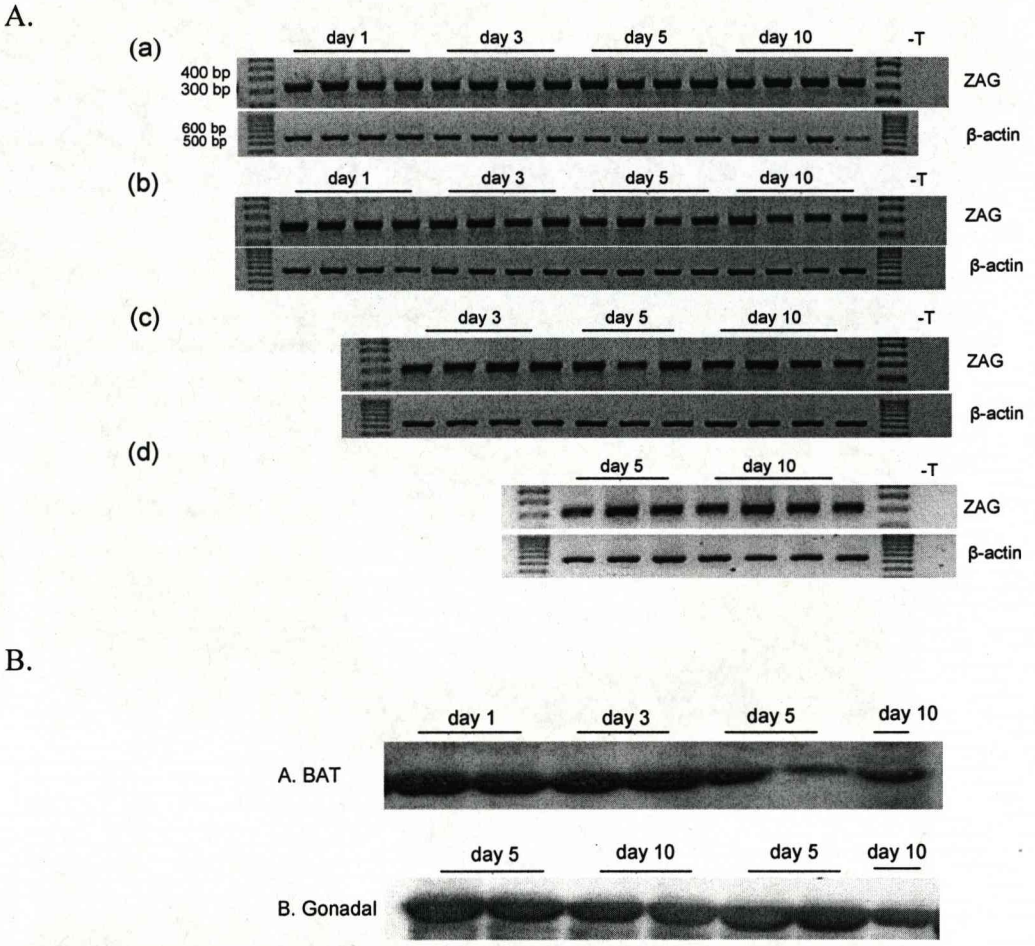

(A) Gene expression of ZAG in liver (a), subcutaneous WAT (b), gonadal WAT (c) and BAT (d) from 1, 3, 5 and 10-days old rats were examined by RT-PCR; PCR was performed at 30 cycles for ZAG and 23 cycles for β-actin (B) Protein expression of ZAG in BAT and gonadal WAT depots of the same animals were examined by western blotting. –T, no template control; BAT, interscapular brown adipose tissue

Figure 6.2 Gene expression of leptin and adiponectin in WAT depots and BAT of rat neonates

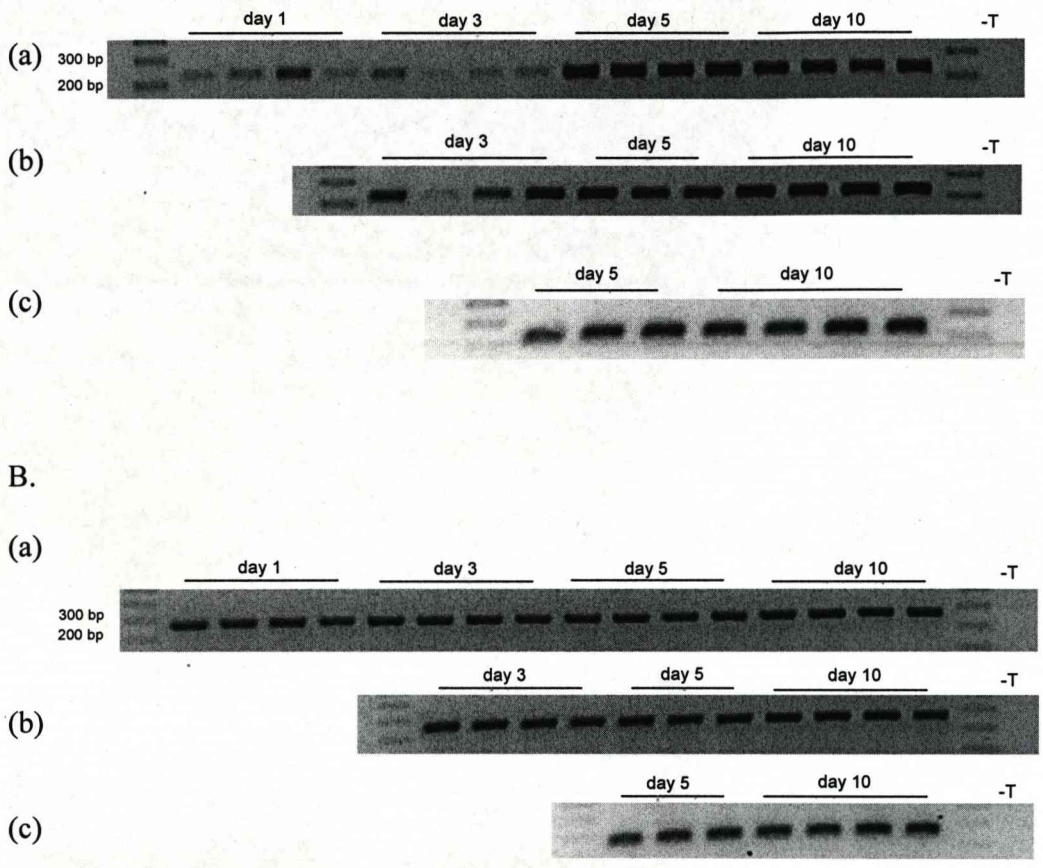

Gene expression of leptin (A) and adiponectin (B) in subcutaneous WAT (a), gonadal WAT (b) and BAT (c) from 1, 3, 5 and 10-days old rats were examined by RT-PCR; (1) at 30 cycles for leptin; and (2) at 28 cycles for adiponectin; 1µl cDNA was used as a template; -T, no template control

6.3.2 Total body weight and adipose tissue depots during early postnatal development

In order to establish the pattern of ZAG expression postnatally a larger scale study was designed. Groups of five female rats were sacrificed at days 1, 3, 5, 7, 10, 15, 21 and 32 after birth. Weaning was initiated at day 21, with rats having *ad libitum* access to lab chow from day 18. As shown in Figure 6.3, their total body weight increased very rapidly, with the greatest increase being observed between days 21 and 32, when their weight almost doubled. In this study, only a tiny amount of subcutaneous WAT could be sampled at day 1, with increased amounts thereafter, while the perirenal and gonadal depots could only be sampled from days 5 and 7 respectively. This again demonstrates that after birth the amount of subcutaneous fat increases rapidly, while it takes longer for the internal fat depots to develop. The amount of BAT, on the other hand, reached its peak at day 15 but gradually decreased thereafter (Figure 6.3). As a percentage of total body weight (Figure 6.4), both perirenal and gonadal WAT depots steadily increased rapidly although not so abruptly, to reach maximum values at day 21. In contrast, BAT gradually declined in terms of relative weight from day 5 onwards.

6.3.3 ZAG expression patterns in adipose tissue postnatally

Real-time PCR results (Figure 6.5) revealed no differences in ZAG mRNA levels between different time points in the case of the subcutaneous depot. On the other hand, ZAG mRNA levels in gonadal WAT were significantly decreased at day 21 and thereafter, the same being observed in the perirenal depot at day 32. Interestingly, ZAG mRNA levels in BAT continually declined from day 3 onwards.

The levels of ZAG protein expression (Figure 6.6) in subcutaneous (A), perirenal (B), gonadal (C) and BAT (D) were then analysed at days 7, 21 and 32 using western blotting. Similar to what was observed for mRNA levels, protein expression levels declined in all depots with time, including in the subcutaneous site. Interestingly, in perirenal WAT and BAT, ZAG levels of protein expression were lowest at day 21.

Figure 6.3 Developmental changes in body weight and weight of adipose tissue depots in rat neonates

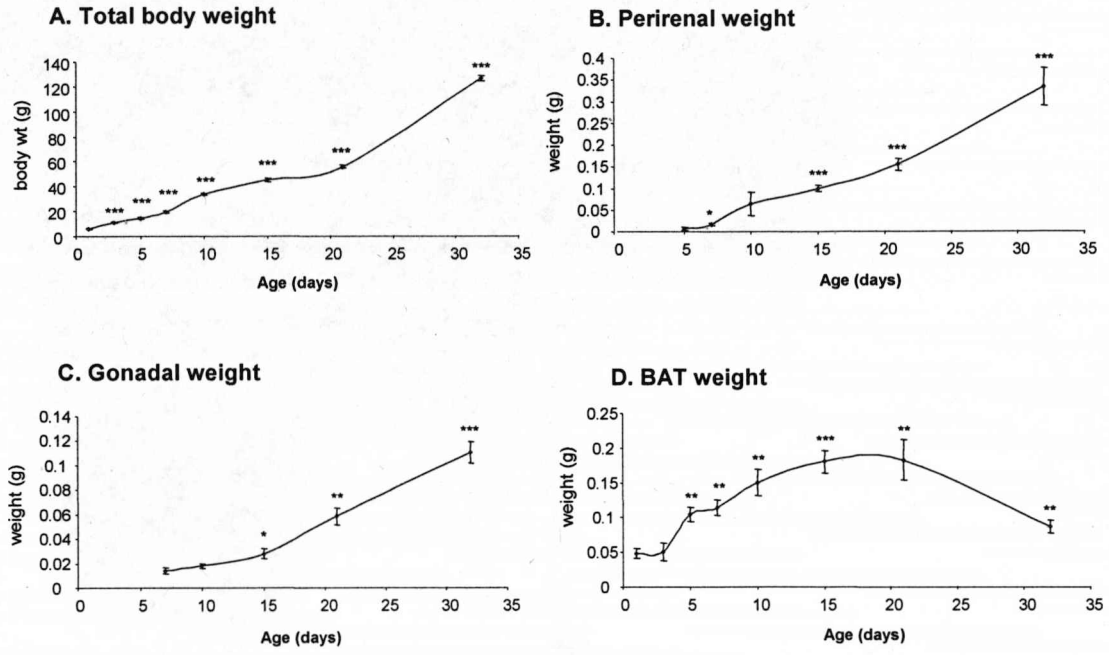

Total body weight was measured following sacrifice, while individual depots were weighed after dissection. Results are presented as means ± SE (bars) for five rats at each time point. $^{*}P < 0.05$, $^{**}P < 0.01$, $^{***}P < 0.001$ compared to day 1 for total body weight and BAT, day 5 for perirenal and day 7 for gonadal WAT (one-way ANOVA).

Figure 6.4 Developmental changes in weight of WAT depots and BAT relative to body weight in rat neonates

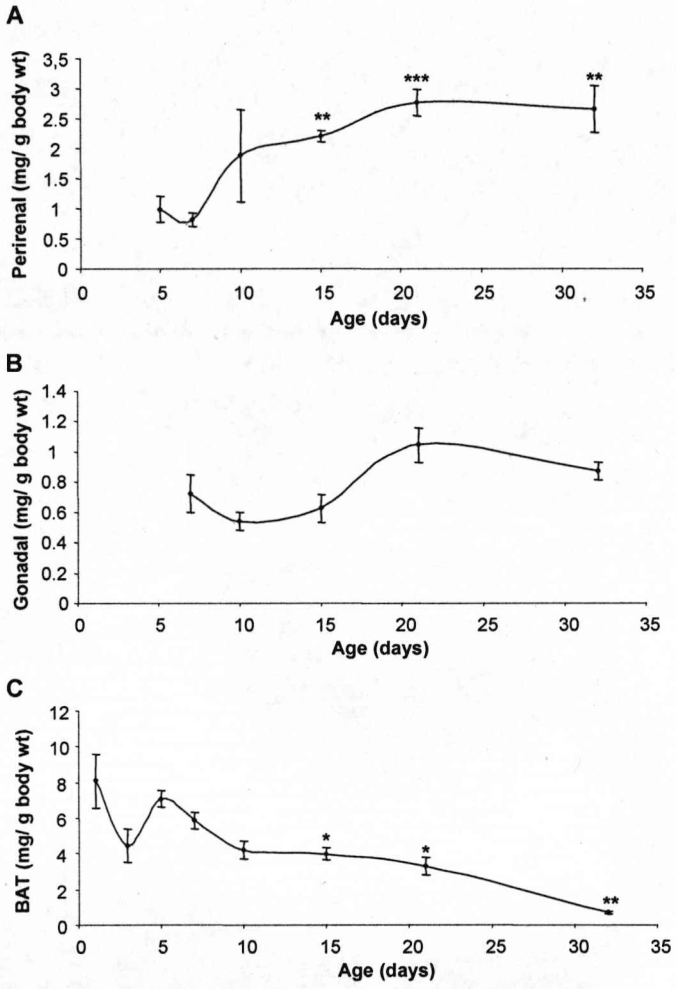

For total body weight, rats were weighed after being sacrificed, while individual depots were weighed after dissection. Perirenal WAT (A), gonadal WAT (B) and BAT (C) weights are presented relative to total body weight [tissue (g)/ body weight (g)]. Results are presented as means ± SE (bars) for five rats at each time point. $^{*}P < 0.05$, $^{**}P < 0.01$, $^{***}P < 0.001$ compared to day 1 for total body weight and BAT, day 5 for perirenal and day 7 for gonadal WAT.

Figure 6.5 *ZAG* gene expression in adipose tissue depots of neonatal rats

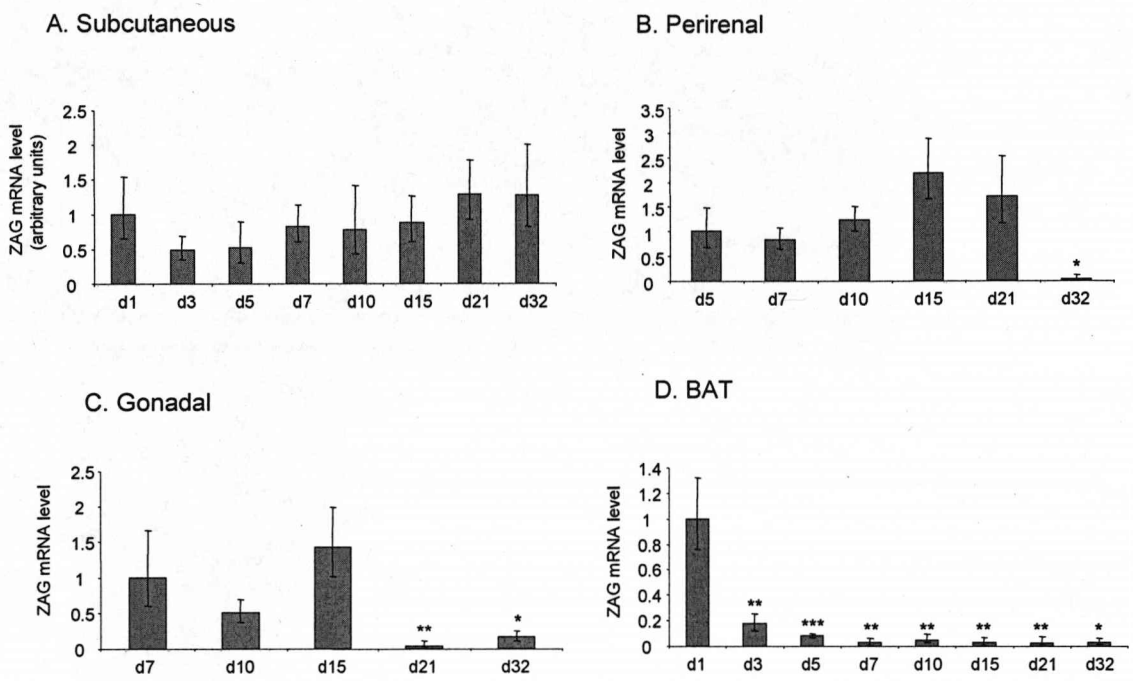

Adipose tissue depots were dissected from rats at each time point and total RNA was extracted. Real-time PCR was used for the relative quantification of ZAG mRNA levels. Results are expressed relative to the ZAG mRNA levels in each depot at day 1 postnatally or day 5 for perirenal and day 7 for gonadal WAT and are presented as means ± SE (bars) for 4-5 rats. $^{*}P < 0.05$, $^{**}P < 0.01$ and $^{***}P < 0.001$ (one-way ANOVA).

Figure 6.6 ZAG protein levels in adipose tissue depots of rat neonates

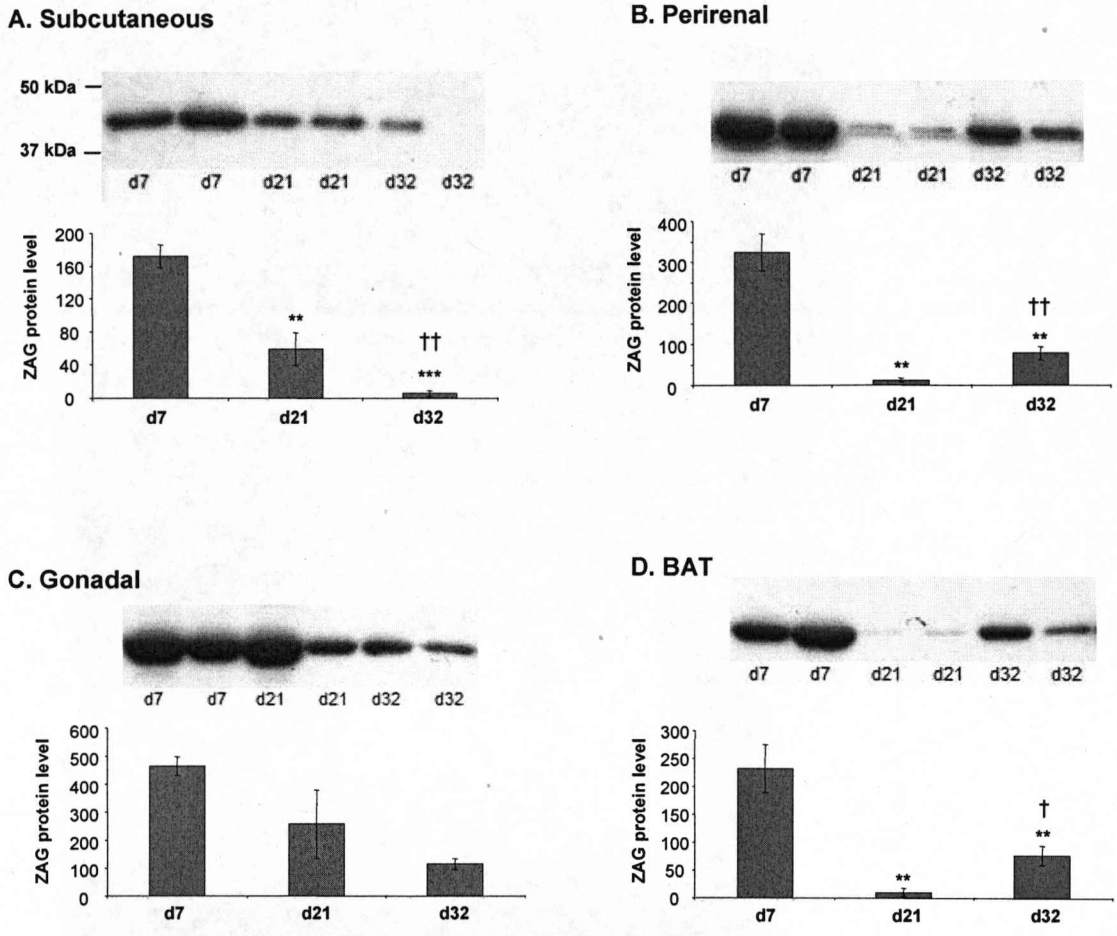

Protein samples were extracted from adipose tissue depots dissected from neonate rats at age of 7, 21 and 32-days old and then were analysed by western blotting followed by densitometric analysis. Representative blots are shown and results are presented as means ± SE (bars) for 4-5 rats at each time point. $^{*}P < 0.05$, $^{**}P < 0.01$ and $^{***}P < 0.001$; results are relative to ZAG protein expression at day 7 (one-way ANOVA). $^{\dagger}P < 0.05$, $^{\dagger\dagger}P < 0.01$; results are comparisons between days 21 and 32 (unpaired Student's *t*-test).

6.3.4 Postnatal expression of ZAG in the liver of rat neonates

As previously mentioned, the liver is the main site of ZAG production in the body. Indeed from day 1 ZAG mRNA levels in the liver were significantly higher than in subcutaneous WAT, and the difference was increased with time (Figure 6.7A). The patterns of ZAG expression in the liver postnatally were further studied in greater detail. As shown in Figure 6.7B, contrary to the expression pattern in adipose tissue, ZAG mRNA levels in the liver were gradually increased, reaching a 10-fold increase by day 32 compared to day 1.

6.3.5 Expression patterns of several adipokines in adipose tissue postnatally

As a reference to ZAG and in order to further explore how the metabolic changes occurring in adipose tissue during early postnatal development affect the expression of adipokines, the expression patterns of several adipokines were analysed using real-time PCR. mRNA levels of leptin, adiponectin, NGF, MCP-1 and IL-6 were analysed in subcutaneous, perirenal, and gonadal WAT and in BAT of newborn rats at days 1, 3, 5, 7, 10, 21 and 32 postnatally.

6.3.5.1 Gene expression pattern of leptin in rat adipose tissue during postnatal development

As aforementioned, leptin was evident in adipose tissue at day 1 after birth and thereafter (Figure 6.2). As shown in Figure 6.8, leptin mRNA levels in subcutaneous WAT were gradually increased from day 1 onwards; reaching a peak at day 15, when they were almost 250-fold higher than at day 1, and then slightly declined at days 21 and 32. In perirenal WAT, leptin mRNA levels gradually increased, reaching a peak at day 32, being 20-fold higher than at day 1. In gonadal WAT, however, there were no statistically significant changes in expression levels until day 32, at which point leptin mRNA levels were 5-fold higher than at day 7. Finally, in BAT leptin expression was significantly increased at all time points compared to day 1, and peaked at day 10 with a 20-fold higher level.

Figure 6.7 *ZAG* gene expression in the liver of rat neonates

(A)

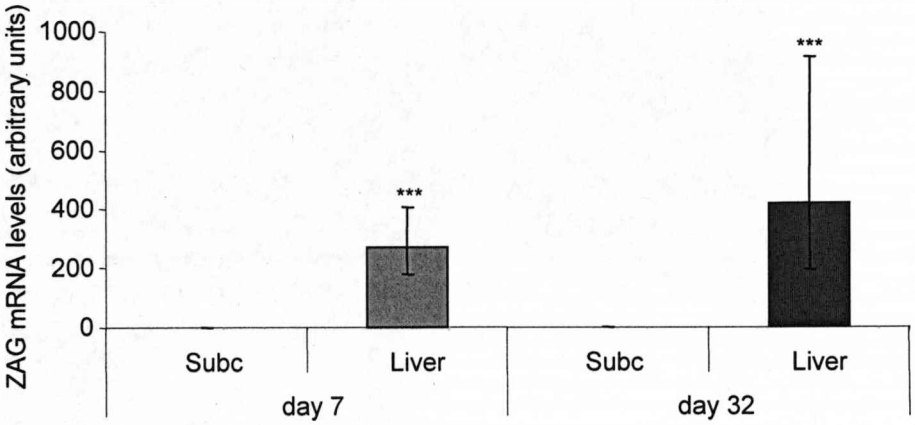

(B)

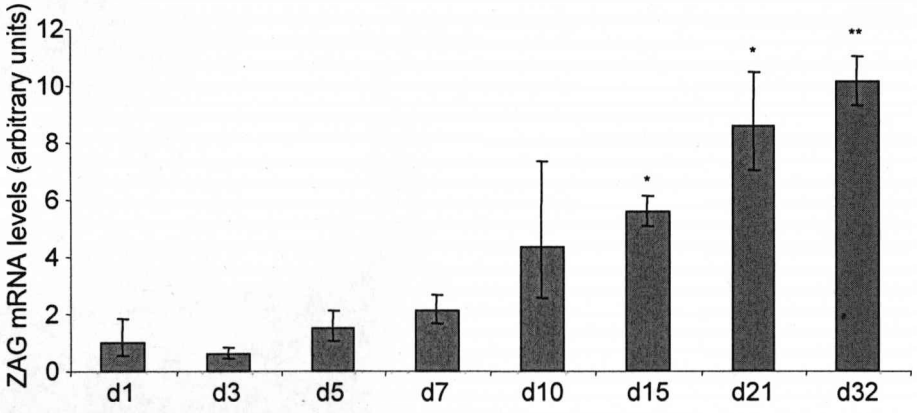

Liver was dissected from rats at each time point and total RNA was extracted. Real-time PCR was used for (A) the comparison between ZAG mRNA levels in subcutaneous WAT and liver at days 7 and 32 postnatally (unpaired Student's *t*-test); and (B) the relative quantification of ZAG mRNA levels in the liver of neonate rats up to day 32. $^{*}P < 0.05$, $^{**}P < 0.01$, $^{***}P < 0.01$. Results are expressed relative to the ZAG mRNA levels in subcutaneous WAT (A) or liver at day 1 postnatally (B) and are presented as means ± SE (bars) for 4-5 rats (one-way ANOVA).

Figure 6.8 Leptin gene expression in adipose tissue depots of neonatal rats

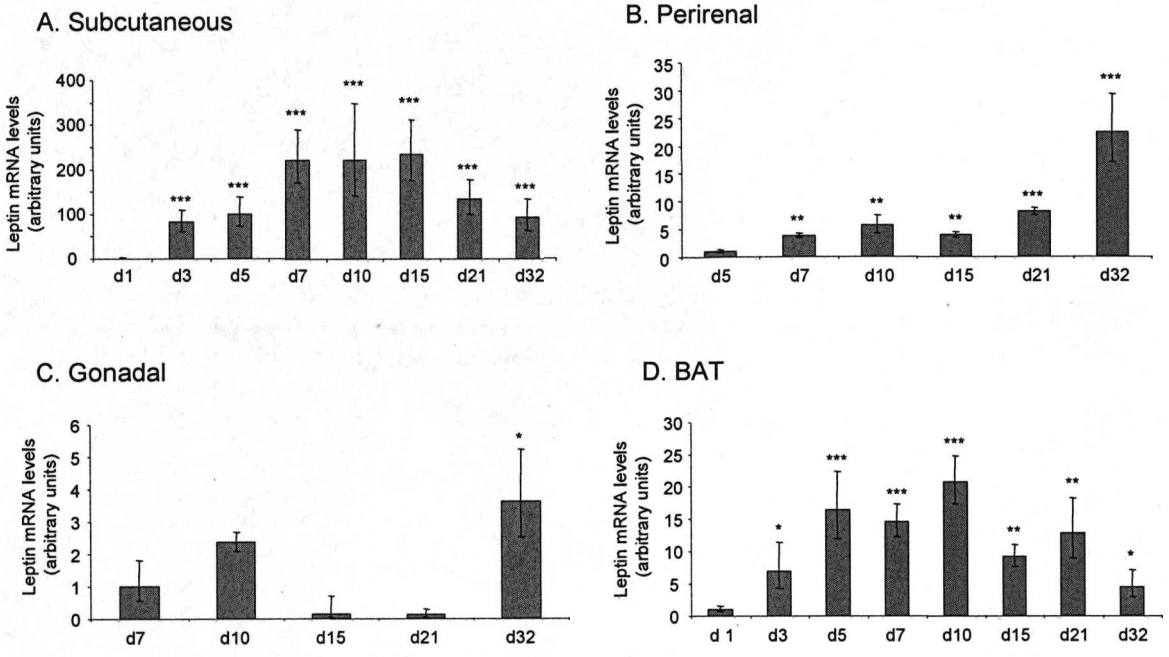

Adipose tissue depots were dissected from rats at each time point and total RNA was extracted. Real-time PCR was used for the relative quantification of leptin mRNA levels. Results are expressed relative to the leptin mRNA levels in each depot at day 1 postnatally or day 5 for perirenal and day 7 for gonadal WAT and are presented as means ± SE (bars) for 4-5 rats. $^{*}P < 0.05$, $^{**}P < 0.01$ and $^{***}P < 0.001$ (one-way ANOVA).

6.3.5.2 Gene expression pattern of adiponectin in rat adipose tissue during postnatal development

The pattern of expression of adiponectin in WAT depots and BAT postnatally was similar to that of leptin (Figure 6.9). In the subcutaneous depot, adiponectin mRNA levels were increased significantly from day 3 relative to day 1, reaching a 5-fold increase at day 15, while at days 21 and 32 the levels fell again. In the perirenal depot there was a gradual increase in adiponectin levels, peaking at day 32 (8-fold higher compared to day 1), while in the gonadal depot, adiponectin levels were significantly suppressed at weaning but increased again at day 32. Finally, in BAT there were no changes in the levels of adiponectin expression throughout the early postnatal development.

6.3.5.3 Gene expression pattern of NGF in rat adipose tissue during postnatal development

NGF was evident in adipose tissue at day 1 postnatally and thereafter. As shown in Figure 6.10, no changes were observed in NGF mRNA levels in subcutaneous and perirenal WAT until day 32, when the expression levels were significantly suppressed. There was a small increase in NGF mRNA at day 21 compared to day 7 in gonadal WAT. In BAT, NGF levels were significantly reduced at day 7, 21 and 32 relative to day 1.

6.3.5.4 Gene expression pattern of MCP-1 in rat adipose tissue during postnatal development

MCP-1 was also expressed at day 1 after birth and thereafter. As shown in Figure 6.11, there were no fluctuations in MCP-1 mRNA levels in the subcutaneous depot until day 21, while it was significantly reduced at day 32. However, in perirenal WAT MCP-1 mRNA levels were significantly increased at days 10, 15 and 32, when they peaked. Weaning though led to downregulation of MCP-1 in the gonadal depot, which was also the case in BAT. In the latter, MCP-1 was downregulated at most time points compared to day 1.

Figure 6.9 Adiponectin gene expression in adipose tissue depots of neonatal rats

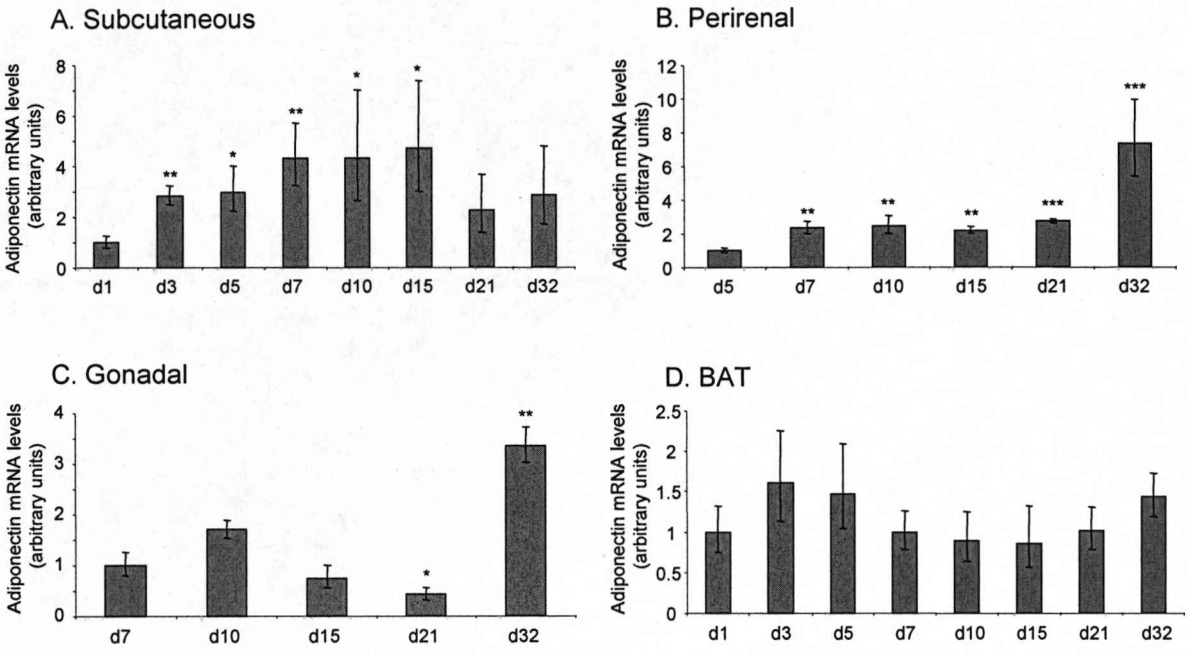

Adipose tissue depots were dissected from rats at each time point and total RNA was extracted. Real-time PCR was used for the relative quantification of adiponectin mRNA levels. Results are expressed relative to the adiponectin mRNA levels in each depot at day 1 postnatally or day 5 for perirenal and day 7 for gonadal WAT and are presented as means ± SE (bars) for 4-5 rats. $^{*}P < 0.05$, $^{**}P < 0.01$ and $^{***}P < 0.001$ (one-way ANOVA).

Figure 6.10 *NGF* gene expression in adipose tissue depots of neonatal rats

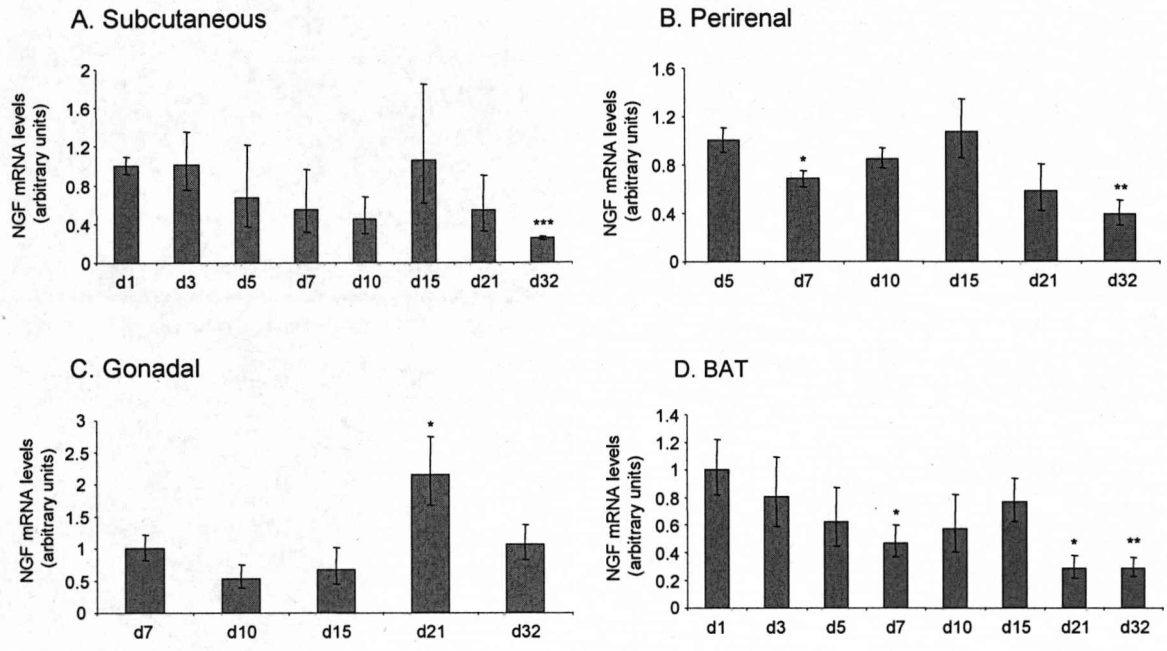

Adipose tissue depots were dissected from rats at each time point and total RNA was extracted. Real-time PCR was used for the relative quantification of NGF mRNA levels. Results are expressed relative to the NGF mRNA levels in each depot at day 1 postnatally or day 5 for perirenal and day 7 for gonadal and are presented as means ± SE (bars) for 4-5 rats. $^{*}P < 0.05$, $^{**}P < 0.01$ and $^{***}P < 0.001$ (one-way ANOVA).

Figure 6.11 *MCP-1* gene expression in adipose tissue depots of neonatal rats

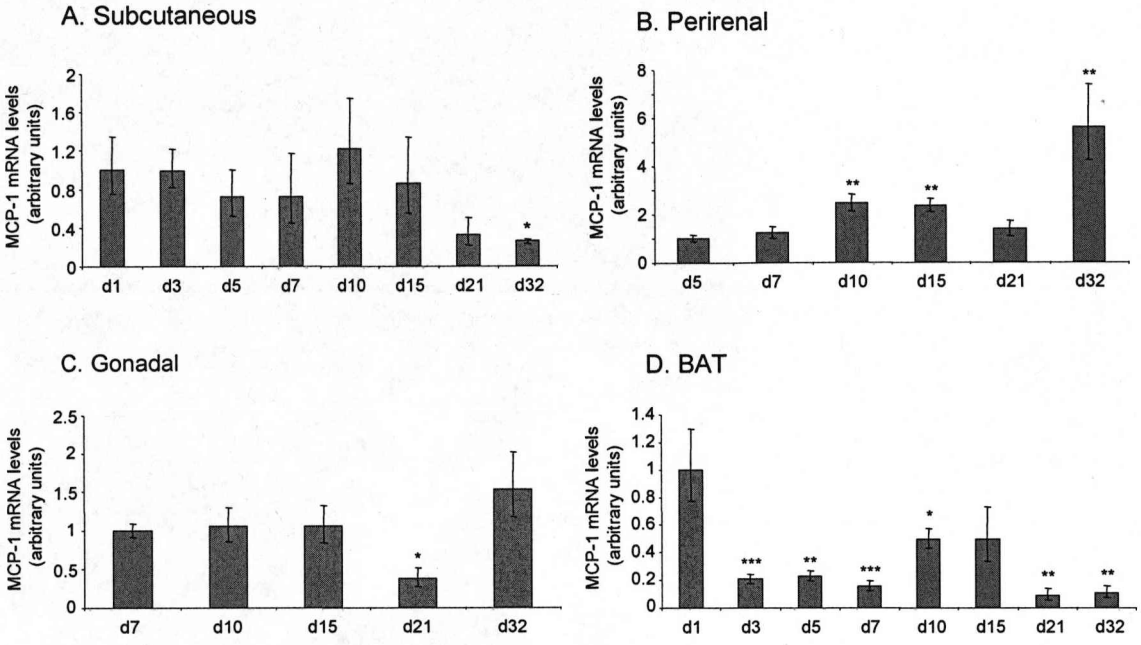

Adipose tissue depots were dissected from rats at each time point and total RNA was extracted. Real-time PCR was used for the relative quantification of MCP-1 mRNA levels. Results are expressed relative to the MCP-1 levels in each depot at day 1 postnatally or day 5 for perirenal and day 7 for gonadal and are presented as means ± SE (bars) for 4-5 rats. $^{*}P < 0.05$, $^{**}P < 0.01$ and $^{***}P < 0.001$ (one-way ANOVA).

6.3.5.5 Gene expression pattern of IL-6 in rat adipose tissue during postnatal development

Finally, IL-6 was also evident in adipose tissue at day 1 after birth and thereafter. As shown in Figure 6.12, mRNA levels were increased at days 10 and 15 in subcutaneous and perirenal. In the latter, however, the level peaked at day 32 (100-fold). At days 21 and 32, the levels were also increased in the gonadal depot. In BAT, IL-6 mRNA levels were significantly downregulated from day 3 onwards.

6.3.6 Comparison of ZAG mRNA levels in different adipose depots at days 1, 21 and 32 postnatally

Although RT-PCR analysis has shown that ZAG is present from day 1 postnatally in all sites tested, it has been shown that there are some differences in the levels of its expression among different sites. There is also some evidence that this pattern may change at different stages during postnatal development. To address this point, the ZAG mRNA levels were compared at days 1 in BAT and subcutaneous WAT at days 7 as it is the first time points at which all four depots were enough to sample, and 32, as this is when some of the major changes had previously been observed not only in ZAG expression pattern but also in the other adipokines. Very interestingly, as shown in Figure 6.13, at day 1, ZAG mRNA levels were higher (18-fold) in subcutaneous WAT compared to BAT. At day 7 and 32, ZAG was still significantly more abundant in the subcutaneous depot compared to the other depots.

Although no major differences were observed in ZAG mRNA levels at different time points during the early stages of development, some interesting patterns were observed in the case of leptin (Figure 6.14) and adiponectin (Figure 6.15) during the same experiment. At day 1 postnatally, leptin mRNA levels were significantly higher in BAT (12-fold) compared to subcutaneous WAT. By day 7 however, the levels were higher in subcutaneous (10-fold) compared to perirenal WAT, while still quite high in BAT. This pattern was completely changed by day 32, when leptin mRNA was more abundant in the internal WAT depots.

Figure 6.12 *IL-6* gene expression in adipose tissue depots of neonatal rats

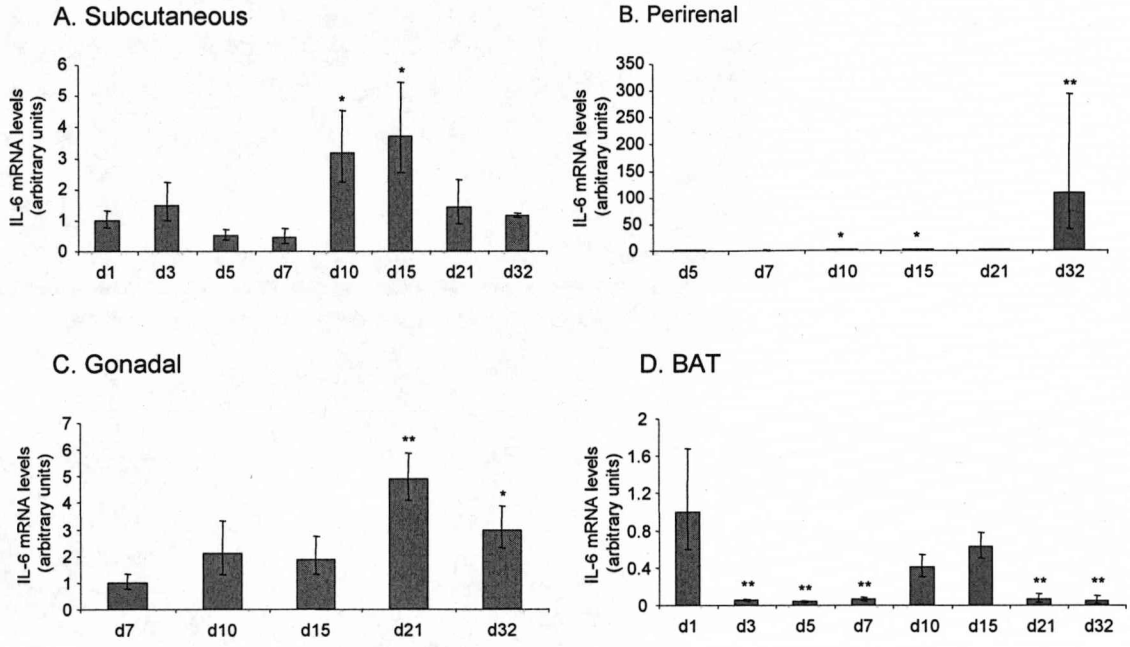

Adipose tissue depots were dissected from rats at each time point and total RNA was extracted. Real-time PCR was used for the relative quantification of IL-6 mRNA levels. Results are expressed relative to the IL-6 mRNA levels in each depot at day 1 postnatally or day 5 for perirenal and day 7 for gonadal and are presented as means ± SE (bars) for 4-5 rats. $^{*}P < 0.05$, $^{**}P < 0.01$ and $^{***}P < 0.001$ (one-way ANOVA).

Figure 6.13 Depot differences in *ZAG* gene expression in adipose tissue of neonatal rats

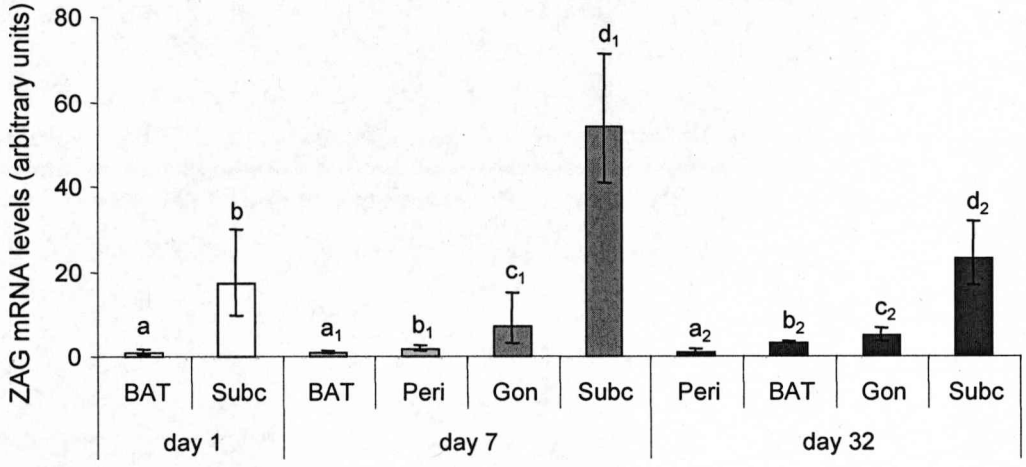

Samples from four adipose tissue depots of neonatal rats at days 1, 7 and 32 were analysed by real-time PCR for the relative quantification of ZAG mRNA levels. Results are expressed relative to ZAG mRNA levels in BAT (day 1 & 7) or peri (day 32) and are presented as means ± SE (bars) for 5 rats. Subc, subcutaneous; peri, perirenal; gon, gonadal; BAT, interscapular brown adipose tissue. $^{a}P < 0.01$ vs Subc; $^{a1}P < 0.001$ vs subc; $^{b1}P < 0.001$ vs subc, $^{c1}P < 0.05$ vs subc; $^{a2}P < 0.001$ vs subc, $^{b2}P < 0.001$ vs subc, $^{c2}P < 0.01$ vs subc (Student's *t*-test for comparisons between 2 groups and one-way ANOVA for comparisons between two or more groups).

Figure 6.14 Depot differences in leptin gene expression in adipose tissue of neonatal rats

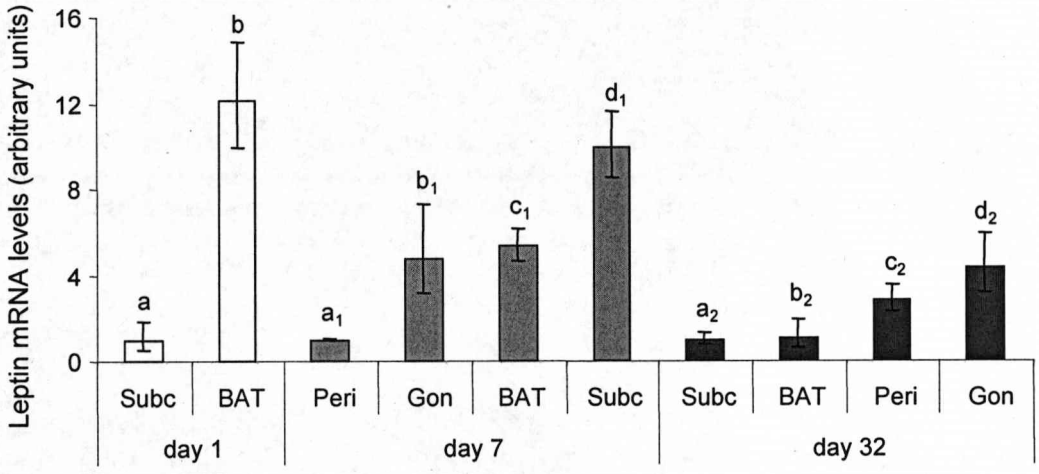

Samples from four adipose tissue depots of neonatal rats at days 1, 7 and 32 were analysed by real-time PCR for the relative quantification of leptin mRNA levels. Results are expressed relative to leptin mRNA levels in subc (day 1 & 32) or peri (day 7) and are presented as means ± SE (bars) for 5 rats. Subc, subcutaneous; peri, perirenal; gon, gonadal; BAT, interscapular brown adipose tissue. $^{a}P < 0.01$ vs BAT; $^{a1}P < 0.001$ vs BAT; $P < 0.001$ vs subc; $^{c1}P < 0.05$ vs subc; $^{a2}P < 0.05$ vs peri, $P < 0.01$ vs gon; $^{b2}P < 0.05$ vs gon (Student's *t*-test for comparisons between 2 groups and one-way ANOVA for comparisons between two or more groups).

The observations made on adiponectin were similar to those made on leptin. Although at day 1, adiponectin mRNA levels were equal in BAT and subcutaneous WAT, at day 7 the concentration in the latter was increased by 3-fold. At day 32, however, adiponectin mRNA levels were 20-fold higher in gonadal and 7-fold in perirenal WAT compared to BAT.

Figure 6.15 Depot differences of adiponectin gene expression in adipose tissue of neonatal rats

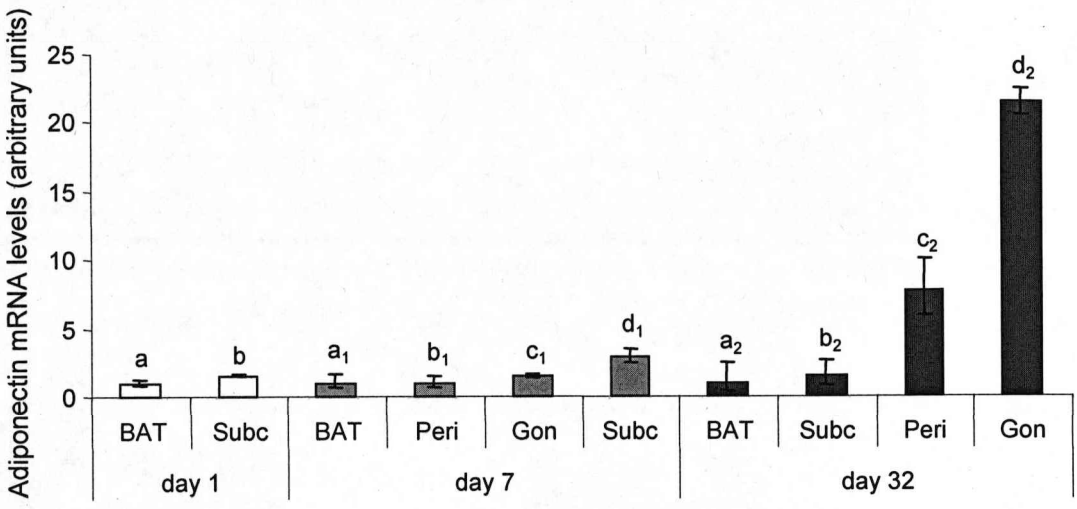

Samples from four adipose tissue depots of neonatal rats at days 1, 7 and 32 were analysed by real-time PCR for the relative quantification of adiponectin mRNA levels. Results are expressed relative to adiponectin mRNA levels in BAT at each time point and are presented as means ± SE (bars) for 5 rats. Subc, subcutaneous; peri, perirenal; gon, gonadal; BAT, interscapular brown adipose tissue. $^{a1}P < 0.05$ vs subc; $^{b1}P < 0.05$ vs subc, $^{c1}P < 0.05$ vs subc; $^{a2}P < 0.05$ vs gon, $^{b2}P < 0.05$ vs peri, $P < 0.01$ vs gon; $^{c2}P < 0.05$ vs gon (Student's *t*-test for comparisons between 2 groups and one-way ANOVA for comparisons between two or more groups).

6.4 Discussion

Little is known so far about the onset of the ZAG system in adipose tissue and its role in the early stages of postnatal development. The studies described here demonstrate that ZAG, both mRNA and protein, is expressed in subcutaneous WAT and BAT of one-day old rats, this being the point at which WAT can in practice be sampled from the subcutaneous region, the major fat depot during the suckling period. A signal for ZAG mRNA was also detected in perirenal and gonadal WAT as soon as they were large enough to be sampled postnatally. Moreover ZAG mRNA was expressed from day 1 postnatally in the liver. As previously discussed, the metabolism of rat adipose tissue during the time course of early development undergoes some major changes (Herrera & Amusquivar, 2000). The strong signal observed for ZAG mRNA and protein expression from day 1 postnatally suggests that the glycoprotein might play a role in the regulation of adipose tissue metabolism from the early stages of postnatal development.

The extensive study of the ontogenic pattern of ZAG expression in subcutaneous, perirenal and gonadal WAT revealed that there are no substantial changes during suckling in ZAG levels in WAT, the expression not being affected by the rapid accumulation of fat, primarily subcutaneously, during this period. Furthermore, as later discussed, ZAG expression is higher during suckling than post-weaning. As previously discussed (section 6.1), immediately after birth and throughout suckling, the rate of lipolysis is enhanced (Gruen *et al.*, 1980). ZAG is a lipid-mobilising factor, which stimulates lipolysis in mature adipocytes *in vitro* (Todorov *et al.*, 1998), while administration of ZAG to mice induces a rapid reduction in body fat and increases serum free fatty acid levels via the activation of hormone-sensitive lipase through increased intracellular cAMP levels (Hirai *et al.*, 1998). Immediately after birth, and until lactation is fully established, usually after 2-3 days, the mobilisation of lipids via lipolysis is essential for the maintenance of life. During this period, there is a rapid change from carbohydrate to lipids as the major energy source (Fisher, 1976). This enhanced lipolytic activity appears to be regulated by catecholamine release, resulting in cAMP production and increased protein kinase C activity (Kimura & Warshaw, 1983; Bahnsen *et al.*,

1984). Thus ZAG might play a role in the regulation of lipolysis at this early stage of postnatal life.

Consistent with previous reports (Rayner *et al.*, 1997), leptin production, assuming that mRNA levels reflect rates of production, on the other hand dramatically increased in subcutaneous WAT, peaking at day 15. A gradual increase in leptin levels was also detected in the perirenal depot, although at a smaller scale. Since leptin is involved in the regulation of energy balance, these results support its potential to play this role from early in postnatal life. Adiponectin showed similar patterns, although to a smaller extent.

It was shown in Chapter 3 that in the adult mouse there are marked differences between depots in the relative contribution to total ZAG production in adipose tissue, the mRNA and protein levels being much higher in the internal depots (omental and perirenal) than in subcutaneous tissue. In contrast, as demonstrated in this chapter, in the suckling period, the subcutaneous fat appears to be the key source of ZAG of the adipose tissues tested. The same was observed for leptin, as previously demonstrated (Rayner *et al.*, 1997) and adiponectin. Although in adult rodents visceral fat appears metabolically more active and the expression of most adipokines is significantly upregulated compared to subcutaneous WAT, it seems that this is not the case in the early suckling period; at this time the subcutaneous depot is the main site of adipokines production. However, as discussed in the next paragraphs, this pattern of expression changes considerably during the post-weaning period, by which point the mass of visceral fat has substantially increased.

Weaning, the switch from a high-fat to a high-carbohydrate diet revealed a site-specific effect in the expression of the adipokines examined. ZAG mRNA levels in gonadal WAT were reduced compared to both day 1 and day 15, while protein levels were reduced in subcutaneous WAT compared to day 7 and were at their minimum in the perirenal depot. These changes in ZAG expression as a result of a change in the diet suggest that ZAG could be sensitive to nutritional changes, as also suggested in Chapter 4, where ZAG was shown to exhibit a depot specific reaction in response to high-fat diet, its

mRNA levels increasing in epididymal while being reduced in subcutaneous WAT of the high-fat diet fed group. Furthermore, they also suggest that the decrease of ZAG synthesis could be due to the metabolic changes occurring in WAT during this period, the main one being a rapid increase in lipogenic activity, as previously discussed (Gruen *et al.*, 1980). The observation that the reduction in protein levels in subcutaneous and perirenal sites was not accompanied by a similar change in mRNA levels is most probably caused by post-transcriptional effects.

By day 32, animals have settled into the high-carbohydrate diet initiated at weaning, and lipogenesis is increased, adipocytes being filled with fat as a result (Herrera & Amusquivar, 2000). Furthermore, by this point, internal fat depots have considerably increased in size as opposed to the suckling period, when the subcutaneous depot is the main WAT site. As a result of these morphological and metabolic changes, substantial changes were observed at day 32 in the expression of the tested adipokines particularly in internal depots. ZAG levels, both in perirenal and gonadal WAT were highly reduced, as revealed by mRNA and protein analysis. A slight increase in ZAG protein levels in perirenal WAT and BAT might link to a small peak in lipolytic activity of adipose tissue shortly after weaning (Gruen *et al.*, 1980).

Both leptin and adiponectin on the other hand show a different pattern. They were both increased in perirenal and gonadal depots, the latter being their main WAT production site at this stage as shown from the depots comparisons. Indeed, after weaning, there seems to be a rapid switch from subcutaneous to internal adipose tissue as the main source of leptin and adiponectin, which is evident by day 32. This is the same pattern of differential expression that has previously been observed in Chapter 3 and reported for leptin in adult mice (Hardie *et al.*, 1996). ZAG, however, at this stage is still mainly expressed in subcutaneous WAT. However, it would be assumed that there is a switch later on during development as in 10-week old mice it is mainly expressed in omental and perirenal depots. Studies covering a longer period of postnatal development would make it possible to further explore this.

IL-6, MCP-1 and NGF have been linked to body weight control, obesity and insulin sensitivity, as well as inflammation in adipose tissue (Prins, 2002; Wood & Trayhurn, 2006). There have been no reports so far on their expression in adipose tissue during early postnatal development. The current study demonstrates that all three are expressed in WAT of rat neonates from day 1 of life. During suckling there were only small changes in the mRNA levels in all three WAT depots tested, the effects being depot specific, including an increase in MCP-1 mRNA levels in perirenal WAT at days 10 and 15 and in IL-6 mRNA levels in both subcutaneous and perirenal WAT at days 10 and 15 compared to day 1. In adult rodents, IL-6 has been reported to be implicated in stimulating lipolysis (Path *et al.*, 2001), being mainly synthesized by visceral fat (Fried *et al.*, 1998). According to the present data, though, IL-6 might also be involved in the regulation of lipolysis occurring during suckling, as indicated by an increase in its mRNA levels at day 10 and 15 in subcutaneous and perirenal WAT depots. The same was observed in response to weaning, which had only small depot-specific effects in the expression of the adipokines in WAT. The most dramatic effects on the expression of the three adipokines were however observed at day 32 postnatally.

Interestingly at day 32, NGF mRNA is suppressed in subcutaneous and perirenal WAT, although not altered in the gonadal depot, its main production site in adult mice (Peeraully *et al.*, 2004). Furthermore, MCP-1 is also suppressed in the subcutaneous, but increased in perirenal WAT, while a substantial increase in IL-6 production in the latter was observed. Although no depots comparisons were carried out for these adipokines, the present data suggests that as for leptin and adiponectin, they are mainly synthesized by visceral WAT at that stage of postnatal development. So at this stage, it is likely that most of the adipokines start showing the patterns found in adult rodents, thus accounting for the high metabolic activity observed in internal depots of adult rodents compared to subcutaneous WAT (Kelley, 2004). However, not all of the observed changes in mRNA levels during early postnatal development could be explained in relation to the function of these adipokines in rat WAT at this stage.

The heterogeneity of WAT and the differences between different depots, as previously discussed in Chapter 3 are thus evident in the current study as well. Although WAT undergoes major metabolic changes during early postnatal development, these probably affect specific depots in different degrees. Such differences may also be related to regional differences in the production of adipose-derived factors, as previously reported (Mohamed-Ali, 1998), which also change during the course of postnatal development, as specifically shown in the case of leptin and adiponectin in this study.

Apart from WAT, BAT also plays an important role in the early postnatal development, especially soon after birth as it is the site of non-shivering thermogenesis. This study demonstrates that ZAG is expressed in BAT of rats by/or soon after birth. The mRNA and protein levels are at their peak at day 1, but fell significantly thereafter. Of all adipokines tested, ZAG's reduction in BAT from day 3 onwards was the most dramatic, indicating that ZAG may have a role in the metabolic activities of BAT at or soon after birth. Furthermore, ZAG has been shown to increase UCP-1 expression in mouse BAT (Bing *et al.*, 2002) and in primary cultured brown adipocytes (Sanders & Tisdale, 2004).

In addition to ZAG, the other five adipokines tested were expressed in BAT at day 1 postnatally. Leptin, whose presence in BAT in rat neonates has previously been reported (Dessolin *et al.*, 1997), gradually increased in BAT, peaked at day 10, and started declining thereafter. Very interestingly, depot difference analysis revealed that leptin synthesis is higher in BAT at day 1 compared to subcutaneous WAT. However, as mentioned above, by day 7, leptin expression in subcutaneous WAT is higher than in BAT. No changes were observed in adiponectin mRNA levels in BAT throughout the early postnatal development. On the other hand, similarly to ZAG, NGF, MCP-1 and IL-6 mRNA levels in BAT started decreasing during suckling, this being most dramatic at weaning. The increasing levels of leptin in BAT throughout early stages of postnatal development may support a previous suggestion that BAT thermogenesis may be involved in the control of food intake in neonates. It was suggested that both in humans and rats a feeding episode occurs during an episode of increased sympathetic nervous system activity that stimulates BAT thermogenesis and increases body temperature; BAT

thermogenesis being important in the control of meal size, relating it to thermoregulatory needs (Himms-Hagen, 1995 a & b).

Finally, the fact that ZAG is mainly produced in the liver of adult mice was further supported in the current study, as it was shown that from the very early stages of postnatal development, there is a significant difference between ZAG mRNA levels in the liver and subcutaneous WAT. Contrary to what was observed in adipose tissue, ZAG mRNA levels in the liver were gradually increased during the early stages of postnatal development, peaking at day 32 (~10-fold compared to day 1). This might indicate that levels of circulating ZAG would also increase, although further studies on serum circulating levels are needed to clarify this notion.

In conclusion, ZAG is expressed in WAT and BAT of rat neonates from day 1 postnatally (or earlier), the subcutaneous depot being its main site of production within adipose tissue. Its ontogenic pattern of expression may be linked or contribute to the metabolic changes occurring within the tissues at different phases of postnatal development. An interesting observation is that in contrast to most adipokines tested, ZAG levels are higher in WAT during the suckling period than after weaning, suckling being characterised by low lipogenic and high lipolytic activity within the depots, the reverse being the case after weaning. These results may suggest that ZAG might contribute to the high lipolytic and low lipogenic activity which characterises WAT during the suckling period.

Chapter 7

General Discussion

7.1 Introduction

Adipose tissue is now considered as a major endocrine organ, and more than fifty adipose tissue secreted factors, known as adipokines, have been identified so far, their number continually increasing. As already discussed in Chapter 1 (section 1.4), adipokines have numerous functions and are involved in a broad range of physiological conditions. However, many of the functions and underlying mechanisms are still unknown. The complexity of adipose tissue studies is due to the diversity of the roles of these factors and the fact that in a number of cases they are not specific to adipose tissue. In order to establish the secretory function of adipose tissue, the key challenge after identifying a new secreted factor is to establish its role and to assess how its production is regulated with alterations in adiposity and energy flux, present in conditions such as obesity, fasting, and cachexia. ZAG, a lipid-mobilising factor, has been recently identified as a novel adipokine, the protein being secreted by human adipocytes (Bao *et al.*, 2005). The studies in this thesis were thus designed to further explore ZAG function and regulation in adipose tissue using both *in vivo* (rodent models) and *in vitro* (3T3-L1 adipocytes) approaches.

7.2 Previous work

Little is known of ZAG expression in adipose tissue and previous studies exploring the expression of ZAG in rodents using northern blotting analysis, which is effective for the analysis of highly expressed genes, had failed to detect ZAG mRNA in adipose tissue (Ueyama *et al.*, 1992). However, RT-PCR and real-time PCR are much more sensitive methods for detecting an mRNA and it was shown in 2004 by Bing and co-workers that the *ZAG* gene is actually expressed in mouse adipose tissue and murine adipocytes (Bing *et al.*, 2004). That study formed the basis for the development of the current work in different directions, as it was the first evidence that ZAG could have a local (possibly paracrine) role in adipose tissue. For example, since ZAG was detected in all major adipose tissue depots as part of that study, it was of interest to explore the possibility that there might be significant differences in the levels of its expression among specific depots,

the same being the case for differences in ZAG levels in mature adipocytes and the stromal vascular fraction of these depots, both at the mRNA and protein level.

Studying ZAG expression and regulation in adipose tissue is significant for an additional reason. As discussed in detail in chapter 1, ZAG is identical to lipid-mobilising factor (LMF) and administration of ZAG purified from the urine of patients with cancer, leads to a significant decrease in body fat of both normal and *ob/ob* mice as it increases fat breakdown while it does not affect muscle mass (Hirai *et al.*, 1998). This lipolytic effect is mediated through the β_3-adrenoreceptor (Russell *et al.*, 2002). This led to the suggestion that ZAG could be a possible treatment for obesity (Tisdale, 2003), a chronic low-grade inflammatory state with considerable health consequences (Trayhurn & Wood, 2004). Since the main obesity phenotype is the expansion of fat at different sites, understanding of the role of ZAG in adipose tissue and in lipid metabolism could provide further insight into its function and potential. Studies so far have provided evidence that ZAG is involved in the induction of lipolysis in adipose tissue, but that ZAG could also exert its effects by inhibiting lipogenesis.

7.3 Current study

The studies presented in Chapters 3, 4, 5, and 6 were carried out in order to explore the expression and regulation of ZAG in adipose tissue, both under normal and pathophysiological conditions. For this reason, two main approaches were used: *in vivo* studies in mice and rats, and *in vitro* studies using 3T3-L1 adipocytes. Following collection of samples, both mRNA and protein levels were examined using real-time PCR and western blotting respectively. It would be expected in such a study to also measure circulating levels of the protein of interest. However, an Enzyme Linked Immunosorbant Assay (ELISA) kit for ZAG has not yet been commercially available and it was not one of the aims of this thesis to develop one. Although, it was initially attempted to assess changes in circulating levels by western blotting, these trials were not successful, as a number of non-specific bands were detected on the blots, even at very low concentrations

of protein, making it very hard to distinguish ZAG and particularly making it impossible to measure the intensity of these bands by densitometric analysis.

Furthermore, adipose tissue is not the main synthesis site for ZAG in the body, and adipose tissue most probably contributes a low percentage of circulating ZAG. This is evident by previous studies which failed to detect ZAG in adipose tissue, but also by the current study. As discussed in Chapter 6, the difference between ZAG expression in the subcutaneous WAT and the liver (which is its main synthesis site) is very high from the early stages of postnatal development. This sometimes has made studies on adipose tissue rather challenging, especially when studying a condition in which ZAG expression was suppressed, or when a certain agent applied to the adipocytes *in vitro* led to its downregulation. This is also likely to be the main reason for variation in some studies and lack of statistical significance, although a certain trend was evident. Availability of larger groups of samples could have possibly solved this problem.

In the following paragraphs, the main findings of this thesis are summarised, together with mention of some initial results from experiments which have not been presented in the Results Chapters. In addition, in most cases, ZAG expression was studied in reference to other adipokines, primarily leptin. Leptin was mainly used as it is the most studied adipokine and its regulation under most conditions has been extensively examined, both in humans and rodents. In all cases, the results obtained for leptin were consistent with those already described by previous studies. These included the highest levels of leptin being in mouse epididymal WAT, the adipocyte-specific expression, the acute downregulation by fasting, the increase in genetic models of obesity and the increasing levels during early postnatal development. Other adipokines were also studied in certain experiments, such as adiponectin and IL-6, as both have established roles in metabolic regulation, insulin sensitivity and inflammation.

7.4 ZAG expression in adipose tissue

It has been shown in the current study that ZAG is expressed in rodent liver, subcutaneous WAT and BAT from day 1 postnatally and in all other WAT depots as soon as they become sufficient to be sampled. Whether ZAG is also expressed prenatally has not been addressed yet, although it would be very interesting to explore whether it is expressed in the fetus. However, rodents would not be an ideal model for a study of that kind, as WAT depots develop primarily postnatally. Quantitative analysis during early postnatal development revealed that in WAT, weaning at day 21 induced a reduction in ZAG mRNA and protein levels, suggesting that ZAG could possibly be involved in early adipose tissue mass development. Furthermore, throughout early postnatal development, subcutaneous WAT appears to be the main adipose tissue site of ZAG synthesis. However, as revealed from the experiments described in Chapter 3, in the adult mouse ZAG is most highly expressed in visceral fat, particularly omental. This is in line with the previous observation that rates of lipolysis are higher in omental WAT, which is also characterised by high levels of β_3-adrenoreceptors; ZAG having been suggested to exert its lipolytic effect through this type of receptor (Russell *et al.*, 2002). There thus seems to be a switch at some point during development from high levels of ZAG in subcutaneous to high levels in visceral fat. This is also the case for leptin, as has previously been reported (Rayner *et al.*, 1997), and adiponectin, although in these cases the changes happen soon after weaning.

There is an ongoing debate and intensive research on what the differences in the expression levels of most adipokines in different fat sites mean and whether this is associated with regional variations of adipocyte function. Apart from morphological variations, different depots exhibit different metabolic characteristics, this differential expression of adipokines being the major one. Furthermore, differences have been reported between species. For example, in the case of leptin, although in adult rodents leptin is preferentially expressed in epididymal WAT, as also shown in the results presented in Chapter 3, in humans leptin levels are higher in subcutaneous compared to omental WAT (Masuzaki *et al.*, 1995; van Harmelen *et al.*, 1997; Zhang *et al.*, 1999). It

has been suggested that this regional variation in the expression of leptin might play a role in controlling the size of different fat depots (Montague *et al.*, 1997; van Harmelen *et al.*, 1997). In contrast, from some recent findings in our group, it has been shown that in the dog, although leptin is expressed in all major WAT sites, there are no specific inter-depot differences in its expression levels (Ryan, personal communication). Another well established difference between subcutaneous and visceral depots, as shown by both *in vivo* and *in vitro* investigations, is the regional variations in the lipolytic activity of adipose tissue sites, the rate of lipolysis being higher in the visceral, especially the omental region. The lipolytic $\beta_{1, 2, 3}$ adrenoreceptors are most active in the visceral fat cells, while the antilipolytic insulin receptors, α_2 adrenoreceptors and adenosine receptors are most active in the subcutaneous adipocytes (Arner, 1995). However, the physiological significance of these differences is still not fully understood. A study carried out on preadipocytes isolated from the stromal vascular fraction of adipose tissue in order to explore whether regional variations in adipocyte function are primary events or effects of external factors derived from the circulation, suggested that omental and subcutaneous adipocytes might originate from precursor cells that are genetically different or that are programmed differentially by the surrounding tissue before their differentiation (van Harmelen *et al.*, 2002).

Although for a factor to be classified as an adipokine, it does not have to be exclusively expressed in adipose tissue, it has to be established that it is expressed and secreted by mature adipocytes. In the initial study, ZAG had been detected by RT-PCR both in the mature adipocytes and stromal vascular fraction of epididymal WAT. In the study described in Chapter 3, it was shown using quantitative analyses (real-time PCR and western blotting), that ZAG is equally expressed in the two fractions of subcutaneous, epididymal and perirenal WAT. This means that other cells contribute to ZAG levels in WAT and indeed ZAG has previously been detected using immunohistochemical analysis in many types of endothelial and epithelial cells (Tada *et al.*, 1991). It would be interesting to further determine ZAG expression in the different types of cells present in the stromal vascular fraction of adipose tissue depots; for example, whether it is expressed in the macrophages.

In contrast to other adipokines, such as leptin and resistin, mouse ZAG may not function as a marker of adipocyte differentiation. This is evident both by the presence of ZAG in the WAT stromal vascular fraction, as a major part of it consists of undifferentiated or immature adipocytes, as well as by the data presented in Chapter 5, where it was shown that in 3T3-L1 cells the *ZAG* gene was expressed both pre- and post-differentiation. Contrary to that observation, a recent study in SGBS human cells has shown that ZAG is a marker of early adipocyte differentiation (Bao *et al.*, 2005). This might be attributable to the difference between mouse and human, as the homology between the two species is not particularly high and only reaches about 60%, apart from regions important in lipid metabolism where the similarity is 100%.

The present study also demonstrates that ZAG, both mRNA and protein, is expressed in mouse and rat BAT, an important site of lipid utilization. As discussed in Chapter 1, BAT contributes to the regulation of energy homeostasis through UCP-1, which uncouples mitochondrial respiration, thus generating heat (Ricquier & Bouillaud, 2000). It has been shown that ZAG promotes lipid utilization *via* upregulation of BAT UCP-1 mRNA and protein expression in normal mice (Bing *et al.*, 2002) and in primary cultured primary adipocytes (Sanders & Tisdale, 2004) stimulating oxygen uptake by isolated BAT (Hirai *et al.*, 1998). The observation that ZAG expression is higher in rat BAT at day 1 postnatally, its levels being significantly reduced thereafter, could suggest that ZAG might have a role in the metabolic activities of BAT at or soon after birth.

7.5 Regulation of ZAG expression in adipose tissue

The first pathophysiological condition to be studied was obesity and as demonstrated in Chapter 3, ZAG levels are reduced in genetic models of obesity (*ob/ob* mouse and *fa/fa* rats). This is consistent with a recently published study, where it was shown that ZAG is reduced in obese women (Dahnlman *et al.*, 2005). It is thus likely that there is a link between obesity and reduced ZAG expression and as previously discussed, this could be attributed to numerous reasons, such as the increased degree of lipogenesis and the extensive loss of β_3 adrenoreceptors in WAT in both genetic and dietary obesity in mice

(Boschman, 2001). The downregulation of ZAG in obesity could also be partly explained by the fact that administration of leptin in 3T3-L1 adipocytes induced a reduction in ZAG mRNA levels, while adiponectin had the opposite effect, as shown in Chapter 5. However, in the study on *ob/ob* mouse, it was only possible to analyse the mRNA levels, while ZAG protein was not measured due to limited samples. Further protein analysis would show whether these changes are also observed at the protein level.

In addition to obesity, whether diet has a role in the modulation of ZAG expression in adipose tissue was examined. As described in Chapter 4, ZAG expression was studied in two different types of nutritional manipulation. In the first case, animals were fasted for 16 hours, while in the second, mice were fed a high-fat diet for 12 weeks. However, as shown in Chapter 5, a clear pattern in the changes of ZAG expression as a result of dietary changes failed to be established. ZAG mRNA levels in WAT were reduced as a result of short-term fasting, although a similar change was not observed in protein levels. This observation appears to argue against a local role in lipid mobilization. In contrast, ZAG mRNA levels were significantly increased both in BAT and liver of the same animals as a result of food deprivation. Although it has been proposed in Chapter 5 that this could be a result of an initial energy conservation mechanism, further experiments would be necessary to prove whether this is the case. These could include experiments in animals fasted for a longer period, as well as experiments in which re-feeding would follow the fasting period. Furthermore, since after 16 hours, the loss observed in total body weight is mostly due not to actual loss of fat, the decrease observed in ZAG mRNA levels could actually be because of another primary effect of fasting.

On the other hand, a high-fat diet induced a depot-specific response in ZAG mRNA levels, the levels reducing in subcutaneous while increasing in epididymal WAT. The fact that ZAG is sensitive to changes in the diet is supported by the observation in Chapter 6 that ZAG mRNA and protein levels in all WAT depots tested reduced as a result of weaning; weaning represents a switch from a high-fat diet characteristic of milk to a high-carbohydrate diet. This sensitivity to dietary alterations is further illustrated by the fact that although after 12 weeks, the animals kept on a high-fat diet were obese, the effects

observed were not the same as in WAT depots from genetically obese models. However, in all cases, other mechanisms are involved, so using the current data it is not possible to fully explain the observed changes in ZAG levels.

The observation that adiponectin induces *ZAG* gene expression *in vitro* might be suggestive of ZAG's anti-inflammatory role in adipose tissue. Indeed, there is some further evidence arising both from studies described in this thesis and the parallel studies in human adipocytes that ZAG is involved in the inflammatory response, its effect being most probably anti-inflammatory. Firstly, ZAG levels are reduced in adipose tissue depots of genetic models of obesity. Since obesity is now recognised as a low-grade inflammatory state, mainly due to the elevated circulating levels of several markers of inflammation, such as TNFα and acute-phase proteins (Trayhurn & Wood, 2004), it is possible that similarly to adiponectin, which is known to be reduced in obesity and has an established anti-inflammatory role, ZAG may also have anti-inflammatory properties.

Furthermore, as shown in Chapter 5, 15d-PGJ_2, a potent anti-inflammatory agent, strongly induces *ZAG* gene expression, while both PGE_2 and $PGF_{2\alpha}$, which act as inflammatory mediators (Straus & Glass, 2001), inhibit its expression in 3T3-L1 adipocytes in a dose dependent manner. The observation that PGE_2 induces IL-6, an inflammatory regulator in adipose tissue, further supports this suggestion. However, both the pro-inflammatory cytokines TNFα and IL-6 did not affect ZAG mRNA levels in 3T3-L1 adipocytes, although the former induced a significant dose-dependent decrease in human SGBS cells (Bao *et al.*, 2005). Similarly, LPS administration to the 3T3-L1 adipocytes had no effect. In contrast, studies in WAT samples from mice treated with LPS for 4 hours showed a significant decrease in ZAG mRNA levels in epididymal and perirenal WAT, while there was no change observed in ZAG levels in WAT of mice treated with LPS for 12 hours, and thus a connection failed to be established (Tzanavari, unpublished observations). A role for ZAG as an anti-inflammatory agent in adipose tissue is further supported by the finding that rosiglitazone, a selective PPARγ agonist, has a stimulatory effect on ZAG gene expression; this also indicates that the PPARγ nuclear receptor is involved in the regulation of ZAG synthesis.

Apart from rosiglitazone, Δ^{12}-PGJ_2 and 15d-PGJ_2, the two metabolites of PGJ_2, have strong stimulatory effects on ZAG gene expression. While 15d-PGJ_2 is the highest affinity natural ligand for PPARγ identified so far, Δ^{12}-PGJ_2 also binds PPARγ, but with a much lower affinity (Forman *et al.*, 1995). The reasons for the different effects of prostaglandins on ZAG expression in adipocytes could be attributed to their various functions identified so far and their involvement in many pathophysiological conditions. The main finding, however, of this work is that prostaglandins are key regulators of *ZAG* gene expression in adipose tissue and have the greatest effects on its levels identified in the studies carried out for this thesis. The effects of prostaglandins on different adipokines have just recently started being explored and so far it has been reported that prostaglandins influence the expression of some key adipokines as well, including adiponectin, IL-6, MCP-1 and NGF (Bulló *et al.*, 2005; Peeraully *et al.*, 2006). The regulation of ZAG by prostaglandins seems worth further exploration by studying in the first instance ZAG levels in the media of the adipocytes and then by conducting a time-course analysis of their effects on ZAG expression.

One of the problems encountered during the work presented in this thesis was with the quantification of protein levels from western blots and as a result, in a few studies, such as fasting, the changes observed at the mRNA level were not mirrored by protein analysis, especially when changes were not substantial. One reason for that could be due to the fact that real-time PCR is a much more sensitive technique than western blotting. Secondly, although for mRNA analysis five to eight samples were used for each group, four to five samples were usually used for protein work (for practical reasons). Finally, these variations could be due to post-transcriptional events or time lag in mRNA levels leading to changes in protein and differential roles of secretion. In all cases however, equal protein loading was confirmed by Ponceau S staining.

7.6 Future work

The work presented in this thesis has laid the foundations for future studies. Some have already been mentioned above as they would complete already constructed experiments,

such as assessing the changes in ZAG circulating levels in all the animal models, as well as in the media from adipocytes treated with different agents. Furthermore, and as aforementioned, interesting information on ZAG expression and regulation in adipose tissue would be provided by studies on primary adipocytes, as they would show whether the inter-depots differences in ZAG expression observed in Chapters 3 and 4 are primary events. A further issue is that as demonstrated in Chapter 3, ZAG is equally expressed in mature adipocytes and the stromal vascular fraction of WAT depots, consisting of preadipocytes and a number of other cell types, including macrophages. Considering that ZAG could be an inflammation-related adipokine, it is important to further explore the relative importance of both fractions in ZAG regulation in the obese state.

It has been discussed in Chapter 1 (section 1.2.1.5) that knockout mice have so far been useful tools in the study of adipose tissue, as in the case of POMC and MC3R knockout models (Butler & Cone, 2003). The construction of a knockout mouse *in vivo* or RNA silencing *in vitro* could provide useful information on the function of ZAG in adipose tissue and the organism as a whole.

In many occasions, and as has also been shown in Chapter 5, where it was demonstrated that both leptin and adiponectin have an effect on ZAG expression, these factors affect one another. Similarly, ZAG stimulates the expression of adiponectin in transfected 3T3-L1 cells (Gohda *et al.*, 2003). This, as well as other similarities observed between the two adipokines, suggests a functional relation between them. Furthermore, although there are numerous such observations in the literature, it is worth mentioning that TNFα has, for example, been shown to have major effects on the expression of many adipokines in adipocytes (Wang & Trayhurn, 2006), the same being the case for prostaglandins (Bulló *et al.*, 2005). Thus, in order to be able to unfold the complexity of the endocrine function of adipose tissue, it is crucial to try and understand the relations between different adipokines.

Furthermore, it has previously been shown that there is a 10-fold increase in ZAG mRNA levels in white adipose tissue of MAC16 adenocarcinoma bearing mice, a widely

used model for studying cancer cachexia, compared to control mice (Bing *et al.*, 2004). Cachexia also characterises other pathophysiological conditions, including AIDS and sepsis. It was observed while carrying out the work described here that ZAG mRNA levels were 20-fold higher in the epididymal WAT of a sepsis model mouse, in which sepsis was induced by faecal material injection (Tzanavari, unpublished observations). However, these results have not been presented here, as they suggested that ZAG expression could also be induced due to stress (injection) and further work to explore whether this is the case has not been carried out yet due to time restrictions. It would, however, be very interesting to further investigate this.

Finally, so far, all evidence on ZAG expression and regulation in adipose tissue comes from studies in rodents and humans. Considering the differences among different species, useful information could also be provided from studies on ZAG regulation in adipose tissue of other species. Companion animals, especially the dog, have started being used in adipose tissue research due to the increasing occurrence of obesity in these animals. It has recently been shown that several key adipokines, including leptin, adiponectin, PAI-1 and IL-6, are expressed in canine adipose tissue and dog mature adipocytes (Eisele *et al.*, 2005). Very recently and as part of some studies conducted in our group on the dog, ZAG has been detected by RT-PCR in all major dog WAT depots (Ryan & Tzanavari, unpublished observations).

7.7 Concluding remarks

In conclusion, the work presented in this thesis has provided key information on the regulation and possible role of ZAG in adipose tissue, as certain aspects that could contribute to its regulation were examined for the first time. The findings presented further support the suggestion that ZAG contributes to the local modulation of lipid metabolism.

REFERENCES

Abel ED, Peroni O, Kim JK, Kim YB, Boss O, Hadro E, Minnemann T, Shulman GI & Kahn BB (2001). Adipose-selective targeting of the GLUT4 gene impairs insulin action in muscle and liver. *Nature* **409**, 729-733.

Ahima RS, Saper CB, Flier JS & Elmquist JK (2000). Leptin regulation of neuroendocrine systems. *Front Neuroendocrinol* **21**, 263-307.

Ailhaud G (2001). Development of white adipose tissue and adipocyte differentiation. In: *Adipose Tissues*, pp 27-55. Edited by Suzanne Klaus, Landes Bioscience.

Araki T, Gejyo F, Takagaki K, Haupt H, Schwick HG, Burgi W, Marti T, Schaller J, Rickli E, Brossmer R & et al. (1988). Complete amino acid sequence of human plasma Zn-alpha 2-glycoprotein and its homology to histocompatibility antigens. *Proc Natl Acad Sci U S A* **85**, 679-683.

Arch JR (1989). The brown adipocyte beta-adrenoceptor. *Proc Nutr Soc* **48**, 215-223.

Arch JR (2001). The beta 3-adrenergic system and beta 3-adrenergic agonists. *Rev Endocr Metab Disord* **2**, 385-393.

Arch JR, Ainsworth AT, Cawthorne MA, Piercy V, Sennitt MV, Thody VE, Wilson C & Wilson S (1984). Atypical beta-adrenoceptor on brown adipocytes as target for anti-obesity drugs. *Nature* **309**, 163-165.

Argiles JM, Lopez-Soriano J, Busquets S & Lopez-Soriano FJ (1997). Journey from cachexia to obesity by TNF. *Faseb J* **11**, 743-751.

Argiles JM, Moore-Carrasco R, Fuster G, Busquets S & Lopez-Soriano FJ (2003). Cancer cachexia: the molecular mechanisms. *Int J Biochem Cell Biol* **35**, 405-409.

Arita Y, Kihara S, Ouchi N, Takahashi M, Maeda K, Miyagawa J, Hotta K, Shimomura I, Nakamura T, Miyaoka K, Kuriyama H, Nishida M, Yamashita S, Okubo K, Matsubara K, Muraguchi M, Ohmoto Y, Funahashi T & Matsuzawa Y (1999). Paradoxical decrease of an adipose-specific protein, adiponectin, in obesity. *Biochem Biophys Res Commun* **257**, 79-83.

Arner P (1998). Not all fat is alike. *Lancet* **351**, 1301-1302.

Arner P, Hellstrom L, Wahrenberg H & Bronnegard M (1990). Beta-adrenoceptor expression in human fat cells from different regions. *J Clin Invest* **86**, 1595-1600.

Backhed F, Ding H, Wang T, Hooper LV, Koh GY, Nagy A, Semenkovich CF & Gordon JI (2004). The gut microbiota as an environmental factor that regulates fat storage. *Proc Natl Acad Sci U S A* **101**, 15718-15723.

Bae SK, Kim SR, Kim JG, Kim JY, Koo TH, Jang HO, Yun I, Yoo MA & Bae MK (2006). Hypoxic induction of human visfatin gene is directly mediated by hypoxia-inducible factor-1. *FEBS Lett* **580**, 4105-4113.

Bahnsen M, Burrin JM, Johnston DG, Pernet A, Walker M & Alberti KG (1984). Mechanisms of catecholamine effects on ketogenesis. *Am J Physiol* **247**, E173-180.

Bao Y, Bing C, Hunter L, Jenkins JR, Wabitsch M & Trayhurn P (2005). Zinc-alpha2-glycoprotein, a lipid mobilizing factor, is expressed and secreted by human (SGBS) adipocytes. *FEBS Lett* **579**, 41-47.

Barr VA, Lane K & Taylor SI (1999). Subcellular localization and internalization of the four human leptin receptor isoforms. *J Biol Chem* **274**, 21416-21424.

Barsh GS, Farooqi IS & O'Rahilly S (2000). Genetics of body-weight regulation. *Nature* **404**, 644-651.

Bartness TJ & Bamshad M (1998). Innervation of mammalian white adipose tissue: implications for the regulation of total body fat. *Am J Physiol* **275**, R1399-1411.

Bastard JP, Jardel C, Bruckert E, Blondy P, Capeau J, Laville M, Vidal H & Hainque B (2000). Elevated levels of interleukin 6 are reduced in serum and subcutaneous adipose tissue of obese women after weight loss. *J Clin Endocrinol Metab* **85**, 3338-3342.

Beattie JH, Wood AM, Trayhurn P, Jasani B, Vincent A, McCormack G & West AK (2000). Metallothionein is expressed in adipocytes of brown fat and is induced by catecholamines and zinc. *Am J Physiol Regul Integr Comp Physiol* **278**, R1082-1089.

Bell-Parikh LC, Ide T, Lawson JA, McNamara P, Reilly M & FitzGerald GA (2003). Biosynthesis of 15-deoxy-delta12,14-PGJ2 and the ligation of PPARgamma. *J Clin Invest* **112**, 945-955.

Berglund O, Frankel BJ & Hellman B (1978). Development of the insulin secretory defect in genetically diabetic (db/db) mouse. *Acta Endocrinol (Copenh)* **87**, 543-551.

Bertile F, Criscuolo F, Oudart H, Le Maho Y & Raclot T (2003). Differences in the expression of lipolytic-related genes in rat white adipose tissues. *Biochem Biophys Res Commun* **307**, 540-546.

Bertile F & Raclot T (2004). Differences in mRNA expression of adipocyte-derived factors in response to fasting, refeeding and leptin. *Biochim Biophys Acta* **1683**, 101-109.

Bing C, Brown M, King P, Collins P, Tisdale MJ & Williams G (2000). Increased gene expression of brown fat uncoupling protein (UCP)1 and skeletal muscle UCP2 and UCP3 in MAC16-induced cancer cachexia. *Cancer Res* **60**, 2405-2410.

Bing C, Russell ST, Beckett EE, Collins P, Taylor S, Barraclough R, Tisdale MJ & Williams G (2002). Expression of uncoupling proteins-1, -2 and -3 mRNA is induced by an adenocarcinoma-derived lipid-mobilizing factor. *Br J Cancer* **86**, 612-618.

Bing C, Bao Y, Jenkins J, Sanders P, Manieri M, Cinti S, Tisdale MJ & Trayhurn P (2004). Zinc-alpha2-glycoprotein, a lipid mobilizing factor, is expressed in adipocytes and is up-regulated in mice with cancer cachexia. *Proc Natl Acad Sci U S A* **101**, 2500-2505.

Bjorntorp P (1991). Metabolic implications of body fat distribution. *Diabetes Care* **14**, 1132-1143.

Blum WF, Englaro P, Hanitsch S, Juul A, Hertel NT, Muller J, Skakkebaek NE, Heiman ML, Birkett M, Attanasio AM, Kiess W & Rascher W (1997). Plasma leptin levels in healthy children and adolescents: dependence on body mass index, body fat mass, gender, pubertal stage, and testosterone. *J Clin Endocrinol Metab* **82**, 2904-2910.

Bolinder J, Kager L, Ostman J & Arner P (1983). Differences at the receptor and postreceptor levels between human omental and subcutaneous adipose tissue in the action of insulin on lipolysis. *Diabetes* **32**, 117-123.

Borglum JD, Pedersen SB, Ailhaud G, Negrel R & Richelsen B (1999). Differential expression of prostaglandin receptor mRNAs during adipose cell differentiation. *Prostaglandins Other Lipid Mediat* **57**, 305-317.

Bornstein SR, Abu-Asab M, Glasow A, Path G, Hauner H, Tsokos M, Chrousos GP & Scherbaum WA (2000). Immunohistochemical and ultrastructural localization of leptin and leptin receptor in human white adipose tissue and differentiating human adipose cells in primary culture. *Diabetes* **49**, 532-538.

Boschmann M (2001). Heterogeneity of adipose tissue metabolism. In: *Adipose tissues*, pp 131-157. Edited by Suzanne Klaus, Landes Bioscience.

Bottner A, Kratzsch J, Muller G, Kapellen TM, Bluher S, Keller E, Bluher M & Kiess W (2004). Gender differences of adiponectin levels develop during the progression

of puberty and are related to serum androgen levels. *J Clin Endocrinol Metab* **89**, 4053-4061.

Bray GA (2004). How do we get fat? An epidemiologic and metabolic approach. *Clin Dermatol* **22**, 281-288.

Bruun JM, Pedersen SB & Richelsen B (2000). Interleukin-8 production in human adipose tissue. inhibitory effects of anti-diabetic compounds, the thiazolidinedione ciglitazone and the biguanide metformin. *Horm Metab Res* **32**, 537-541.

Bruun JM, Pedersen SB & Richelsen B (2001). Regulation of interleukin 8 production and gene expression in human adipose tissue in vitro. *J Clin Endocrinol Metab* **86**, 1267-1273.

Bruun JM, Lihn AS, Pedersen SB & Richelsen B (2005). Monocyte chemoattractant protein-1 release is higher in visceral than subcutaneous human adipose tissue (AT): implication of macrophages resident in the AT. *J Clin Endocrinol Metab* **90**, 2282-2289.

Brysk MM, Lei G, Adler-Storthz K, Chen Z, Brysk H, Tyring SK & Arany I (1999). Zinc-alpha2-glycoprotein expression as a marker of differentiation in human oral tumors. *Cancer Lett* **137**, 117-120.

Bullo M, Garcia-Lorda P, Megias I & Salas-Salvado J (2003). Systemic inflammation, adipose tissue tumor necrosis factor, and leptin expression. *Obes Res* **11**, 525-531.

Bullo M, Peeraully MR & Trayhurn P (2005). Stimulation of NGF expression and secretion in 3T3-L1 adipocytes by prostaglandins PGD2, PGJ2, and Delta12-PGJ2. *Am J Physiol Endocrinol Metab* **289**, E62-67.

Burgi W & Schmid K (1961). Preparation and properties of Zn-alpha 2-glycoprotein of normal human plasma. *J Biol Chem* **236**, 1066-1074.

Busquets S, Garcia-Martinez C, Olivan M, Barreiro E, Lopez-Soriano FJ & Argiles JM (2006). Overexpression of UCP3 in both murine and human myotubes is linked with the activation of proteolytic systems: a role in muscle wasting? *Biochim Biophys Acta* **1760**, 253-258.

Bustin SA (2002). Quantification of mRNA using real-time reverse transcription PCR (RT-PCR): trends and problems. *J Mol Endocrinol* **29**, 23-39.

Bustin SA & Mueller R (2005). Real-time reverse transcription PCR (qRT-PCR) and its potential use in clinical diagnosis. *Clin Sci (Lond)* **109**, 365-379.

Butler AA, Marks DL, Fan W, Kuhn CM, Bartolome M & Cone RD (2001). Melanocortin-4 receptor is required for acute homeostatic responses to increased dietary fat. *Nat Neurosci* **4**, 605-611.

Butler AA & Cone RD (2003). Knockout studies defining different roles for melanocortin receptors in energy homeostasis. *Ann N Y Acad Sci* **994**, 240-245.

Calle EE, Rodriguez C, Walker-Thurmond K & Thun MJ (2003). Overweight, obesity, and mortality from cancer in a prospectively studied cohort of U.S. adults. *N Engl J Med* **348**, 1625-1638.

Campfield LA, Smith FJ, Guisez Y, Devos R & Burn P (1995). Recombinant mouse OB protein: evidence for a peripheral signal linking adiposity and central neural networks. *Science* **269**, 546-549.

Caspar-Bauguil S, Cousin B, Galinier A, Segafredo C, Nibbelink M, Andre M, Casteilla L & Penicaud L (2005). Adipose tissues as an ancestral immune organ: site-specific change in obesity. *FEBS Lett* **579**, 3487-3492.

Castan I, Valet P, Quideau N, Voisin T, Ambid L, Laburthe M, Lafontan M & Carpene C (1994). Antilipolytic effects of alpha 2-adrenergic agonists, neuropeptide Y, adenosine, and PGE1 in mammal adipocytes. *Am J Physiol* **266**, R1141-1147.

Castracane VD, Kraemer RR, Franken MA, Kraemer GR & Gimpel T (1998). Serum leptin concentration in women: effect of age, obesity, and estrogen administration. *Fertil Steril* **70**, 472-477.

Chance WT, Balasubramaniam A, Dayal R, Brown J & Fischer JE (1994). Hypothalamic concentration and release of neuropeptide Y into microdialysates is reduced in anorectic tumor-bearing rats. *Life Sci* **54**, 1869-1874.

Chandran M, Phillips SA, Ciaraldi T & Henry RR (2003). Adiponectin: more than just another fat cell hormone? *Diabetes Care* **26**, 2442-2450.

Chen H, Charlat O, Tartaglia LA, Woolf EA, Weng X, Ellis SJ, Lakey ND, Culpepper J, Moore KJ, Breitbart RE, Duyk GM, Tepper RI & Morgenstern JP (1996). Evidence that the diabetes gene encodes the leptin receptor: identification of a mutation in the leptin receptor gene in db/db mice. *Cell* **84**, 491-495.

Christiansen T, Richelsen B & Bruun JM (2005). Monocyte chemoattractant protein-1 is produced in isolated adipocytes, associated with adiposity and reduced after weight loss in morbid obese subjects. *Int J Obes (Lond)* **29**, 146-150.

Chua SC, Jr., Chung WK, Wu-Peng XS, Zhang Y, Liu SM, Tartaglia L & Leibel RL (1996). Phenotypes of mouse diabetes and rat fatty due to mutations in the OB (leptin) receptor. *Science* **271**, 994-996.

Cianflone K, Xia Z & Chen LY (2003). Critical review of acylation-stimulating protein physiology in humans and rodents. *Biochim Biophys Acta* **1609**, 127-143.

Cid MC, Grant DS, Hoffman GS, Auerbach R, Fauci AS & Kleinman HK (1993). Identification of haptoglobin as an angiogenic factor in sera from patients with systemic vasculitis. *J Clin Invest* **91**, 977-985.

Cinti S, Frederich RC, Zingaretti MC, De Matteis R, Flier JS & Lowell BB (1997). Immunohistochemical localization of leptin and uncoupling protein in white and brown adipose tissue. *Endocrinology* **138**, 797-804.

Cinti S (2001). The adipose organ: morphological perspectives of adipose tissues. *Proc Nutr Soc* **60**, 319-328.

Cinti S (2005). The adipose organ. *Prostaglandins Leukot Essent Fatty Acids* **73**, 9-15.

Civitarese AE, Jenkinson CP, Richardson D, Bajaj M, Cusi K, Kashyap S, Berria R, Belfort R, DeFronzo RA, Mandarino LJ & Ravussin E (2004). Adiponectin receptors gene expression and insulin sensitivity in non-diabetic Mexican Americans with or without a family history of Type 2 diabetes. *Diabetologia* 47, 816-820.

Clement K, Garner C, Hager J, Philippi A, LeDuc C, Carey A, Harris TJ, Jury C, Cardon LR, Basdevant A, Demenais F, Guy-Grand B, North M & Froguel P (1996). Indication for linkage of the human OB gene region with extreme obesity. *Diabetes* 45, 687-690.

Collins S, Cao W, Daniel KW, Dixon TM, Medvedev AV, Onuma H & Surwit R (2001). Adrenoceptors, uncoupling proteins, and energy expenditure. *Exp Biol Med (Maywood)* **226**, 982-990.

Considine RV, Sinha MK, Heiman ML, Kriauciunas A, Stephens TW, Nyce MR, Ohannesian JP, Marco CC, McKee LJ, Bauer TL & et al. (1996). Serum immunoreactive-leptin concentrations in normal-weight and obese humans. *N Engl J Med* **334**, 292-295.

Coppack SW (2001). Pro-inflammatory cytokines and adipose tissue. *Proc Nutr Soc* **60**, 349-356.

Costa G, Bewley P, Aragon M & Siebold J (1981). Anorexia and weight loss in cancer patients. *Cancer Treat Rep* **65 Suppl 5**, 3-7.

Cryer A & Jones HM (1978). Changes in the lipoprotein lipase (clearing-factor lipase) activity of white adipose tissue during development of the rat. *Biochem J* **172**, 319-325.

Curtis-Prior PB (1975). Prostaglandins and obesity. *Lancet* **1**, 897-899.

Dahlman I, Kaaman M, Olsson T, Tan GD, Bickerton AS, Wahlen K, Andersson J, Nordstrom EA, Blomqvist L, Sjogren A, Forsgren M, Attersand A & Arner P (2005). A unique role of monocyte chemoattractant protein 1 among chemokines in adipose tissue of obese subjects. *J Clin Endocrinol Metab* **90**, 5834-5840.

Damcott CM, Sack P & Shuldiner AR (2003). The genetics of obesity. *Endocrinol Metab Clin North Am* **32**, 761-786.

Daniels J (2006). Obesity: America's epidemic. *Am J Nurs* **106**, 40-49, quiz 49-50.

Das UN (2001). Is obesity an inflammatory condition? *Nutrition* **17**, 953-966.

De Benedetti F, Alonzi T, Moretta A, Lazzaro D, Costa P, Poli V, Martini A, Ciliberto G & Fattori E (1997). Interleukin 6 causes growth impairment in transgenic mice through a decrease in insulin-like growth factor-I. A model for stunted growth in children with chronic inflammation. *J Clin Invest* **99**, 643-650.

Deckelbaum RJ & Williams CL (2001). Childhood obesity: the health issue. *Obes Res* **9 Suppl 4**, 239S-243S.

Dessolin S, Schalling M, Champigny O, Lonnqvist F, Ailhaud G, Dani C & Ricquier D (1997). Leptin gene is expressed in rat brown adipose tissue at birth. *Faseb J* **11**, 382-387.

Diez-Itza I, Sanchez LM, Allende MT, Vizoso F, Ruibal A & Lopez-Otin C (1993). Zn-alpha 2-glycoprotein levels in breast cancer cytosols and correlation with clinical, histological and biochemical parameters. *Eur J Cancer* **29A**, 1256-1260.

Diez JJ & Iglesias P (2003). The role of the novel adipocyte-derived hormone adiponectin in human disease. *Eur J Endocrinol* **148**, 293-300.

do Nascimento CO, Hunter L & Trayhurn P (2004). Regulation of haptoglobin gene expression in 3T3-L1 adipocytes by cytokines, catecholamines, and PPARgamma. *Biochem Biophys Res Commun* **313**, 702-708.

Dulloo AG & Samec S (2000). Uncoupling Proteins: Do They Have a Role in Body Weight Regulation? *News Physiol Sci* **15**, 313-318.

Einstein FH, Atzmon G, Yang XM, Ma XH, Rincon M, Rudin E, Muzumdar R & Barzilai N (2005). Differential responses of visceral and subcutaneous fat depots to nutrients. *Diabetes* **54**, 672-678.

Elmquist JK (2001). Hypothalamic pathways underlying the endocrine, autonomic, and behavioral effects of leptin. *Int J Obes Relat Metab Disord* **25 Suppl 5**, S78-82.

Enerback S & Gimble JM (1993). Lipoprotein lipase gene expression: physiological regulators at the transcriptional and post-transcriptional level. *Biochim Biophys Acta* **1169**, 107-125.

Engeli S, Negrel R & Sharma AM (2000). Physiology and pathophysiology of the adipose tissue renin-angiotensin system. *Hypertension* **35**, 1270-1277.

Engeli S, Schling P, Gorzelniak K, Boschmann M, Janke J, Ailhaud G, Teboul M, Massiera F & Sharma AM (2003). The adipose-tissue renin-angiotensin-aldosterone system: role in the metabolic syndrome? *Int J Biochem Cell Biol* **35**, 807-825.

Engstrom G, Hedblad B, Stavenow L, Lind P, Janzon L & Lindgarde F (2003). Inflammation-sensitive plasma proteins are associated with future weight gain. *Diabetes* **52**, 2097-2101.

Esposito K, Pontillo A, Ciotola M, Di Palo C, Grella E, Nicoletti G & Giugliano D (2002). Weight loss reduces interleukin-18 levels in obese women. *J Clin Endocrinol Metab* **87**, 3864-3866.

Esposito K, Pontillo A, Giugliano F, Giugliano G, Marfella R, Nicoletti G & Giugliano D (2003). Association of low interleukin-10 levels with the metabolic syndrome in obese women. *J Clin Endocrinol Metab* **88**, 1055-1058.

Evans WK, Makuch R, Clamon GH, Feld R, Weiner RS, Moran E, Blum R, Shepherd FA, Jeejeebhoy KN & DeWys WD (1985). Limited impact of total parenteral nutrition on nutritional status during treatment for small cell lung cancer. *Cancer Res* **45**, 3347-3353.

Faggioni R, Fantuzzi G, Fuller J, Dinarello CA, Feingold KR & Grunfeld C (1998). IL-1 beta mediates leptin induction during inflammation. *Am J Physiol* **274**, R204-208.

Fain JN, Leffler CW, Bahouth SW, Rice AM & Rivkees SA (2000). Regulation of leptin release and lipolysis by PGE2 in rat adipose tissue. *Prostaglandins Other Lipid Mediat* **62**, 343-350.

Fain JN, Kanu A, Bahouth SW, Cowan GS, Jr., Hiler ML & Leffler CW (2002). Comparison of PGE2, prostacyclin and leptin release by human adipocytes versus explants of adipose tissue in primary culture. *Prostaglandins Leukot Essent Fatty Acids* **67**, 467-473.

Fain JN, Madan AK, Hiler ML, Cheema P & Bahouth SW (2004). Comparison of the release of adipokines by adipose tissue, adipose tissue matrix, and adipocytes from visceral and subcutaneous abdominal adipose tissues of obese humans. *Endocrinology* **145**, 2273-2282.

Fain JN & Madan AK (2005). Insulin enhances vascular endothelial growth factor, interleukin-8, and plasminogen activator inhibitor 1 but not interleukin-6 release by human adipocytes. *Metabolism* **54**, 220-226.

Faust IM, Johnson PR, Stern JS & Hirsch J (1978). Diet-induced adipocyte number increase in adult rats: a new model of obesity. *Am J Physiol* **235**, E279-286.

Fay WP (2004). Plasminogen activator inhibitor 1, fibrin, and the vascular response to injury. *Trends Cardiovasc Med* **14**, 196-202.

Fearon KC (1992). The mechanisms and treatment of weight loss in cancer. *Proc Nutr Soc* **51**, 251-265.

Fearon KC & Preston T (1990). Body composition in cancer cachexia. *Infusionstherapie* **17 Suppl 3**, 63-66.

Feingold KR, Doerrler W, Dinarello CA, Fiers W & Grunfeld C (1992). Stimulation of lipolysis in cultured fat cells by tumor necrosis factor, interleukin-1, and the interferons is blocked by inhibition of prostaglandin synthesis. *Endocrinology* **130**, 10-16.

Fernandez-Real JM & Ricart W (2003). Insulin resistance and chronic cardiovascular inflammatory syndrome. *Endocr Rev* **24**, 278-301.

Festa A, D'Agostino R, Jr., Williams K, Karter AJ, Mayer-Davis EJ, Tracy RP & Haffner SM (2001). The relation of body fat mass and distribution to markers of chronic inflammation. *Int J Obes Relat Metab Disord* **25**, 1407-1415.

Flier JS, Cook KS, Usher P & Spiegelman BM (1987). Severely impaired adipsin expression in genetic and acquired obesity. *Science* **237**, 405-408.

Flower L, Gray R, Pinkney J & Mohamed-Ali V (2003). Stimulation of interleukin-6 release by interleukin-1beta from isolated human adipocytes. *Cytokine* **21**, 32-37.

Forman BM, Tontonoz P, Chen J, Brun RP, Spiegelman BM & Evans RM (1995). 15-Deoxy-delta 12, 14-prostaglandin J2 is a ligand for the adipocyte determination factor PPAR gamma. *Cell* **83**, 803-812.

Forman BM, Chen J & Evans RM (1997). Hypolipidemic drugs, polyunsaturated fatty acids, and eicosanoids are ligands for peroxisome proliferator-activated receptors alpha and delta. *Proc Natl Acad Sci U S A* **94**, 4312-4317.

Frederich RC, Lollmann B, Hamann A, Napolitano-Rosen A, Kahn BB, Lowell BB & Flier JS (1995). Expression of ob mRNA and its encoded protein in rodents. Impact of nutrition and obesity. *J Clin Invest* **96**, 1658-1663.

Fredrix EW, Soeters PB, Wouters EF, Deerenberg IM, von Meyenfeldt MF & Saris WH (1991). Effect of different tumor types on resting energy expenditure. *Cancer Res* **51**, 6138-6141.

Fried SK, Bunkin DA & Greenberg AS (1998). Omental and subcutaneous adipose tissues of obese subjects release interleukin-6: depot difference and regulation by glucocorticoid. *J Clin Endocrinol Metab* **83**, 847-850.

Friedman JM & Halaas JL (1998). Leptin and the regulation of body weight in mammals. *Nature* **395**, 763-770.

Fruhbeck G, Gomez-Ambrosi J, Muruzabal FJ & Burrell MA (2001). The adipocyte: a model for integration of endocrine and metabolic signaling in energy metabolism regulation. *Am J Physiol Endocrinol Metab* **280**, E827-847.

Fruhbeck G & Salvador J (2000). Relation between leptin and the regulation of glucose metabolism. *Diabetologia* **43**, 3-12.

Fu Y, Luo N, Klein RL & Garvey WT (2005). Adiponectin promotes adipocyte differentiation, insulin sensitivity, and lipid accumulation. *J Lipid Res* **46**, 1369-1379.

Fujita H, Fujishima H, Morii T, Koshimura J, Narita T, Kakei M & Ito S (2002). Effect of metformin on adipose tissue resistin expression in db/db mice. *Biochem Biophys Res Commun* **298**, 345-349.

Fukuhara A, Matsuda M, Nishizawa M, Segawa K, Tanaka M, Kishimoto K, Matsuki Y, Murakami M, Ichisaka T, Murakami H, Watanabe E, Takagi T, Akiyoshi M, Ohtsubo T, Kihara S, Yamashita S, Makishima M, Funahashi T, Yamanaka S, Hiramatsu R, Matsuzawa Y & Shimomura I (2005). Visfatin: a protein secreted by visceral fat that mimics the effects of insulin. *Science* **307**, 426-430.

Gerhardt CC, Romero IA, Cancello R, Camoin L & Strosberg AD (2001). Chemokines control fat accumulation and leptin secretion by cultured human adipocytes. *Mol Cell Endocrinol* **175**, 81-92.

Giacobino JP (1996). Role of the beta3-adrenoceptor in the control of leptin expression. *Horm Metab Res* **28**, 633-637.

Gil-Campos M, Canete RR & Gil A (2004). Adiponectin, the missing link in insulin resistance and obesity. *Clin Nutr* **23**, 963-974.

Gilroy DW, Colville-Nash PR, Willis D, Chivers J, Paul-Clark MJ & Willoughby DA (1999). Inducible cyclooxygenase may have anti-inflammatory properties. *Nat Med* **5**, 698-701.

Giordano A, Frontini A, Murano I, Tonello C, Marino MA, Carruba MO, Nisoli E & Cinti S (2005). Regional-dependent increase of sympathetic innervation in rat white adipose tissue during prolonged fasting. *J Histochem Cytochem* **53**, 679-687.

Giulietti A, Overbergh L, Valckx D, Decallonne B, Bouillon R & Mathieu C (2001). An overview of real-time quantitative PCR: applications to quantify cytokine gene expression. *Methods* **25**, 386-401.

Gohda T, Makita Y, Shike T, Tanimoto M, Funabiki K, Horikoshi S & Tomino Y (2003). Identification of epistatic interaction involved in obesity using the KK/Ta mouse as a Type 2 diabetes model: is Zn-alpha2 glycoprotein-1 a candidate gene for obesity? *Diabetes* **52**, 2175-2181.

Goodman MN, Larsen PR, Kaplan MM, Aoki TT, Young VR & Ruderman NB (1980). Starvation in the rat. II. Effect of age and obesity on protein sparing and fuel metabolism. *Am J Physiol* **239**, E277-E286.

Gordon JN, Green SR & Goggin PM (2005). Cancer cachexia. *Qjm* **98**, 779-788.

Grako KA, McClain DA & Olefsky JM (1994). Hybrid formation between endogenous mouse and transfected human tyrosine kinase-deficient (A/K1018) insulin receptors leads to decreased insulin sensitivity in 3T3-L1 adipocytes. *Mol Endocrinol* **8**, 682-692.

Greenwood MR & Hirsch J (1974). Postnatal development of adipocyte cellularity in the normal rat. *J Lipid Res* **15**, 474-483.

Gregoire FM (2001). Adipocyte differentiation: from fibroblast to endocrine cell. *Exp Biol Med (Maywood)* **226**, 997-1002.

Grinberg DR, Ramirez I, Vilaro S, Reina M, Llobera M & Herrera E (1985). Starvation enhances lipoprotein lipase activity in the liver of the newborn rat. *Biochim Biophys Acta* **833**, 217-222.

Grosvenor M, Bulcavage L & Chlebowski RT (1989). Symptoms potentially influencing weight loss in a cancer population. Correlations with primary site, nutritional status, and chemotherapy administration. *Cancer* **63**, 330-334.

Gruen R, Kava R & Greenwood MR (1980). Development of basal lipolysis and fat cell size in the epididymal fat pad of normal rats. *Metabolism* **29**, 246-253.

Gualillo O, Eiras S, Lago F, Dieguez C & Casanueva FF (2000). Elevated serum leptin concentrations induced by experimental acute inflammation. *Life Sci* **67**, 2433-2441.

Guan XM, Yu H & Van der Ploeg LH (1998). Evidence of altered hypothalamic pro-opiomelanocortin/ neuropeptide Y mRNA expression in tubby mice. *Brain Res Mol Brain Res* **59**, 273-279.

Halaas JL, Gajiwala KS, Maffei M, Cohen SL, Chait BT, Rabinowitz D, Lallone RL, Burley SK & Friedman JM (1995). Weight-reducing effects of the plasma protein encoded by the obese gene. *Science* **269**, 543-546.

Hale LP, Price DT, Sanchez LM, Demark-Wahnefried W & Madden JF (2001). Zinc alpha-2-glycoprotein is expressed by malignant prostatic epithelium and may serve as a potential serum marker for prostate cancer. *Clin Cancer Res* **7**, 846-853.

Hales CN, Luzio JP & Siddle K (1978). Hormonal control of adipose-tissue lipolysis. *Biochem Soc Symp*, 97-135.

Hamann A, Flier JS & Lowell BB (1996). Decreased brown fat markedly enhances susceptibility to diet-induced obesity, diabetes, and hyperlipidemia. *Endocrinology* **137**, 21-29.

Hardie LJ, Rayner DV, Holmes S & Trayhurn P (1996). Circulating leptin levels are modulated by fasting, cold exposure and insulin administration in lean but not Zucker (fa/fa) rats as measured by ELISA. *Biochem Biophys Res Commun* **223**, 660-665.

Harper LA (1973). Laboratory problems in the diagnosis of trachoma. *Trans Ophthalmol Soc U K* **93**, 641-645.

Hata AN & Breyer RM (2004). Pharmacology and signaling of prostaglandin receptors: multiple roles in inflammation and immune modulation. *Pharmacol Ther* **103**, 147-166.

Haugen F, Jorgensen A, Drevon CA & Trayhurn P (2001). Inhibition by insulin of resistin gene expression in 3T3-L1 adipocytes. *FEBS Lett* **507**, 105-108.

Hauner H, Skurk T & Wabitsch M (2001). Cultures of human adipose precursor cells. *Methods Mol Biol* **155**, 239-247.

Hausman DB, DiGirolamo M, Bartness TJ, Hausman GJ & Martin RJ (2001). The biology of white adipocyte proliferation. *Obes Rev* **2**, 239-254.

Hausman GJ (1985). Anatomical and enzyme histochemical differentiation of adipose tissue. *Int J Obes* **9 Suppl 1**, 1-6.

Havel PJ (2001). Peripheral signals conveying metabolic information to the brain: short-term and long-term regulation of food intake and energy homeostasis. *Exp Biol Med (Maywood)* **226**, 963-977.

Havel PJ, Kasim-Karakas S, Dubuc GR, Mueller W & Phinney SD (1996). Gender differences in plasma leptin concentrations. *Nat Med* **2**, 949-950.

Heptulla R, Smitten A, Teague B, Tamborlane WV, Ma YZ & Caprio S (2001). Temporal patterns of circulating leptin levels in lean and obese adolescents: relationships to insulin, growth hormone, and free fatty acids rhythmicity. *J Clin Endocrinol Metab* **86**, 90-96.

Herberg L & Coleman DL (1977). Laboratory animals exhibiting obesity and diabetes syndromes. *Metabolism* **26**, 59-99.

Herrera E & Amusquivar E (2000). Lipid metabolism in the fetus and the newborn. *Diabetes Metab Res Rev* **16**, 202-210.

Herschman HR, Reddy ST & Xie W (1997). Function and regulation of prostaglandin synthase-2. *Adv Exp Med Biol* **407**, 61-66.

Himms-Hagen J (1990). Brown adipose tissue thermogenesis: interdisciplinary studies. *Faseb J* **4**, 2890-2898.

Himms-Hagen J (1995a). Does thermoregulatory feeding occur in newborn infants? A novel view of the role of brown adipose tissue thermogenesis in control of food intake. *Obes Res* **3**, 361-369.

Himms-Hagen J (1995b). Role of brown adipose tissue thermogenesis in control of thermoregulatory feeding in rats: a new hypothesis that links thermostatic and glucostatic hypotheses for control of food intake. *Proc Soc Exp Biol Med* **208**, 159-169.

Hirai K, Hussey HJ, Barber MD, Price SA & Tisdale MJ (1998). Biological evaluation of a lipid-mobilizing factor isolated from the urine of cancer patients. *Cancer Res* **58**, 2359-2365.

Hirai H, Tanaka K, Yoshie O, Ogawa K, Kenmotsu K, Takamori Y, Ichimasa M, Sugamura K, Nakamura M, Takano S & Nagata K (2001). Prostaglandin D2 selectively induces chemotaxis in T helper type 2 cells, eosinophils, and basophils via seven-transmembrane receptor CRTH2. *J Exp Med* **193**, 255-261.

Hotamisligil GS, Shargill NS & Spiegelman BM (1993). Adipose expression of tumor necrosis factor-alpha: direct role in obesity-linked insulin resistance. *Science* **259**, 87-91.

Hotta K, Funahashi T, Arita Y, Takahashi M, Matsuda M, Okamoto Y, Iwahashi H, Kuriyama H, Ouchi N, Maeda K, Nishida M, Kihara S, Sakai N, Nakajima T, Hasegawa K, Muraguchi M, Ohmoto Y, Nakamura T, Yamashita S, Hanafusa T & Matsuzawa Y (2000). Plasma concentrations of a novel, adipose-specific protein, adiponectin, in type 2 diabetic patients. *Arterioscler Thromb Vasc Biol* **20**, 1595-1599.

Hube F, Lietz U, Igel M, Jensen PB, Tornqvist H, Joost HG & Hauner H (1996). Difference in leptin mRNA levels between omental and subcutaneous abdominal adipose tissue from obese humans. *Horm Metab Res* **28**, 690-693

Hube F & Hauner H (1999). The role of TNF-alpha in human adipose tissue: prevention of weight gain at the expense of insulin resistance? *Horm Metab Res* **31**, 626-631..

Hug C & Lodish HF (2005). Medicine. Visfatin: a new adipokine. *Science* **307**, 366-367.

Hussey HJ & Tisdale MJ (1994). Effect of polyunsaturated fatty acids on the growth of murine colon adenocarcinomas in vitro and in vivo. *Br J Cancer* **70**, 6-10.

Ikeda H (1994). KK mouse. *Diabetes Res Clin Pract* **24 Suppl**, S313-316.

Ingalls AM, Dickie MM & Snell GD (1950). Obese, a new mutation in the house mouse. *J Hered* **41**, 317-318.

Inukai K, Nakashima Y, Watanabe M, Takata N, Sawa T, Kurihara S, Awata T & Katayama S (2005). Regulation of adiponectin receptor gene expression in diabetic mice. *Am J Physiol Endocrinol Metab* **288**, E876-882.

Issad T, Coupe C, Ferre P & Girard J (1987). Insulin resistance during suckling period in rats. *Am J Physiol* **253**, E142-148.

Janke J, Engeli S, Gorzelniak K, Luft FC & Sharma AM (2002). Resistin gene expression in human adipocytes is not related to insulin resistance. *Obes Res* **10**, 1-5.

Jequier E & Tappy L (1999). Regulation of body weight in humans. *Physiol Rev* **79**, 451-480.

Jones TH (1994). Interleukin-6 an endocrine cytokine. *Clin Endocrinol (Oxf)* **40**, 703-713.

Jourdan ML, Wang LC & Christopherson RJ (1984). Effects of fasting and aminophylline on norepinephrine-stimulated non-shivering thermogenesis. *Life Sci* **34**, 1101-1109.

Jowsey IR, Murdock PR, Moore GB, Murphy GJ, Smith SA & Hayes JD (2003). Prostaglandin D2 synthase enzymes and PPARgamma are co-expressed in mouse 3T3-L1 adipocytes and human tissues. *Prostaglandins Other Lipid Mediat* **70**, 267-284.

Juge-Aubry CE, Somm E, Pernin A, Alizadeh N, Giusti V, Dayer JM & Meier CA (2005). Adipose tissue is a regulated source of interleukin-10. *Cytokine* **29**, 270-274.

Juhan-Vague I, Alessi MC, Mavri A & Morange PE (2003). Plasminogen activator inhibitor-1, inflammation, obesity, insulin resistance and vascular risk. *J Thromb Haemost* **1**, 1575-1579.

Kadowaki T & Yamauchi T (2005). Adiponectin and adiponectin receptors. *Endocr Rev* **26**, 439-451.

Kalant D, Cain SA, Maslowska M, Sniderman AD, Cianflone K & Monk PN (2003). The chemoattractant receptor-like protein C5L2 binds the C3a des-Arg77/acylation-stimulating protein. *J Biol Chem* **278**, 11123-11129.

Kather H & Simon B (1979). Effects of some naturally occurring prostaglandins of the D-, E-, and I-type and synthetic analogues on adenylate cyclase of human fat cell ghosts. *Res Exp Med (Berl)* **176**, 25-29.

Kershaw EE & Flier JS (2004). Adipose tissue as an endocrine organ. *J Clin Endocrinol Metab* **89**, 2548-2556.

Kersten S (2001). Mechanisms of nutritional and hormonal regulation of lipogenesis. *EMBO Rep* **2**, 282-286.

Kersten S, Mandard S, Tan NS, Escher P, Metzger D, Chambon P, Gonzalez FJ, Desvergne B & Wahli W (2000). Characterization of the fasting-induced adipose

factor FIAF, a novel peroxisome proliferator-activated receptor target gene. *J Biol Chem* **275**, 28488-28493.

Kim KH, Lee K, Moon YS & Sul HS (2001). A cysteine-rich adipose tissue-specific secretory factor inhibits adipocyte differentiation. *J Biol Chem* **276**, 11252-11256.

Kimura RE & Warshaw JB (1983). Metabolic adaptations of the fetus and newborn. *J Pediatr Gastroenterol Nutr* **2 Suppl 1**, S12-15.

Klaus S (2001). Brown Adipose Tissue: Thermogenic function and its physiological regulation. In: *Adipose tissues*. Edited by Suzanne Klaus, Landes bioscience.

Kliewer SA, Lenhard JM, Willson TM, Patel I, Morris DC & Lehmann JM (1995). A prostaglandin J2 metabolite binds peroxisome proliferator-activated receptor gamma and promotes adipocyte differentiation. *Cell* **83**, 813-819.

Koerner A, Kratzsch J & Kiess W (2005). Adipocytokines: leptin--the classical, resistin--the controversical, adiponectin--the promising, and more to come. *Best Pract Res Clin Endocrinol Metab* **19**, 525-546.

Kokkoris P & Pi-Sunyer FX (2003). Obesity and endocrine disease. *Endocrinol Metab Clin North Am* **32**, 895-914.

Kopelman PG (2000). Obesity as a medical problem. *Nature* **404**, 635-643.

Korhonen T & Saarela S (2005). Role of adiposity hormones in the mouse during fasting and winter-acclimatization. *Comp Biochem Physiol A Mol Integr Physiol* **140**, 217-223.

Kralisch S, Klein J, Lossner U, Bluher M, Paschke R, Stumvoll M & Fasshauer M (2005). Hormonal regulation of the novel adipocytokine visfatin in 3T3-L1 adipocytes. *J Endocrinol* **185**, R1-8.

Krogh-Madsen R, Plomgaard P, Keller P, Keller C & Pedersen BK (2004). Insulin stimulates interleukin-6 and tumor necrosis factor-alpha gene expression in human subcutaneous adipose tissue. *Am J Physiol Endocrinol Metab* **286**, E234-238.

Krzyzanowska K, Mittermayer F, Krugluger W, Kopp HP & Schernthaner G (2006). Increase in visfatin after weight loss induced by gastroplastic surgery. *Obesity (Silver Spring)* **14**, 1886-1889.

Kubis N & Levy BI (2004). Angiogenic effect of prostaglandin I 2 in relation with its effect on PPAR nuclear receptors. *J Mol Cell Cardiol* **36**, 331-332.

Lagathu C, Bastard JP, Auclair M, Maachi M, Capeau J & Caron M (2003). Chronic interleukin-6 (IL-6) treatment increased IL-6 secretion and induced insulin resistance in adipocyte: prevention by rosiglitazone. *Biochem Biophys Res Commun* **311**, 372-379.

Lee GH, Proenca R, Montez JM, Carroll KM, Darvishzadeh JG, Lee JI & Friedman JM (1996). Abnormal splicing of the leptin receptor in diabetic mice. *Nature* **379**, 632-635.

Lei G, Arany I, Selvanayagam P, Rajaraman S, Ram S, Brysk H, Tyring SK & Brysk MM (1997). Detection and cloning of epidermal zinc-alpha 2-glycoprotein cDNA and expression in normal human skin and in tumors. *J Cell Biochem* **67**, 216-222.

Lewis GF, Carpentier A, Adeli K & Giacca A (2002). Disordered fat storage and mobilization in the pathogenesis of insulin resistance and type 2 diabetes. *Endocr Rev* **23**, 201-229.

Livak KJ & Schmittgen TD (2001). Analysis of relative gene expression data using real-time quantitative PCR and the 2(-Delta Delta C(T)) Method. *Methods* **25**, 402-408.

Llobera M, Montes A & Herrera E (1979). Lipoprotein lipase activity in liver of the rat fetus. *Biochem Biophys Res Commun* **91**, 272-277.

Lonnqvist F, Krief S, Strosberg AD, Nyberg S, Emorine LJ & Arner P (1993). Evidence for a functional beta 3-adrenoceptor in man. *Br J Pharmacol* **110**, 929-936.

Lopez IP, Marti A, Milagro FI, Zulet Md Mde L, Moreno-Aliaga MJ, Martinez JA & De Miguel C (2003). DNA microarray analysis of genes differentially expressed in diet-induced (cafeteria) obese rats. *Obes Res* **11**, 188-194.

Lopez IP, Milagro FI, Marti A, Moreno-Aliaga MJ, Martinez JA & De Miguel C (2005). High-fat feeding period affects gene expression in rat white adipose tissue. *Mol Cell Biochem* **275**, 109-115.

Ma LJ, Mao SL, Taylor KL, Kanjanabuch T, Guan Y, Zhang Y, Brown NJ, Swift LL, McGuinness OP, Wasserman DH, Vaughan DE & Fogo AB (2004). Prevention of obesity and insulin resistance in mice lacking plasminogen activator inhibitor 1. *Diabetes* **53**, 336-346.

Maeda K, Okubo K, Shimomura I, Mizuno K, Matsuzawa Y & Matsubara K (1997). Analysis of an expression profile of genes in the human adipose tissue. *Gene* **190**, 227-235.

Maeda N, Takahashi M, Funahashi T, Kihara S, Nishizawa H, Kishida K, Nagaretani H, Matsuda M, Komuro R, Ouchi N, Kuriyama H, Hotta K, Nakamura T, Shimomura I & Matsuzawa Y (2001). PPARgamma ligands increase expression and plasma concentrations of adiponectin, an adipose-derived protein. *Diabetes* **50**, 2094-2099.

Makover A, Soprano DR, Wyatt ML & Goodman DS (1989). Localization of retinol-binding protein messenger RNA in the rat kidney and in perinephric fat tissue. *J Lipid Res* **30**, 171-180.

Mantzoros CS, Qu D, Frederich RC, Susulic VS, Lowell BB, Maratos-Flier E & Flier JS (1996). Activation of beta(3) adrenergic receptors suppresses leptin expression and mediates a leptin-independent inhibition of food intake in mice. *Diabetes* **45**, 909-914.

Marcus C, Ehren H, Bolme P & Arner P (1988). Regulation of lipolysis during the neonatal period. Importance of thyrotropin. *J Clin Invest* **82**, 1793-1797.

Massiera F, Bloch-Faure M, Ceiler D, Murakami K, Fukamizu A, Gasc JM, Quignard-Boulange A, Negrel R, Ailhaud G, Seydoux J, Meneton P & Teboul M (2001a). Adipose angiotensinogen is involved in adipose tissue growth and blood pressure regulation. *Faseb J* **15**, 2727-2729.

Massiera F, Seydoux J, Geloen A, Quignard-Boulange A, Turban S, Saint-Marc P, Fukamizu A, Negrel R, Ailhaud G & Teboul M (2001b). Angiotensinogen-deficient mice exhibit impairment of diet-induced weight gain with alteration in adipose tissue development and increased locomotor activity. *Endocrinology* **142**, 5220-5225.

Masuzaki H, Ogawa Y, Isse N, Satoh N, Okazaki T, Shigemoto M, Mori K, Tamura N, Hosoda K, Yoshimasa Y & et al. (1995). Human obese gene expression. Adipocyte-specific expression and regional differences in the adipose tissue. *Diabetes* **44**, 855-858.

Masuzaki H, Hosoda K, Ogawa Y, Shigemoto M, Satoh N, Mori K, Tamura N, Nishi S, Yoshimasa Y, Yamori Y & Nakao K (1996). Augmented expression of *obese* (*ob*) gene during the process of obesity in genetically obese-hyperglycemic Wistar fatty (fa/fa) rats. *FEBS Lett* **378**, 267-271.

Matsuzawa Y (2005). Adiponectin: Identification, physiology and clinical relevance in metabolic and vascular disease. *Atheroscler Suppl* **6**, 7-14.

Matsuzawa Y, Funahashi T, Kihara S & Shimomura I (2004). Adiponectin and metabolic syndrome. *Arterioscler Thromb Vasc Biol* **24**, 29-33.

Mertens I & Van Gaal LF (2002). Obesity, haemostasis and the fibrinolytic system. *Obes Rev* **3**, 85-101.

Miyazawa-Hoshimoto S, Takahashi K, Bujo H, Hashimoto N, Yagui K & Saito Y (2005). Roles of degree of fat deposition and its localization on VEGF expression in adipocytes. *Am J Physiol Endocrinol Metab* **288**, E1128-1136.

Mohamed-Ali V, Goodrick S, Rawesh A, Katz DR, Miles JM, Yudkin JS, Klein S & Coppack SW (1997). Subcutaneous adipose tissue releases interleukin-6, but not tumor necrosis factor-alpha, in vivo. *J Clin Endocrinol Metab* **82**, 4196-4200.

Mohamed-Ali V, Pinkney JH & Coppack SW (1998). Adipose tissue as an endocrine and paracrine organ. *Int J Obes Relat Metab Disord* **22**, 1145-1158.

Moitra J, Mason MM, Olive M, Krylov D, Gavrilova O, Marcus-Samuels B, Feigenbaum L, Lee E, Aoyama T, Eckhaus M, Reitman ML & Vinson C (1998). Life without white fat: a transgenic mouse. *Genes Dev* **12**, 3168-3181.

Mokdad AH, Bowman BA, Ford ES, Vinicor F, Marks JS & Koplan JP (2001). The continuing epidemics of obesity and diabetes in the United States. *Jama* **286**, 1195-1200.

Molina JM, Premdas FH, Klenck RE, Eddlestone G, Oldham SB & Lipson LG (1984). The dynamic insulin secretory response of isolated pancreatic islets of the diabetic mouse. Evidence for a gene dosage effect on insulin secretion. *Diabetes* **33**, 1120-1123.

Montague CT, Prins JB, Sanders L, Digby JE & O'Rahilly S (1997). Depot- and sex-specific differences in human leptin mRNA expression: implications for the control of regional fat distribution. *Diabetes* **46**, 342-347.

Nam DK, Lee S, Zhou G, Cao X, Wang C, Clark T, Chen J, Rowley JD & Wang SM (2002). Oligo(dT) primer generates a high frequency of truncated cDNAs through internal poly(A) priming during reverse transcription. *Proc Natl Acad Sci U S A* **99**, 6152-6156.

Nechad M, Ruka E & Thibault J (1994). Production of nerve growth factor by brown fat in culture: relation with the in vivo developmental stage of the tissue. *Comp Biochem Physiol Comp Physiol* **107**, 381-388.

Negishi M, Sugimoto Y & Ichikawa A (1995). Prostaglandin E receptors. *J Lipid Mediat Cell Signal* **12**, 379-391.

Nielsen S, Guo Z, Johnson CM, Hensrud DD & Jensen MD (2004). Splanchnic lipolysis in human obesity. *J Clin Invest* **113**, 1582-1588.

Nisoli E, Tonello C, Benarese M, Liberini P & Carruba MO (1996). Expression of nerve growth factor in brown adipose tissue: implications for thermogenesis and obesity. *Endocrinology* **137**, 495-503.

Niswender KD, Morton GJ, Stearns WH, Rhodes CJ, Myers MG, Jr. & Schwartz MW (2001). Intracellular signalling. Key enzyme in leptin-induced anorexia. *Nature* **413**, 794-795.

O'Rahilly S, Farooqi IS, Yeo GS & Challis BG (2003). Minireview: human obesity-lessons from monogenic disorders. *Endocrinology* **144**, 3757-3764.

Oliver P, Pico C & Palou A (2001a). Differential expression of genes for uncoupling proteins 1, 2 and 3 in brown and white adipose tissue depots during rat development. *Cell Mol Life Sci* **58**, 470-476.

Oliver P, Pico C & Palou A (2001b). Ontogenesis of leptin expression in different adipose tissue depots in the rat. *Pflugers Arch* **442**, 383-390.

Oliver P, Pico C, Serra F & Palou A (2003). Resistin expression in different adipose tissue depots during rat development. *Mol Cell Biochem* **252**, 397-400.

Ouchi N, Kihara S, Arita Y, Maeda K, Kuriyama H, Okamoto Y, Hotta K, Nishida M, Takahashi M, Nakamura T, Yamashita S, Funahashi T & Matsuzawa Y (1999). Novel modulator for endothelial adhesion molecules: adipocyte-derived plasma protein adiponectin. *Circulation* **100**, 2473-2476.

Ouchi N, Kihara S, Arita Y, Okamoto Y, Maeda K, Kuriyama H, Hotta K, Nishida M, Takahashi M, Muraguchi M, Ohmoto Y, Nakamura T, Yamashita S, Funahashi T & Matsuzawa Y (2000). Adiponectin, an adipocyte-derived plasma protein, inhibits endothelial NF-kappaB signaling through a cAMP-dependent pathway. *Circulation* **102**, 1296-1301.

Path G, Bornstein SR, Gurniak M, Chrousos GP, Scherbaum WA & Hauner H (2001). Human breast adipocytes express interleukin-6 (IL-6) and its receptor system: increased IL-6 production by beta-adrenergic activation and effects of IL-6 on adipocyte function. *J Clin Endocrinol Metab* **86**, 2281-2288.

Pecqueur C, Couplan E, Bouillaud F & Ricquier D (2001). Genetic and physiological analysis of the role of uncoupling proteins in human energy homeostasis. *J Mol Med* **79**, 48-56.

Peeraully MR, Jenkins JR & Trayhurn P (2004). NGF gene expression and secretion in white adipose tissue: regulation in 3T3-L1 adipocytes by hormones and inflammatory cytokines. *Am J Physiol Endocrinol Metab* **287**, E331-339.

Peeraully MR, Sievert H, Bullo M, Wang B & Trayhurn P (2006). Prostaglandin D(2) and J (2)-series (PGJ (2), Delta (12)-PGJ (2)) prostaglandins stimulate IL-6 and MCP-1, but inhibit leptin, expression and secretion by 3T3-L1 adipocytes. *Pflugers Arch* **453**, 177-187.

Phillips MS, Liu Q, Hammond HA, Dugan V, Hey PJ, Caskey CJ & Hess JF (1996). Leptin receptor missense mutation in the fatty Zucker rat. *Nat Genet* **13**, 18-19.

Pi-Sunyer FX (2002). The obesity epidemic: pathophysiology and consequences of obesity. *Obes Res* **10 Suppl 2**, 97S-104S.

Plata-Salaman CR (2000). Central nervous system mechanisms contributing to the cachexia-anorexia syndrome. *Nutrition* **16**, 1009-1012.

Poitou C, Viguerie N, Cancello R, De Matteis R, Cinti S, Stich V, Coussieu C, Gauthier E, Courtine M, Zucker JD, Barsh GS, Saris W, Bruneval P, Basdevant A, Langin D & Clement K (2005). Serum amyloid A: production by human white adipocyte and regulation by obesity and nutrition. *Diabetologia* **48**, 519-528.

Pola R, Gaetani E, Flex A, Aprahamian TR, Bosch-Marce M, Losordo DW, Smith RC & Pola P (2004). Comparative analysis of the in vivo angiogenic properties of stable prostacyclin analogs: a possible role for peroxisome proliferator-activated receptors. *J Mol Cell Cardiol* **36**, 363-370.

Pond CM & Mattacks CA (1991). The effects of noradrenaline and insulin on lipolysis in adipocytes isolated from nine different adipose depots of guinea-pigs. *Int J Obes* **15**, 609-618.

Prins JB (2002). Adipose tissue as an endocrine organ. *Best Pract Res Clin Endocrinol Metab* **16**, 639-651.

Rajala MW, Qi Y, Patel HR, Takahashi N, Banerjee R, Pajvani UB, Sinha MK, Gingerich RL, Scherer PE & Ahima RS (2004). Regulation of resistin expression and circulating levels in obesity, diabetes, and fasting. *Diabetes* **53**, 1671-1679.

Rayner DV, Dalgliesh GD, Duncan JS, Hardie LJ, Hoggard N & Trayhurn P (1997). Postnatal development of the ob gene system: elevated leptin levels in suckling fa/fa rats. *Am J Physiol* **273**, R446-450.

Rayner DV & Trayhurn P (2001). Regulation of leptin production: sympathetic nervous system interactions. *J Mol Med* **79**, 8-20.

Rennie KL & Jebb SA (2005). Prevalence of obesity in Great Britain. *Obes Rev* **6**, 11-12.

Rodriguez AM, Elabd C, Delteil F, Astier J, Vernochet C, Saint-Marc P, Guesnet J, Guezennec A, Amri EZ, Dani C & Ailhaud G (2004). Adipocyte differentiation of multipotent cells established from human adipose tissue. *Biochem Biophys Res Commun* **315**, 255-263.

Rosen ED & Spiegelman BM (2000). Molecular regulation of adipogenesis. *Annu Rev Cell Dev Biol* **16**, 145-171.

Rothwell NJ & Stock MJ (1979). A role for brown adipose tissue in diet-induced thermogenesis. *Nature* **281**, 31-35.

Ruan H, Hacohen N, Golub TR, Van Parijs L & Lodish HF (2002). Tumor necrosis factor-alpha suppresses adipocyte-specific genes and activates expression of preadipocyte genes in 3T3-L1 adipocytes: nuclear factor-kappaB activation by TNF-alpha is obligatory. *Diabetes* **51**, 1319-1336.

Ruan H & Lodish HF (2003). Insulin resistance in adipose tissue: direct and indirect effects of tumor necrosis factor-alpha. *Cytokine Growth Factor Rev* **14**, 447-455.

Ruan Y, Kan H, Cano C & Malik KU (1996). Modulation of beta-adrenergic receptor-stimulated lipolysis in the heart by prostaglandins. *Am J Physiol* **271**, E556-562.

Rubin H (2003). Cancer cachexia: its correlations and causes. *Proc Natl Acad Sci U S A* **100**, 5384-5389.

Russell ST, Hirai K & Tisdale MJ (2002). Role of beta3-adrenergic receptors in the action of a tumour lipid mobilizing factor. *Br J Cancer* **86**, 424-428.

Samad F, Yamamoto K, Pandey M & Loskutoff DJ (1997). Elevated expression of transforming growth factor-beta in adipose tissue from obese mice. *Mol Med* **3**, 37-48.

Sanchez LM, Lopez-Otin C & Bjorkman PJ (1997). Biochemical characterization and crystalization of human Zn-alpha2-glycoprotein, a soluble class I major histocompatibility complex homolog. *Proc Natl Acad Sci U S A* **94**, 4626-4630.

Sanchez LM, Chirino AJ & Bjorkman P (1999). Crystal structure of human ZAG, a fat-depleting factor related to MHC molecules. *Science* **283**, 1914-1919.

Sanchis D, Busquets S, Alvarez B, Ricquier D, Lopez-Soriano FJ & Argiles JM (1998). Skeletal muscle UCP2 and UCP3 gene expression in a rat cancer cachexia model. *FEBS Lett* **436**, 415-418.

Sanders PM & Tisdale MJ (2004). Effect of zinc-alpha2-glycoprotein (ZAG) on expression of uncoupling proteins in skeletal muscle and adipose tissue. *Cancer Lett* **212**, 71-81.

Sarraf P, Frederich RC, Turner EM, Ma G, Jaskowiak NT, Rivet DJ, 3rd, Flier JS, Lowell BB, Fraker DL & Alexander HR (1997). Multiple cytokines and acute inflammation raise mouse leptin levels: potential role in inflammatory anorexia. *J Exp Med* **185**, 171-175.

Sartipy P & Loskutoff DJ (2003). Monocyte chemoattractant protein 1 in obesity and insulin resistance. *Proc Natl Acad Sci U S A* **100**, 7265-7270.

Sawyer N, Cauchon E, Chateauneuf A, Cruz RP, Nicholson DW, Metters KM, O'Neill GP & Gervais FG (2002). Molecular pharmacology of the human prostaglandin D2 receptor, CRTH2. *Br J Pharmacol* **137**, 1163-1172.

Schafer K, Fujisawa K, Konstantinides S & Loskutoff DJ (2001). Disruption of the plasminogen activator inhibitor 1 gene reduces the adiposity and improves the metabolic profile of genetically obese and diabetic ob/ob mice. *Faseb J* **15**, 1840-1842.

Scherer PE, Williams S, Fogliano M, Baldini G & Lodish HF (1995). A novel serum protein similar to C1q, produced exclusively in adipocytes. *J Biol Chem* **270**, 26746-26749.

Schling P & Loffler G (2002). Cross talk between adipose tissue cells: impact on pathophysiology. *News Physiol Sci* **17**, 99-104.

Schwartz MW, Prigeon RL, Kahn SE, Nicolson M, Moore J, Morawiecki A, Boyko EJ & Porte D, Jr. (1997). Evidence that plasma leptin and insulin levels are associated with body adiposity via different mechanisms. *Diabetes Care* **20**, 1476-1481.

Shellock FG, Riedinger MS & Fishbein MC (1986). Brown adipose tissue in cancer patients: possible cause of cancer-induced cachexia. *J Cancer Res Clin Oncol* **111**, 82-85.

Shillabeer G, Kumar V, Tibbo E & Lau DC (1998). Arachidonic acid metabolites of the lipoxygenase as well as the cyclooxygenase pathway may be involved in regulating preadipocyte differentiation. *Metabolism* **47**, 461-466.

Sigrist S, Bedoucha M & Boelsterli UA (2000). Down-regulation by troglitazone of hepatic tumor necrosis factor-alpha and interleukin-6 mRNA expression in a murine model of non-insulin-dependent diabetes. *Biochem Pharmacol* **60**, 67-75.

Sjoholm K, Palming J, Olofsson LE, Gummesson A, Svensson PA, Lystig TC, Jennische E, Brandberg J, Torgerson JS, Carlsson B & Carlsson LM (2005). A microarray search for genes predominantly expressed in human omental adipocytes: adipose tissue as a major production site of serum amyloid A. *J Clin Endocrinol Metab* **90**, 2233-2239.

Skurk T, Herder C, Kraft I, Muller-Scholze S, Hauner H & Kolb H (2005). Production and release of macrophage migration inhibitory factor from human adipocytes. *Endocrinology* **146**, 1006-1011.

Slaviero KA, Read JA, Clarke SJ & Rivory LP (2003). Baseline nutritional assessment in advanced cancer patients receiving palliative chemotherapy. *Nutr Cancer* **46**, 148-157.

Smith PA & Kaplan ML (1980). Development of hepatic and adipose tissue lipogenesis in the fa/fa rat. *Int J Biochem* **11**, 217-228.

Smith U (2002). Resistin--resistant to defining its role. *Obes Res* **10**, 61-62.

Sporn MB, Roberts AB, Wakefield LM & de Crombrugghe B (1987). Some recent advances in the chemistry and biology of transforming growth factor-beta. *J Cell Biol* **105**, 1039-1045.

Spranger J, Kroke A, Mohlig M, Bergmann MM, Ristow M, Boeing H & Pfeiffer AF (2003). Adiponectin and protection against type 2 diabetes mellitus. *Lancet* **361**, 226-228.

Staiger H, Kaltenbach S, Staiger K, Stefan N, Fritsche A, Guirguis A, Peterfi C, Weisser M, Machicao F, Stumvoll M & Haring HU (2004). Expression of adiponectin receptor mRNA in human skeletal muscle cells is related to in vivo parameters of glucose and lipid metabolism. *Diabetes* **53**, 2195-2201.

Starnes T, Broxmeyer HE, Robertson MJ & Hromas R (2002). Cutting edge: IL-17D, a novel member of the IL-17 family, stimulates cytokine production and inhibits hemopoiesis. *J Immunol* **169**, 642-646.

Stefan N & Stumvoll M (2002). Adiponectin--its role in metabolism and beyond. *Horm Metab Res* **34**, 469-474.

Steppan CM, Bailey ST, Bhat S, Brown EJ, Banerjee RR, Wright CM, Patel HR, Ahima RS & Lazar MA (2001). The hormone resistin links obesity to diabetes. *Nature* **409**, 307-312.

Steppan CM & Lazar MA (2004). The current biology of resistin. *J Intern Med* **255**, 439-447.

Stout RD & Suttles J (2004). Functional plasticity of macrophages: reversible adaptation to changing microenvironments. *J Leukoc Biol* **76**, 509-513.

Straczkowski M, Dzienis-Straczkowska S, Stepien A, Kowalska I, Szelachowska M & Kinalska I (2002). Plasma interleukin-8 concentrations are increased in obese subjects and related to fat mass and tumor necrosis factor-alpha system. *J Clin Endocrinol Metab* **87**, 4602-4606.

Straus DS & Glass CK (2001). Cyclopentenone prostaglandins: new insights on biological activities and cellular targets. *Med Res Rev* **21**, 185-210.

Sugden MC, Grimshaw RM, Lall H & Holness MJ (1994). Regional variations in metabolic responses of white adipose tissue to food restriction. *Am J Physiol* **267**, E892-899.

Tada T, Ohkubo I, Niwa M, Sasaki M, Tateyama H & Eimoto T (1991). Immunohistochemical localization of Zn-alpha 2-glycoprotein in normal human tissues. *J Histochem Cytochem* **39**, 1221-1226.

Takahashi K, Mizuarai S, Araki H, Mashiko S, Ishihara A, Kanatani A, Itadani H & Kotani H (2003). Adiposity elevates plasma MCP-1 levels leading to the increased CD11b-positive monocytes in mice. *J Biol Chem* **278**, 46654-46660.

Tartaglia LA, Dembski M, Weng X, Deng N, Culpepper J, Devos R, Richards GJ, Campfield LA, Clark FT, Deeds J, Muir C, Sanker S, Moriarty A, Moore KJ, Smutko JS, Mays GG, Wool EA, Monroe CA & Tepper RI (1995). Identification and expression cloning of a leptin receptor, OB-R. *Cell* **83**, 1263-1271.

Tchernof A, Nolan A, Sites CK, Ades PA & Poehlman ET (2002). Weight loss reduces C-reactive protein levels in obese postmenopausal women. *Circulation* **105**, 564-569.

Tisdale MJ (2002). Cachexia in cancer patients. *Nat Rev Cancer* **2**, 862-871.

Todorov PT, McDevitt TM, Meyer DJ, Ueyama H, Ohkubo I & Tisdale MJ (1998). Purification and characterization of a tumor lipid-mobilizing factor. *Cancer Res* **58**, 2353-2358.

Towbin H, Staehelin T & Gordon J (1979). Electrophoretic transfer of proteins from polyacrylamide gels to nitrocellulose sheets: procedure and some applications. *Proc Natl Acad Sci U S A* **76**, 4350-4354.

Tracey KJ, Morgello S, Koplin B, Fahey TJ, 3rd, Fox J, Aledo A, Manogue KR & Cerami A (1990). Metabolic effects of cachectin/tumor necrosis factor are

modified by site of production. Cachectin/tumor necrosis factor-secreting tumor in skeletal muscle induces chronic cachexia, while implantation in brain induces predominantly acute anorexia. *J Clin Invest* **86**, 2014-2024.

Trayhurn P, Thomas ME, Duncan JS & Rayner DV (1995). Effects of fasting and refeeding on ob gene expression in white adipose tissue of lean and obese (oblob) mice. *FEBS Lett* **368**, 488-490.

Trayhurn P, Duncan JS, Rayner DV & Hardie LJ (1996). Rapid inhibition of ob gene expression and circulating leptin levels in lean mice by the beta 3-adrenoceptor agonists BRL 35135A and ZD2079. *Biochem Biophys Res Commun* **228**, 605-610.

Trayhurn P, Duncan JS, Hoggard N & Rayner DV (1998). Regulation of leptin production: a dominant role for the sympathetic nervous system? *Proc Nutr Soc* 57, 413-419.

Trayhurn P, Hoggard N, Mercer JG & Rayner DV (1999). Leptin: fundamental aspects. *Int J Obes Relat Metab Disord* **23 Suppl 1**, 22-28.

Trayhurn P, Duncan JS, Wood AM & Beattie JH (2000). Regulation of metallothionein gene expression and secretion in rat adipocytes differentiated from preadipocytes in primary culture. *Horm Metab Res* **32**, 542-547.

Trayhurn P & Beattie JH (2001). Physiological role of adipose tissue: white adipose tissue as an endocrine and secretory organ. *Proc Nutr Soc* **60**, 329-339.

Trayhurn P & Wood IS (2004). Adipokines: inflammation and the pleiotropic role of white adipose tissue. *Br J Nutr* **92**, 347-355.

Trayhurn P & Wood IS (2005). Signalling role of adipose tissue: adipokines and inflammation in obesity. *Biochem Soc Trans* **33**, 1078-1081.

Tsuboi H, Sugimoto Y, Kainoh T & Ichikawa A (2004). Prostanoid EP4 receptor is involved in suppression of 3T3-L1 adipocyte differentiation. *Biochem Biophys Res Commun* **322**, 1066-1072.

Tsuchida A, Yamauchi T, Ito Y, Hada Y, Maki T, Takekawa S, Kamon J, Kobayashi M, Suzuki R, Hara K, Kubota N, Terauchi Y, Froguel P, Nakae J, Kasuga M, Accili D, Tobe K, Ueki K, Nagai R & Kadowaki T (2004). Insulin/Foxo1 pathway regulates expression levels of adiponectin receptors and adiponectin sensitivity. *J Biol Chem* **279**, 30817-30822.

Ueyama H, Naitoh H & Ohkubo I (1994). Structure and expression of rat and mouse mRNAs for Zn-alpha 2-glycoprotein. *J Biochem (Tokyo)* **116**, 677-681.

Utsunomiya N, Ohagi S, Sanke T, Tatsuta H, Hanabusa T & Nanjo K (1998). Organization of the human carboxypeptidase E gene and molecular scanning for mutations in Japanese subjects with NIDDM or obesity. *Diabetologia* **41**, 701-705.

Valasek MA & Repa JJ (2005). The power of real-time PCR. *Adv Physiol Educ* **29**, 151-159.

Van Gaal LF & Michiels JJ (2005). Obesity, health issues, and cardiovascular disease. *Semin Vasc Med* **5**, 1-2.

van Harmelen V, Dicker A, Ryden M, Hauner H, Lonnqvist F, Naslund E & Arner P (2002). Increased lipolysis and decreased leptin production by human omental as compared with subcutaneous preadipocytes. *Diabetes* **51**, 2029-2036.

Vassaux G, Gaillard D, Ailhaud G & Negrel R (1992a). Prostacyclin is a specific effector of adipose cell differentiation. Its dual role as a cAMP- and Ca(2+)-elevating agent. *J Biol Chem* **267**, 11092-11097.

Vassaux G, Gaillard D, Darimont C, Ailhaud G & Negrel R (1992b). Differential response of preadipocytes and adipocytes to prostacyclin and prostaglandin E2: physiological implications. *Endocrinology* **131**, 2393-2398.

Vega JA, Garcia-Suarez O, Hannestad J, Perez-Perez M & Germana A (2003). Neurotrophins and the immune system. *J Anat* **203**, 1-19.

Visser M, Bouter LM, McQuillan GM, Wener MH & Harris TB (1999). Elevated C-reactive protein levels in overweight and obese adults. *Jama* **282**, 2131-2135.

Vozarova B, Weyer C, Hanson K, Tataranni PA, Bogardus C & Pratley RE (2001). Circulating interleukin-6 in relation to adiposity, insulin action, and insulin secretion. *Obes Res* **9**, 414-417.

Wabitsch M, Brenner RE, Melzner I, Braun M, Moller P, Heinze E, Debatin KM & Hauner H (2001). Characterization of a human preadipocyte cell strain with high capacity for adipose differentiation. *Int J Obes Relat Metab Disord* **25**, 8-15.

Wajchenberg BL (2000). Subcutaneous and visceral adipose tissue: their relation to the metabolic syndrome. *Endocr Rev* **21**, 697-738.

Wallenius K, Wallenius V, Sunter D, Dickson SL & Jansson JO (2002). Intracerebroventricular interleukin-6 treatment decreases body fat in rats. *Biochem Biophys Res Commun* **293**, 560-565.

Wang B, Jenkins JR & Trayhurn P (2005). Expression and secretion of inflammation-related adipokines by human adipocytes differentiated in culture: integrated response to TNF-alpha. *Am J Physiol Endocrinol Metab* **288**, E731-740.

Wang B & Trayhurn P (2006). Acute and prolonged effects of TNF-alpha on the expression and secretion of inflammation-related adipokines by human adipocytes differentiated in culture. *Pflugers Arch* **452**, 418-427.

Wang SM, Fears SC, Zhang L, Chen JJ & Rowley JD (2000). Screening poly(dA/dT)-cDNAs for gene identification. *Proc Natl Acad Sci U S A* **97**, 4162-4167.

Warren S (1932). The immediate causes of death in cancer. *Am J Med Sci* **184**, 610-615.

Way JM, Gorgun CZ, Tong Q, Uysal KT, Brown KK, Harrington WW, Oliver WR, Jr., Willson TM, Kliewer SA & Hotamisligil GS (2001). Adipose tissue resistin expression is severely suppressed in obesity and stimulated by peroxisome proliferator-activated receptor gamma agonists. *J Biol Chem* **276**, 25651-25653.

Weisberg SP, McCann D, Desai M, Rosenbaum M, Leibel RL & Ferrante AW, Jr. (2003). Obesity is associated with macrophage accumulation in adipose tissue. *J Clin Invest* **112**, 1796-1808.

Wellen KE & Hotamisligil GS (2003). Obesity-induced inflammatory changes in adipose tissue. *J Clin Invest* **112**, 1785-1788.

Wicha MS, Liotta LA & Kidwell WR (1979). Effects of free fatty acids on the growth of normal and neoplastic rat mammary epithelial cells. *Cancer Res* **39**, 426-435.

Wigmore SJ, Fearon KC & Ross JA (1997). Modulation of human hepatocyte acute phase protein production in vitro by n-3 and n-6 polyunsaturated fatty acids. *Ann Surg* **225**, 103-111.

Wood IS, Wang B, Jenkins JR & Trayhurn P (2005). The pro-inflammatory cytokine IL-18 is expressed in human adipose tissue and strongly upregulated by TNFalpha in human adipocytes. *Biochem Biophys Res Commun* **337**, 422-429.

Wood IS & Trayhurn P (2006). Adipokines and the signaling role of adipose tissue in inflammation and obesity. *Future Lipidol* **1**, 81-89.

Yamamoto Y, Hirose H, Saito I, Nishikai K & Saruta T (2004). Adiponectin, an adipocyte-derived protein, predicts future insulin resistance: two-year follow-up study in Japanese population. *J Clin Endocrinol Metab* **89**, 87-90.

Yamauchi T, Kamon J, Ito Y, Tsuchida A, Yokomizo T, Kita S, Sugiyama T, Miyagishi M, Hara K, Tsunoda M, Murakami K, Ohteki T, Uchida S, Takekawa S, Waki

H, Tsuno NH, Shibata Y, Terauchi Y, Froguel P, Tobe K, Koyasu S, Taira K, Kitamura T, Shimizu T, Nagai R & Kadowaki T (2003). Cloning of adiponectin receptors that mediate antidiabetic metabolic effects. *Nature* **423**, 762-769.

Yang Q, Graham TE, Mody N, Preitner F, Peroni OD, Zabolotny JM, Kotani K, Quadro L & Kahn BB (2005). Serum retinol binding protein 4 contributes to insulin resistance in obesity and type 2 diabetes. *Nature* **436**, 356-362.

Yang WS, Lee WJ, Funahashi T, Tanaka S, Matsuzawa Y, Chao CL, Chen CL, Tai TY & Chuang LM (2001). Weight reduction increases plasma levels of an adipose-derived anti-inflammatory protein, adiponectin. *J Clin Endocrinol Metab* **86**, 3815-3819.

Zhang HH, Kumar S, Barnett AH & Eggo MC (1999). Intrinsic site-specific differences in the expression of leptin in human adipocytes and its autocrine effects on glucose uptake. *J Clin Endocrinol Metab* **84**, 2550-2556.

Zhang Y, Proenca R, Maffei M, Barone M, Leopold L & Friedman JM (1994). Positional cloning of the mouse obese gene and its human homologue. *Nature* **372**, 425-432.

Zhang Y, Matheny M, Zolotukhin S, Tumer N & Scarpace PJ (2002). Regulation of adiponectin and leptin gene expression in white and brown adipose tissues: influence of beta3-adrenergic agonists, retinoic acid, leptin and fasting. *Biochim Biophys Acta* **1584**, 115-122.

Zigman JM & Elmquist JK (2003). Minireview: From anorexia to obesity--the yin and yang of body weight control. *Endocrinology* **144**, 3749-3756.

Zucker LM & Antoniades HN (1972). Insulin and obesity in the Zucker genetically obese rat "fatty". *Endocrinology* **90**, 1320-1330.